Novel Approaches to Drug Development by Applications of Accelerator Mass Spectrometry

GC Young

Doctor of Philosophy

2016

NOVEL APPROACHES TO DRUG DEVELOPMENT BY APPLICATIONS OF ACCELERATOR MASS SPECTROMETRY

Graeme Charles Young

A commentary submitted in partial fulfilment of the requirements of the University of Lincoln for the degree of Doctor of Philosophy

This research was sponsored by GlaxoSmithKline Research and Development Ltd., UK.

September 2016

Abstract

Accelerator Mass Spectrometry (AMS) is an extremely sensitive nuclear physics isotope ratio technique with growing application to clinical pharmaceutical drug development. The papers discussed in this commentary demonstrate a wide variety of clinical study designs that incorporate the use of radiocarbon (^{14}C) as a tracer, with subsequent analysis by AMS. The focus of the commentary is application of AMS as an enabling technique aimed towards novel investigations of the absorption, distribution, metabolism, excretion and pharmacokinetics (ADME-PK) of new therapeutic drugs in humans. The impact and contributions to this field of research are demonstrated through discussion and critical examination of selected examples of the author's peer-reviewed publications in this area. The first use of AMS in a clinical study for a new drug in development is included, along with other ADME-PK studies with potential new medicines. The commentary details the expanding scope of AMS over recent years to encompass experiments designed to yield previously unattainable data.
Developments of scientific practices, where the author has contributed intellectual, leadership and practical insight to achieve significant improvements in the generation of knowledge, are highlighted throughout the commentary. The ongoing and future development of AMS, as well as the emergence of techniques as potential alternatives to AMS to provide deep insight into the research of new medicines are also discussed.

Contents

Glossary, Abbreviations and Definitions

[<u>underlined bold</u> in the text**]**

Term	Definition
Absolute bioavailability (F)	F is the fraction of an extravascular dose of unchanged drug that reaches the systemic circulation, commonly known as absolute bioavailability (also see bioavailability below). To determine F, an intravenous reference dose administration is necessary
ADME	Absorption, Distribution, Metabolism and Excretion
Allometric scaling	Inter-species prediction of pharmacokinetic parameters, typically scaled relative to body weight or surface area
Antineutrino ($\bar{\upsilon}$)	A lepton antimatter particle emitted along with an electron during radioactive β^--decay
ANU (Australian National University) Sugar/Sucrose	is a crop of sugar harvested in 1969-1971 with a precisely defined ^{12}C:^{13}C:^{14}C ratio; used as a standard for normalisation of data from the AMS and as a quality control
AMS	Accelerator Mass Spectrometry
AUC	Area Under the drug concentration:time Curve
Autoinduction	Where the administration of a drug leads to increased expression of a given metabolising enzyme responsible for the

	metabolism of that drug. Typically observed following repeated dosing
Autoradiolysis	Dissociation of molecules by free radicals from nuclear radiation; cleavage of one or several chemical bonds resulting from exposure to high-energy flux
Bioanalytical/bioanalysis	Analysis of drug (or metabolite) in biological matrix using an individual analyte specific assay
Bioavailability	Fraction of the dose of drug that reaches the systemic circulation
Biosphere	The ecosystem of the earth and living organisms that inhabit it
Bq	Becquerel – unit of radioactivity; 60 dpm = 1 Bq
B-Raf	A gene on chromosome 7q34 that encodes a protein of the raf/mil family of serine/threonine protein kinases
^{14}C	A radioactive isotope of carbon
Carbon carrier	A known (usually petrochemical) source of carbon added to samples as an isotope dilutor
Cathode	Graphite (or gas) sample holder for analysis by AMS
CCK	Cholecystokinin
Cold	Terminology often used when describing non-radiolabelled doses or samples [as opposed to “hot” for radioactive]
cpm and dpm	cpm - counts per minute; the number of radioactive particles (electrons in the context of this commentary) directly detected by a scintillation counter. The

	value for cpm is adjusted for counting efficiency to provide the number of disintegrations per minute (dpm). dpm = [cpm/(% efficiency)]x 100
CL (clearance)	Clearance –the volume of blood from which drug is irreversibly removed per unit time (eg. L/h)
COPD	Chronic Obstructive Pulmonary Disease
Cross-over study design	Study design where two or more dose administrations are given on separate occasions to the same subject (with a washout period between doses)
Cryogenic transfer	Process by which carbon dioxide gas (at circa -70°C) in a sealed quartz glass tube is transferred and solidified under vacuum into a borosilicate glass tube (at circa -190°C) driven by the temperature differential of the environment in the two tubes
Cytochromes P450; CYP3A4	A group of mixed function oxygenases responsible for metabolism of over 85% of marketed drugs (Kwon, 2001); CYP3A4 is the most prevalent isoform
Disproportionate metabolites	Metabolites present in humans at higher concentrations than in (at least one) of the toxicology study species
Direct AMS	Analysis of samples by AMS (without any chromatographic separation) to provide total radioactivity data
DMPK	Drug Metabolism and Pharmacokinetics
Dosimetry	A series of experiments that are used to calculate dose of ionising radiation that

	will be received by the human body
EMA	European Medicines Authority
E_{max}	The maximum energy carried by an electron emitted during β^-—decay
FDA	(US) Food and Drug Administration
Flip-flop kinetics	Phenomenon observed if the rate of absorption is slower than the rate of elimination (or if one of the distribution rates is slower than elimination rate)
First pass metabolism	The process by which drugs absorbed from the gastrointestinal pass through the liver where they are metabolised (to varying degrees) before reaching the systemic circulation
FTIH	First Time In Human
GSK	GlaxoSmithKline Research and Development Ltd.
Hepatic extraction	Removal of the drug by the liver from the blood flowing through it (via metabolism or biliary elimination) prior to it reaching the systemic circulation as defined by the extraction ratio
HPLC	High Performance Liquid Chromatography
ICH M3	International Conference on Harmonisation M3 – ICH guideline M3(R2) on non-clinical safety studies for the conduct of human clinical trials and marketing authorisation for pharmaceuticals; combines regulatory positions across the world
Intrinsic clearance	intrinsic ability for the liver to remove

	drug by metabolism – determined in vitro (eg. in hepatocytes) therefore not limited by blood flow or by protein binding
Isotope dilution	Isotope ratio of a sample is quantitatively altered usually by the addition of a known amount of a selected isotope in order to deliberately alter the isotopic ratio eg. an organic substance originating from petrochemical sources is depleted of ^{14}C. Therefore when added to a biological sample with a given ^{14}C:^{12}C ratio, the effect is to quantitatively increase the ratio of ^{12}C
IV	Intravenous administration
keV	kiloelectron Volts
KIE	Kinetic Isotope Effect
LC	Liquid Chromatography
LC+AMS	Bioanalytical assay of specific individual analyte isolated through off-line fractionation following liquid chromatography with subsequent analysis by AMS (distinct from metabolite profiling where multiple analytes i.e. drug and metabolites, are analysed)
LC-MS	Liquid Chromatograph interfaced to a Mass Spectrometer (often shortened to this even when MS fragmentation is carried out ie. LC-MS/MS or LC-MS^n)
LoD	Limit of Detection; the lowest quantity of analyte that can be distinguished from

	the absence of a signal for that analyte within a stated confidence (eg. a multiple of signal:noise ratio)
LoQ	Limit of Quantification; lowest concentration at which the analyte can be detected with predefined bias and precision
LSC	Liquid Scintillation Counting/Counter; a method of quantifying decay through radioactive emissions
Mass balance (in vivo)	Recovery of the radioactive dose administered via collections of excreta (urine and faeces mainly)
Mass (of drug) equivalents per unit sample volume eg. pg trametinib equiv./mL	Concentration of total drug-related material is converted from radioactive units to a mass that relates to parent drug based on the administered specific activity of the dose
MDR1-MDCKII	Multi-Drug Resistance Madin-Darby Canine Kidney (cell monolayers)
MEK	Mitogen-activated protein Kinase
Metabolite	Product of metabolism (biotransformation of parent drug, or of another metabolite)
Metabolite profiling	An assessment of the presence and quantification of the range of drug metabolites observed in any post-dose matrix analysed. A metabolite profile is typically performed by radiochromatography
Microdose	Drug administered to humans does not exceed 1% of the **NOAEL** in animals, or 1%

	of the predicted pharmacologic dose based on animal data, or as 100 μg of a new drug, whichever dose is lowest.
Microtracer	An isotopically labelled substance (radioactive or stable isotope) administered intravenously concomitant to a considerably higher extravascular dose. The microtracer dose is low enough to avoid any perturbance of the pharmacokinetics of the extravascular dose
Modern	Terminology used to denote the ^{14}C present at the natural level in 1950 [13.56 dpm/g C]. A term inherited from radiocarbon dating by AMS, but still used in other AMS applications
MS	Mass Spectrometry
NMR	Nuclear Magnetic Resonance spectroscopy
NOAEL	No Adverse Effect Level [relates to absence of toxicity in animal toxicology studies]
Parametric release	An approach through which sterility procedures for dose manufacture is established for non-labelled product and the same procedure then applied to ^{14}C-labelled drug, to expedite release for intravenous dosing to humans
PET	Positron Emission Tomography
P-glycoprotein	Permeability glycoprotein; a cell membrane bound efflux transporter of xenobiotics

Pharmacokinetics	Study of the time course of drug absorption, distribution, metabolism, and excretion – described through mathematical models
Polymorphic	In respect to enzymes responsible for metabolism of xenobiotics, distinctly different expression populations exist (eg. poor and extensive metabolisers)
Radiocarbon dating	Determination of carbon isotope ratios in a sample to provide a chronological date
RDM	Radioactive Drug-related Material i.e. ^{14}C-parent drug and metabolites which still contain the ^{14}C label (≈ Total radioactivity)
Specific radioactivity	Radioactivity per unit mass (or mole) of a stated element or compound
SSAMS	Single Stage Accelerator Mass Spectrometer
Sv	Sievert ; unit of committed effective dose of ionising radiation exposure
$t_{1/2}$	Pharmacokinetic parameter: describes the period of time for a given concentration of analyte to be reduced to exactly half of it's initial concentration by clearance Radioactivity parameter: describes the time taken for the activity of a given amount of a radioactive substance to decay to half of it's initial value
Time-adjusted proportional pools	Plasma samples combined such that the volume of each included in the pool is proportional to the time period between collections. The drug concentration in the

	pool is equivalent to that of the $AUC_{(0-t)}$ (where t is the time the last sample was taken that is included in the pool). (Hop et al., 1998)
t_{max}	Time at which maximum concentrations of analyte are present in the systemic circulation [observed]
TopCount	Equipment for radiodetection using solid scintillant in a microplate
Total Radioactivity	Sum of all ^{14}C radiolabelled (drug related) material in any given sample
Tributyrin	1,2,3-tributyrylglycerol; commonly used as a carbon carrier in graphitisation
UPLC	Ultra High Pressure Liquid Chromatography
Volume of distribution	Theoretical volume of body fluid that would be required to contain the total amount of drug at the same concentration as that measured in biological fluid (blood, plasma or serum)

Figures

PAGE

*** Indicates accreditation**

Declaration

I hereby declare that the basis for this work is as described in Appendices to this Commentary and as otherwise acknowledged.
This work has not been previously submitted for a degree to the University of Lincoln or at any other University.

Acknowledgements

I would like to thank all of the following –

- Dr. Graham Lappin, visiting Professor to the University of Lincoln, for his critical, generous and often humorous guidance throughout the course of my PhD preparations. Also for offering his support at the outset – can't thank you enough Graham!!

- Dr. Driton Vllasaliu, Senior Lecturer at the University of Lincoln, for his support in helping me navigate the requirements for the preparation and submission of my PhD Commentary – I very much enjoyed learning from you Driton, thank you!

- My GSK colleagues, in particular, Gordon Dear for his support throughout the PhD process; Will Ellis, Clive Felgate, Steven Corless and Adrian Pereira for their exemplary technical assistance and insights over many years. We have been through some significant ups and downs together but AMS has been a success, in no small part due to your efforts! And to Mike Tucker and the InMass crew – without you there would be no instrument on which to make the strides forward that we have – BIG Thankyou to you all!

- I would like to acknowledge Xceleron Inc. (formerly Xceleron Ltd. and before that CBAMS Ltd. [Centre for Biomedical AMS Ltd.]) for their support on many studies, particularly prior to 2004. We developed the science together, during many years of interactions, and in so doing many medicines have been helped on their way to the patients who need them.

- My parents for providing me with the opportunity to step on the path to this in the beginning – I know they are both proud of me and I thank them from the bottom of my heart.

- Last but by no means least, my wife Alison, who has provided love, support and encouragement for many years – whilst listening to me ramble on about AMS in all aspects *ad nauseum*!

"What we do in life echoes in eternity"
Marcus Aurelius (Roman Emperor, 161 to 180AD)

Scope of the Commentary

This commentary will focus on some of the applications of Accelerator Mass Spectrometry *(**AMS**)* to drug development specific to the experience and expertise gained by this author in support of experiments conducted by GlaxoSmithKline Research and Development Ltd. (**GSK**). Many applications that are described in the commentary are well established, if not widely adopted today. This however, is a relatively recent advent and the commentary is based upon the progressive development history of the technique in which the author played a significant role, as evidenced by the publications.

Clinical applications are the focus of this commentary and therefore there is only brief mention of applications that have also taken place under the author's stewardship, such as non-clinical studies, eg. in vivo animal and in vitro efforts. Additionally, applications which are often inextricably linked to AMS, such as **microdosing** in humans are also largely excluded from this commentary. References that included such work where the author has contributed are provided for completeness in Appendix 1 of the commentary (Cahn et al., 2013), (Mahar et al., 2012).

The commentary is based upon papers centered around the theme of AMS use to support human **ADME** studies and intravenous **microtracer** pharmacokinetic studies. These will be described in more detail later, but importantly the learnings from application of AMS to the support of these studies, by this author, has driven significant developments of the science in this field. The knowledge derived from these works has then enabled confident design of a combined human ADME/microtracer study for a new drug in development. The details of this will be covered in the future perspectives section of this commentary. Longer term future aspirations for AMS in drug development are also addressed.

1. Introduction

The following sections will provide background information on the principles of the application of radioisotopes as tracers in the study of **pharmacokinetics** and drug metabolism in the development of medicines. In particular, the use of the isotope ^{14}C and its measurement in biological matrices using AMS will be addressed. A selection of published works by this author, which demonstrate novel application of AMS in drug development, will then be presented and will form the main basis for this commentary. Throughout the commentary, evidence will be shown for the contribution that this author has made to the field of biomedical AMS over many years. Finally, the possible directions for future development and advancement of this area of science will be outlined.

1.1. Pharmacokinetics and Drug Metabolism

The study of drug metabolism and pharmacokinetics (**DMPK**) concerns the processes of absorption, distribution, metabolism and excretion (ADME) of drugs and the mathematical description of concentrations of a drug and its **metabolites** over time. DMPK data are used in the safety evaluation of drugs throughout their development towards safe and efficacious medicines, and thereafter as marketed products.

1.2. Use of radioisotopes as metabolic tracers in drug development

Radioisotopes, in particular **^{3}H** and **^{14}C**, are widely used in the pharmaceutical industry as radioisotopic tracers to facilitate an understanding of the ADME properties of new drugs under development as future medicines. They provide the ability to trace a drug and its metabolites through living organisms by differentiating it from the myriad of other endogenous molecules present. This information is of use in determining the metabolic fate of the drug and in confirming the validity of the animal species used in toxicology studies to support administration to humans. Although ^{3}H is widely used

for in vitro studies and in early experiments in drug discovery, due to its facile inclusion in chemical structures and high **specific activity**, loss of the isotope from molecules due to tritium exchange limits its use in vivo. For in vivo studies, particularly those conducted in humans, ^{14}C is the preferred radioisotopic tracer for the following reasons:

1) It can be chemically incorporated into the structural skeleton of a drug molecule.

2) It can be located in specific molecular moieties that are metabolically stable thus allowing the molecule and any drug-related metabolites to be quantitatively traced through the relevant experiments.

3) The half-life of radioactive decay of ^{14}C is 5700 ± 30 years (as recently assessed (Kutschera, 2013)) and therefore places no time restrictions on experiments.

4) ^{14}C is a low energy β^--emitter (**E_{max}** = 156 **keV**) and therefore presents few safety concerns (although there are still limitations in terms of its administration to human subjects; see below and (ICRP, 1992)).

5) ^{14}C has a relatively small kinetic isotope effect (**KIE**) (discussed further below).

6) The rate of radioactive decay is unaffected by environmental factors (eg. temperature, pH, molecular form) and so their measurement is fully quantitative without the need for authentic matched standards.

The use of ^{14}C has a number of practical limitations however, due to the long decay half-life of this isotope (Kutschera, 2013). Relatively high radioactive doses lead to the need for **dosimetry** to assess the burden of ionising radiation exposure to human subjects in the context of clinical trials with ^{14}C-labelled drugs. Equally, even with administration of such relatively high doses of ^{14}C, the data generated may be truncated due to inadequate sensitivity of measurement of the radioactivity present in samples over sufficient periods of time (Bowers et al., 2013) as depicted in Figure 12.

To achieve relatively short sample counting times a large number of ^{14}C atoms must be present in the sample if decay counting is to be used as the detection methodology (see section 1.3.1). However, the long half-life does allow a more relaxed approach to be taken with regard to sample handling and analysis times as the ^{14}C content will not be reduced significantly within the normal timeframe of experimentation. This is not the case for shorter half-life tracers such as ^{11}C (β^+-emitter commonly used in **PET** imaging), which has a half-life of only 20 minutes; leading to severe limitations on the practicalities regarding the timescale of its application and detection, although this isotope also has its place in drug development and research, and indeed has been used alongside ^{14}C in at least one clinical study (Wagner et al., 2011).

As stated above, inclusion of ^{14}C in organic molecules does not lead to significant kinetic isotope effects. The KIE is the change in the rate of a chemical reaction when one of the atoms in the reactants is substituted with one of its elemental isotopes. Formally, it is the ratio of rate constants (k) for the reactions involving the light (kL) and the heavy (kH) isotopically substituted reactants as described in Equation 1:

$$KIE = \frac{kL}{kH} \qquad \textbf{(Equation 1)}$$

It can be seen from Equation 1 that the larger the relative mass of the isotopes the greater the magnitude of the KIE. The relative difference in atomic mass between the light and heavy isotopes decreases as the atomic mass increases. In the case of tritium, there is a 3-fold difference from its lighter ^{1}H isotope. This has been shown to lead to changes in reaction times by specific enzymes in the order of 2.5-fold (Damgaard, 1977). For ^{14}C, there is only a 1.2-fold mass difference from its lighter ^{12}C isotope, which results in an essentially negligible impact on reaction rates (see work on carboxylation of ^{13}C-ribulose biphosphate (Roeske and O'Leary, 1985)). Moreover, such small KIEs are likely to be indistinguishable from experimental biological variations in vivo. In short, incorporation of ^{14}C into a molecule will have no significant impact upon potential reaction paths or rates and hence no significant effect upon the biological fate of the molecule under investigation.

1.3. Measurement of ^{14}C

^{14}C is commonly quantified by measuring the number of electrons emitted over a given time during β^--decay by a technique known as liquid scintillation counting (**LSC**). A calibrated LSC converts the number of electrons detected to the number of decay events for any given period of time. Typically, the raw units of radioactive measurement from an LSC instrument are counts per minute (**cpm**), which are then converted to disintegrations per minute via instrument calibration*. Disintegrations per minute (**dpm**) is the fundamental unit of radioactivity and other units are derived from this (1 Becquerel = 60 dpm, 1 Curie = 2.22×10^{12} dpm).

Liquid scintillation counters have been in common use in drug metabolism laboratories for many years with the first commercial instrument having been built in 1954 (reviewed by (Lappin, 2015)). The energy of emitted electrons is absorbed by the liquid scintillant's π orbital electrons, which re-emit the energy upon returning to the ground state, as photons of light. Early instruments suffered from high background (equivalent to 100 dpm or more) and as with any analytical instrumentation, the higher the background, the lower the signal to noise ratio and therefore the poorer the sensitivity (i.e. the higher the limit of detection (**LoD**)). In scintillation counting, there are a variety of sources of potential background, including cosmic radiation, chemical luminescence from scintillants and electronic noise. To address the sensitivity issue, a combined approach was taken to reduce noise, ranging from use of lead shielding (to reduce cosmic radiation ingress) to sophisticated electronic solutions and complex scintillation cocktail developments. The background in modern LSC instruments is about 10 dpm. Traditionally, the limit of quantification (**LoQ**) for LSC is defined as multiples of background (typically two to three-fold, depending on the laboratory). A typical LoQ for LSC is 25 dpm (Lappin and Temple, 2006).

* Liquid scintillation counters are calibrated using a quench curve that can involve complex mathematical algorithms. The details of this technique are outside of the scope of this commentary. Methods of quench curve correction are discussed in Chapter-8 of Lappin and Temple (2006).

In liquid scintillation counting the sample is dissolved in a chemical cocktail consisting of a solvent and a liquid scintillator thus bringing the radionuclide into close molecular contact with the scintillator. Liquid scintillation counting was - before the advent of AMS and indeed remains so for relatively high radioactive content samples - the preferred method for analysing relatively low energy emitters such as β-particles (electrons), which are produced during the radioactive decay of ^{14}C (Equation 2):

$$^{14}_{6}C \longrightarrow {}^{14}_{7}N + e^{-} + \bar{\upsilon} \qquad \textbf{(Equation 2)}$$

As shown by the reaction above, by emitting an electron (a negatively charged β-particle) and an electron **<u>antineutrino</u>** ($\bar{\upsilon}$), a ^{14}C neutron decays to a proton and the ^{14}C transmutes to the stable (non-radioactive) isotope nitrogen-14 (^{14}N).
Due to the long half-life of ^{14}C (as stated in the previous section; 5700 years, or ~3 billion minutes), only 2×10^{-8}% of the ^{14}C in a sample decays in one minute, making decay counting extremely inefficient.

1.3.1 Analytical Sensitivity

Although manufacturers of liquid scintillation counters have taken steps to reduce background noise through the use of multiple photomultipliers, comprehensive shielding and complex electronics, the LoQs are still somewhat restricted for the reasons discussed below.

Notwithstanding noise from instrument electronics, the limitation on the LoQ for LSC is dependent upon the ability to measure a given number of electrons emitted from an analyte radionuclide, against those electrons arising from background radioactivity. The LoQ in LSC is defined statistically, typically by counting a sufficient number of decay events to achieve a 95.5% confidence interval (i.e. within two standard deviations of the mean). It therefore follows that the fewer the number of decay events in any given period, the longer the count time on the instrument as shown in Equation 3:

(Equation 3)*

$$\boldsymbol{t = \frac{1}{cpm}\left(\frac{200}{\%2\sigma}\right)^2}$$

Where t is the count time,

σ is the standard deviation,

2%2σ (often shortened as shown here to %2σ) is the 95.5% confidence interval of a determined value being within two standard deviations of the mean value.

* Equation 3 uses cpm; the conversion to dpm by the computer software of the LSC, takes into account efficiency of the counting process within the LSC instrument.

To demonstrate the impact of the above, if 1 million cpm are counted to 2%2σ, then a count time of only 0.6 seconds is required. If 10 cpm are counted to 2%2σ then the count time increases to 16.6 hours. The count times therefore become impractically long for samples containing low amounts of ^{14}C.

In addition to the above, complex statistical methods have to be applied for very low level counting by LSC, to enable reliable background subtraction. These are outside of the scope of the current commentary, but typically involve estimating background over 3 to 5-fold the time required for sample measurement. Reliable low level LSC can therefore be extremely time consuming and may take up to several days per sample.

The number of disintegration events for a radioisotope, in any given time period, is dependent upon its radioactive $t_{½}$ as shown in Equation 4. This defines the maximum specific activity for any given isotope:

dpm/mol = (ln2/ t½) x Avogadro's constant (Equation 4)

The natural Log of 2 (ln2) = 0.6931,
$t_{½}$ for ^{14}C = 5700 years = 3.0 $x10^{9}$ minutes,
Avogadro's constant = 6.0221 x 10^{23} atoms or molecules per mole,

Thus, every mole of ^{14}C emits 1.39 x 10^{14} dpm,

Thus, to generate 1 dpm, 4.33 $x10^{9}$ atoms of ^{14}C are required.

As stated in section 1.3, in most laboratories the LoQ for LSC is 25 dpm, which means that approximately 1 x 10^{11} atoms of ^{14}C have to be present in the sample, thus limiting the sensitivity to the high picomole range.

To highlight the impact of this inefficiency of LSC, in the world of archeology for **radiocarbon dating** of famous artefacts such as the Shroud of Turin using LSC, a large piece (probably around the size of a handkerchief) would have been required to be sampled, by destructive analysis, for sufficient sensitivity to be achieved. It was largely for these reasons that a more sensitive method of ^{14}C detection was sought, which culminated in the development of accelerator mass spectrometry (AMS) in the mid-1970s (Bennett et al., 1977).

The advent of AMS provided sufficient sensitivity improvement over that of LSC to allow dating through analysis of only a few milligrams of material (Damon et al., 1989). The first experiment applying AMS to investigations in the biomedical field occurred in 1997 (see section 1.5). AMS was subsequently applied to drug development.

AMS was adopted into use for drug development because it was recognised that certain clinical studies carried an unacceptably high risk of radioactive exposure to human volunteers if supported by LSC. In retrospect it became clear that in some cases studies would not have attained ethical approval without the extremely sensitive analysis offered by AMS (see section 3.2.2). For example, a human radiolabel study was not conducted for such ethical reasons for dutasteride, a 5α-reductase inhibitor, due to its extremely long elimination half-life in humans (approx. 5 weeks) and excretion mass balance could only be assessed using a ^{19}fluorine-**NMR** (^{19}F-NMR) approach (GSK data on file). Although beyond the scope of this commentary, applying ^{19}F-NMR to mass balance studies is problematic as it relies on a fluorine atom being present in the structure of the molecule of interest and it is insensitive in comparison to AMS.

Although ^{14}C is a commonly used isotopic tracer, ^{13}C is also used, particularly in studies in humans, because it has the advantage of being a stable isotope and so there are no issues of radioactive exposure. There is however a significant disadvantage with ^{13}C; an inherently higher LoQ because of its relatively high background.

The natural abundance of ^{13}C is around 1.1% of total carbon in the living **biosphere**, whereas ^{14}C is present as the rare isotope at one part per trillion (1:10^{12}). Doubling the concentration of both isotopes in 1 mg of carbon requires 900 nmol of ^{13}C, but only 98 amol of ^{14}C. Assuming equivalent detection of the two isotopes, this produces a 10 billion times increase in sensitivity for compounds labeled with ^{14}C over those labeled with ^{13}C.

This commentary focuses solely on the application of ^{14}C in AMS and drug development.

1.3.2 Application of AMS

AMS has been used instead of, or as a supplemental analytical tool to, LSC for the following reasons:

1) Reduced radiation burden. In instances where the drug under development has shown retention of either the parent drug or **RDM** (radioactive drug related material) in non-clinical studies (see clinical study example in **Commentary paper 2**, section 3.2) a clinical study can be successfully conducted using a vastly reduced amount (in the region of a thousand fold) of radioactivity in the dose, thus leading to reduced exposure of the subject to ionising radiation. Studies in paediatric or patient populations further re-enforce the need to keep radiation burden to a minimal level.

2) Flexibility of study design, e.g. multiple doses. The possibility of reduced radiation burden to the subject then allows for more than one radioactive dose to be administered if required, either as pulse doses (see **Commentary paper 5**, section 3.5) or even as multiple repeat doses of radioactivity (Iyer et al., 2012). Prior to the advent of AMS such studies in human subjects were extremely rare.

3) The ability to extend sample collection over longer periods of time. It is possible to monitor the pharmacokinetics and excretion of the drug under investigation such that samples can be collected for weeks or even months after dosing (see **Commentary papers 2 and 3**, sections 3.2 and 3.3, and (Clifford et al., 1998)), rather than just for up to one week which is the conventional approach for human ADME studies. When using higher doses of radioactive drug, subjects can only be discharged from the clinic once levels being excreted have reached acceptable amounts. AMS allows for very low levels of radioactivity to be administered thereby enabling subjects to be released from clinics at any time and they may even return at later dates to

provide more samples should there be a requirement to further define the excretion profile.

4) Concomitant dosing. The design and application of the microtracer study has been revolutionised through the use of AMS (see **Commentary papers 6 and 7**, section 3.6).

1.3.3 Sample preparation (Graphitisation) for AMS

Unlike LSC, where radioactive samples are added directly to liquid scintillant, samples for analysis by AMS require prior preparation to extract elemental carbon ('graphite') prior to isotope ratio measurement. This occurs via a two step process of oxidation to CO_2 and then reduction to graphite (Vogel, 1992); see Equation 5 and Equation 6 below. AMS provides an isotope ratio of ^{14}C : ^{12}C from which ^{14}C per mg carbon is derived (see section 1.3.5). It is important to note here that for a reliable measurement to be made the sample preparation process must preserve the isotope ratio of the initial sample and KIEs (known as **isotope fractionation** in this context (Vogel, 1992)) that might occur during sample preparation must be avoided. Such a disruption to the isotope ratio during graphitisation can occur when excess nitrogen is present in the sample – urine samples are prone to this effect so care must be taken to ensure that this is minimised through sample dilution or increased time for the **cryogenic transfer** step to occur. The mechanism for the nitrogen effect remains obscure, but has been observed empirically (Vogel et al., 2010).

Quartz tubes containing the "biological sample" with the addition of supplemental carbon source (**carbon carrier**) as required (see section 1.3.5.1 and Figure 5) and copper (II) oxide wire (in excess at ~50 mg) are dried under vacuum in a centrifugal evaporator. The quartz tubes are then sealed into separate evacuated larger quartz tubes prior to combustion at 900°C for two hours. The CO_2 thus formed is cryogenically transferred into evacuated borosilicate tubes containing zinc powder and titanium dihydride blend at 8.3:1, w:w ratio (~160 mg) and cobalt catalyst (~6 mg) and the tubes are sealed using a high temperature torch, as shown in Figure 1, Figure 2 and Figure 3. The reduction tubes are then heated to 500°C for 4 hours, followed by 550°C for 6 hours to complete the graphitisation process (see the oxidation and reduction reactions summarised below). Carbon as graphite, deposited on the cobalt, is pressed into aluminium **cathode**s and analysed by AMS.

From the above description it can be seen that sample preparation is a demanding process, taking up to three days post preparation of the biological sample itself in

readiness for the graphitisation phase of the sample preparation. This explains the interest in finding alternative approaches to a more rapid sample preparation procedure or avoidance of it entirely, such as direct injection of harvested gas (CO_2) directly into the AMS instrument source (see section 1.4).

Figure 1. Stage 1 graphitisation rig (photograph of set up at GSK*).

Dried sample is sealed into an evacuated tapered quartz tube containing copper (II) oxide, then subsequently placed in a furnace.

Combustion Stage:

CuO + Sample (containing carbon) $\xrightarrow{\text{(900°C for 2 hours)}}$ **$Cu + CO_2 + H_2O$** **(Equation 5)**

* Photograph provided with permission from GSK.

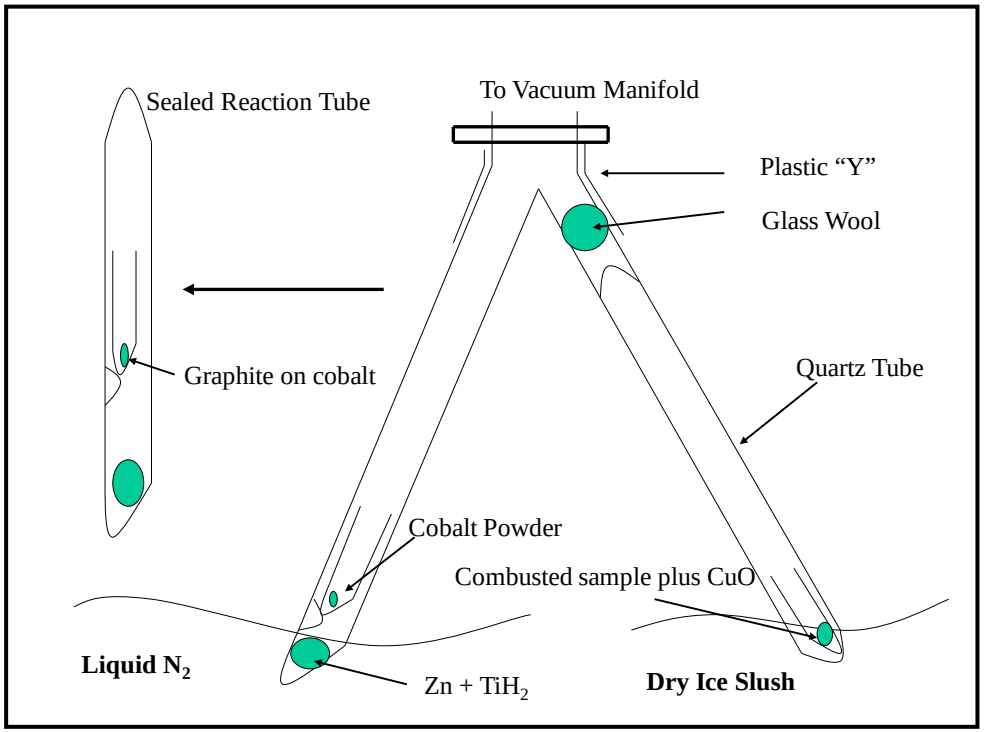

Figure 2. Diagram of graphitisation* – showing the set up for cryogenic transfer of CO_2.

Following sample combustion, the quartz tube is inserted into the Y-piece, gas transferred and the sealed reaction tube is placed back into the furnace.

Note – plastic disposable Y-piece (as shown in the diagram above) was changed to re-usable metal unit (shown in the photograph below) following investigation in our laboratory which demonstrated no sample-to-sample carryover occurred.

* Diagram prepared by the author.

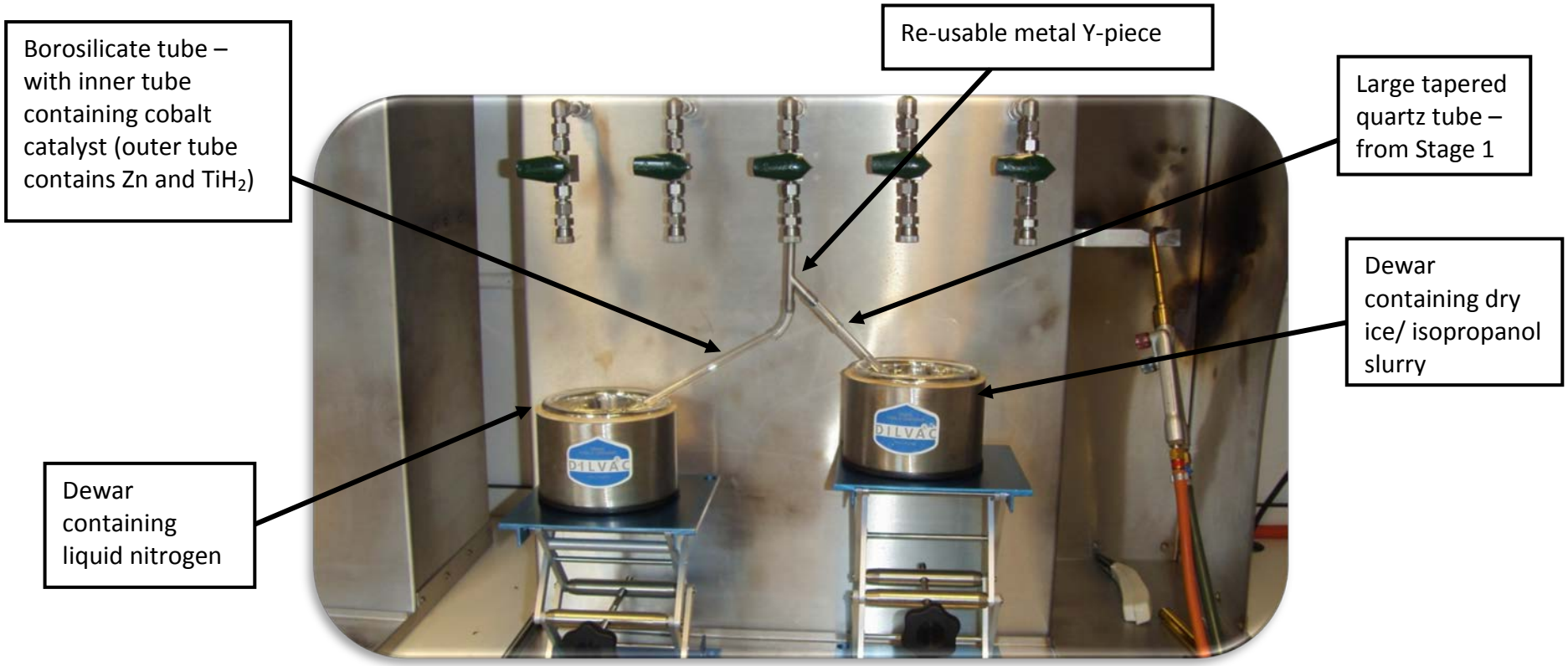

Figure 3. Stage 2 graphitisation rig (photograph of set up at GSK*).

Reduction Stage (following cryogenic transfer of CO_2 from combustion tube):

$$2Zn + 2TiH_2 + 3CO_2 \xrightarrow{\text{(500°C for 4 hrs + 550°C for 6 hrs [+Cobalt])}} 2ZnO + 2TiO + 2H_2O + 3C \qquad \textbf{(Equation 6)}$$

* Photograph provided with permission from GSK.

The graphite pressed into the cathode is ionised using a sputtering caesium ion beam (Cs^+) which generates negative carbon ions; this is crucial as it removes the possibility of interference from $^{14}N^-$, which is unstable and does not survive past the ion source. The ^{12}C, ^{13}C and ^{14}C ions produced are separated based on their mass/charge ratio, sequentially accelerated to high velocities using a high potential difference (250kV-10 MV; depending on the AMS design), and separately counted. The results are typically expressed as isotope ratios, which are normalised to the ratio provided by the consensus value standard (see section 1.3.5), thus accounting for any variability in instrument response. The radiocarbon content of the graphite samples can then be calculated based upon carbon content, sample volume analysed, extraction recovery and initial specific activity to provide the drug or drug-related material concentration (a detailed explanation is given in sections 1.3.5 and 1.3.5.1).

Unlike decay counting, which counts electrons emitted during β^--decay, AMS counts individual ^{14}C atoms and, typically, just 1000 are considered adequate to give a reliable result to provide statistical assurance to the 3% precision level ((√1000/1000)x100 = 3%)*.

However, taking into account differences in background ^{14}C content between sample types and the larger amount of sample that can be analysed by LSC, the inherent sensitivity of the AMS instrument translates in practice to a 300 to 500-fold lower limit of quantification for direct AMS measurements compared with **total radioactivity** analysis using LSC. To put this into context, if the LoQ by LSC for a plasma sample is 25 dpm/mL, then with AMS the LoQ is between 0.08 – 0.05 dpm/mL. With generation of good cathode currents (> 5 µAmp high energy for $^{12}C^{+1}$; see later in this section), analysis times are usually in the region of < 10 minutes per cathode for biomedical work, whereas for carbon dating, to achieve higher precision, lower throughput can be tolerated and the analysis time per cathode can take several hours of measurement.

*As an aside, for radiocarbon dating purposes the desired precision is usually at the 1% level, which requires upwards of 10,000 counts [(√10000/10000)x100 = 1%]

1.3.4 AMS instrumentation

The architecture of a standard 250kV AMS instrument used for biomedical AMS (Young et al., 2008) is shown in Figure 4 below. This design of instrument provided all of the AMS data generated by GSK, from 2005 onwards.

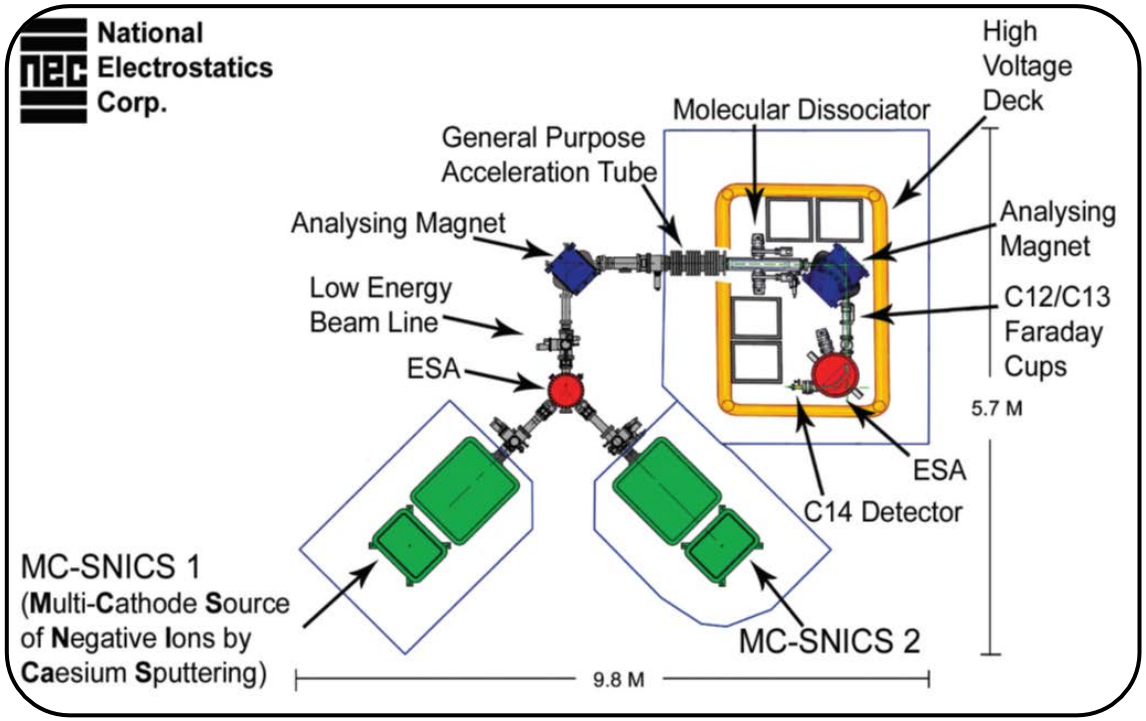

Figure 4. Schematic of Single Stage Accelerator Mass Spectrometer (SSAMS) instrument at GSK*.

* Reproduced by kind permission of National Electrostatics Corp., Madison, Wisconsin, USA.

The graphite samples in the aluminium cathodes are placed on a wheel which is loaded into one of the two MC-SNICS (Multi-Cathode Source of Negative Ions by Caesium Sputtering), depicted in green in Figure 4. Multiple ionic species are generated by the source including monoionic $^{12}C^-$, $^{13}C^-$, $^{14}C^-$ and $^{16}O^-$, as well as molecular species such as $^{12}CH_2^-$ and $^{13}CH^-$.

The mixed ion beam is pre-accelerated through the first electrostatic analyser (ESA; red in Figure 4), which removes some interfering ions and then directs the beam towards the first analysing magnet (blue in Figure 4) that sequentially selects for masses of 12, 13 and 14 in "jumping cycles" of 500 µs, 2100 µs and 0.1 second, respectively. This initial crude filtering of ions selects for $^{12}C^-$, $^{13}C^-$ and $^{14}C^-$, but also allows molecular interferences of the same m/z values (such as $^{12}CH_2^-$) to pass through towards the accelerator. The anionic beam passes into the acceleration tube where ions are accelerated through a potential difference of 290 kV*. The beam enters a cell containing low-pressure argon (known as the molecular dissociator) where molecular species are destroyed, as they collide with the gas, leaving only monoionic species. Through this process electrons are stripped from the outer orbitals of mono-anionic carbon species resulting in cations ranging from C^{+1} to C^{+4}, with the singly charged species being the most abundant at this energy. Creation of positively charged carbon ions removes interference from all of the remaining molecular isobars such as $^{12}CH_2^+$ and $^{13}CH^+$, since these are unstable in the molecular dissociator. After the acceleration tube the ions pass through the second analysing magnet, which further separates out the ions by mass/charge ratio and hence the singly charged ions are selected. $^{12}C^{+1}$ and $^{13}C^{+1}$ are quantified by Faraday cups, whilst $^{14}C^{+1}$ ions then pass through to a final ESA which focuses the ion beam to the detector and removes any remaining background interference. The detector is a silicon surface barrier detector that counts individual atoms of $^{14}C^{+1}$ that are incident upon it. The instrument thus generates measurements of the ratios of the three isotopes of carbon (^{12}C, ^{13}C and ^{14}C) present in the graphite sample.

* Ions are extracted out of the ion source by a potential difference of -40kV and accelerated by a final potential difference of up to +250kV, thereby producing total potential difference of 290kV

1.3.5 Data acquisition and calculations

Analysis of sample radiocarbon within an environment where it is present in the atmosphere and many surrounding organic molecules is very challenging. There is therefore a vital need for a thorough understanding of the carbon inventory for any sample under analysis. Typically a sample analysed by AMS requires between 1-2 mg carbon for a reliable measurement. In some cases the sample provides this mass of carbon during graphitisation. For example, plasma is consistently 4.1% carbon (see section 3.1.4) and so 49 µL will provide 2 mg carbon. Not all sample types contain adequate amounts of carbon, urine for example is only approximately 0.5 % carbon (Kim et al., 2011). These types of sample are supplemented with a known amount of additional carbon (called "carbon carrier"). Ideally carbon carrier is derived from petrochemical sources that are essentially devoid of ^{14}C*. Addition of carbon carrier that contains ^{12}C but not ^{14}C, dilutes the ^{12}C:^{14}C isotopic ratio and therefore this has to be taken into account during any calculations as described in section 1.3.5.1. Fractions collected from liquid chromatography contain very low levels of carbon and so require the addition of carbon carrier prior to analysis, but this is a somewhat special case discussed in section 1.3.5.1. This isotopic dilution is an extremely useful approach, particularly when the total carbon content of the sample of interest is negligible (say in the nanogram range and can be effectively made inconsequential by the addition of an excess of carbon from the carrier – often 1000x dilution) which allows the denominator of the below equation (Equation 7) to effectively be a fixed and known value. This then facilitates the interpretation of the data from the AMS to provide the ^{14}C content for unknown samples.

$$\textbf{The } {}^{14}\textbf{C} : {}^{12}\textbf{C ratio of a sample} = \frac{\textbf{Total } {}^{14}\textbf{C (drug + biological sample + carrier)}}{\textbf{Total } {}^{12}\textbf{C (drug + biological sample + carrier)}} \qquad \textbf{(Equation 7)}$$

* Some batches of carbon carrier derived from petrochemicals have been known to contain ^{14}C and this is discussed below.

Thus, AMS measures the ^{14}C:^{12}C content of a sample derived from all sources of carbon in the sample.

The ^{14}C:^{12}C ratio of a sample is normalised using data generated from a known certificated standard eg. Australian National University Sugar (**ANU**) which is graphitised for analysis by AMS. Another set of synthetic graphite instrument standards are also run to monitor instrument background and further process controls to check that no cross-contamination, or environmental contamination has occurred. The ^{14}C : ^{12}C isotope ratio data provided are then used to calculate concentration values for prepared biological samples as described below.

AMS data are provided as isotope ratios, with the most important one being ^{14}C:^{12}C, although ^{13}C:^{12}C are measured to ensure that the transmission ratio of all measured carbon isotopes remains constant throughout the analysis with no fractionation.

Due to the origins of AMS in carbon dating, the instrument output is typically expressed in units of percent **Modern** Carbon, which can be confusing for those involved in development of pharmaceuticals. Modern, being 100%, is defined as the atmospheric ^{14}C:^{12}C isotope ratio in 1950. Because of atmospheric bomb tests after this date, background pMC had risen and ANU sugar (used as an AMS standard) harvested in 1969-1971 is certified at a consensus value of 150.61 pMC. 1 Modern, or 100 pMC is defined as follows:

100 pMC = 0.01356 dpm/mg C (Mook and Plicht van der, 1999)

Thus, $\text{pMC} \times 0.0001356 = \text{dpm}^{14}\text{C/mg C}$

and $(\text{dpm}^{14}\text{C/mg}) \times \text{mg C in sample} = \text{dpm}^{14}\text{C}$

and $\text{dpm}^{14}\text{C} / \text{volume of sample } (\mu\text{L}) \times 1000 = \text{dpm}^{14}\text{C /mL.}$

The dpm^{14}C/mL value and specific activity of the drug dosed are used to calculate mass per unit volume (eg. pg/mL) values.

So, (dpm^{14}C/mL)/ specific activity (dpm/pg) = pg/mL

The fact that ANU sugar is used as a universal single concentration standard for instrument data normalisation may seem questionable considering that samples analysed may be quite different in concentration to this standard. However, AMS is known to be linear over five orders of magnitude (Vogel and Love, 2005), (Keck et al., 2010) and of course the sample analysed in the instrument is always the same matrix (graphite) so there are no matrix variability effects to cause any analytical differences. For **bioanalytical** (**LC+AMS**) assay applications there would be additional spiked biological matrix matched standards prepared as further sample processing standards.

It is important to state that the assay range is impacted by the specific activity of the material used to prepare standards. The back-calculation of data from the AMS, to mass concentration of drug and drug-related material for samples is equally impacted by the specific activity of the dosed material.

Carbon carriers are chosen from petrochemical sources that are essentially devoid of ^{14}C due to their vast geological age. The choice of carrier has changed over the past decade or so; in fact GSK's early practice (before 2004) was to use **tributyrin** as a carrier. Tributyrin was the carrier used by the Lawrence Livermore National Laboratories (LLNL), California, USA (the first practitioners of biomedical AMS). Although a convenient material to use for such a purpose, containing less than modern levels of ^{14}C, tributyrin did still contain ^{14}C (at 26 pMC when sourced from Aldrich Chemical Co.) and so it seemed counter intuitive to deliberately add this in to materials low in ^{14}C. Liquid paraffin was subsequently used until around 2008, but this was difficult to pipette (required in very small volume) due to its viscosity. Use of liquid paraffin was therefore prone to error which could have a large effect on data generated (as stated it provides the total carbon value). The author advocated the switch to an aqueous based carbon carrier, which resulted in sodium benzoate

solution (prepared in chromatography grade water to a concentration of 90 mg/mL) being selected, which is now in common use. The level of carbon present in the sodium benzoate solution was calculated on the basis of the molecular weight of the solid material which was known to be pure. The data from the AMS and the carbon content of the sodium benzoate solution (58%) are combined to provide radiocarbon levels for each sample.

1.3.5.1 Calculation of analyte concentration from an isotope ratio

AMS provides a measurement of the ^{14}C:^{12}C isotope ratio in units of pMC, but these data have to be converted to mass concentrations of drug in a given body compartment to be useful in drug development applications. Typically, the compartment sampled is blood plasma and so the required units of drug concentration are mass of drug per volume plasma (typically ng, or pg drug per mL of plasma).

As stated above, to calculate the drug concentration from the isotope ratio requires knowledge of the total carbon in the sample, as described by Equation 8 below (Salehpour et al., 2008).

In some cases, such as when the total radioactivity (^{14}C) of plasma is measured, there is sufficient naturally occurring carbon present within the sample (the limitation is dependent upon AMS instrument design but typically a minimum of 1 mg carbon is required) to allow sufficient graphite to be prepared for analysis.

$$K = (R_m - R_n)\,\Psi\,(W/L) \qquad \text{(Equation 8)}$$

Where K = analyte concentration (mass equivalents per unit volume),
R_m = ^{14}C:^{12}C isotope ratio of analyte (pMC),
R_n = natural background ^{14}C:^{12}C isotope ratio of the sample (pMC),
Ψ = carbon mass fraction in the sample,
W = molecular mass of the analyte,
L = specific molar radioactivity (pMC/mole).

In other cases the sample does not contain sufficient carbon to allow direct analysis as depicted in Figure 5. Under these circumstances additional carbon is added in the form of "carrier carbon" (see section 1.3.5). Providing vast excess of carbon carrier is added to the sample then Ψ in Equation 8 is assumed to be the mass of carbon carrier added.

In the early days of biomedical AMS it was thought that carrier carbon merely bulked up the mass of carbon to facilitate analysis, for sample handling and generation of sufficient current from the ion beam. Where samples were analysed directly, for example where a small volume of urine was taken for analysis, then the "carrier carbon" hypothesis was correct. In the case of LC fractions, however, it was found that another factor had to be taken into account when adding carbon to the sample, namely the procedural recovery. Plasma samples are solvent extracted and analysed by LC and therefore there are potential procedural losses during the process. The addition of carrier alters the isotope ratio in such a way that Equation 8 assumes 100% of the original analyte in the matrix (e.g. plasma) is recovered in the fraction. Any loss of sample in extraction, or LC separation, results in a proportional error to the calculation of mass of drug per volume sample from the isotope ratio. These losses have to be taken into account in any calculation of mass of drug per volume sample, as shown in Equation 9 by including an additional function, θ, which represents the fraction of the analyte recovered. The value for θ ranges from 0-1 (Lappin et al., 2008) (also see Figure 5).

$$K = (R_D\ \Phi)/(L_m\ \theta) \qquad \textbf{(Equation 9)}$$

K = mass concentration of drug,
RD = R_m-R_n (as defined in Equation 8)

Φ is the equivalent of Ψ (in Equation 8), but whereas Ψ is the intrinsic carbon in the sample, Φ is the amount of carbon added as "carrier". It assumes that the mass of carbon in the sample (eg. LC fraction) is negligible as volatiles such as LC solvents are evaporated off leaving insignificant levels of contaminants such that ideally only carbon from drug-related material remains. The total carbon present is then equal to that added as the carrier. The amount of carrier carbon added is often in excess of 1000-fold of that present in the sample.

L_m = specific activity (expressed in terms of pMC/mass).

θ = fraction recovered, i.e. if there is a procedural loss of 20% during extraction and preparation by LC, then $\theta = 0.8$.

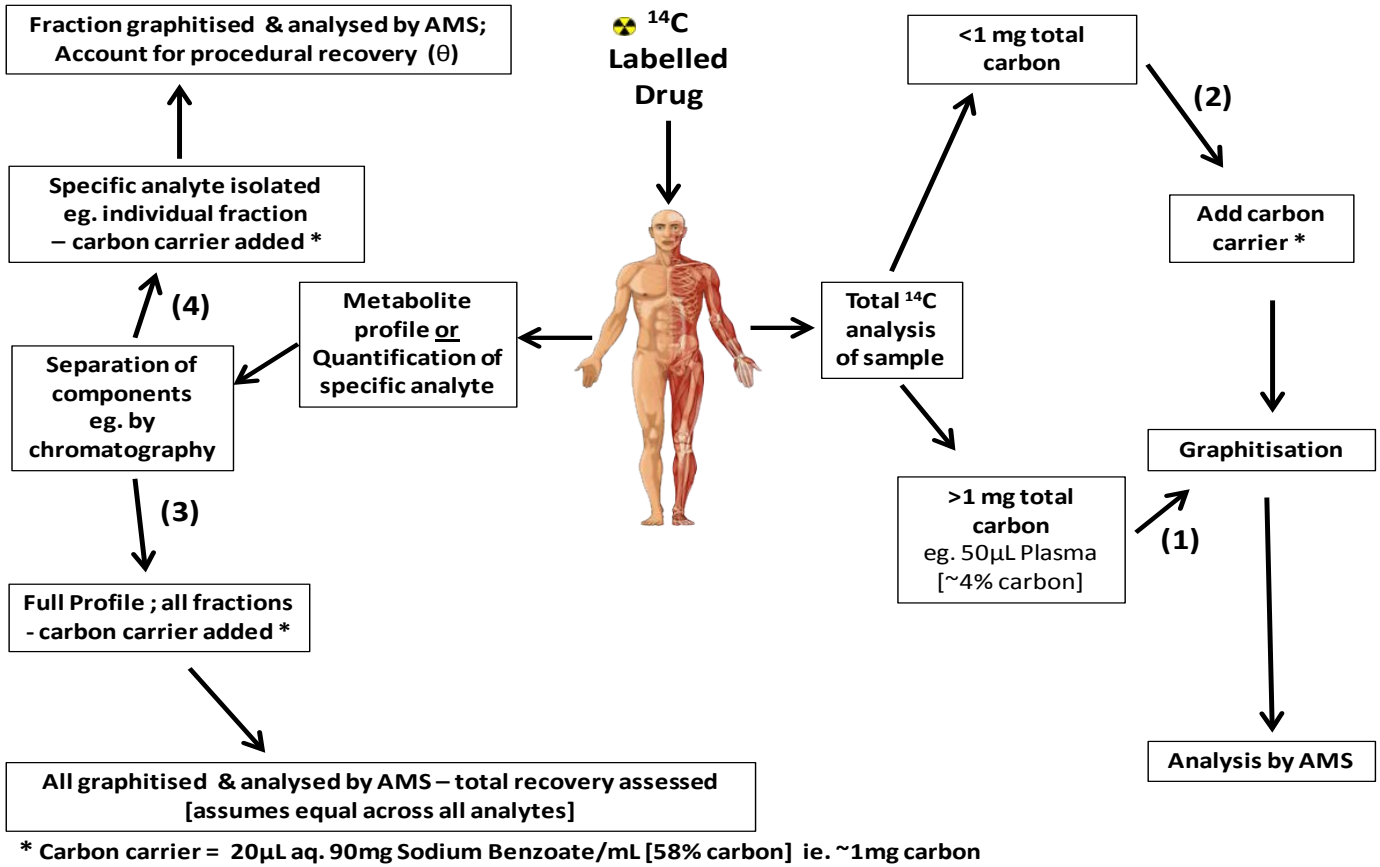

Figure 5. Outline of the procedures for analysis by AMS depending on sample origin*.

Total ^{14}C analysis by AMS [without (1) and with (2) addition of carbon carrier], **metabolite profiling** (3) and isolated individual analyte assay by LC+AMS (4).

* Prepared by the author.

1.4. Instrumentation advances

A brief history of development of AMS instrumentation is provided in Appendix 7. The most recent evolutions of the AMS instrument technology – further reduction in the footprint of the instruments – can be seen in the schematic in Appendix 9. A photograph of the GSK SSAMS is shown in Figure 6.

Instrument size reduction was a useful practical improvement in itself, but the real breakthrough was around sample introduction and interfacing of the instrument with direct introduction of gas (carbon dioxide from the combusted sample, with a helium carrier). This approach removed much of the resource-intense, low sample throughput of the graphitisation process, whilst offering apparent further improved sensitivity. Particularly for metabolite profiling, this improvement in sample throughput could bring a step change in the application of AMS to drug development by removing the time-consuming graphitisation process. There are at this time only a very few systems capable of this in an automated fashion (Bronk et al., 2004), (Wacker et al., 2013), (Roberts et al., 2013), (van Duijn et al., 2014) and there are limited data in the public domain to demonstrate the improvements over graphite (the author is currently working with others to see if this can be addressed, but this is outside the scope of this commentary). Sample-to-sample carry-over seems to be a constant concern for the analysis of gas, but again there is hope that this can be managed and/or reduced with further interfacing and instrument development research. Certainly some drug development research, such as for paediatric drug applications, is being established through such technological advances (Mooij et al., 2014).

Currently, sample preparation via liquid chromatography is performed to produce fractions that are collected into separate tubes or well plates, followed by off-line analysis by AMS. Because of the off-line nature of the analysis, the term LC+AMS is now commonly used, rather than LC-AMS which would infer a direct on-line interface between the LC and the AMS. Gas (CO_2 injection) sources are being investigated that would directly couple the LC and the AMS, but the engineering challenges have not been overcome at the time of writing this commentary and so the fraction collection

method persists. Details of efforts to couple the LC to the AMS (Thomas et al., 2013) are outside the scope of this commentary, although the author has collaborated with groups who are working on gas interfacing (Daniel et al., 2013).

Figure 6. Photograph of the GSK SSAMS*.

Ion source 1 (of 2) containing a sample holder wheel can be seen on the right, with the high energy deck in the background.

* Photograph provided with permission from GSK.

1.5. First Biomedical uses of AMS for ^{14}C

Although analysis of ^{14}C by AMS dominates the applications of AMS in general, the technology has been used for analysis of 55 radionuclides and for a very wide range of applications covering everything from analysis of extraterrestrial materials, environmental applications and archaeological or geological dating (carbon and other elements) (Kutschera, 2013). A poignant example of the use of AMS for analysis of a radionuclide is that employed for the calculation of radiation doses received by the survivors of the Hiroshima and Nagasaki atomic bomb explosions in August 1945. ^{63}Ni (half-life of 100.1 years) was produced by fast A-bomb neutrons via the reaction from ^{63}Cu (copper). The analysis of copper samples from sources such as lightning rods of buildings at various distances from the blast epicentres, including that from the roof of the now Hiroshima Peace Memorial, has allowed such an assessment of radiation to be made, many years after it occurred (Ruhm et al., 2007).

Prior to the emergence of AMS the toxicity of environmental carcinogens were tested in animals at inappropriately high doses due to the limitations of suitably sensitive analytical technology. The use of AMS for biomedical applications first appeared at LLNL, California, in the 1990s to determine the relevance of high-dose animal data for human exposure (Turteltaub et al., 1997). The dose-response curves for ^{14}C-MeIQx (2-amino-3,8-dimethylimidazo[4,5-f]quinoxaline; one of a range of mutagenic/carcinogenic heterocyclic amines formed during the cooking of protein-rich foods) were determined in rodents at low doses under both single-dose and chronic dosing regimens. Historically, the human exposure to MeIQx had been estimated to range from ng/person/day to a few microgram/person/day. In contrast, as inferred above, animal studies had previously been conducted at doses in excess of 10 mg/kg/day. MeIQx-DNA adduct levels in a variety of tissues were compared following oral administration of ^{14}C-MeIQx at doses over four orders of magnitude. Adducts in humans were shown to be around 10-fold higher compared to the mouse, but the biological significance remains debatable. This study demonstrated the utility of AMS as a very sensitive analytical tool that could facilitate new experimental designs.

GSK first used ^{14}C AMS in a range of in-vitro and non-clinical studies before embarking on application of the technique to clinical study support ((Young and Ellis, 2007) and unpublished works).

1.6. Applications of ^{14}C AMS in drug discovery and development

Experiments conducted on new drugs in development using AMS across the pharmaceutical industry were first focussed on human ADME studies for molecules that had persistent retention such as long pharmacokinetic elimination half-lives or high melanin binding where radioactive exposure to ^{14}C would be problematic. Following these initial applications there was a shift of focus to microdosing studies and more recently to microtracer studies.

It should be noted, however, that there have been a wide variety of applications of biomedical ^{14}C AMS, well beyond the uses for human ADME and clinical microtracer studies that the author has focussed on in this Commentary. It is worth mentioning some of these here, in outline, particularly those that may yet have application in exciting areas of research in the pharmaceutical industry; indeed the author is aware that some of these new applications are already being progressed (see below).

Most of the applications of AMS in the pharmaceutical industry have been on "small molecule" DMPK-type applications. There have, however, been some applications to investigate ADME properties of larger molecules such as peptides and proteins (Rickert et al., 2005), (Lappin et al., 2006), (Vlaming et al., 2015); fundamental systems biology applications to investigate production of different cell types in humans, e.g. production only at birth or generated throughout lifetime (Shapiro et al., 1991), (Heinemeier et al., 2013); investigations of drug uptake into tissues other than blood cells or the systemic circulation (Chen et al., 2010) and (Lappin et al., 2013a); tracing the fate of nanoparticles in vivo (Wang et al., 2014); metabolic flux measurements (Stewart et al., 2010); and target turnover assessments (personal communication with Dr. Graham Lappin) - labelling of the biological target itself rather than the drug to investigate the rate at which a target is turned over and thus facilitate development of a better understanding of what attributes of drugs are required to provide pharmacological engagement to ultimately produce efficacy. This latter application may turn out to be the most impactful advance for biomedical AMS in drug discovery and development.

2. Works published

2.1. Introduction

A comprehensive listing of the author's contributions to the field of AMS based research in general, including further peer reviewed publications, conference poster abstracts, book chapters, invited conference speaker listings and external collaborations, is provided in Appendix 1.

During drug development and particularly before large scale clinical trials are carried out, there is an expectation from regulatory authorities that the drug metabolism and pharmacokinetics of the drug are understood. It is of course also good scientific practice and in the interest of the drug development researchers that the molecule under development as a medicine is well established for safety assessment purposes. The human ADME study is a cornerstone of this assessment.

AMS has been used for investigations in a number of human ADME studies in the author's laboratory (Young et al., 2001), (Hughes et al., 2008), (Harrell et al., 2013), (Bowers et al., 2013), (Mamaril-Fishman et al., 2014), (Dave et al., 2014) and (Negash et al., 2015). These have ranged from initial investigative or pilot approaches (Young et al., 2001) to those where we have investigated highly potent, low dose drugs for intended inhaled use (Hughes et al., 2008), (Harrell et al., 2013), (high dose) low specific radioactivity drugs (Mamaril-Fishman et al., 2014), (Negash et al., 2015), repeat dose design to investigate enzyme **autoinduction** (Dave et al., 2014), and "hybrid LSC-AMS" studies where both scintillation counting and AMS instrumentation were required to provide the data (Bowers et al., 2013). In all cases, the study designs at the outset, or samples generated from the studies necessitated the use of AMS to allow the study to deliver on its objectives.

Seven peer reviewed research papers, which included major contributions from the author of this commentary (Appendix 3) were selected for critical review for the

purpose of this commentary. Five of these papers include reports of human ADME studies.

Additionally, a significant and more recent development in the utility of AMS is its application to enable the generation of intravenous pharmacokinetics of new drugs through the microtracer approach (see section 3.6). Two of the seven papers were selected for critical assessment to address this application and a planned combination human ADME/microtracer study is also outlined (section 4.1).

3. Principal papers published as basis for this Commentary

1) **Young, G**., W. Ellis, J. Ayrton, E. Hussey and B. Adamkiewicz (2001). "Accelerator mass spectrometry (AMS): recent experience of its use in a clinical study and the potential future of the technique." Xenobiotica **31**(8-9): 619-632.

2) **Young, G**. and W. J. Ellis (2007). "AMS in Drug Development at GSK." Nuclear Instruments and Methods in Physics Research **B 259**: 752-757.

3) Bowers, G. D., D. Tenero, P. Patel, P. Huynh, J. Sigafoos, K. O'Mara, **G. C.Young**, E. Dumont, E. Cunningham, M. Kurtinecz, P. Stump, J. J. Conde, J. P. Chism, M. J. Reese, Y. L. Yueh and J. F. Tomayko (2013). "Disposition and metabolism of GSK2251052 in humans: a novel boron-containing antibiotic." Drug Metab Dispos **41**(5): 1070-1081.

4) Harrell, A. W., S. K. Siederer, J. Bal, N. H. Patel, **G. C. Young**, C. C. Felgate, S. J. Pearce, A. D. Roberts, C. Beaumont, A. J. Emmons, A. I. Pereira and R. D. Kempsford (2013). "Metabolism and disposition of vilanterol, a long-acting β(2)-adrenoceptor agonist for inhalation use in humans." Drug Metab Dispos **41**(1): 89-100.

5) Dave, M., M. Nash, **G. C. Young**, H. Ellens, M. H. Magee, A. D. Roberts, M. A. Taylor, R. W. Greenhill and G. W. Boyle (2014). "Disposition and metabolism of darapladib, a lipoprotein-associated phospholipase A2 inhibitor, in humans." Drug Metab Dispos **42**(3): 415-430.

6) Denton, C. L., E. Minthorn, S. W. Carson, **G. C. Young**, L. E. Richards- Peterson, J. Botbyl, C. Han, R. A. Morrison, S. C. Blackman and D. Ouellet (2013). "Concomitant oral and intravenous pharmacokinetics of dabrafenib, a BRAF inhibitor, in patients with BRAF V600 mutation-positive solid tumors." J Clin Pharmacol **53**(9): 955-961.

7) Leonowens, C., C. Pendry, J. Bauman, **G. C. Young**, M. Ho, F. Henriquez, L. Fang, R. A. Morrison, K. Orford and D. Ouellet (2014). "Concomitant oral and intravenous

pharmacokinetics of trametinib, a **MEK** inhibitor, in subjects with solid tumours." Br J Clin Pharmacol **78**(3): 524-532.

These specific papers were selected as they provide a measure of the breadth of application of AMS by the author, particularly around the theme of human ADME and clinical microtracer studies. They also demonstrate the impact of the studies and their contribution to the advancement of this field of research.

Each of the papers is summarised and discussed in section 3.1 to section 3.8 below. **See Appendix 3 for supporting letters from lead authors and detail of the contributions made by this author to each of these published works.**

3.1. Commentary paper 1

Young, G., W. Ellis, J. Ayrton, E. Hussey and B. Adamkiewicz (2001). "Accelerator mass spectrometry (AMS): recent experience of its use in a clinical study and the potential future of the technique." Xenobiotica **31**(8-9): 619-632.

3.1.1. Objectives

The use of AMS for a pilot human ADME study was described in this study with the following objectives:

1) To determine the rates and routes of excretion of a new chemical entity (NCE), GI181771 (a **CCK**-A agonist for potential use in appetite suppression), following oral administration to healthy volunteers.

2) To determine the biotransformation pathways for GI181771 in humans.

3) To investigate the utility of AMS to facilitate human ADME with reduced radiation burden to the subjects.

Studies designed to meet these objectives by applying AMS are relatively commonplace today within the pharmaceutical industry (and certainly within GSK). However, at the time this work was conducted (around 2000-2001) no such clinical study had been previously reported. **Commentary paper 1** was the first to report the application of AMS for the analysis of samples obtained in a clinical study with a NCE. Prior to this publication others had conducted preliminary and evaluation studies with pharmaceuticals, but these were using in vitro dilutions to scale from the range of LSC to AMS (Kaye et al., 1997), (Garner et al., 2000), or from studies involving human volunteers in nutritional research. Such a study was the analysis of folic acid in a single subject with the low ^{14}C dose added to dietary intake on a single occasion, and

subsequent assessment of extended elimination of the dose (3.7 k**Bq**) over one year (Clifford et al., 1998).

3.1.2. Clinical study design

In this clinical study, six healthy male human volunteers were administered 2.7 mg of ^{14}C-GI181771 (121 Bq), which equated to an exposure to ionising radiation of only 0.06 μ**Sv**, as shown in Figure 7. This was more than 1000-fold lower than for most conventional radioactive dose human ADME studies and nearly 17-fold below the targeted threshold of ionising radiation exposure of 1 μSv. At the time, this was seen as a very attractive proposition, i.e. to be able to conduct a clinical study with radiocarbon labeled drug producing exposure to ionising radiation at such a low level. At targeted exposures of <1 μSv certain approvals and enabling work were not required, such as those to facilitate dosimetry (see section 1.2).

To put the level of radioactivity used in such studies (and subsequent ionising radiation exposure) into context, a 70 kg human adult subject's natural ^{14}C content is in the region of 3.7 kBq (Vogel et al., 2010), so this clinical study barely raised the exposure to ionising radiation in the study subjects to above background (<5% increase).

As the regulatory authorities became more familiar with the concept of AMS and the consequential lowering of ^{14}C doses, over the intervening years and in several parts of the world, up to 37 kBq can now be administered to human subjects without the need for dosimetry data*. These changes accelerate study implementation and reduce the enabling package resource burden placed upon such clinical experiments.

* The assumption being that a dose of 37 kBq will produce an exposure to ionising radiation of <1 μSv.

Design:
6 Healthy human subjects;
Single oral dose of 2.7 mg ^{14}C-GI181771
(121 *Bq*)

Samples :

- Blood for serum [for parent drug & RDM concentrations & metabolite profiling]
- Faeces and urine [for mass balance and metabolite profiling]

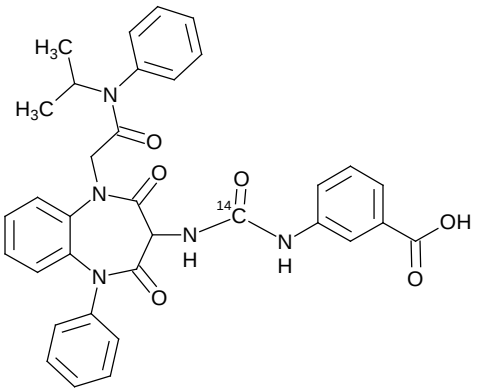

^{14}C-GI181771*

Main data outputs:

- Parent drug concentrations in serum (by **LC-MS**)
- Total radioactivity in serum (by direct AMS)
- Excretion mass balance assessment (by direct AMS)
- Metabolite profile (faeces only; by LC+AMS) – insufficient sensitivity for metabolite profiling of serum due to the tiny ^{14}C dose administered.
    - Definition of limits of detection by direct AMS (and LC+AMS) for a range of different biological matrices

Figure 7. Schematic of clinical study design 1.

* Structure was not included in **Commentary paper 1**

3.1.3. Clinical study data output and impact

Despite the extremely low amount of radioactivity administered, **mass balance** in recovery of administered radioactivity was achieved (mean of 92.2%; standard deviation (SD) of 16.1%). It was shown that systemic concentration of total ^{14}C was up to 8-fold greater than for parent drug. Total ^{14}C is a measure of **RDM** and represents exposure to parent drug plus its metabolites (or those metabolites retaining the ^{14}C tracer). GI181771 was therefore extensively metabolised, resulting in 8-fold greater exposure of metabolites compared to parent drug. Bearing in mind that this drug was thought to act locally in the gut, without the need for absorption into the systemic circulation, these data contribute to decision making relevant to safety cover for systemic metabolites in animal species when extrapolated to humans.

This study showed the potential of AMS to support extremely low ^{14}C dose administrations to humans, as well as defining its limitations since it turned out that the dose of ^{14}C-labelled drug was too low for all study endpoints to be achieved. The situation was exacerbated by the fact that the drug was designed to be poorly absorbed (for treatment of appetite suppression through local action in the gut). Due to adverse pharmacology in the preceding clinical study (GSK data on file), the human ADME study under discussion had to be re-designed with a reduction in the clinical dose only a short time before dosing. The ^{14}C dose was reduced by 20-fold (radiolabel dose material had already been prepared) which then compromised the endpoint of metabolite profiling for blood serum samples. Indeed, were this drug to have been filed for marketing approval, it is likely that a further human ADME study would have been required to deliver on the initial study objectives. In retrospect, the study could have been more appropriately designed, but these were the early days of AMS and there was little experience with required ^{14}C doses and the sensitivity of the assays.

Data from the study nevertheless provided a good understanding of the drug's ADME properties at an early stage of clinical development, well in advance of progression to large scale clinical trials*. Despite the 8-fold difference in RDM to parent drug, the only metabolite of GI181771 detected in human faeces was an acyl glucuronide of parent drug (see Figure 5 of the paper) and this was minor in magnitude. It was known from pre-clinical work for this drug (unpublished) that the acyl glucuronide was present as the major metabolite in bile from rat. Nowadays, a bile collection would be included in the clinical study design (see section 3.4.4) and had this been available at the time then perhaps a better understanding of whether the glucuronide concentration was decreased due to breakdown back to parent drug by gut microflora activity could have been ascertained (Hawksworth et al., 1971).

Such data provision around the development of understanding of metabolite exposures in safety testing is in alignment with not only good scientific practice, but also with the expectations set out in regulatory guidance (**FDA**, 2008). The data has significant impact upon assessments for potential drug-drug interactions where therapies are co-administered. Again, there is guidance in place that describes expectations of regulatory authorities and re-enforces the need for generation of knowledge in this regard ((FDA, 2012) and (**EMA**, 2013); Appendix V).

* The paper used the term "radiocarbon", rather than (total) radioactivity as is commonly used. Radiocarbon has since been seen as a misleading term, when used in the way it was in the paper, as it does not properly describe what is being reflected by the measurement of radiocarbon (and carbon in general) in the samples, i.e. radiocarbon being the traced isotope, but effectively the traced molecule itself is being measured and not just the carbon it contains.

This paper (note that the study was published in 2001) also discussed the possible future direction of the technology for biomedical applications – much of which came to pass over the years since this publication, including microdosing (see Scope of Commentary), parent drug pharmacokinetics by AMS **(see Commentary papers 6 and 7),** analysis of late timepoint samples **(see Commentary paper 2)**, smaller sample sizes (Salehpour et al., 2008), use of other isotopes (eg. ^{41}Ca, ^{129}I (Vogel and Love, 2005)), the need for increased sample throughput via simpler sample preparation and/or on-line interfacing (Thomas et al., 2013), (Wacker et al., 2013) and instrument size and cost reduction possibilities (Klody et al., 2005).

Some of these advances, at least in part, have become reality due to the published and presented works of the author (see Appendix 1). This author was encouraged by other scientists in the field to present and publish our work since we were, and still are, unique amongst pharmaceutical companies in our advancement of AMS capabilities.

3.1.4. Technical considerations and reflections

Some of the technical approaches taken in this work* were deemed to be poor practice and were subsequently improved upon with continued application experience. At the time of conducting this clinical study, the practice for carbon content assessment was to analyse all samples that were likely to have measurable endogenous carbon present so that the individual sample carbon was known and used in the calculation of the isotope ratio conversion to derive the unknown ^{14}C concentration (see section 1.3.5). Subsequent to this, following investigations at other laboratories ((Keck et al., 2010), Xceleron Inc. – communicated through GSK sponsored study reports) and GSK's own experience, it was found that in most instances, where a carbon carrier was not added, particularly for whole blood or blood plasma samples, a generic value could be used (e.g. in the region of 4.1% for plasma). It was found that the carbon content of such samples (at least from healthy human subjects) did not vary greatly, i.e. coefficient of variation of < 5% (Kim et al., 2011). It is therefore recognised that a generally small, but acceptable, error will occur. This is deemed to be acceptable since it is outweighed by inherent biological variations and other accepted analytical variabilities (typical tolerances of +/- 15% for bioanalytical assays). Also, the effort required to analyse carbon content of all samples is outweighed by acceptance of the potential level of error that is implicit by using a generic value. It would, however, be ideal (as long as the measurement of carbon content is accurate enough) for it to be measured for every individual sample, as is the approach with the gas ion source used in a recent modification to the AMS interface (van Duijn et al., 2014), particularly for sample types that are notoriously non-homogeneous such as faecal sample preparations.

* An example being the use of a slurry for preparation of faecal homogenates; pipetting difficulties due to the nature of the material involved. This was improved upon through use of a freeze drying approach, to produce a powder that could be more easily handled in small, representative quantity for mass balance data provision.

Through analysis of clinical samples the limits of quantification for a range of biological matrices were defined (see Table 4 in **Commentary paper 1**). This encompassed both direct analysis by AMS and LC+AMS approaches. This fundamental information helped the author and colleagues to design many subsequent studies through development of the understanding of what influence endogenous carbon has on detection limits. Also, what could be achieved through different sample clean-up procedures, such as protein precipitation or chromatographic separations, became clearer through design and conduct of these experiments

In these early works, concerns about inadvertent cross-contamination (of ^{14}C) were significant for researchers in this field. Therefore, precautions were taken to try to avoid the likelihood of this occurring, notwithstanding the fact that the environment which surrounds us contains ^{14}C in the form of $^{14}CO_2$. Typical precautions taken included use of segregated clean laboratory approaches, disposable laboratory supplies wherever possible, work procedures which entailed processing samples of low ^{14}C content ahead of those containing higher levels and use of human subjects (and animals) naive to ^{14}C study exposure. Over time and through extensive research, it has been determined in our laboratory that contamination is indeed an issue for both the sample preparation areas and equipment, as well as for the AMS ion source itself, but with meticulous practices, these issues are manageable.

All of the analysis of samples detailed in this paper used a 5 MV tandem accelerator instrument, and it was not until 2005 that GSK's own instrument (a single stage 250 kV accelerator) came into use (see section 1.3.4). The data generated by these two different types of AMS were the subject of a separate publication by this author and co-workers ((Young et al., 2008) – not listed as one of the papers providing the basis for this Commentary). In brief summary, this publication provided bioanalytical data showing that for the analysis of biological samples (blood, plasma and urine) spiked with a range of low level concentrations of ^{14}C, below those that could be detected by LSC, equivalent data (correlation coefficient values of >0.99 for all matrices) were provided through analysis of separate graphites generated from the same biological samples on the 5 MV and the 250 kV instruments.

It is worth noting that a direct comparison of two GSK SSAMS instruments (see Appendix 8) was carried out through analysis of the same graphite samples on both instruments and the data (unpublished) showed remarkable reproducibility with percent differences of <5% for all graphites (albeit <20 in number), measured as being >20 pMC and about 3-fold the acceptable limit generated for background carbon carrier in our laboratory. This was as expected since the reproducibility of the AMS instruments for analysis of carbon is well founded (Damon et al., 1989) and indeed is the basis for consensus values being generated for AMS as inter-laboratory standards (see section 1.3.5).

These type of data supported the production of increased numbers of what are termed compact, or sub-compact, AMS instruments and these are now in common use for the analysis of carbon in both the biomedical and wider carbon dating fields. Much of the practical work included in **Commentary paper 1** was groundbreaking at the time* and provided the foundation for later sample preparation and study designs, both within GSK and beyond to the wider biomedical AMS field.

* The extremely low specific activity material used required that a new approach was taken to assess the radiochemical purity of the dosed material. Common practice is now as per this study, i.e. to check the purity of the high specific activity material that is initially synthesised and of the cold material drug substance that it would be formulated with, but not to assess the final (blended or re-crystallised) drug product itself.

3.2. Commentary paper 2

Young, G. and W. J. Ellis (2007). "AMS in Drug Development at GSK." Nuclear Instruments and Methods in Physics Research **B 259**: 752-757. This paper contains elements of review of previous works by this author, but also contains original research which is the focus of this section of the commentary.

3.2.1. Objectives

The novel use of AMS for a low radioactive dose clinical study for a compound with potential for prolonged retention of radioactive drug-related material was described with the following objectives:

1) To provide information on rates and routes of excretion of the NCE, SB773812, including extension of excreta collections in anticipation of retention of drug-related material.

2) Provision of metabolite profiling (biotransformation) data.

3) To investigate the feasibility of achieving acceptable mass balance for a low dose of ^{14}C with incomplete/interval collections of excreta.

3.2.2. Clinical study design

SB773812 is a high affinity D_3, 5-HT_{2A}, 5-HT_{2C} and 5-HT_6 receptor antagonist, that was being developed for treatment of antipsychotic-like behaviour (Catafau et al., 2011). A human ADME study was conducted in Phase 1 of development due to uncertainty over which toxicology species should be used for assessment of safety cover limits. It is important in drug development to understand the ADME profile in the species used in the toxicology (safety assessment) studies, so that the relevance, or otherwise, to humans can be established as the data from humans becomes available.

In the rat, elimination of the dose of ^{14}C-SB773812 was complete by 96 hours post-dose, whilst in the dog elimination was protracted, with radioactivity continuing to be excreted 312 hours after dose administration (GSK internal reports and (Iverson and Smith, 2016)). There were also metabolic route differences between the toxicology study species, such that in rat the main metabolic pathway was cleavage of the ether bond, whilst in dog N-demethylation and N-oxidation were the principal metabolic routes. The differences in the ADME profile of SB773812 between the non-clinical species made the human ADME study difficult to design e.g. how long blood and excreta samples should be collected for.

Due to the slow elimination of drug-related material in the dog, a second study in this species was performed following a single dose of ^{14}C-drug to enable tissue and excreta metabolite profiles to be monitored over a 13 day period. In this second study the major metabolite in dog plasma and several organ tissues, at 312 hours was M9 (N-demethylated SB773812, see Figure 8, known to be a target pharmacologically active metabolite).

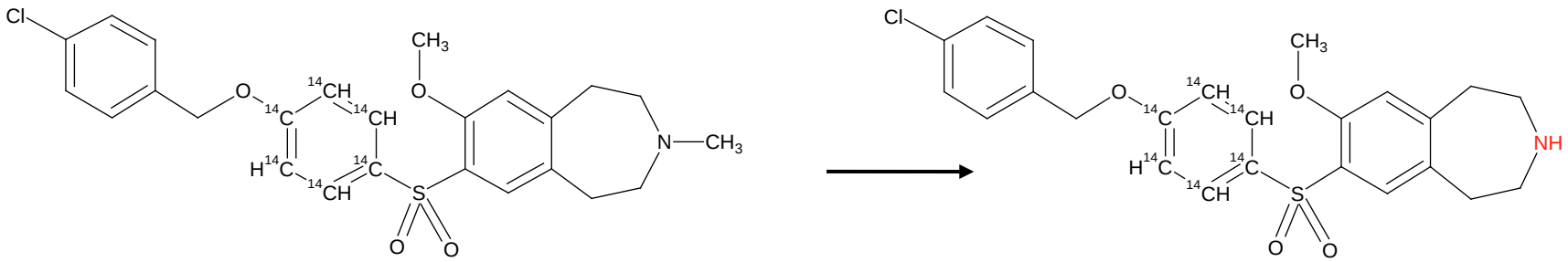

SB773812 **M9**

Figure 8. Biotransformation of SB773812 to M9 (N-demethylated metabolite of SB773812).

The structures show the positions of the ^{14}C-label.

A clinical study was therefore designed as outlined in Figure 9, to take account of the concerns (based on data from the dog) that there may be considerable retention of drug-related material in humans and therefore excess exposure to ionising radiation, were the usual magnitude of ^{14}C dose to be administered. It is worth pointing out that in cases where the metabolism of a drug varies across species, the design of the clinical study often becomes complicated. Moreover, the radioactive dose that can be administered is very difficult to assess in terms of being sufficient for subsequent analysis but at the same time, not to cause excessive exposure to ionising radioactivity. The advent of AMS, where doses of ^{14}C could be reduced considerably, ameliorated these difficulties considerably.

The dose of radioactivity in the current study was kept low (18.5 kBq, being ~200-fold lower than that used conventionally) and the excreta collection period was extended out to eight weeks, with interval (24 h) collections of excreta weekly and then bi-weekly after the initial two week continuous collection. The interval collections were included due to logistical limitations on incarceration of the human subjects beyond the initial two week period, and because a full understanding of the (potential) extent of retention of drug or metabolites was warranted, so as to put the human data into context with the animal data.

Design:
5 Healthy human subjects;
Single oral dose of 16 mg ^{14}C-SB773812 (18.5 k*Bq*)

Samples :

- Blood for plasma [for parent drug & RDM concentrations & metabolite profiling]
- Extended collections of Faeces and Urine [for mass balance and metabolite profiling] - with weekly and bi-weekly interval collections after 15 days to 8 weeks

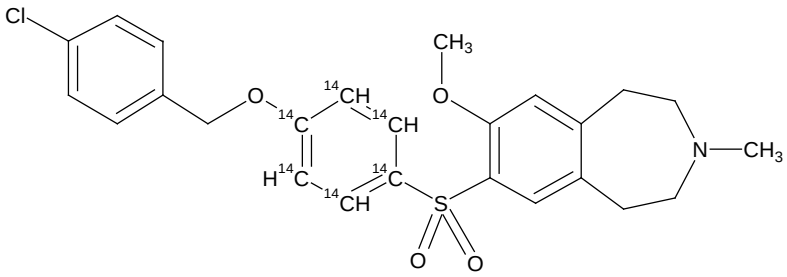

^{14}C-SB773812

Main data outputs:

- Parent drug concentrations in plasma (by LC-MS)
- Total radioactivity in plasma (by direct AMS)
- Excretion mass balance assessment (by direct AMS)
- Metabolite profiles of all matrices (plasma by LC+AMS; other matrices by **Topcount**)
    - Established limit of possibility for reliable metabolite profiling [0.06 dpm on column for multiple metabolites; >7 in this instance (see Figure 10)]

Figure 9. Schematic of clinical study design 2.

3.2.3. Clinical study data output and impact

In this study, the sensitivity of AMS was such that mass balance of ^{14}C recovery was achieved (mean of 77.1%; SD of 5.4%, for continual excreta collection to two weeks) despite the low dose of radioactivity and the need for extended collections, with intervals, to provide extrapolated cumulative recovery (increased to 86.4%). As shown in this paper (Figure 4), total radioactivity was still above background in plasma samples at 480 hours post-dose (LoQ was ~ 1 ng SB773812 equivalents/mL), with a terminal elimination half-life of >150 hours, confirming that elimination of SB773812 related material in human was protracted and was comparable to dog. Thus, the decision to adopt the low ^{14}C dose approach for this study was well justified.

The example chromatographic profile in **Commentary paper 2** (Figure 2) (Young and Ellis, 2007) shows a detailed profile containing multiple metabolite peaks, obtained from only 0.06 dpm injected onto the HPLC column. To put this into context, this is approximately 3,000-fold lower than could be achieved using a scintillation counting approach, such as Topcount (Bruin et al., 2006). Through analysis of the metabolite profiles generated against time after dosing, M9 was determined as being largely the causal agent for the protracted elimination profile, demonstrating predisposition for this metabolite to accumulate upon repeat dosing. Despite the slow elimination of M9 (and other metabolites of SB773812) sufficient cover in the toxicology species for the major active metabolite was demonstrated and the other major metabolites were well represented in both toxicological species.

The data provided evidence that the dog was the more relevant toxicology species for safety assessment of SB773812 and contributed to the position for validation of the toxicology species used in the safety assessment program for this drug under development.

3.2.4. Technical considerations and reflections

In addition to the clinical study described above, **Commentary paper 2** also described the first use of AMS in providing metabolite profile data from a clinical study where scintillation counting approaches did not provide sufficient sensitivity to deliver on the experimental objectives. The author termed the type of application of AMS to clinical experiments, where conventionally high doses of radioactivity were used (circa 3.7 MBq) and where many of the study objectives could be met using non-AMS approaches, as "hybrid LSC - AMS" studies.

These were distinct from experiments that were designed to be supported by AMS, for most endpoints by first intent, particularly during the transition stage when AMS was not well established for use in biomedical experiments. In the initial stages, where GSK had access to the AMS, studies were often designed without much consideration being given to the potential need to resort to the use of this technology, although this approach changed radically over time. In this study, the samples required dilution (by a factor of 25) as the ^{14}C concentrations were too high for more direct analysis by AMS, but were also too low in radioactive content to be analysed by alternative radiodetection methods. This provided useful experience in metabolite profiling by AMS. Through such work, our laboratory was able to establish the frequency with which to fractionate samples (a requirement for both metabolite profiling and individual analyte measurement by AMS; see Figure 10) to be able to reconstruct high quality chromatograms providing a suitable level of resolution. In this respect, it is important to be able to generate metabolite profiles that fully describe the range and quantity of metabolites present in any given sample so that the data can be used (along with metabolite identification) to build a thorough understanding of the ADME of the drug under test.

Through experience, fraction collections of one every 12 seconds for the whole chromatogram have become normal practice for separations by HPLC, when using a chromatographic mobile phase flow rate of 1 mL/minute. This has generally facilitated provision of very detailed chromatograms with sufficient resolution between closely eluting peaks to allow quantification of each individual, but particularly the major, drug-related component. It is worth pointing out that our laboratory have used **UPLC** less frequently as the methods transferred to our laboratory, for support by AMS, have been previously developed on HPLC systems. For metabolite profiling of clinical samples using detection by AMS, retention time comparisons need to be made with chromatograms generated from non-clinical samples and it is important to maintain consistency between the experiments carried out across the species since AMS does not provide structural identification of the analytes (other than ^{14}C:^{12}C content). If UPLC is used, with inherently shorter chromatographic separation times versus HPLC, more rapid fraction collections are required to maintain analyte peak resolution. At this time little data can be found in the literature which provides metabolite profiles generated using UPLC with detection by AMS, although there is evidence that UPLC is being used (Xu et al., 2012) and that the fractions analysed in at least one case (see Figure 1 of (Morris et al., 2015)) are not frequent enough to provide resolution of many of the individual drug metabolites present in the samples.

On occasion the frequency of collection has been increased in our laboratory to as many as one fraction every three seconds, but for a chromatographic run time of, for example 60 minutes per sample, this generates a logistically unmanageable number of samples for individual graphitisation (1200 fractions), which equates to about three working weeks of continual sample graphitisation for one scientist. This approach has only been used for special cases where there has been a need to improve resolution for a portion of the chromatographic run. Based on this experience, our group invoked the practice of not collecting all of the chromatogram in an effort to reduce the number of fractions that had to be graphitised (as was the case for profiling in this clinical study), but sometimes found that this led to a need for repeat of work and so was inefficient and not a thorough investigation of the samples. Calculation of recovery of drug-related material from the LC system is a necessity when the

percentage contribution of each component is converted to actual concentrations and to provide confidence that the chromatogram is suitably representative of everything drug-related that was present in the initial sample. Therefore, current practice is typically for all fractions to be collected for subsequent analysis by AMS, which increases the initial work load, but often reduces the requirement for re-analyses.

The sample preparation described above is extremely labour intensive and thus makes the desire for a more on-line LC-AMS approach very appealing (Thomas et al., 2013) (see section 1.4). In contrast to this, especially early on in the use of AMS for such biomedical investigations, other scientists in the field used relatively infrequent fractionation such as only one fraction for every 30 seconds, or even one per minute (Buchholz et al., 1999), (Garner et al., 2002). This led to a loss of resolution and, in the author's opinion, a reduction in overall quality of the data through poor definition of peak retention time and quantity of each individual component. However, such practices were to some degree understandable as the costs associated with analysis of large numbers of samples by AMS were (and still are) often seen as prohibitive, or resource use inefficient. Over time, the practices that were established in our laboratory, as in Figure 10, have become more commonly applied across the biomedical AMS field in such experiments (eg. (Lee et al., 2016)).

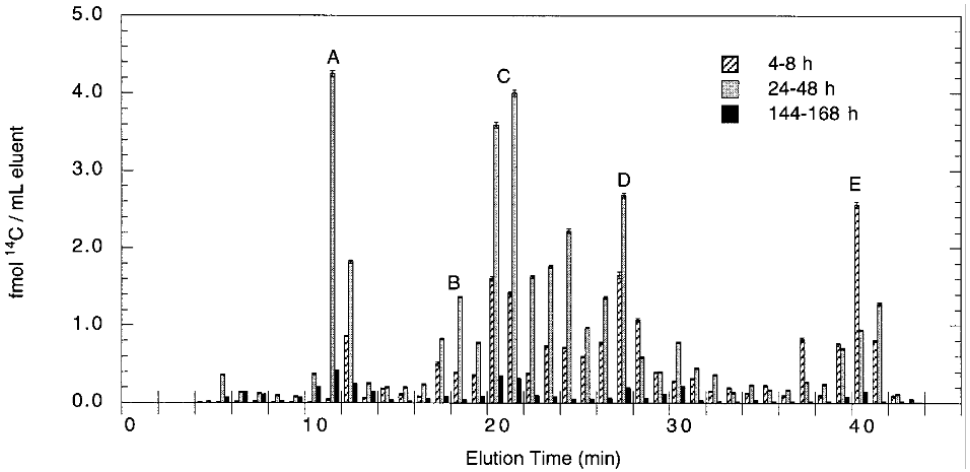

(a) **Reproduced from Buchholz et al., 1999*** – fractions collected only once every minute leading to generation of a histogram.

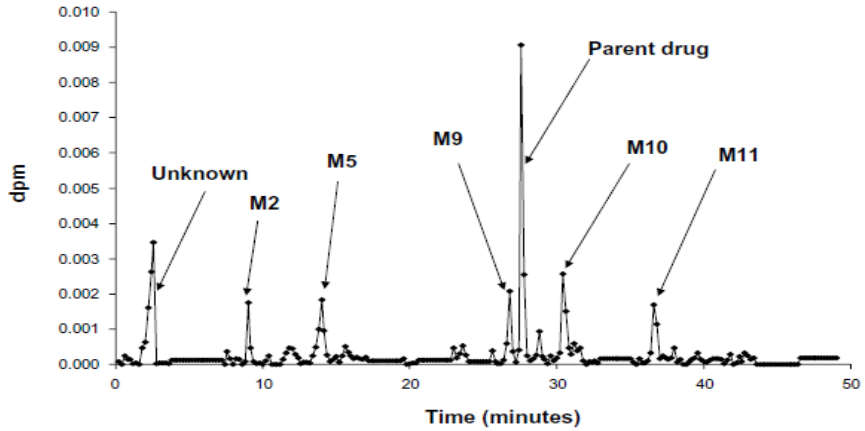

(b) **Reproduced from Commentary paper 2** – fractions collected every 12 seconds leading to generation of a detailed reconstructed chromatogram.

Figure 10. Comparison of fraction collection frequencies.

* Reprinted with permission from BUCHHOLZ, B. A. *et al.*, Copyright (1999) American Chemical Society.

In **Commentary paper 2**, this author put forward the potential that automation of the graphitisation process may be developed as a path towards higher throughput analysis. This has not materialised in any tangible and significant way (there is a low throughput automated approach which is commercially available, but is targeted at carbon dating laboratory use with preparation of up to only 21 samples per day; the Automated Graphitisation Equipment (Ionplus, 2016)). Instead, as stated earlier, advances have been made to increase throughput via direct gas interfacing of an elemental (usually termed CHN) analyser, to the AMS (van Duijn et al., 2014). This is a promising approach, but is still in the early phases of adoption.

Commentary paper 2 encompasses a number of different experiments spanning eight years of application of AMS to non-clinical (in vitro and animal) and clinical investigations. These works defined the reach of AMS in drug development and also provided focus on where it could add most value as an enabling technology. There were instances when AMS was applied where the decision to do so was perhaps questionable (eg. in vitro metabolism assessments at extremely low concentrations (data on file at GSK)), but in any case the experiences gained were used to design improved experiments that followed, with definition of frequency of fraction collection being a good example of that. AMS was usually applied in these experiments because the drug was potent and therefore would be low dose, providing a challenge to sensitivity limits for conventional detection methodologies.

3.3. Commentary paper 3

Bowers, G. D., D. Tenero, P. Patel, P. Huynh, J. Sigafoos, K. O'Mara, **G. C.Young**, E. Dumont, E. Cunningham, M. Kurtinecz, P. Stump, J. J. Conde, J. P. Chism, M. J. Reese, Y. L. Yueh and J. F. Tomayko (2013). "Disposition and metabolism of GSK2251052 in humans: a novel boron-containing antibiotic." Drug Metab Dispos **41**(5): 1070-1081.

3.3.1. Objectives

1) To determine the rates and routes of excretion of a novel boron containing NCE, GSK2251052 (AN3365), following oral administration to healthy volunteers.

2) To determine the biotransformation pathways for GSK2251052 in humans.

3) To investigate the utility of AMS to provide systemic exposure data supplemental to that provided by LSC.

3.3.2. Clinical study design

The study involved a high dose of 1500 mg ^{14}C-GSK2251052 (0.6 MBq) by the intravenous route (driven by the high predicted therapeutic dose) as outlined in Figure 11 and necessitated support by AMS for analysis of late timepoint plasma samples. The intravenous route was used as this drug was intended for treatment of systemic infections in a critical care setting. The high sensitivity of AMS was required due to the anticipated low concentrations of drug-related material in plasma and the low specific activity of the dose (the radioactive dose was towards the low end of a conventional dose of ^{14}C to humans (commonly 3.7 MBq is administered)).

In a previous ADME study with ^{14}C-GSK2251052 in the rat, excretion of radioactivity was not complete with evidence of melanin binding of drug-related material through

retention in the uveal tract of the eye, to 840 hours after dosing (unpublished material). The resultant dosimetry calculations then limited the radioactive dose in humans to 0.69 MBq, so as not to exceed the 100 µSv regulatory limit (lower end of Category IIa, ICRP 1992; see Appendix 10).

In this clinical study, there was an apriori extended excreta collection period of 14 days since the radioactive dose was too low to allow the assessment of excreted radioactivity to be used as release criteria for the volunteers – normal practice in a mass balance study. There was an objective to obtain a thorough understanding of the systemic exposure to drug-related material, particularly as some concerns existed about the potential mechanism for retention arising from the novel mechanism of action for this drug (Mendes et al., 2013) (binding of the cycloboronate ring to inhibit the bacterial enzyme, Leucyl tRNA synthetase, which prevents protein synthesis and thus bacterial growth).

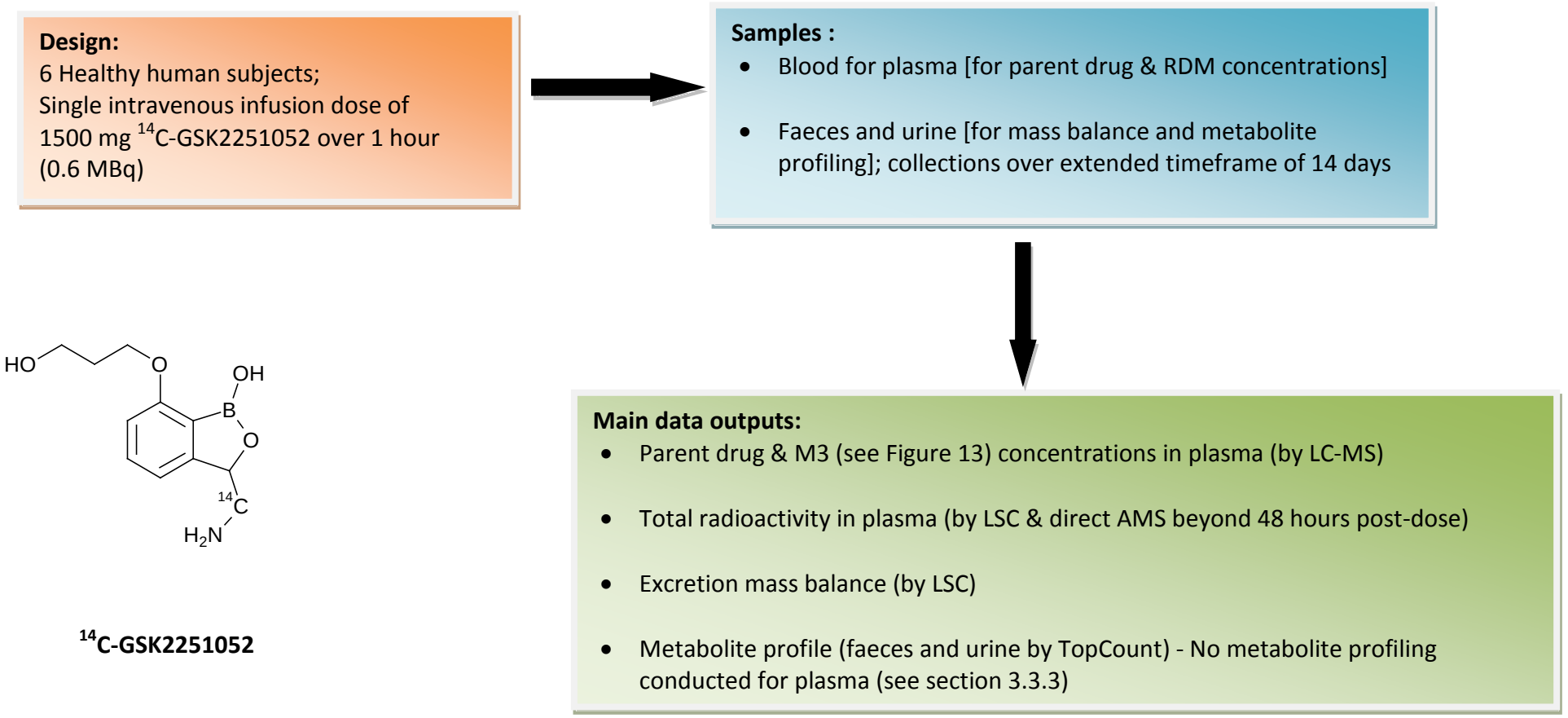

Figure 11. Schematic of clinical study design 3.

3.3.3. Clinical study data output and impact

AMS was used for the analysis of late timepoint blood plasma samples, where the amounts of ^{14}C had reduced to below the lower limit of quantification (870 ng GSK2251052 equivalents/mL of plasma; 20 dpm/mL) for analysis by LSC. Good concordance was observed between the data provided through use of LSC for early timepoints (plasma analysis), and of AMS for analysis of samples at later timepoints as shown in Figure 12.

The total radioactivity data were compared to liquid chromatography with mass spectrometric detection (LC-MS) data for parent drug and a particular individual non-active metabolite, M3 (oxidation of GSK2251052 to a carboxylic acid metabolite; see Figure 3 of the paper and Figure 13 in this commentary).

Systemic concentrations of total radioactivity closely aligned to the sum of the systemic concentrations of parent drug and M3, thereby indicating that no significant quantities of other metabolites were present. Further to this, parent drug elimination half-life in plasma was defined as being much shorter (11.6 hours) than for total radioactivity, i.e. parent drug and metabolite(s) (96 hours). This longer half-life for RDM, largely driven by reduced **clearance** (see Table 1 in the paper), was similar to that of the M3 metabolite (~77 hours) and it was therefore not necessary to conduct further metabolite profiling analysis on plasma samples. This significantly reduced the resources/costs that were required to support the study.

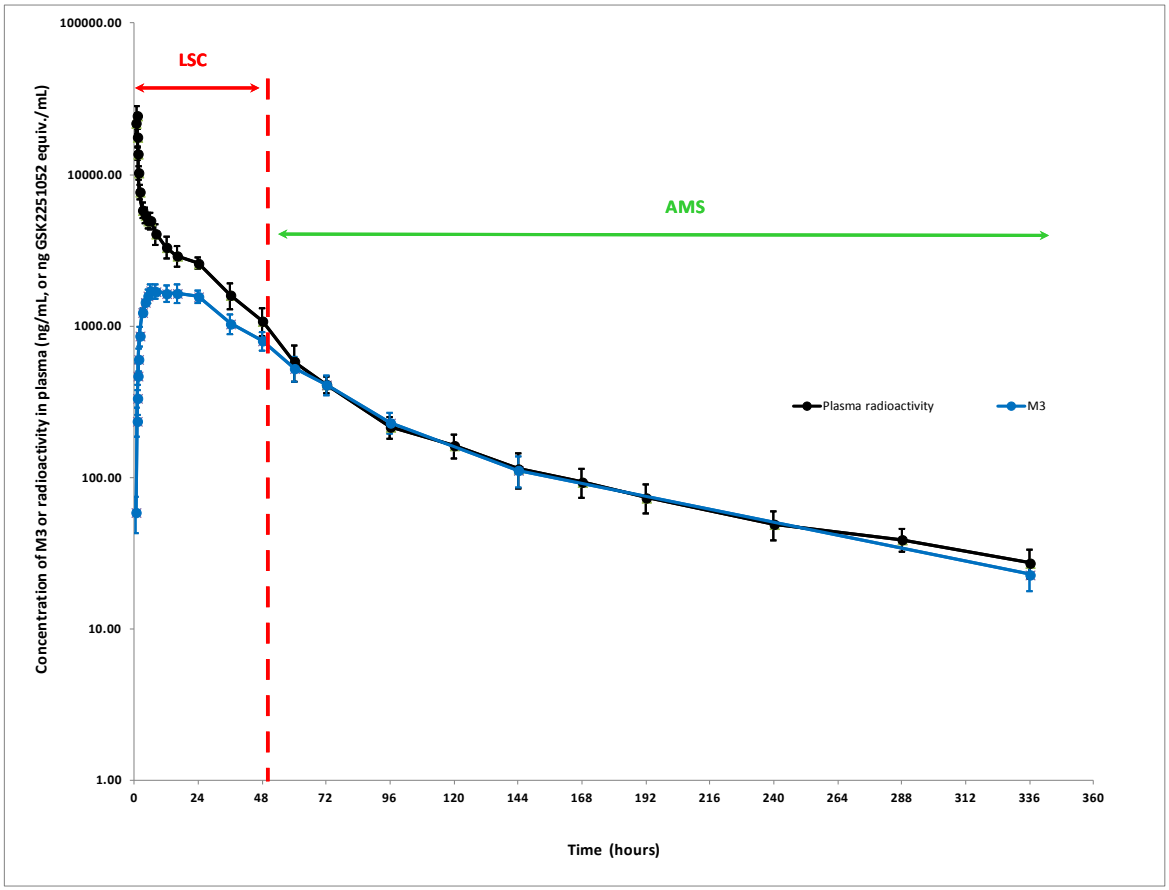

Figure 12. Concentration- time plot showing the transition from LSC data to AMS data for total radioactivity in plasma.

(Adapted from Figure 3 in **Commentary paper 3**, with addition of error bars and indicators of analytical technique applied).

Mean (n=6) plasma concentrations of metabolite M3 (●, ng/mL) and total plasma radioactivity (●, ng GSK2251052 equivalents/mL).

Left of the vertical dashed line, plasma radioactivity concentrations were measured using LSC (before 48h). Right of the dashed line, the plasma radioactivity concentrations were measured using AMS (48 hours and later). LoQ for the LC-MS specific assay for M3 was 5 ng/mL ; LoQ for AMS for total radioactivity was 27.2 ng GSK2251052 equivalents/mL.

Good mass balance was achieved (95% (range from 92.7 to 99.9%) within 192 hours, 8 days) with the majority of excretion of RDM via the urine (a mean of 87.4% of the dose). GSK2251052 was eliminated both as unchanged drug in the urine (it was absent from faeces) and as metabolites, with the M3 as the only other major RDM present in urine. There was nevertheless, continued excretion of radioactivity into the urine throughout the 14 days of collections (see Figure 4 in the paper showing only M3 present in the later timepoint (120 – 336 hours) pooled urine sample), consistent with the long half-life of the M3 metabolite in plasma.

This type of information (overall body burden to drug-related material) is important as it provides knowledge from which assessments of likelihood for accumulation of drug and metabolites can be determined upon repeated administration (i.e. the marked differences between clearance of parent drug versus RDM in this case highlight the need for this knowledge).

The paper also investigated the mechanism of formation of the major metabolite, M3. Alcohol dehydrogenase and aldehyde dehydrogenase were implicated in the formation of M3 via in vitro and in vivo experiments. Both of these are **polymorphic** enzymes so there is an inherent risk associated with variability in extent of metabolism across individuals (Eriksson et al., 2001). These risks need to be considered as lack of antibiotic efficacy could occur in some patients, e.g. in the case of subjects who are extensive metabolisers of GSK2251052 (to M3). An example population may be alcoholics who have induced levels of ALDH due to ethanol abuse (Nilius, 1983).

Unfortunately, around the time of conducting the human ADME study, antibiotic resistance issues occurred in the clinic in a separate efficacy study for GSK2251052, which precluded further development of this molecule and so further mechanistic studies were abandoned.

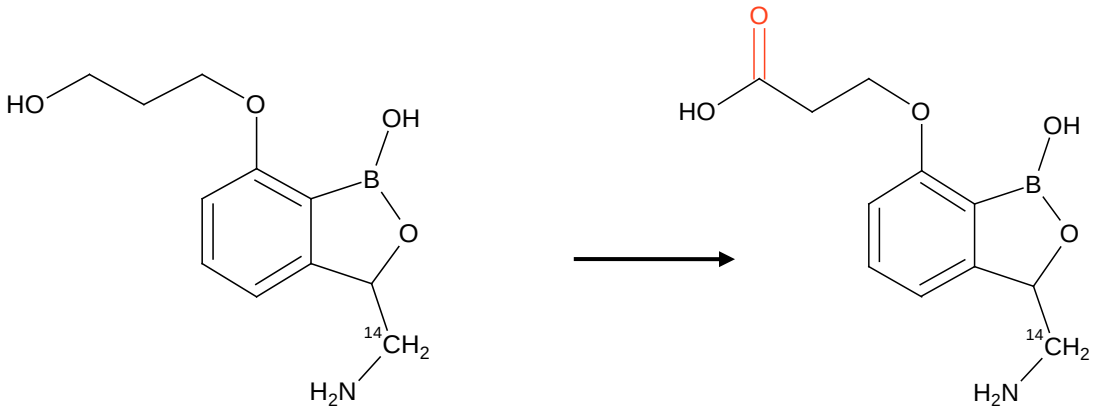

GSK2251052 **M3**

Figure 13. Biotransformation of GSK2251052 to M3 (carboxylic acid metabolite of GSK2251052).

The structures show the position of the ^{14}C-label.

3.3.4. Technical considerations and reflections

As can be seen from Figure 12 above, taking into account variability around the independent sample analysis conducted for the specific LC-MS assay of the M3 metabolite and the direct analysis by AMS for total radioactivity (as indicated by the error bars), the mean data from both data sets from around 72 hours after dosing is close to superimposable, justifying the decision made not to conduct metabolite profiling on the plasma samples, as mentioned above.

The total radioactivity data from analysis by direct AMS from this study led to development of our approach to defining the LoQ for radioactive drug related material in plasma, based upon specific activity of the drug being investigated. This was achieved by measurement of endogenous radiocarbon from control blood plasma taken from 25 individual subjects and a statistical definition was made of confidence intervals for ability to discriminate drug-related material from background radioactivity. It was established that the LoQ for drug related material could be defined at concentrations ≥15% above background with 99% confidence, or ≥10% with 95% confidence, thus the default position became the former in most cases. This LoQ assessment is in broad agreement with the work of other laboratories ((Keck et al., 2010) and direct communication with Xceleron Ltd.). The practice established in our group, of taking multiple predose plasma samples (one at screening of the subjects, one pre-study on Day -1 and one on Day 1 of the study), served to re-enforce the assurity of background radioactivity measured in each human subject. Note that the accepted LoQ definition for LSC is more empirically determined (see section 1.3).

The LoQ, which is expressed in dpm/mL of plasma, could then be converted into the units of drug equivalents per volume of plasma using the specific activity of the drug dose (e.g. expressed in units of dpm per picogram) to provide an LoQ in a comparable manner to other analytical techniques such as LC-MS, rather than in dpm as is the normal practice for LSC (see section 1.3).

3.4. Commentary paper 4

Harrell, A. W., S. K. Siederer, J. Bal, N. H. Patel, **G. C. Young**, C. C. Felgate, S. J. Pearce, A. D. Roberts, C. Beaumont, A. J. Emmons, A. I. Pereira and R. D. Kempsford (2013). "Metabolism and disposition of vilanterol, a long-acting β(2)-adrenoceptor agonist for inhalation use in humans." Drug Metab Dispos **41**(1): 89-100.

3.4.1. Objectives

1) To determine the rates and routes of excretion of vilanterol (a potent, low dose long acting β2-agonist NCE for inhalation use), following oral administration to healthy volunteers.

2) To determine the biotransformation pathways for vilanterol in humans.

3) To examine the utility of AMS and duodenal bile collection to investigate biliary elimination of vilanterol in humans following an oral dose administration.

3.4.2. Clinical study design

The accepted practice for assessment of ADME in humans for inhaled therapies is through administration of ^{14}C-labelled drug by surrogate routes, such as intravenous or oral administration. There is precedent for the administration of ^{14}C-labelled drug by inhalation to humans (Affrime et al., 2000), but it is fraught with logistical difficulties, not least being the fact that a dry powder of material incorporating the labelled drug is likely to be different in terms of physical properties, such as crystalline form and particle sizes from the marketed (non-labelled) medicine.
The intravenous route is a surrogate for systemic exposure to drug related material absorbed via the lung and the oral route represents the majority of the dose swallowed and delivered to the gastrointestinal tract from an oral inhalation dose (see section 4.1.2).

The intravenous route was not used in the human ADME (excretion balance) study for vilanterol due to radiolytic instability over the period required for manufacture and release of the dose*. This study, depicted in Figure 14, therefore involved administration of vilanterol by the oral route only. It is accepted that oral administration will not entirely represent the same rates and routes of ADME as per the entire dose administered by oral inhalation, but nevertheless it is accepted as a practically feasible surrogate approach by regulatory authorities for human ADME studies of inhaled therapies (Hughes et al., 2008), (Kagan et al., 2012).

Autoradiolysis was found to be reduced through use of lower specific activity material, so although the therapeutic dose of this drug was predicted to be 25 µg, a higher total dose of ^{14}C-vilanterol of 200 µg [74 kBq] was used in the human ADME study (see section 3.4.4 for further explanation of the reason for choice of dose). Existing safety information, from prior toxicological and clinical studies, supported the administration of the supra-therapeutic dose of 200 µg of vilanterol to humans.

* Stability for up to two weeks was required. Note that through the newer approach of **parametric release** , stability and sterility assurance for only 24 hours is required.

Design:
6 Healthy human subjects;
Single oral dose of 200 µg ^{14}C-vilanterol (74 kBq)

Samples :

- Blood for plasma [for parent drug, RDM concentrations & metabolite profiling]
- Faeces and urine [for mass balance and metabolite profiling]
- Duodenal bile [for metabolite profiling]

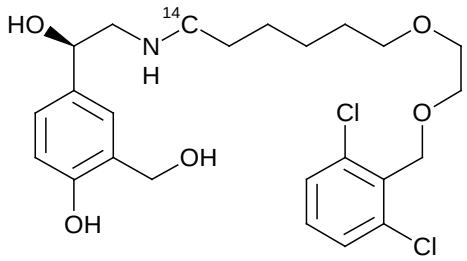

^{14}C-vilanterol

Main data outputs:

- Parent drug concentrations (by LC-MS)
- Total radioactivity in plasma (by direct AMS)
  - Derivation of pharmacokinetic parameters in plasma [very limited for parent drug*]
- Excretion mass balance (by direct AMS)
- Metabolite profiles (plasma, urine, faeces [bile not reported (see section 3.4.4)]; by LC+AMS and LC-MS); in vitro assessment of pharmacological activity of metabolites

Figure 14. Schematic of clinical study design 4.

* Due to most concentrations being <LoQ of the specific LC-MS assay.

3.4.3. Clinical study data output and impact

To estimate the extent of **first pass metabolism** of a drug in humans*, one approach is to compare the unchanged parent drug concentration with RDM in plasma, at an early sample timepoint following oral administration. The choice of timepoint is a matter of judgement, but it should be late enough that the drug has had time to undergo significant absorption, but insufficient time to be metabolised in the systemic circulation. Minimal first pass metabolism is indicated if the RDM and the parent drug are present at very similar concentrations, whereas a notable difference between parent and RDM concentrations is indicative of first pass metabolism.

The assumption is that first pass metabolism occurs either in the wall of the gastrointestinal (GI) tract, in the liver before the drug reaches the systemic circulation, or a combination of both. However, there are a number of caveats to this assumption:

1) that the drug was stable in the GI tract prior to absorption (e.g. metabolism by the gut microbiota, or facile degradation in stomach acid were not significant.

2) that systemic metabolism is not exceptionally rapid.

3) that the incorporated radioisotope was in a position stable to metabolism, so that the core of the molecule is traced (see section 1.2).

* The importance of understanding the extent of first pass metabolism of the drug and indeed drug metabolism by the liver in general is discussed later (see section 4).

Notwithstanding these points, it is generally recognised that comparison of parent and RDM early in the absorption phase of a concentration-time profile gives a reasonable estimate of the magnitude of first pass metabolism (Lappin and Garner, 2005).

In the case of vilanterol, at 30 minutes after dosing the mean concentration of the RDM in plasma was 935 pg vilanterol equivalents/mL (SD of 323 pg vilanterol equiv./mL), whilst parent drug was at a mean of only 2.3 pg/mL (SD was not calculated as vilanterol concentration was >LoQ in only one individual sample) or <0.5% of the circulating drug-related material as highlighted in Figure 15.

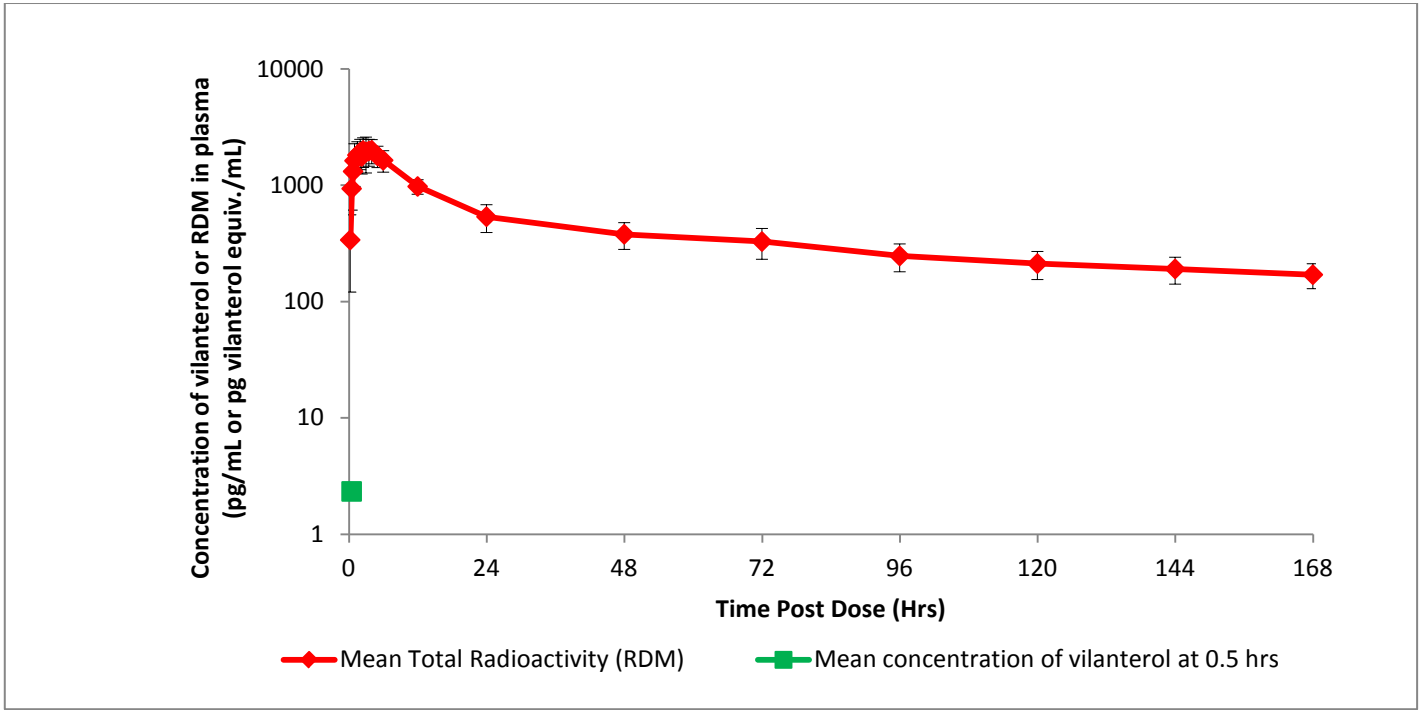

Figure 15. Mean concentrations (n=6) of vilanterol and total radioactivity in plasma after oral administration of ^{14}C-vilanterol to humans.

(Adapted from Figure 2 in **Commentary paper 4**, with the addition of error bars.)

The difference in mean plasma concentrations of radioactivity (pg vilanterol equiv./mL) versus concentrations of unchanged vilanterol (pg/mL) are highlighted on this concentration–time semi-log plot. Note that the vilanterol data represents a quantifiable concentration in a single subject (at 14 pg/mL) at 0.5 hours after administration i.e. for five of the six subjects the concentrations were below the LoQ and treated as being zero for the purpose of representation of the mean data (2.3 pg/mL).

Additionally, in the mouse and rat, following oral administration of vilanterol, concentrations of unchanged parent drug were determined from samples taken from the cannulated hepatic portal vein (HPV) and compared to those of parent drug in plasma from the systemic (SYS) circulation (cardiac puncture) (see cartoon of first pass effect assessment in the rodent, through analysis of HPV and SYS samples; Figure 16). These investigations showed significantly higher concentrations (> 10-fold) of vilanterol in hepatic portal vein plasma, at 15 minutes after dosing, indicating extensive first pass metabolism in these species (GSK internal reports). Additionally, **intrinsic clearance** of vilanterol was very high in human liver microsomes in vitro and moderately high in microsomes prepared from the gastro-intestinal mucosa (GSK internal reports). The commentary paper (Figure 5E) also shows that incubation of vilanterol with human hepatocytes in vitro resulted in complete metabolic turnover of vilanterol to metabolites. All indications were therefore that vilanterol underwent significant first pass metabolism, including following oral dosing to humans. This is of significance for vilanterol, as the extensive pre-systemic metabolism to inactive metabolites reduces the propensity for it to cause off-target side effects, including tachycardia, since the concentrations in the systemic circulation are very low indeed.

A low mass balance of ^{14}C-recovery was obtained for the clinical study (mean of ~72%, SD of 4.4%), although the overall reason for the low recovery was not clear. In the paper, several arguments for the low recovery were presented, including technical limitations related to the low radioactive dose. The most likely reason, in this author's opinion, is the fact that there were measurable concentrations of above background radioactivity in plasma at the end of the collection period (168 hours), i.e. elimination of drug-related material was not complete. There was a long terminal elimination half-life for total radioactivity (in excess of a mean of 146 hours; CV of 15%), which was not stated in the paper and yet excreta samples were only collected for 7 days after dosing. The implication then is that near complete ^{14}C-recovery was never likely to be achieved with this excreta collection period.

As stated in the paper and in a supporting reference of historical mass balance data (Roffey et al., 2007), incomplete mass balance is common with an expectation that 80% or greater is generally recovered using routine methodology, but it is recognised that the methodology used for this study could not be described as routine, as outlined i.e. low radioactive dose and use of AMS.

The data obtained (see **Commentary paper 4**) showed that metabolite profiles could be provided by AMS, even for such a low dose of drug to human subjects. The major metabolites observed in humans were appropriately present in the non-clinical species used in the safety evaluation of vilanterol, providing validation of the toxicology species used in development of this drug. This study highlighted the complications associated with determining the human ADME for potent low dose drugs for inhalation. Nevertheless, mitigation of any concern around the poor mass balance ^{14}C-recovery was the low therapeutic dose of vilanterol.

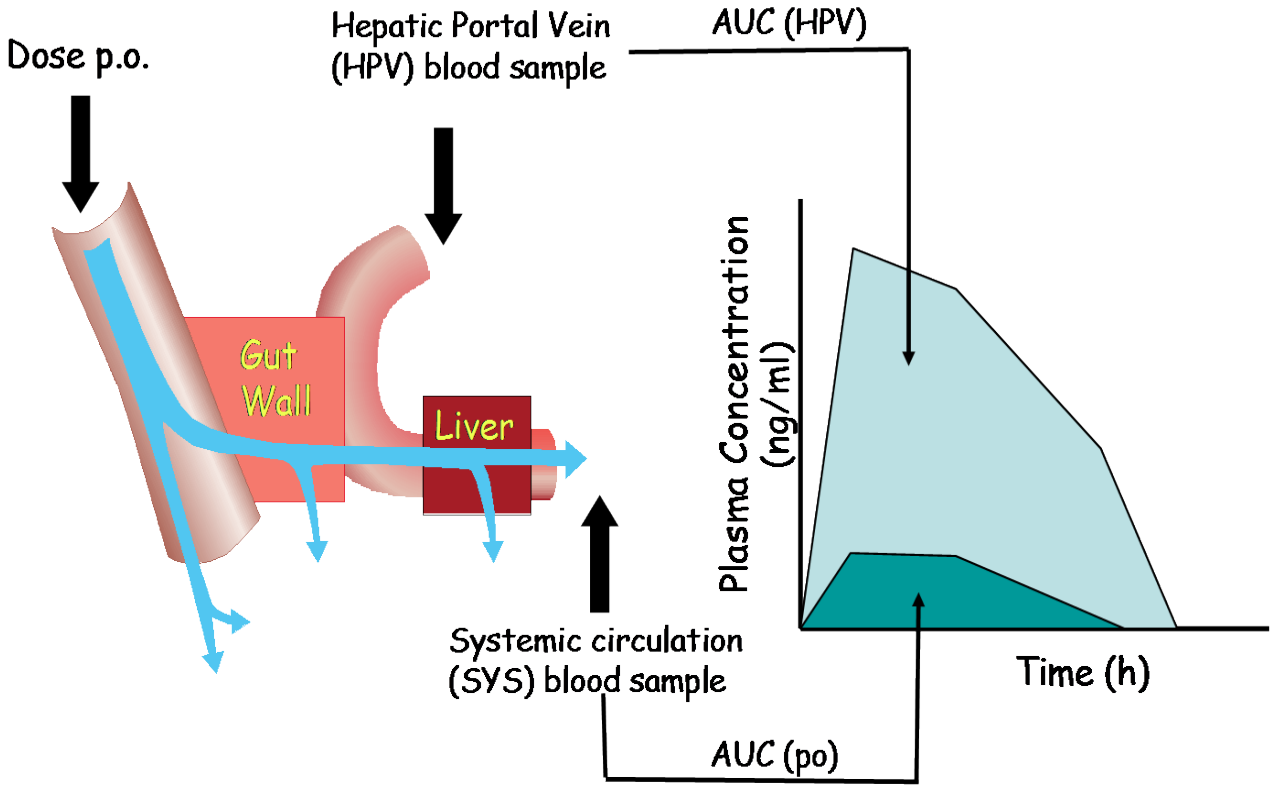

Figure 16. Cartoon of sample analysis and exposure assessment in the rodent before and after first pass through the liver*.

* With permission from GSK.

3.4.4. Technical considerations and reflections

The major objective of an ADME study destined for submission to the regulatory authorities is to identify rates and routes of metabolism of the drug under test in humans. Discovery of any metabolites unique to humans would be the outcome of major concern for this investigation. However, the extremely low therapeutic dose for vilanterol, along with existing clinical safety data (GSK, 2016) and independent monitoring of several specific metabolites (using LC-MS assays) of known on-target potency in other clinical trials, may have been expected to negate the need for a human ADME study. This, however, was not the view of at least one regulatory authority, so this study was designed to provide an increased level of understanding of the ADME-PK of vilanterol in advance of regulatory approval of the marketing application for this medicine.

The supra-therapeutic dose of 200 μg (with associated lowered specific activity) that was selected for this study was chosen by the GSK clinical study team. At the outset in the planning of the study, this author proposed that the study could be conducted at the therapeutic dose (25 μg, even with the dose of lowered ionising radiation) and that study objectives would still be met, but on this occasion that opinion was not supported by others in the clinical study team. This highlights one of the challenges of collaborating with scientists who are unfamiliar with the AMS technology. As experience with the AMS technology grows across the pharmaceutical industry, such arguments will be easier to make in the future.

Until recently, it was common practice in drug development to limit biliary elimination data to the rat and less commonly from other species. This is because bile duct cannulation surgery is required which is amenable to the rat, but difficult to ethically justify in the dog and particularly in the monkey. Data on biliary excretion in humans was almost always absent and assumptions were made from extrapolation purely from the rat. The likelihood of a compound being excreted in bile is in part related to its molecular weight and the threshold above which this is more likely, than via renal elimination, varies across species (Hirom et al., 1972). Other factors, including active

transport, further complicate prediction from animals to humans (Fagerholm, 2008) as there are notable species differences in transporters (Chu et al., 2013). It is potentially concerning that the only data pertaining to biliary excretion therefore comes from the rat, even though it is well known that these data could be misleading when applied to humans. In some cases, analysis of faeces may provide some insight to biliary elimination in humans, but this may also be misleading if metabolites are formed by gut microflora. In addition, metabolites formed in the liver and eliminated in bile can undergo further metabolism before excretion in the faeces, or they can be reabsorbed and be absent from the faeces altogether.

Sampling of human bile was historically difficult to justify to provide a wider understanding of this route of elimination of drug related material in humans due to the invasive nature of the sample collection (Lennernas et al., 1992). Several studies recruited healthy volunteers who have been fitted with oroenteric tubes, which facilitate the sampling of duodenal bile. The majority of these studies used an adaptation of the Loc-I-Gut technique (Lennernas et al., 1992). Nevertheless, the technical difficulty in sampling directly from the gallbladder or duodenum, not to mention high study running costs and the need for suitably qualified personnel, means that the studies are very rarely conducted.

The vilanterol study applied a new approach to the collection of human duodenal bile using the Entero-test™ string, which has developed from seminal work conducted at GSK (Guiney et al., 2011). The Entero-test™ is comprised of a weighted (steel ball bearing) and adsorbent nylon string, inside a gelatine capsule. The proximal end of the string is attached to the cheek of the subject and the capsule is swallowed. The capsule dissolves in the stomach and the string reaches the duodenum. Contraction of the gall bladder is induced by a small food stimulus and a small portion of the bile (~1mL of the total volume which is likely between 350 and 600 mL per day (Boyer and Bloomer, 1974), (Davies and Morris, 1993), dependent on, for example, food intake), is adsorbed onto the string. The string is then retrieved through the mouth and the bile collected for later analysis (the ball bearing becomes unattached and passes through the gastrointestinal tract).

Biliary secretion is a potentially major route of elimination of drugs and their metabolites from the body. As a result, elimination of compounds by this route can impact the systemic exposure, toxicity and pharmacological effects of drugs. In the absence of knowledge around the biliary disposition of a drug, the relative importance of different routes of metabolism and their relationship to overall clearance may be misinterpreted. This makes the non-invasive Entero-test™ string approach a very attractive proposition for DMPK scientists to be able to gather this kind of information for new drugs in development. It should be noted however, that Entero-test™ results in a single bile sample per subject and although it provides qualitative information on biliary metabolites, it does not provide data on the magnitude or kinetics of biliary elimination. This type of information is best attained via an intravenous administration of drug (further detail provided below).

In the case of the vilanterol study, very little information was gained from the Entero-test™ approach, which is in part likely due to the complications of the low dose and the oral dose route being used (potential for contamination of the bile with drug swallowed into the gastrointestinal tract). However, there have been several experiments where the Entero-test™ approach has been more successfully applied in clinical studies. In the human ADME study for GSK2140944, gepotidacin, a bacterial topoisomerase inhibitor (a new class of antibiotic), strings collected following intravenous administration were analysed in our laboratory (Negash et al., 2015). The data obtained, as shown in the metabolism pathway schematic in Figure 17, indicated that the predominant metabolite present in faeces (M2) was not the same as that observed in bile (M4). In fact, the data indicate that the metabolite M2, present in faeces, was likely due to hydrolysis of M4 (the major circulating metabolite of GSK2140944) by gut microbial activity, and this was subsequently not detected by metabolite profiling of faecal samples. This clearly demonstrated the value of insight provided by analysis of the human bile, which otherwise would have been lost in the assessment of metabolite burden.

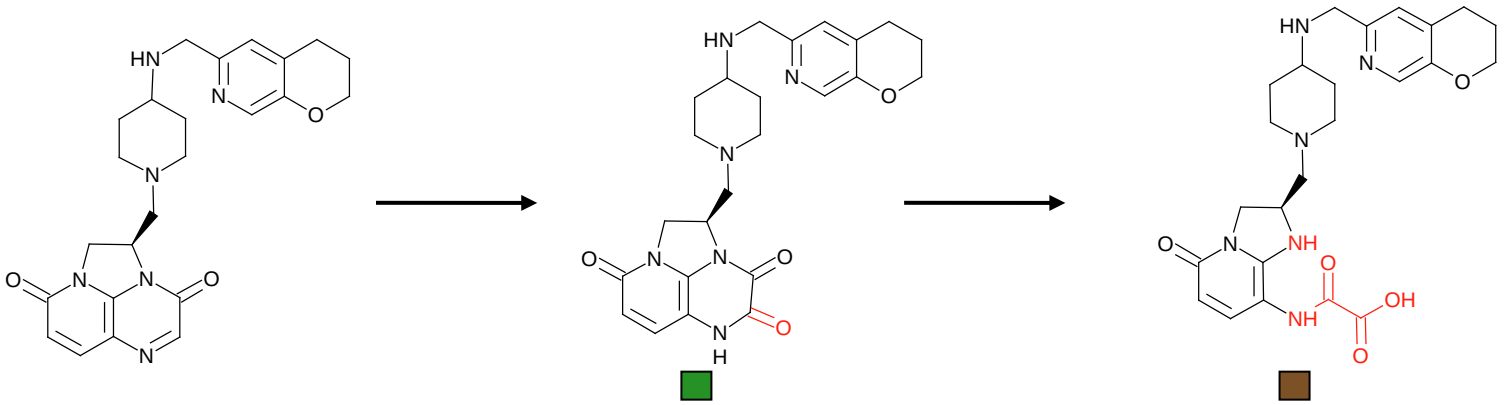

Figure 17. Biotransformation of GSK2140944 to M4 (oxidative metabolite of GSK2140944) and M2 (hydrolysis product of M4) in human*.

Major metabolite in duodenal bile
Major metabolite in faeces

* Structures reproduced with permission from NEGASH, K., *et al.*, 2015, with addition of bile and faecal major metabolite indicators.

The Entero-test™ approach has been used by our laboratory in other human ADME or early microtracer studies for drugs in development ((Mamaril-Fishman et al., 2014) and unpublished works), where this has proven to be very valuable in elucidating routes of metabolism, such as direct glucuronidation of parent drug. In such instances, had only faeces samples been analysed the significance of such metabolic routes and the metabolite burden to the humans would not have been fully understood. This is because the glucuronide is converted back to the aglycone (parent drug) in the gastrointestinal tract (Hawksworth et al., 1971), meaning that the parent drug rather than the metabolite would have been observed in faeces.

As highlighted above, several of these investigations demonstrate the value of the Entero-test™ method in providing a contribution to the overall understanding of ADME of the drug. The approach is particularly useful when combined with a radioactive dose administered intravenously, as there is no complication from the potential contamination of the bile sample due to unabsorbed dose, as can be the case when it is administered by the oral route, i.e. any drug-related radioactivity detected on the string has to be present due to biliary elimination of drug-related material. It is also noteworthy that the sensitivity of the AMS enables study designs and analyses that would otherwise be impossible to achieve; the bile sample volume collected represents a very small proportion of the total volume excreted and hence there is a low amount of drug-related material present (assuming biliary elimination of drug-related material occurs), providing a challenge for detection by other means.

With current knowledge of the microtracer approach (see an in depth explanation of the principles of this in section 3.6) it is possible that administration of vilanterol by the intravenous route for the human ADME study could have been attempted. Dosing by the intravenous route would have provided information on pre-systemic metabolism through comparisons that could be made to data from the metabolite profile following oral dosing. This would have enabled deconvolution of metabolism in the systemic circulation from that due to first pass metabolism following oral administration. In fact, **Commentary paper 4** overstates the surety of the extensive nature of first pass metabolism in the absence of this information.

3.5. Commentary paper 5

Dave, M., M. Nash, **G. C. Young**, H. Ellens, M. H. Magee, A. D. Roberts, M. A. Taylor, R. W. Greenhill and G. W. Boyle (2014). "Disposition and metabolism of darapladib, a lipoprotein-associated phospholipase A2 inhibitor, in humans." Drug Metab Dispos **42**(3): 415-430.

3.5.1. Objectives

1) To determine the rates and routes of excretion of an NCE, darapladib, following single intravenous and single and repeat oral (proposed therapeutic route) administrations to healthy subjects.

2) To determine the biotransformation pathways for darapladib following both routes of administration and following single and repeat oral administration in humans.

3) To utilise AMS to investigate the reason for altered pharmacokinetics of darapladib following repeated administration.

3.5.2. Clinical study design

Predictions of modelled systemic exposure, based upon the existing single oral dose elimination half-life pharmacokinetic data for darapladib (an inhibitor of lipoprotein-associated phospholipase A2) in humans indicated that repeat dose administration would result in significant accumulation (130-200%) in the systemic circulation. However, following repeated administration of darapladib at oral doses up to 80 mg once daily, concentrations in plasma were only 30-60% higher compared to those after a single oral dose. A likely hypothesis for this difference between the predictions and the subsequent clinical study data was that darapladib exhibited time-dependent

changes in its pharmacokinetics due to autoinduction of one or more of the enzymes involved in its metabolism, which then led to an increase in clearance of darapladib.

A human ADME study was therefore designed to include a test of this hypothesis i.e. to investigate the extent, if any, of metabolic autoinduction following repeat oral dose administration of darapladib.

The study, illustrated in Figure 18, was of a four stage cross-over design, as follows:

Stage 1: a single intravenous administration of 8 mg of ^{14}C-darapladib [1.85 MBq], followed by a minimum washout period of 21 days.

Stage 2: administration of a single oral dose of 80 mg of ^{14}C-darapladib [740 kBq], followed by a minimum washout period of 21 days.

Stage 3: administration of non-labelled darapladib as daily 160 mg doses for 14 days. The doses were given in the form of enteric coated tablets as this molecule was prone to degradation under acidic conditions, such as those of the stomach, to produce a potentially genotoxic species, 4-fluorobenzyl chloride (see Figure 19).

Stage 4: on Day 11 of stage 3, a single oral dose of 80 mg of ^{14}C-darapladib [740 kBq] was administered.

Design:
8 Healthy human subjects; cross-over – washout of 21 days minimum between the intravenous (stage 1) and oral dose (stage 2)

(1) Single 3 hour intravenous infusion dose of 8 mg ^{14}C-darapladib (1.85 M*Bq*)

(2) Single oral dose of 80 mg ^{14}C-darapladib (740 k*Bq*)

(3) Repeat oral [*cold*] doses of 160 mg for 14 days

(4) Single oral dose of 80 mg ^{14}C-darapladib (740 k*Bq*) [on Day 11 of stage 3]

Samples :

- Blood for plasma [for parent drug, RDM concentrations & metabolite profiling]
- Faeces and urine [for mass balance and metabolite profiling]

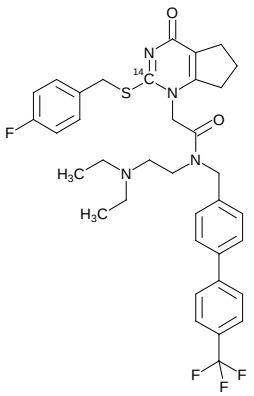

^{14}C-darapladib

Main data outputs:

- Parent drug & active metabolite (M4) concentrations in plasma (by LC-MS) following intravenous and oral administration
- Total radioactivity in plasma (by LSC [intravenous dose] and by direct AMS [oral doses])
  - Derivation of pharmacokinetics of darapladib in plasma following single intravenous and single and repeat oral doses
- Excretion mass balance assessment (by LSC)
- Metabolite profiles (plasma (by LC+AMS) & faeces (by TopCount); both routes and following single and repeat oral dose admin. Urine was not profiled due to <1% dose excreted by renal elimination*

Figure 18. Schematic of clinical study design 5.

* It is common practice to make a judgement as to whether to carry out metabolite identification and quantification of excreta samples based on the percent of the dose excreted by that route.

Blood samples (for plasma) and excreta samples (faeces and urine) were collected over time for stages 1, 2 and 4. All samples were analysed for total radioactivity by LSC or AMS as required. Plasma samples were additionally analysed by LC-MS specifically for parent drug and an equipotent pharmacologically active metabolite of darapladib (M4; SB553253), which is depicted in Figure 19, to further establish the relationships between systemic exposure to active drug-related material and clinical efficacy.

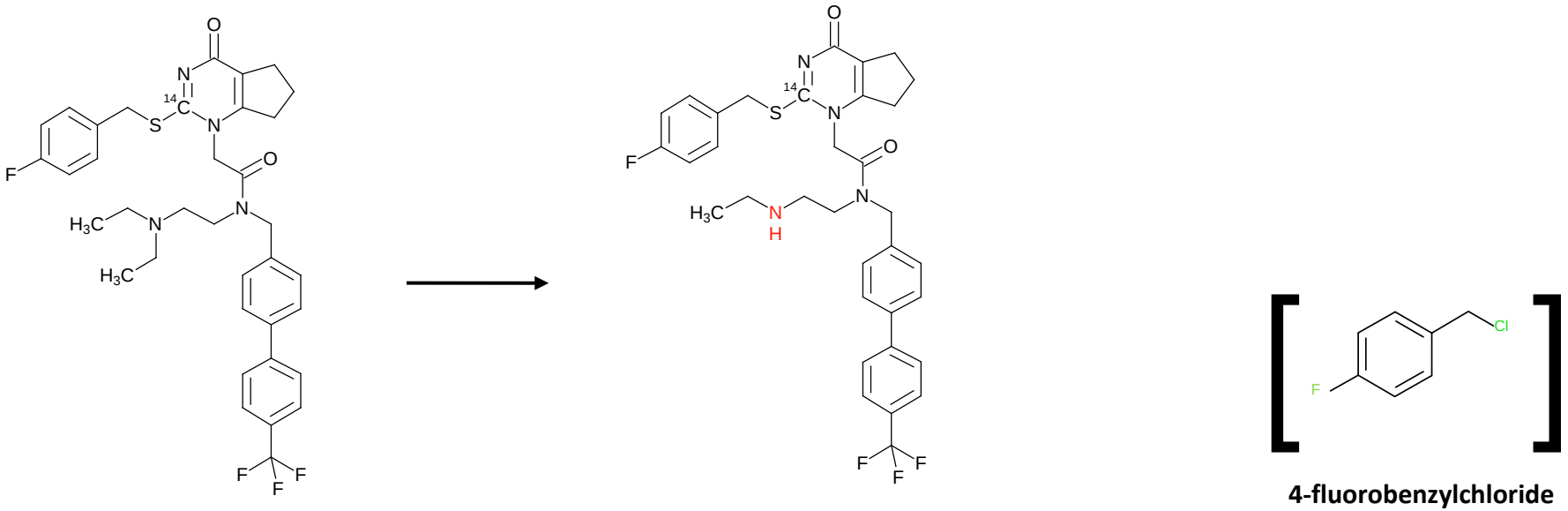

Darapladib **SB553253 (M4)** **4-fluorobenzylchloride**

Figure 19. Biotransformation of darapladib to SB553253 (N-desethyl metabolite of darapladib) & structure of 4-fluorobenzyl chloride.

The structures show the position of the ^{14}C-label, where present.

3.5.3. Clinical study data output and impact

This study was relatively complex in design, set out to assist with understanding of the pharmacokinetic properties and metabolism of darapladib following oral and intravenous administration and both single and repeated oral doses to humans. The mean mass balance recovery for oral ^{14}C-darapladib pulse dose administrations for stages 2 and 4 was >93% (SD of <8%) by 8 days after administration, whereas recovery was lower (mean of 86%; SD of 4.4%) at 21 days after intravenous administration (stage 1). Following oral darapladib dose administration, a large proportion of the dose was either unabsorbed or cleared via first pass metabolism. The slightly lower ^{14}C-recovery (within the timeframe of the excreta sample collections) following intravenous administration may result from these dose route differences and may be compounded by the potential sequestration of darapladib (a tertiary amine with a pKa of 8.4) into lysosomes by virtue of its physicochemical properties (Kaufmann and Krise, 2007) (i.e. darapladib is a cationic amphiphilic drug and has a very high **volume of distribution** of 833 L, indicating distribution into peripheral tissue compartments).

The retention of drug-related material (all ^{14}C dose stages of the study), combined with collection periods that did not allow full characterisation of concentrations of radioactivity in plasma to suitably late time points after administration, meant that extrapolated pharmacokinetics of total drug-related radioactivity could not be provided; e.g. extrapolation of **AUC** to infinity beyond the last time point sampled, would have been inappropriate, at >20% of the area under the drug concentration-time profile, and as such prone to error (EMA, 2001). The commentary paper did not explain the impact of this data absence, but this limitation is not critical for data interpretation as the AUC to the last timepoint provides an adequate assessment of the systemic exposure.

The intravenous dose was included as from animal study data (GSK internal reports) it was predicted that absorption in humans would be low. Therefore, if the study was

conducted with oral administration only, then analyses of faeces samples potentially containing unchanged parent drug would not help elucidate to what extent the parent drug had been absorbed prior to being excreted in faeces. The intravenous dose and metabolite profiling of the faeces samples from both routes of administration indicated that absorption from an oral dose was much higher (at ≥43 %) than previously believed. In fact, the metabolite profiling of faeces following intravenous administration showed a large proportion of intact parent drug to be present. This indicated that absorption could be even higher than established through analysis of faeces samples after oral administration, i.e. otherwise intact parent drug present in the faeces collected following oral dosing may have been assumed to be entirely from unabsorbed dose. This type of information is useful as it can, for example, guide dose formulation development if absorption was believed to be dissolution rate or solubility limited*, which was apparently not the case for darapladib.

In stage 1, the pulse dose of radiolabelled darapladib fully reflects the totality of the drug-related material present in the system (in this case the human) at the time of sampling. However, the pulse dose of radiolabelled drug in stage 4 of the study, following repeated oral **cold** dose administrations (stage 3) has a limitation in this regard, in that the drug-related material that is present in samples from the repeated doses of cold drug are not represented through calculation from the specific activity for the pulse dose. This has the impact that chemical mass equivalents of drug and metabolites cannot be calculated for this stage of the study. To explain this further, the administration of repeat doses of unlabelled drug causes an unquantifiable dilution of drug-related material in the systemic circulation, which makes it impossible to convert the radioactivity measurements to mass of drug equivalents. This design limitation in some regards makes the alternative design of repeat tracer doses of ^{14}C-labelled drug more attractive, as the isotopic dilution would not occur since there is no cold drug-related material present. This type of design has its own limitations, with the main one of these being that the doses of radiation have to be very low indeed for each dose administered, so as not to administer cumulative excessive ionising radiation doses to each individual subject.

* It must be borne in mind in the interpretation of the data however, that a solution dose is most often used in the human ADME study, rather than a solid dose formulation eg. tablet or capsule, which are more often the marketed form of the medicine.

The objective of understanding the reduced level of anticipated accumulation (as possibly caused by autoinduction) may have been compromised by discontinuation of the dosing of darapladib during the sample collection period in stage 4. The dosing did continue for some of that period, through days 12-14 following dosing of the ^{14}C-labelled darapladib on day 11, but not for the entire sample collection period. Discontinuation of the dosing of an inducer will result in dissipation of induction over time as illustrated by the prototypical inducer, rifampicin (Niemi et al., 2003), so it can be postulated that this may have occurred during stage 4 of this study. Assessment of accumulation is important in establishing repeat dose regimens for new medicines and in this instance it would appear that further investigations would be warranted to more fully investigate this phenomenon and any potential requirement for dose adjustment following repeated administration. Feasibly this could include analysis of the pharmacokinetics of darapladib following repeated administration, where the dosing is continued beyond the timeframe carried out in this study, i.e. there is no possibility of dissipation of any autoinduction.

The study showed that it was possible to generate a relatively high volume of data with provision of metabolite profiles for many chromatograms. However, as indicated above, the experiments failed to show clear evidence of enzyme induction (the metabolite profiles were very similar following each of the oral pulse doses in stages 2 and 4). In part, as indicated in the paper, it is possible that the need to use **time-adjusted proportional pools** to keep the resources involved to a reasonable level may have contributed to this inability to fully investigate the ADME-PK. However, the analyses did show reduction in drug-related material in plasma after the pulse dose of ^{14}C-darapladib in stage 4 ($AUC_{(0-t)}$ of 320 dpm.h/mL) versus that in stage 2 ($AUC_{(0-t)}$ of 420 dpm.h/mL). It is stated in the commentary paper that darapladib is a substrate of both Cytochrome P450 isoform 3A (CYP3A) and the efflux transporter **P-glycoprotein** (P-gp). It was thus postulated that the lowered systemic exposure to drug-related material in stage 4 may indicate lesser absorption of darapladib across the enterocytes after repeated oral dosing, combined with greater extent of first pass metabolism and/or efflux transport through induction of enzyme and/or efflux transporter activity.

Through the course of large scale clinical trials these types of findings would be further investigated via generation of pharmacokinetics upon long term administration of the new drug under evaluation. Additionally, both population pharmacokinetics in the presence of co-administered medications and specific drug-drug interaction studies would be used to further investigate propensity for inhibition and/or induction of the metabolism and transport of the drug, before and after it becomes a medicine (EMA, 2013).

The presence and quantification of potential human specific and **disproportionate metabolites** were highlighted in this study. This can have far reaching ramifications for a drug under development, such as the need for additional safety studies, including dosing of the metabolite to animals in extreme cases where safety cannot otherwise be established (FDA, 2008). In the case of darapladib, assessments of genotoxic liability, general safety cover and on-target pharmacological activity of the metabolites (i.e. their limited contribution to the activity of parent darapladib) meant that no further work was required.

The genotoxic risk assessments were carried out as stipulated by regulatory guidance (ICH, 2011). If a proven genotoxin is present either as an impurity, degradant or metabolite of a drug, there are wide ranging consequences for the drug as a potential medicine, including potential termination of the drug. For darapladib, extensive assessments showed that loss of the fluorobenzene moiety from the structure of darapladib did not cause consistent genotoxic endpoints in the non-clinical studies conducted. Additionally, the enteric coating used for tablets and the administration of the oral solution dose along with food was shown to limit degradation to potentially produce 4-fluorobenzyl chloride.

The M4 pharmacologically active metabolite (see section 3.5.2) was the only metabolite found to be present in plasma following intravenous administration of darapladib (1% of total RDM) and one of several minor metabolites present following oral administration. None of the metabolites were greater than 6% of drug-related material in plasma and thus contributed little to the pharmacology of darapladib. **Commentary paper 5** states that M4 was routinely analysed in all clinical studies for

darapladib, but the value added in doing this seems questionable (at least to this author) based on the data from this study.

3.5.4. Technical considerations and reflections

There was a minimum 21 day washout period between stage 1 and stage 2 of the darapladib study to attempt to ensure that there was no drug-related material present in samples from the intravenous dose administration when the first oral pulse dose was administered. On reflection, the washout period between dosing phases of the cross-over was not long enough in this study, as was shown by the presence of radioactivity at above background levels in the predose samples from the oral dose session; predose samples contained about 20% of peak post dose concentrations. Pharmacokinetic data modelling was used to subtract concentrations of RDM residual from the intravenous dose session from those in the first oral dose session and although not ideal, there was no significant effect on the data or objectives of the study in this case. This finding was useful for application to subsequent studies as a note of caution in the planning of the length of the washout period between dosing phases for cross-over study design, as demonstrated by Figure 25.

Similar to the study for **Commentary paper 4**, LSC was used alongside AMS for certain elements of this darapladib study, with further demonstration of how these techniques can be used to complement each other. The design could have been altered, as mentioned in the paper, through use of repeated administration of ^{14}C-labelled doses instead of the use of single doses before and after repeated cold dose administrations, as was implemented. Whether this type of repeat dose design is really necessary in general drug development is questionable as a plethora of repeat dose ADME data can be obtained through alternative approaches, such as with NMR and LC-MS, without the need for ^{14}C-labelled drug (Dear et al., 2008).
An unresolved issue in this paper was that of a very poor ^{14}C recovery (only 20% recovery; unpublished data) from one individual subject, following the first oral dose administration. Full investigation of the possible reasons for this provided no satisfactory answer for the cause of the low recovery, e.g. it was shown that this individual had very similar systemic exposure to drug-related material, so it was inferred that the subject had received the correct dose of ^{14}C-darapladib. In the author's experience this finding has occurred in more than one clinical mass balance

study, but even after thorough investigations as to how it may have happened (including re-analysis of samples, checks of the collections of excreta made) no definitive reason has been evident. I would speculate that a possible reason is the formation of pockets in the lining of the digestive tract which can fill with excreta and, as a result, the drug-related material is effectively held in the GI tract for an extended period leading to this poor ^{14}C-recovery within the timeframe of the excreta collections. This phenomenon is known as diverticulosis and is a relatively common condition in the elderly and sometimes caused by poor diet (with up to 5% prevalence in 18-40 year olds) (Tursi, 2016). A possible solution to this could be to administer a laxative to such an individual in a future study, should this occur, in the hope that the improved recovery would be achieved, instead of having to exclude the data from this subject from the data set.

3.6. AMS in Microtracer Studies for Intravenous pharmacokinetics

Over recent years there has been some confusion around the nomenclature used to describe two distinctly different clinical study designs, namely that involving a **microdose** (which can be isotopically labelled or non-labelled), where the total dose of drug administered does not exceed 100 μg (ICH, 2009) and the study design which has become known as a microtracer, as described in this section of the commentary. The term microtracer has been widely adopted in an attempt to distinguish the study design outlined below, from a microdose design, although confusion remains through misuse of the terminologies (Ings, 2009), (Lappin et al., 2013b). This commentary is concerned with the microtracer study design only and should not be confused with microdosing.

Traditionally, clinical **absolute bioavailability** (F) data has been obtained through a cross-over study design, where subjects are administered the reference intravenous dose of drug in one dosing session, followed by a wash-out period, and then the extravascular dose in a separate session. Obtaining absolute bioavailability data for drugs intended for extravascular administration was expensive and time consuming because of the need for the intravenous dose. Administering a drug intravenously required safety toxicology (animal studies in two species) by this route of administration, suitable formulation development and often conduct of a prior clinical dose escalation study to establish a safe dose to be used to meet the objectives of the subsequent absolute bioavailability study.

In some cases, drugs are so insoluble that it has not been feasible to develop intravenous formulations. For example, there is good evidence that ezetimibe is absorbed through the GI tract into the systemic circulation following oral administration to humans (Patrick et al., 2002) and yet its absolute bioavailability is unknown because the drug is too insoluble to administer intravenously (Kosoglou et al., 2005).

Additionally, most drugs are developed for therapeutic administration by the oral route and so enabling activities for administration by the intravenous route are often seen as surplus to requirement and wasteful of precious resources. On the other hand, it has been known for many years that there is value in obtaining knowledge of the definitive pharmacokinetic parameters of clearance (CL), volume of distribution (V) and absolute bioavailability that comes from dosing by the intravenous route (Rowland et al., 1973).

Absolute bioavailability is calculated as shown by Equation 10 below:

$$F = \left[\frac{AUC_{oral}}{AUC_{IV}}\right] x \left[\frac{Dose_{IV}}{Dose_{oral}}\right] \quad \textbf{(Equation 10)}$$

Where AUC is area under the drug concentration:time curve.

Absolutely bioavailability is also related to clearance as follows:

Following intravenous administration, $CL_{iv} = [Dose_{iv}/AUC_{iv}]$ **(Equation 11)**

Following oral administration, $CL_{oral} = F \times [Dose_{oral}/AUC_{oral}]$ **(Equation 12)**

Thus : $F= (CL_{oral} \times AUC_{oral})/Dose_{oral}$ **(Equation 12a)**

The value for CL_{oral} in Equation 12a has to be assumed to be the same as CL_{iv} as it is only possible to measure clearance following an intravenous administration.

The question therefore arises, is the assumption that CL is the same for both the intravenous and oral administrations a reasonable one? The answer is that this is a reasonable assumption providing either (a) CL is independent of plasma drug

concentration, or (b) if CL is dependent upon drug concentration, then the plasma concentrations are the same following intravenous and oral administrations.

Since little is known about the clearance of a drug, or whether its value is dependent upon plasma concentration or not prior to intravenous administration, then the ideal design for a study where absolute bioavailability is determined from separate intravenous and oral administrations, is one where the plasma concentrations attained are the same for both dose routes. To achieve this however, good estimates for the volume of distribution (V) and absolute bioavailability (F) are necessary which, paradoxically, are not known with any certainty until after the intravenous dose has been given. Moreover, there are often toxicological and formulation constraints that limit the intravenous dose that can be administered. Consequently, it is not uncommon to see absolute bioavailability studies where the respective plasma drug concentrations following the oral and intravenous administrations are significantly different, with no comment being made regarding potential non-equivalent clearance (a recent example is the absolute bioavailability of tasimelteon where there was an approximate 5-fold difference in AUCs between the oral and intravenous doses (Torres et al., 2015)). Furthermore, there are examples where the apparent absolute bioavailability appears to be in excess of 100% due to non-equivalent clearance (for example with the vitronectin receptor antagonist (SB-26512) (Ward et al., 2004). Non-equivalent clearance is also thought to be responsible for an approximate 10% error in the determination of F for phenytoin (Jusko et al., 1976). Error in the calculation of F arising from non-equivalent clearance is rarely considered in absolute bioavailability studies, although the effect has been recognised for several decades.

An alternative design to the two-way cross over absolute bioavailability study first emerged in the 1970s, where the oral and intravenous doses were given at the same time, with the intravenous dose isotopically labelled. Plasma samples were analysed by methods that were capable of discriminating between the non-labelled and isotopically labelled drug. In this way, both the oral and intravenous pharmacokinetics could be determined from a single set of plasma samples, thereby virtually eliminating any non-equivalent clearance effects.

In the first study of this type to be reported (Strong et al., 1975) N-acetlyprocainamide (NAPA) was administered by the oral route at a dose of 500 mg, and 250 mg of ^{13}C-NAPA was administered simultaneously by the intravenous route. The design was developed to address issues of non-equivalent clearance and to remove potential temporal effects between dose administrations. There were however, some downsides to the approach taken:

(1) The high intravenous ^{13}C-NAPA dose led to much higher systemic concentrations of drug than by the oral route, which meant that the combination of the drug exposure from intravenous and oral doses was markedly different from that from the oral dose alone and complex kinetic modeling was used to deconvolute the data, to adjust for any differences in pharmacokinetics that arose due to the magnitude of the systemic exposure differences.

(2) A better design would have been to administer the intravenous dose in such a small quantity, so that it did not significantly add to the oral drug concentration. In this way, the measured drug concentrations in plasma arising from the oral dose could be assumed to equal the total drug concentration. Measurements of isotopically labelled drug would also directly provide pharmacokinetics by this route and no deconvolution modelling would be required. The available analytical sensitivity at the time however, placed constraints on how low the intravenous dose could be.

Although this design was used a number of times (eg. (Atkinson et al., 1989), (Preston et al., 1999) and (Heikkinen et al., 2001)), it was not widely adopted because of the magnitude of the intravenous dose required. Deconvolution modelling was seen as an unnecessary step compared to the cross-over absolute bioavailability study design. Moreover, the intravenous dose still required an extensive toxicology package and so this remained a major burden to study conduct. This situation changed however, with the advent of biomedical AMS.

As AMS came to be used in drug development, it offered an extremely sensitive method of isotopic measurement (primarily for ^{14}C). This enabled the intravenous dose to be reduced to such a low level that it became much less likely to contribute to the drug exposure resulting from the oral dose. In addition, the regulatory authorities reacted by essentially removing the need for safety toxicology at such low doses (ICH, 2009). With the requirement for intravenous dose route specific toxicology assessment removed, the way was now open for human intravenous pharmacokinetics to be obtained on a far more routine basis.

A microtracer is an isotopically-labelled substance (which can be a radioactive or stable isotope; in the context of this commentary and the direct experience of the author it has only been the former) administered intravenously concomitantly with higher extravascular dose(s), meeting all of the following criteria:

(1) The intravenous microtracer dose meets the regulatory guidelines for safety evaluation in terms of mass administered and solubility in aqueous (usually saline) formulation.

(2) The intravenous microtracer dose is sufficiently low so that it can be reasonably expected not to perturb the pharmacokinetics of the extravascular dose.

(3) Isotopic analytical methods are available that will allow discrimination between the pharmacokinetics derived from the intravenous and extravascular doses. For example, the LC-MS for the analysis of non-labelled drug and LC+AMS for the ^{14}C-drug quantification.

Note that in the early studies (eg. (Strong et al., 1975)) the extravascular and intravenous doses were given simultaneously. This design has been improved upon more recently and it has become standard practice to administer the intravenous dose as an infusion (e.g. 15 minutes duration) timed to end at the oral $\underline{\mathbf{t}_{max}}$, i.e. the intravenous dose is administered concomitantly with the oral dose rather than simultaneously, to further minimise the possibility of non-equivalent pharmacokinetics

between the different dose routes (specifically during the absorption phase for the oral dose, which an infusion more closely mimics than does a bolus dose). An infusion is also usually preferred over a bolus administration for safety reasons as the infusion pump can be turned off to halt drug delivery if there are adverse safety signals in the subject.

A cartoon of the principles behind microtracer dosing, through administration of a low dose of drug by the intravenous route, along with a much higher dose by an extravascular route, is shown in Figure 20. The intravenous dose must be sufficiently lower than the extravascular dose (usually by a factor of between 100 and 1000) so that it does not perturb the pharmacokinetics of the extravascular dose. The cartoon shows the principle of systemic mixing of the two isotopic forms (^{14}C-labelled and non-labelled) of the drug and the fact that during the extravascular elimination phase both will be cleared at the same rate independent of the isotopic form. Samples taken for isotopic analysis and total drug concentration analysis therefore generate pharmacokinetic data for both the intravenous and extravascular routes of administration.

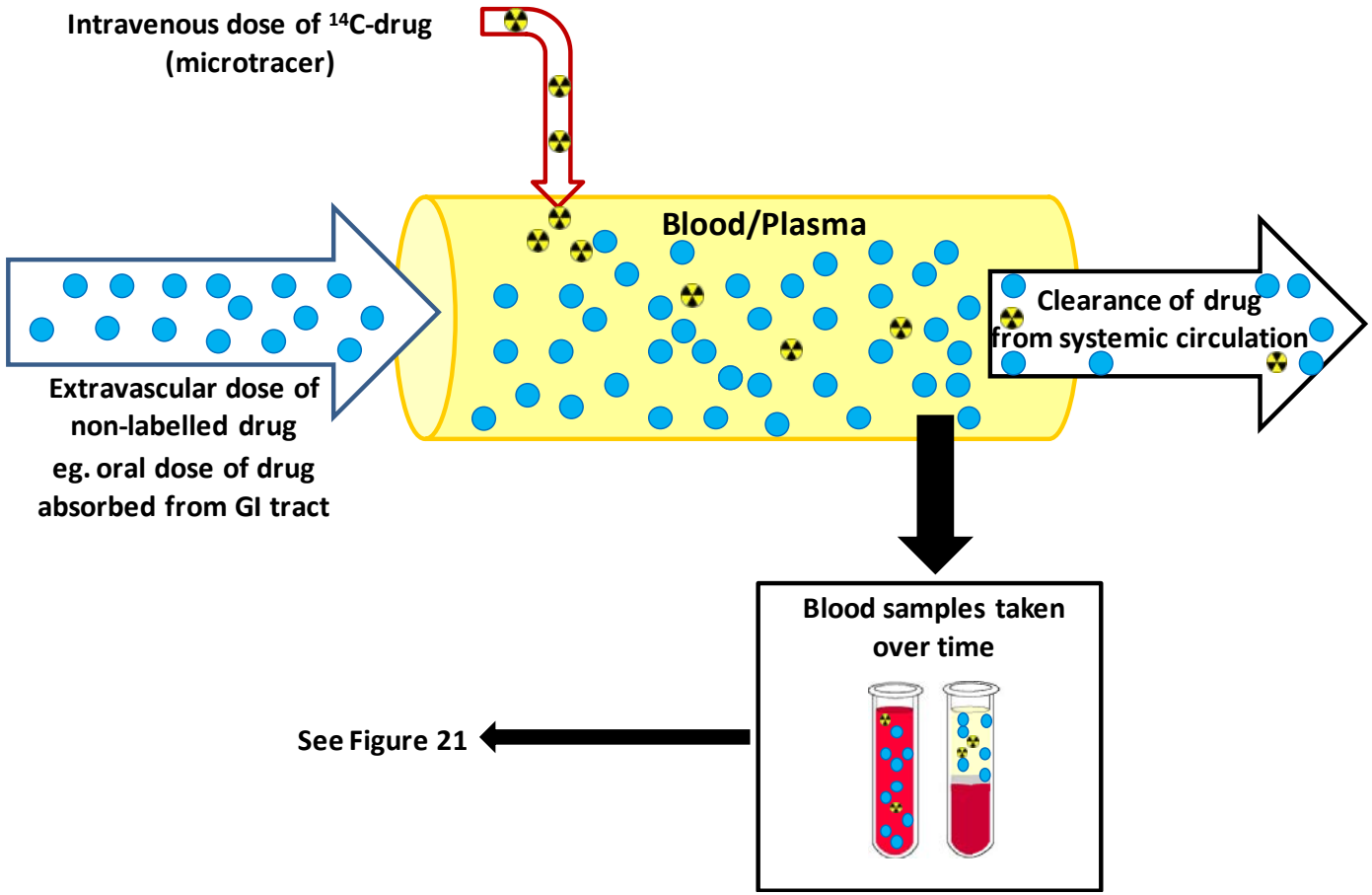

Figure 20. Principles of isotope mixing in systemic circulation during microtracer studies*.

^{14}C-labelled drug from the intravenous dose is effectively diluted into the larger mass of non-labelled drug from the extravascular route dose.

* Figure compiled by G Young and G Lappin.

In summary, the microtracer design has the following advantages over the traditional two-way cross-over study design:

(1) Virtual elimination of non-equivalent clearance effects.

(2) No intravenous toxicology assessment is required in non-clinical species*. The safety data for the intravenous dose can be qualified by the existing oral toxicity studies (ICH, 2009).

(3) Intravenous formulation development can be more straightforward due to the low dose.

(4) No clinical dose escalation study is required to support the intravenous dose

(5) Removal of the temporal effect which might occur when there are two separate dosing occasions

The concept of the microtracer approach is summarised in Figure 21.

* If a novel formulation vehicle is employed for delivery of the intravenous dose, then local tolerance of the vehicle should be assessed (in a non-clinical haemolysis study).

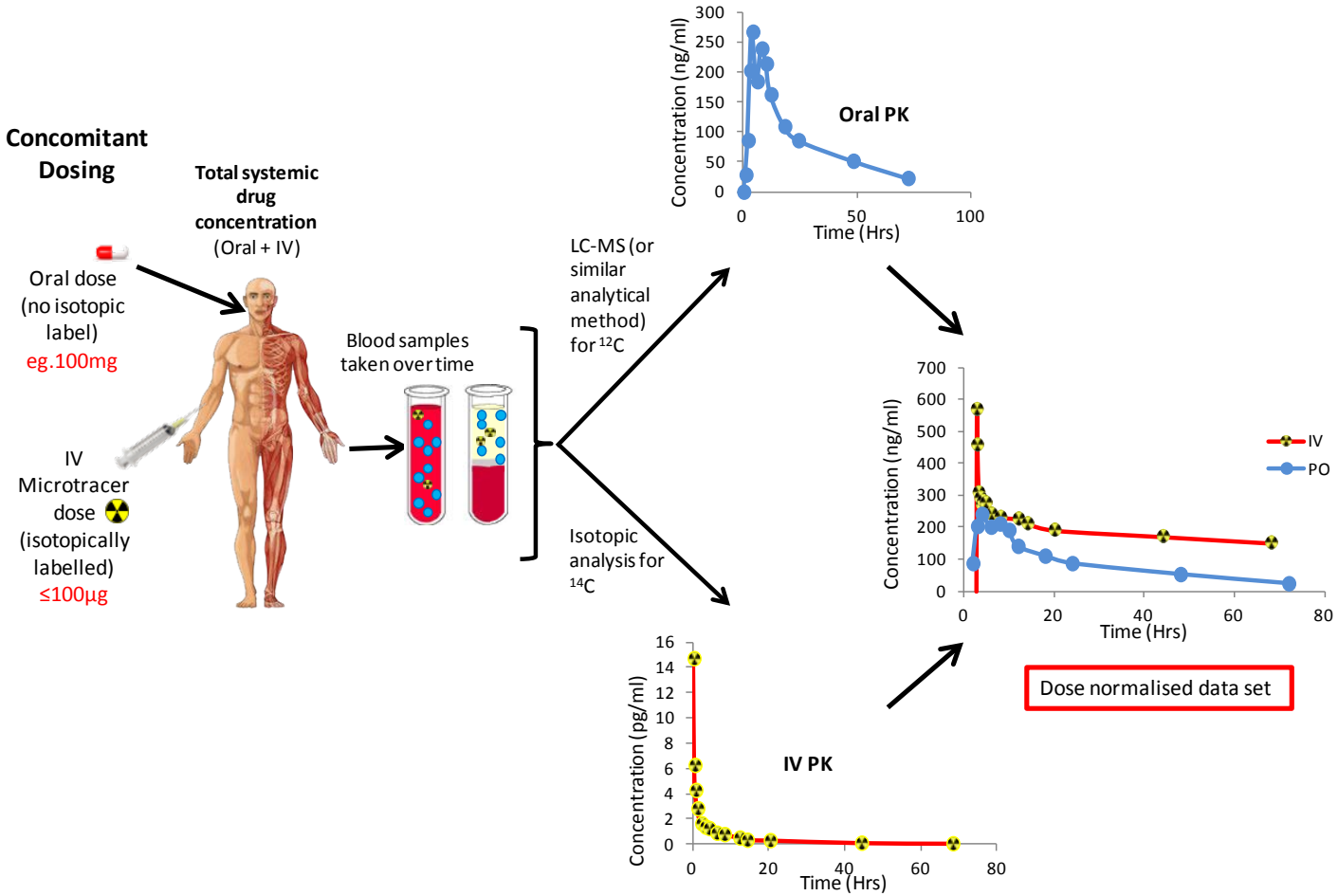

Figure 21. Concomitant oral and intravenous dosing microtracer concept.

(Adapted from Figure 1 of (Lappin, 2016) with permission).

It should be noted that the microtracer could be stable label material rather than ^{14}C; all of the author's experience to date has been with ^{14}C. See section 3.6 for expansion upon some of the pros and cons of use of each of these labels.

GSK has conducted several such clinical studies in recent years (Daley-Yates et al., 2012), (Hoffmann et al., 2013), (Denton et al., 2013), (Leonowens et al., 2014) in different stages of clinical drug development. In the instances when these studies were conducted late on in development, it was to fulfill either real or perceived regulatory requirements for provision of absolute bioavailability data (**Commentary paper 6** – section 3.7 and **Commentary paper 7** – section 3.8). When the studies were conducted early in drug development (eg. (Daley-Yates et al., 2012), (Hoffmann et al., 2013)) it was for definition of absolute bioavailability to help define the reason for variable systemic exposure following extravascular administration* or investigation of routes of elimination of drug via reactive pathways that may raise a safety concern (unpublished works).

From the perspective of the pharmaceutical industry, it is the regulatory requirements for absolute bioavailability data that drives the conduct of these studies. Notwithstanding absolute bioavailability, intravenous dosing of a drug otherwise intended only for extravascular administration also provides a wealth of other information, including:

(1) Assessment of biliary excretion.

(2) First pass metabolism versus systemic metabolism.

(3) Definition of pharmacokinetic parameters such as CL and V (as well as F).

(4) Assessment of renal clearance.

Additionally, there are applications beyond the scope of this commentary including:

(1) Study of conversion from pro-drug to active drug.

* Drugs with low absolute bioavailability tend to exhibit more variability in systemic concentrations achieved following extravascular dose administration.

(2) Formation and elimination of active metabolites.

(3) Pharmacokinetics of metabolite turnover.

* Drugs with low absolute bioavailability tend to exhibit more variability in systemic concentrations achieved following extravascular dose administration.

It should be noted, that since the re-emergence of the microtracer approach as a favoured alternative to the traditional cross-over design for absolute bioavailability assessment, sparked by the use of ^{14}C tracer for this purpose, a number of studies where a ^{13}C-labelled tracer was used have been conducted (Jiang et al., 2012), (Schwab et al., 2013), (Cannady et al., 2015), (de Vries et al., 2016). Advances in the sensitivity of LC-MS since the time of the first study of this type (Strong et al., 1975), has made the use of stable isotope feasible. There are both pros and cons to the choice of which tracer to use (Xu et al., 2014), including considerations around required analytical sensitivity, inclusion of additional objectives over parent drug pharmacokinetics alone, requirement for pre-work to check for possible KIE (in particular where multiple labels have been incorporated (Jiang et al., 2012)), availability of labeled materials and assay development complexities. It is a reflection of the sensitivity challenges for ^{13}C-labelled tracer measurement that studies where this has been applied to date have all used at least a 100 µg dose, whereas AMS has utilised much lower doses, eg. **Commentary paper 7**. This author has no direct experience of ^{13}C microtracer designs but it is his opinion that, as stated in a previous publication (Young and Seymour, 2015), sometimes there are reasons that ^{14}C and AMS are avoided, beyond those relating to science, e.g. availability of equipment and expertise in pharmaceutical companies (all have LC-MS capability) and lack of transparency of the real costs associated with drug development activities in-house (versus external expenditure at a contract research organisation).

Measurement of isotopic concentration by AMS relies upon the analyte chromatographic peak being free from contaminating ^{14}C-labelled compounds which may occur, for example, if a ^{14}C-labelled metabolite co-elutes with parent drug. Unlike mass spectrometry, AMS has no ability to discriminate on the basis of the mass of the analyte and so the purity of the ^{14}C-labelled analyte peak relies solely upon resolution by chromatography.

A thorough investigation of the peak purity could include use of a second chromatographic separation system such as two-dimensional chromatography using two different separation modalities (eg. normal versus reversed-phase) (Simpson et al., 2010), but this is a very time consuming approach and therefore not practical on a routine basis. In the case of a microtracer study, where the unchanged parent drug is the target analyte, a less robust but more routine approach is to use LC-MS for analysis of a time-window across the analyte peak to provide assurance of purity (Bryant et al., 1996). Given the very low dose administered intravenously, LC-MS may not be sufficiently sensitive to detect contaminating metabolites arising from this route of administration. The oral dose is typically >100-fold higher however and so with the assumption that the same metabolite is formed by this route of administration, then LC-MS should be able to detect it.

3.7. Commentary paper 6

Denton, C. L., E. Minthorn, S. W. Carson, **G. C. Young**, L. E. Richards- Peterson, J. Botbyl, C. Han, R. A. Morrison, S. C. Blackman and D. Ouellet (2013). "Concomitant oral and intravenous pharmacokinetics of dabrafenib, a BRAF inhibitor, in patients with BRAF V600 mutation-positive solid tumors." J Clin Pharmacol **53**(9): 955-961.

3.7.1. Objectives

1) To determine the intravenous pharmacokinetics and absolute bioavailability of oral dose administration of the NCE, dabrafenib, using the novel clinical microtracer approach in **B-Raf** positive oncology patients.

2) To determine the number of subjects required to generate the appropriate data and to show the advantage in design flexibility which allowed patients to quickly be moved onto much needed therapy for their cancer treatment.

3.7.2. Clinical study design

Intravenous pharmacokinetics (CL, V and $\mathbf{t_{1/2}}$) of dabrafenib (50 µg; 7.4 kBq) and absolute bioavailability following oral (150 mg) dosing was defined in oncology patients using the microtracer design, as outlined in Figure 22. Provision of this information improves the understanding of the drug ADME-PK. This is important as it allows judgements to be made about the likelihood of inter-patient variability in bioavailability and, combined with data from other studies such as the human ADME, the extent of first pass metabolism can be assessed (see section 3.4.3).

A separate human ADME study with ^{14}C-dabrafenib was conducted in parallel (Bershas et al., 2013) to the microtracer study. The emergent metabolism data was used in the development of the chromatographic separation method for the LC+AMS assay of plasma (to ensure integrity of parent isolation from metabolites for quantification following intravenous administration).

Design:
4 Patients with B-RAF mutation-positive solid tumours;

Single 15 minute intravenous infusion dose of 50 µg ^{14}C-dabrafenib (7.4 k*Bq*) concomitant to a single oral dose of 150 mg dabrafenib

- [Intravenous infusion started at 1.75 hours after oral dose to coincide with oral dose t_{max}]

Samples :

- Blood (for plasma) for parent drug from oral and intravenous doses
  [& RDM from intravenous dose]

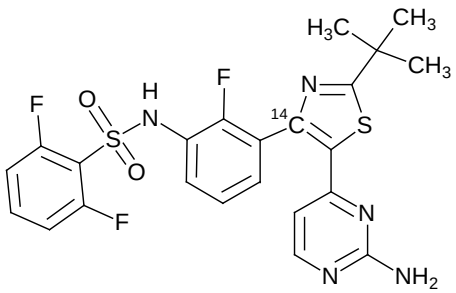

^{14}C-dabrafenib

Main data outputs:

- Parent drug concentrations in plasma from oral dose (by LC-MS)
- Total radioactivity in plasma from intravenous dose (by direct AMS)
- Parent drug concentrations from the intravenous dose (by LC+AMS)
  - Derivation of pharmacokinetic parameters of dabrafenib in plasma including absolute bioavailability from the oral dose relative to the intravenous dose
  - Comparison of predictions of human intravenous PK with clinical data

Figure 22. Schematic of clinical study design 6.

3.7.3. Clinical study data output and impact

The mean (n=4 patients) absolute bioavailability of dabrafenib was determined as being high at 94.5%. This high absolute bioavailability for dabrafenib reflects the low degree of variability in systemic exposure observed following oral administration (bioavailability range* of 79.3 to 106%). Indeed, when absolute bioavailability is used as a decision making criterion for drugs in development, a minimal desired bioavailability limit is often set at around 20% (GSK developability criteria) in an attempt to minimise such variability across subjects. Low bioavailability is not just a cause for concern as a potential source of patient-to-patient variability per se, but is also an inefficient delivery of the active moiety to the systemic target site.

Dabrafenib is a substrate of the efflux transporter P-glycoprotein (P-gp) (data on file at GSK), which is located in tissues including the intestinal epithelium and has the potential to limit absorption through the GI tract (Yang and Liu, 2016). However, dabrafenib also demonstrates a high permeability across epithelial monolayers (1.48×10^{-5} cm/s in an in vitro assessment in **MDR1-MDCKII** cell monolayers at GSK). The high permeability is postulated to negate potential efflux of dabrafenib at the gut wall and it is known that efflux by P-gp may sometimes have only minimal impact upon drug absorption (Wu and Benet, 2005), (Dufek et al., 2013). The high permeability of dabrafenib supports the propensity for it to achieve high bioavailability following oral administration.

The comparison of systemic exposure to parent drug versus that for RDM following intravenous administration of ^{14}C-dabrafenib in this study and following oral administration of ^{14}C-dabrafenib in the human ADME study (Bershas et al., 2013) showed that unchanged dabrafenib represented a very similar proportion of the total radioactive drug-related material in plasma (about 10%) by both routes of administration. This is consistent with dabrafenib undergoing limited first pass metabolism (as demonstrated by the similar proportion of parent drug circulating from

* SD cannot be calculated due to GSK restrictions of access to the full data set.

both dose routes), yet extensive metabolism (about 90% by both routes) in the systemic circulation.

Dosing intervals are based upon the half-life of elimination of the drug ($t_{1/2}$) as this parameter defines the time to reach steady state exposure (related to the number of repeated dose administrations). Although dosing intervals are often fixed in relation to $t_{1/2}$ alone, the half-life is itself a function of CL and V (Equation 13).

$$t_{1/2} = \frac{0.693\,V}{CL} \qquad \textbf{(Equation 13)}$$

Clearance is dependent upon blood flow and as such it is affected by, for example, disease state, hepatic and renal function, age and drug interactions. Changes of clearance can therefore have marked effects on the safety profile of the drug. This understanding of the fundamental pharmacokinetic parameters of the drug can help with avoidance of future safety issues and can guide dosing regimens.
The plasma clearance for dabrafenib was low at 12.0 L/h, being only about 30% of liver blood flow (blood to plasma ratio was about 0.5), which along with the high absolute bioavailability suggested low hepatic extraction and low first pass metabolism of dabrafenib. This is consistent with the understanding of metabolism of dabrafenib from the microtracer and human ADME studies. Dabrafenib had low volume of distribution (45.5 L) and although the clearance was also low there was a resulting short terminal half-life for dabrafenib after intravenous administration (2.6 h).

The elimination half-life of dabrafenib was longer than anticipated from pre-**FTIH** predictions, particularly following oral administration, which showed **flip-flop kinetics** with a prolonged absorption phase after oral administration. The term flip-flop is used to describe the pharmacokinetic phenomenon where the absorption rate is longer than the elimination half-life (that following oral administration, at 4.8 hours, was nearly two-fold greater than following intravenous administration) and has been observed for many drugs (Garrison et al., 2015). This absorption rate limited, longer elimination half-life and protracted decline in concentrations of dabrafenib in plasma

from oral administration was seen as advantageous in providing a better chance for achieving efficacy with this drug.

Dabrafenib has two known active metabolites (hydroxy-dabrafenib and desmethyl-dabrafenib) as shown in Figure 23 (and (Bershas et al., 2013)) both of which are B-raf kinase antagonists. Concentrations of these metabolites in plasma (along with parent dabrafenib) have been measured in several clinical studies and constitute approximately 25% of the total pharmacological activity (data on file at GSK).

Although this has not been done for the metabolites of dabrafenib, the microtracer approach enables PK of active metabolites to be studied. Although ^{14}C-labelled metabolite has to be synthesised, there is still no need for intravenous toxicology with a very low dose. If the parent drug is administered by the oral route and the metabolite is dosed by the intravenous route then the rate of metabolite formation and CL for the metabolite can be measured in the same way as for a prodrug (Annes et al., 2015).

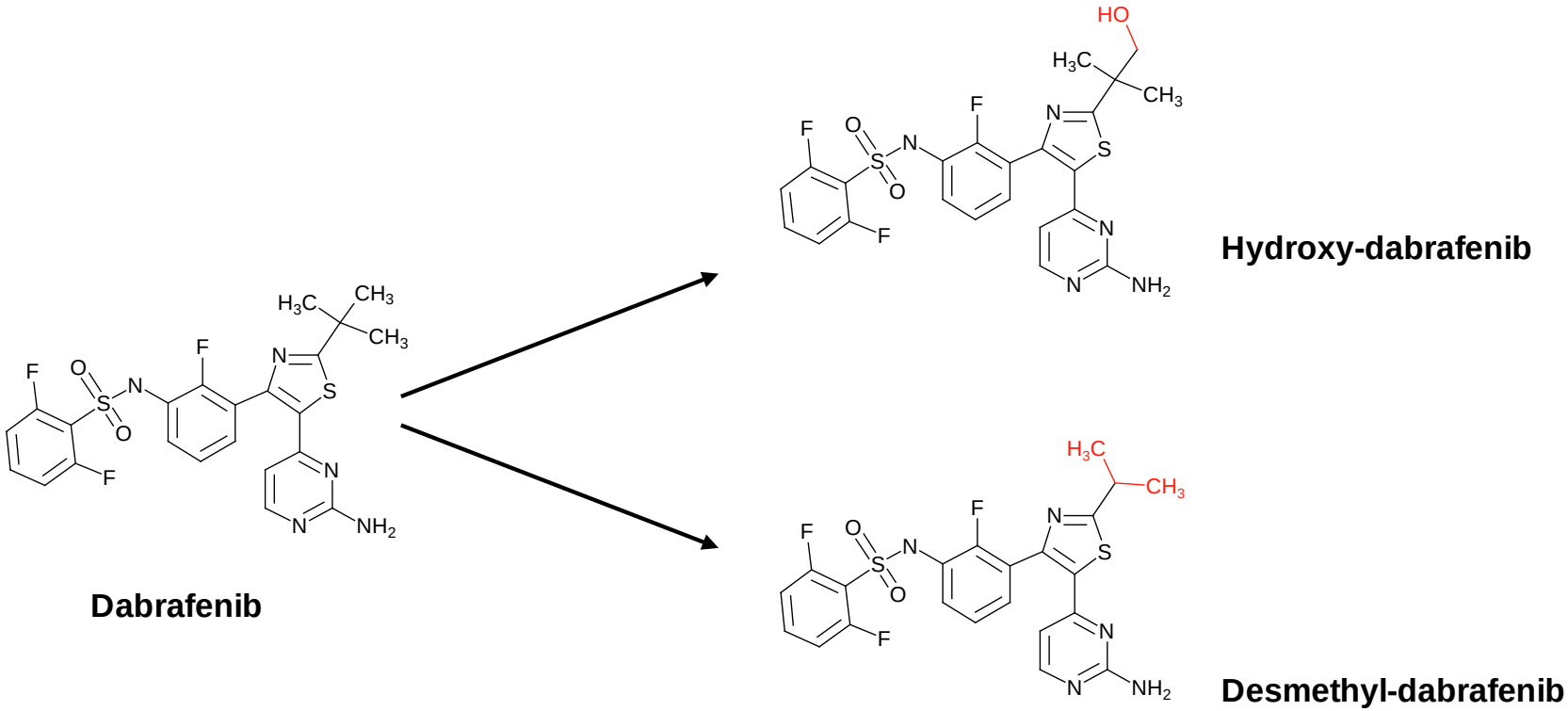

Figure 23. Biotransformation of dabrafenib to hydroxy-dabrafenib and desmethyl-dabrafenib.

3.7.4. Technical considerations and reflections

An LoQ that allowed definition of the intravenous PK of dabrafenib in plasma was achieved (1.86 pg dabrafenib/mL) and the assay was validated against outline criteria as described in the literature (Higton et al., 2012). The assay was shown to be robust and this was demonstrated further post-analysis of study samples through an incurred sample re-analysis (ISR), where a proportion of the study samples were re-analysed and the results were found to be reproducible to the original results within criteria established apriori (repeat analysis results for more than two thirds of samples, within 20% of original values). At the time, there was little experience of carrying out such a robustness check using an LC+AMS assay approach, so it was re-assuring to observe that the assay applied could meet the limits of acceptable performance for this assessment. It is now routine practice in our laboratory and for other AMS researchers involved in such clinical sample LC+AMS assay provision to carry out ISR ((Xu et al., 2012) and personal communication with Xceleron Inc.).

An additional advantage of the use of the ^{14}C approach to the microtracer design (over and above ^{13}C) is that an assessment can be made of total radioactivity to check on the validity of the LC+AMS data, i.e. notwithstanding analytical variability, the data provided by LC+AMS for parent drug cannot be higher than that provided for drug-related material by direct analysis by AMS (Young et al., 2014).

It is also important to note that even at the time of writing this commentary, there are no regulatory guidelines that specifically embrace the bioanalytical LC+AMS assay approach and so it is beholden upon the practitioners (this author included) to apply defensible and appropriate quality scientific practice in the application of such methods.

In the study detailed in **Commentary paper 6**, the LoQ for total radioactivity was considerably higher (due to less sample clean-up) than for the parent specific assay, at 9.77 pg dabrafenib equivalents/mL. Interestingly, although implied, there are no analytical method-focused regulatory guidelines whatsoever specifically for the analysis of total radioactivity in biological samples. Best practices based on good science have been established at laboratories that conduct total radioactivity measurements, but nevertheless methods vary across laboratories.

In contrast, there are bioanalytical regulatory guidelines that are applicable to the LC-MS assay (LoQ of 1 ng/mL) used in support of the considerably higher oral dose. This disparity in expectation of quality for these assay approaches (used to provide complementary data sets from the same clinical studies) has been the focus of AMS researchers in recent years (Young et al., 2014).

The dabrafenib study showed that suitable data could be provided from a low number of subjects (n=4) through the concomitant dosing approach, with the assessment that this design inherently reduced data variability (Ma and Chowdhury, 2016). Additionally, the clinical pharmacokinetic data compared favourably with that from predictions made using **allometric scaling** from non-clinical studies, which gave further confidence in the data provided from this novel study design and application of AMS.

3.8. Commentary paper 7

Leonowens, C., C. Pendry, J. Bauman, **G. C. Young**, M. Ho, F. Henriquez, L. Fang, R. A. Morrison, K. Orford and D. Ouellet (2014). "Concomitant oral and intravenous pharmacokinetics of trametinib, a **MEK** inhibitor, in subjects with solid tumours." Br J Clin Pharmacol **78**(3): 524-532.

3.8.1. Objectives

1) To determine the absolute bioavailability of the NCE, trametinib, using the clinical microtracer approach in patients with metastatic cancer.

2) To determine the number of subjects required to generate the appropriate data and to show the advantage in design flexibility which allowed patients to quickly be moved onto much needed therapy for their cancer treatment.

3.8.2. Clinical study design

Trametinib is a reversible and selective allosteric inhibitor of mitogen-activated protein kinase (MEK)1 and MEK2 activation and kinase activity. The intravenous pharmacokinetics (CL, V and $t_{1/2}$) of trametinib (5 µg; 7.4 kBq) and absolute bioavailability of oral (2 mg) dosing were defined in (n=4) oncology patients using the microtracer design.

Prior clinical pharmacokinetic and tolerability data following oral administration to patients with advanced solid tumours (Infante et al., 2012) indicated that trametinib had an effective elimination half-life in plasma of 4 days. The study also showed that a dose of 3 mg per day was poorly tolerated beyond the first cycle of treatment (up to 21 days) and that the lower dose of 2 mg provided appropriate pharmacokinetics to meet efficacy requirements, indicating that trametinib has a narrow therapeutic index (Gilmartin et al., 2011).

Based upon allometric scaling of pharmacokinetic data for trametinib in animals and the known systemic exposure data from oral administration to humans (GSK data on file), the likely systemic exposure from intravenous administration to humans was predicted. The intravenous dose thus chosen (5 μg) was likely to be low enough to avoid any significant addition to the concentrations of trametinib in plasma from the oral dose (2 mg), resulting in a dose magnitude differential of 400-fold, as presented in Figure 24.

Design:
4 Patients with B-RAF mutation-positive solid tumours;

Single 5 minute intravenous infusion dose of 5 µg ^{14}C-trametinib (7.4 k*Bq*) concomitant to a single oral dose of 2 mg trametinib

- [Intravenous infusion started at 1.5 hours after oral dose to coincide with oral dose t_{max}]

Samples :

- Blood for plasma for parent drug from oral and intravenous doses [& RDM from intravenous dose]

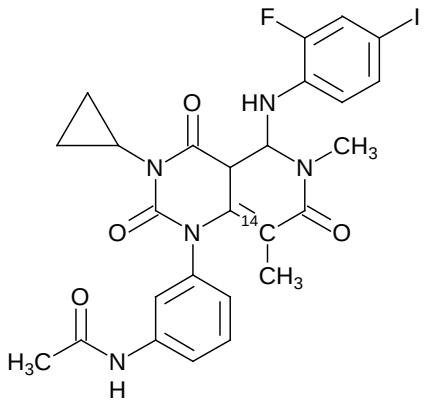

^{14}C-trametinib

Main data outputs:

- Parent drug concentrations in plasma from oral dose (by LC-MS)
- Total radioactivity in plasma from intravenous dose (by direct AMS)
- Parent drug concentrations from the intravenous dose (by LC+AMS)
  - Derivation of pharmacokinetic parameters of trametinib in plasma, including absolute bioavailability from the oral dose relative to the intravenous dose

Figure 24. Schematic of clinical study design 7.

3.8.3. Clinical study data output and impact

The study showed that trametinib had a low blood clearance of 0.94 L/h (only 1% of liver blood flow) and a very high volume of distribution (976 L). The resulting elimination half-life for intravenous administration of trametinib was 10 days.

In a separate human ADME study for trametinib (Ho et al., 2014) there was low mass balance ^{14}C-recovery from patients following oral administration. This can be explained by the intravenous data from this microtracer study as the observed elimination half-life of total radioactive drug-related material was 27 days, whereas the excreta collection period for the human ADME study was only 10 days.

The mean (n=4) absolute bioavailability of trametinib at an oral dose of 2 mg was moderately high at 72.3% (range* of 45.7 to 92.8%), indicating limited likelihood for high inter-patient variability in systemic exposures following oral administration (see section 3.7.3). The apparently narrow therapeutic index for trametinib therefore is less of a concern than otherwise would be the case, were it to demonstrate low bioavailability.

This study indicated a relationship between the clinical PK of trametinib and bodyweight of the subjects, irrespective of route of administration (same variability and rank order across the subjects and dose routes). The reasons for this relationship are likely related to the very high volume of distribution of trametinib, into deep tissue compartments, and indeed the intravenous PK profiles showing a rapid initial distribution phase followed by a protracted elimination phase support this slow elimination from tissues (see Figure 1 of **Commentary paper 7**). Although it would appear that dosage adjustments may need to be considered based upon bodyweight, in fact analysis of data from wider clinical use has shown that factors including bodyweight do not have a clinically important effect on the exposure of trametinib (FDA, 2015). Dosage adjustments are recommended however, based upon observed adverse effects following treatment with trametinib.

* SD cannot be calculated due to GSK restrictions of access to the full data set.

3.8.4. Technical considerations and reflections

From the purely technical standpoint, this study showed that high quality intravenous pharmacokinetic data could be provided from a total dose of only 5 μg (for a drug with a high volume of distribution), through the use of radiolabelled drug and an LC+AMS assay. This clearly demonstrated that the sensitivity of the AMS for detection of ^{14}C-labelled material is such that there can be considerable flexibility in microtracer study designs, which then allows intravenous doses much lower than often considered (usually 100 μg) to be used, if warranted.

A low LoQ was achieved for the LC+AMS assay (1.1 pg trametinib/mL of plasma) and, as for the dabrafenib method, the assay was validated against outline criteria as described in the literature (Higton et al., 2012). The LoQ for total radioactivity was, in this instance, lower than for the parent drug specific assay (at just 0.95 pg trametinib equivalents/mL). The LoQ for the assay of dabrafenib by LC-MS, in support of the oral dose administration, was considerably higher (250 pg/mL).

Also similarly to the dabrafenib microtracer study, this clinical study was carried out in parallel to the conduct of the human ADME study (conventional design, albeit in cancer patients rather than healthy subjects) (Ho et al., 2014). The design for the microtracer study received input from FDA, who reviewed and endorsed the novel study design. FDA did however recommend that the study be conducted in patients (due to perceived safety concerns) with the therapeutic oral dose of 2 mg, rather than at a lower dose of 1 mg in healthy subjects, as had been proposed initially. Due to the efficiency of the (non-crossover) design, patients could quickly be entered into a rollover study, where they received the therapy after completion of this clinical pharmacology study; particularly of note as the design obviated the need for a lengthy washout period (likely in the region of 5 months), as would have been required for a traditional cross-over design arising from the long elimination half-life for trametinib-related material. Such a lengthy washout period would potentially

exacerbate any temporal effects between the two dosing sessions, thereby providing inaccurate data (see section 3.6), particularly so in the case of such cancer patients with rapidly declining health.

Interestingly, the human ADME study for trametinib used the highest possible radioactive dose as allowed by the dosimetry calculations (2.9 MBq; tracer of the same specific activity as used in the microtracer study). The reason the authors cited for taking this approach included the fact that although they were aware that AMS was being used in human ADME studies, the data turnaround time would not readily allow discharge of the patients from the study based upon adequate (≥ 90%) mass balance ^{14}C-recovery. This is a reasonable assessment and one of the ongoing limitations of AMS, which could be addressed through use of improvements such as the gas interface approach (section 1.4).

The dabrafenib and trametinib microtracer studies each only used four subjects. The data obtained showed that there was no need for a larger number of subjects in such studies to provide definition of the intravenous pharmacokinetics. At least 12 subjects are often deemed necessary for traditional cross-over design absolute bioavailability studies (Xu et al., 2015)*, (Ghim et al., 2016)* often because of variability arising from temporal effects. For medicines being developed to treat patients with very limited lifespan projection (as was the case for both dabrafenib and trametinib), such reductions in the size and length of the clinical studies assists in overall drug development timelines and delivery of the medicine to those that need it most.

In the case of trametinib the microtracer and human ADME studies were conducted in parallel but as separate studies, but this does raise the intriguing possibility of combining the studies. This would not only save time and resources but could provide data within a single cohort of subjects. This is certainly possible with a variety of options around the study design (for example, see section 4.1). There has been at least one example of a study (Schwab et al., 2013) where a ^{13}C microtracer was included as a concomitant intravenous dose along with ^{14}C-labelled drug administered by the oral route in a double tracer design in a late stage human ADME study.

* As can be seen from the dates of these references, such studies are still being conducted, so there is yet scope for further adoption of the more efficient and scientifically superior microtracer approach.

This seems a very efficient approach where a human ADME study is planned and absolute bioavailability information is required to meet the expectation of regulatory authorities, but has not yet been provided via another clinical study.

4. Future perspectives

4.1. Combination design: Human ADME and Microtracer

The human ADME study is a regulatory requirement for the development of new drugs and although there is no specific requirement for intravenous pharmacokinetics, the regulatory authorities are increasingly requesting these data in the form of an absolute bioavailability study (Arnold and Lacreta, 2012), (EMA, 2015). The current practice is to conduct the human ADME study and absolute bioavailability study separately, in two different cohorts of volunteers. There is an opportunity, however, to combine the two studies into one clinical study, i.e. that in certain circumstances the microtracer design can be combined with the human ADME design. There is also an opportunity to further refine this approach, to address not only development of orally dosed drugs, but also drugs intended for administration by other extravascular routes, e.g. dermal or inhalation.

Administration of ^{14}C-labelled drug by inhalation of dry powder is fraught with logistical difficulties, for the following reasons:

(1) Incorporation of the labeled material into a dry powder, matching the commercial product in terms of physiochemical properties is challenging (e.g. control of fine particle mass and respirable fraction are critical to reproducible delivery to the lung).

(2) Delivery of the dose to the human subject (and reliable quantification of the exhaled dose) is challenging in terms of containment and contamination risks. As detailed earlier (see section 3.4.2), the standard practice for assessment of ADME in humans for inhaled therapies is through administration of ^{14}C-labelled drug by surrogate routes, such as intravenous or oral administration.

(3) Assessment of systemic bioavailability of drug from an administration by inhalation is usually conducted via a clinical study (see section 3.8.4) separate to the human ADME study.

The use of AMS with intravenous administration of a ^{14}C-microtracer makes it feasible to carry out such clinical investigations efficiently. It is difficult to predict the systemic exposure anticipated from an intravenous dose, based upon clinical data following inhalation as there are so many unknowns eg. fraction of the dose delivered from the device, fraction deposited in the lung and swallowed, absorption through the lung and the gut. It is therefore important to keep the intravenous dose as low as possible to minimise the risk of non-equivalent clearance through a marked difference in the concentrations of drug present in the systemic circulation. This would be a higher risk if a traditional cross-over study design was used.

A study combining inhalation and intravenous routes of administration (as well as oral administration) has been designed at GSK for an NCE, GSK961081*, which at the time of writing has just completed the clinical dosing phases.

Data from such a study will provide an understanding of the route specific metabolism of GSK961081, i.e. the comparison of extent of metabolism and biotransformation pathways following intravenous versus oral administration will highlight the impact of first pass metabolism on the relative systemic exposures of GSK961081 and metabolites (see section 3.4.3 and (Lappin and Garner, 2005)). It is important to understand these aspects for drugs under development as metabolites formed by first pass through the (gut wall and) liver may undergo biliary elimination, thereby reducing systemic exposure to unchanged parent drug and drug-related material. These questions can be key because it is otherwise not possible to distinguish absorption from first pass effects in respect to limited bioavailability without the intravenous reference dose. Assuming the drug target is systemic (as opposed, for example, to luminal gut wall) then limited bioavailability has a consequential reduction on

* The study was designed by this author several years ago but was delayed for project development reasons – at that time this particular design had not been conducted previously.

apparent efficacy and a knock-on effect on dose selection. Equally, in the case of patients with hepatic impairment, changes in **hepatic extraction** can lead to safety implications through a change in the pharmacokinetic profile of the drug (Yu et al., 2014).

As discussed previously, mass balance recovery is a regulatory requirement for new medicines. For an inhaled therapy the designs used are a compromise to the ideal assessment of administration of the labelled drug via inhalation, due to the practical limitations mentioned.

Assessment of bioavailability for an inhaled molecule will provide knowledge of the relative contribution to systemic concentrations of the drug via absorption by the lungs and through the gastrointestinal tract. This is key to understanding, for example, the impact on pharmacokinetic variability in patients with compromised ability to inhale the drug.

4.1.1. Objectives

The main objectives of the clinical study will be –

(1) To compare total radioactivity in plasma relative to parent GSK961081, following a single intravenous microtracer of ^{14}C-GSK961081 (concomitant with an inhaled non-radiolabelled therapeutic dose) and a single oral therapeutic dose of ^{14}C-GSK961081.

(2) To determine the recovery and relative excretion of radioactivity in urine and faeces following a single intravenous microtracer of ^{14}C-GSK961081 (concomitant with an inhaled non-radiolabelled therapeutic dose) and a single oral therapeutic dose of ^{14}C-GSK961081.

(3) To estimate the absolute bioavailability of GSK961081 following oral administration and by inhalation.

The clinical study design as outlined in Figure 25 (www.clinicaltrials.gov reference #NCT02663089) incorporates the intravenous microtracer approach concomitant to an inhaled administration (at a supra-therapeutic dose) as one discrete phase of a human ADME study. GSK961081 contains a dual pharmacophore, as shown in Figure 25, with both long-acting β_2 adrenoceptor agonist activity (LABA) and long-acting anti-muscarinic activity (LAMA) in preclinical studies and is being developed for the potential treatment of chronic obstructive pulmonary disease (**COPD**) (Bateman et al., 2013). The second phase of the study will be an oral administration of GSK961081 at a therapeutic equivalent dose, as a cross- over in the same subjects following a washout period (two weeks). The objectives of the study will only be achieved through the use of multiple analytical techniques and approaches, including AMS as a critical technology, due to both the low ^{14}C doses and the nature of the new chemical entity involved, which is anticipated to have very low bioavailability, probably because of low absorption, based upon existing data from animal studies (data on file at GSK).

GSK961081 is susceptible to hydrolysis across the amide moieties (see Figure 25) which would result in a significant proportion of the substructure being without the ^{14}C-label. It is recognised that depending upon the outcome of the human ADME study, it is possible that another ^{14}C-labelled form of GSK961081 may need to be prepared so that the fate of the erstwhile non-labelled metabolite sub-structure can be traced in subsequent studies.

Design:
6 Healthy human subjects; cross-over – washout of 2 weeks minimum between the intravenous /inhaled (session 1) and oral dose (session 2)

(1) Single 1 hour intravenous infusion dose of 4 µg ^{14}C-GSK961081 (6.22 k*Bq*), concomitant to a single inhaled dose of 1200 µg GSK961081
   - [Inhaled dose administered 5 minutes after intravenous infusion start]

(2) Single oral dose of 200 µg [^{14}C]-GSK961081 (322 k*Bq*)

Samples :
- Blood for plasma [for parent drug, RDM concentrations & metabolite profiling]
- Faeces and urine [for mass balance and metabolite profiling]
- Duodenal bile [for metabolite profiling]

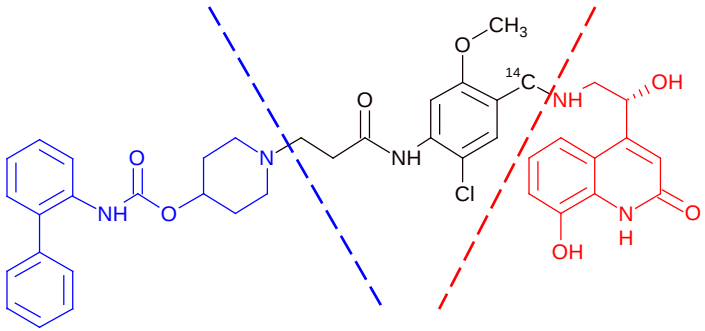

^{14}C-GSK961081*

Main (Planned) data outputs:
- Parent drug concentrations in plasma from inhaled and oral doses (by LC-MS)
- Parent drug concentrations in plasma from intravenous dose (by LC+AMS)
- Total radioactivity in plasma (by direct AMS)
   - Derivation of pharmacokinetic parameters of GSK961081 in plasma
- Excretion mass balance (by direct AMS from intravenous dose; by LSC from oral dose)
- Metabolite profiles (plasma, urine, faeces, bile; by LC+AMS and LC-MS)

Figure 25. Schematic of clinical study design 8 (Potential future publication).

* Regions of pharmacophores; to the left of the blue dashed line is the muscarinic antagonist "head" and to the right of the red dashed line is the β-agonist "head".

4.1.2. Anticipated clinical study endpoints

The total radioactivity measurements in the systemic circulation will likely be provided by analysis by AMS for both intravenous and oral routes, as the concentrations of RDM are anticipated to be too low for analysis by LSC.

Mass balance ^{14}C-recovery will be supported by AMS and LSC for intravenous and oral doses respectively due to the different magnitudes of planned radioactive doses by these routes (6.22 kBq by the intravenous route and 322 kBq by the oral route). The pharmacokinetics of parent drug will be provided by an LC+AMS assay (following intravenous) and by an LC-MS assay (following inhalation and oral administration).

The doses chosen for the study are partly based upon knowledge of the pharmacokinetics of the molecule, but also on the proven understanding of what can be achieved using AMS, as demonstrated through all of the author's previous works.

The intravenous dose will be only 4 μg of ^{14}C-GSK961081 against a concomitant inhaled dose of 1200 μg. The inhalation dose being used is based on prior clinical safety data (Norris and Ambery, 2014) and ease of detection of systemic concentrations of the drug by LC-MS. The intravenous dose was chosen based upon experience that acceptable data should be obtained from this magnitude of dose of drug (and specific activity) (Leonowens et al., 2014) and upon predictions of systemic exposures from the prior clinical studies with GSK961081 (data not shown here).

Following inhalation of drugs to humans, lung deposition is variable and it can be the case that up to ~80% of the dose will be swallowed and delivered to the gastrointestinal tract, rather than deposited in the lung (Thorsson et al., 1998), (Borgstrom et al., 2006), (Newman et al., 2003). At this time, it appears likely that the therapeutic dose for GSK961081 will be around 300 μg by the inhaled route, so the oral dose of 200 μg was chosen based upon an approximation of the fraction of such a therapeutic dose which will be swallowed (rounded for convenience from 240 μg, particularly as this will allow material of the same specific activity to be used for the

intravenous and oral doses, thereby simplifying production and release of the ^{14}C-labelled material).

In this potentially groundbreaking clinical study we will also aim to generate samples that will be used to characterise the metabolite profile of GSK961081 in plasma, urine, faeces, and duodenal bile, to provide a comprehensive understanding of the disposition of GSK961081 in humans. The assessment of biliary elimination, for example, of GSK961081 by AMS following concomitant administration by the intravenous and inhalation routes will only reflect that following intravenous administration, as only the dose following that route of administration is radiolabelled. Nevertheless, along with metabolite profiles from other matrices the information will provide insight into the routes of metabolism and excretion for drug-related material that reaches the systemic circulation. Although these data will be obtained from a non-therapeutic route of administration, it will be representative of a portion of the inhaled dose that enters the systemic circulation and as such still provides valuable information. This will be helpful in building up the overall picture of rates and routes of the ADME of GSK961081 in humans and the mechanisms of drug safety of GSK961081 in humans will be much better understood.

5. Conclusions and Further Work

In the last two decades, AMS has developed from being a little known niche technology, only used as a last resort in drug development, to a more mainstream analytical tool that facilitates flexible clinical study designs, providing deep insights into the pharmacokinetics and metabolic fate of new drugs.

Development of the AMS technology and its application to a variety of clinical studies, through the author's contribution, as evidenced by publications, has been presented in this commentary.

The sensitivity of AMS for detection of ^{14}C-labelled drugs and metabolites has enabled reduced exposure to ionising radiation for human ADME studies, providing safety and ethical improvements that have negated the need for enabling animal studies with less complex dosing formulations and removal of the requirement for dosimetry. AMS has enabled analysis of samples to later timepoints for more complete definition of distribution, metabolism and elimination and microtracer designs. Microtracer studies provide important pharmacokinetic data such as plasma clearance, volume of distribution, absolute bioavailability, definition of extent of first pass metabolism and in combination with bile sample collection, a more thorough understanding of routes of metabolism. A further advance is the use of repeat pulse doses of ^{14}C-labelled drug to allow assessments of ADME-PK under chronic dosing conditions.

Prior to the advent of AMS, some of these experiments required significant resources and supporting safety data, often to such an extent that the studies were not feasible. Some were most probably impossible to perform, such as an intravenous/oral cross-over study with long washout period in patients with progressive disease (for example, as would have been the case for trametinib). Drug development therefore progressed in the absence of data, such as clearance, volume of distribution or absolute bioavailability, which then led to either prolonged development paths or in some cases, increased risk of clinical failure.

Furthermore, the ability to collect duodenal bile from humans non-invasively (the Entero-test™ method), along with the ability to administer ^{14}C more readily by the intravenous route, provided a paradigm shift in the investigation of metabolite burden for drugs under development.

The main contributions to the knowledge highlighted in the commentary were: (1) the first human ADME study supported by AMS for a new drug in development; (2) the investigation of the ADME of a drug with protracted retention in humans; (3) the human ADME of a high dose (thus low specific radioactivity) antibiotic drug; (4) the human ADME for a low dose inhaled respiratory drug by the surrogate route of oral administration; (5) the use of a complex repeat dose ADME study to investigate potential metabolising enzyme autoinduction for a drug in development, and (6) the use of the microtracer approach in oncology patients for two new chemical entities.

A novel combination human ADME and microtracer design was also presented (see section 4) for a drug in development for treatment of COPD, which drew upon the experiences gained through application of AMS over many of the preceding published (and other) works of this author. There has been a recent publication following a similar design, albeit for an oral administration cancer therapy drug, rather than an inhaled therapy (Morcos et al., 2016).

Each of the published studies provided scientific advancement of the technical application of AMS and development of best practices, as well as study design improvements.

This author's view, which seems to be shared by at least some experts in the field of DMPK science (Smith, 2011), (Arnold and Lacreta, 2012), (Lappin, 2016), is that AMS is as yet underutilised and that future years may well demonstrate increased impact of the technology as a more routine tool in drug development. This author hopes to see the ongoing and future development of AMS, to enable a new era of broadened applications (see section 3.6), as well as information rich clinical study designs earlier in drug development. It would be particularly exciting to see the scientific advance of intravenous drug administration as the normal practice, rather than the exception, to provide deep insight into the research of many new medicines.

References

AFFRIME, M. B., CUSS, F., PADHI, D., WIRTH, M., PAI, S., CLEMENT, R. P., LIM, J., KANTESARIA, B., ALTON, K. & CAYEN, M. N. 2000. Bioavailability and metabolism of mometasone furoate following administration by metered-dose and dry-powder inhalers in healthy human volunteers. *J Clin Pharmacol,* 40**,** 1227-1236.

ANNES, W. F., LONG, A., WITCHER, J. W., AYAN-OSHODI, M. A., KNADLER, M. P., ZHANG, W., MITCHELL, M. I., CORNELISSEN, K. & HALL, S. D. 2015. Relative contributions of presystemic and systemic peptidases to oral exposure of a novel metabotropic glutamate 2/3 receptor agonist (LY404039) after oral administration of prodrug pomaglumetad methionil (LY2140023). *J Pharm Sci,* 104**,** 207-214.

ARNOLD, M. E. & LACRETA, F. 2012. When opportunity met aspirational goals: accelerator MS, microdosing and absolute bioavailability studies. *Bioanalysis,* 4**,** 1831-1834.

ATKINSON, A. J., JR., RUO, T. I., PIERGIES, A. A., BREITER, H. C., CONNELLY, T. J., SEDEK, G. S., JUAN, D., HUBLER, G. L. & HSIEH, A. M. 1989. Pharmacokinetics of N-acetylprocainamide in patients profiled with a stable isotope method. *Clin Pharmacol Ther,* 46**,** 182-189.

BATEMAN, E. D., KORNMANN, O., AMBERY, C. & NORRIS, V. 2013. Pharmacodynamics of GSK961081, a bi-functional molecule, in patients with COPD. *Pulm Pharmacol Ther,* 26**,** 581-587.

BENNETT, C. L., BEUKENS, R. P., CLOVER, M. R., GOVE, H. E., LIEBERT, R. B., LITHERLAND, A. E., PURSER, K. H. & SONDHEIM, W. E. 1977. Radiocarbon dating using electrostatic accelerators: negative ions provide the key. *Science,* 198**,** 508-510.

BERSHAS, D. A., OUELLET, D., MAMARIL-FISHMAN, D. B., NEBOT, N., CARSON, S. W., BLACKMAN, S. C., MORRISON, R. A., ADAMS, J. L., JURUSIK, K. E., KNECHT, D. M., GORYCKI, P. D. & RICHARDS-PETERSON, L. E. 2013. Metabolism and disposition of oral dabrafenib in cancer patients: proposed participation of aryl nitrogen in carbon-carbon bond cleavage via decarboxylation following enzymatic oxidation. *Drug Metab Dispos,* 41**,** 2215-2224.

BORGSTROM, L., OLSSON, B. & THORSSON, L. 2006. Degree of throat deposition can explain the variability in lung deposition of inhaled drugs. *J Aerosol Med,* 19**,** 473-483.

BOWERS, G. D., TENERO, D., PATEL, P., HUYNH, P., SIGAFOOS, J., O'MARA, K., YOUNG, G. C., DUMONT, E., CUNNINGHAM, E., KURTINECZ, M., STUMP, P., CONDE, J. J., CHISM, J. P., REESE, M. J., YUEH, Y. L. & TOMAYKO, J. F. 2013. Disposition and metabolism of GSK2251052 in humans: a novel boron-containing antibiotic. *Drug Metab Dispos,* 41**,** 1070-1081.

BOYER, J. L. & BLOOMER, J. R. 1974. Canalicular Bile Secretion in Man studies utilizing the biliary clearance of [^{14}C]mannitol. *The Journal of Clinical Investigation,* 54**,** 773-781.

BRONK, C. R., DITCHFIELD, P. & HUMM, M. 2004. Using a gas ion source for radiocarbon AMS and GC-AMS. *Radiocarbon,* 46**,** 25-32.

BRUIN, G. J., WALDMEIER, F., BOERNSEN, K. O., PFAAR, U., GROSS, G. & ZOLLINGER, M. 2006. A microplate solid scintillation counter as a radioactivity detector for high performance liquid chromatography in drug metabolism: Validation and applications. *Journal of Chromatography A,* 1133**,** 184-194.

BRYANT, D. K., KINGSWOOD, M. D. & BELENGUER, A. 1996. Determination of liquid chromatographic peak purity by electrospray ionization mass spectrometry. *Journal of Chromatography A,* 721**,** 41-51.

BUCHHOLZ, B. A., FULTZ, E., HAACK, K. W., VOGEL, J. S., GILMAN, S. D., GEE, S. J., HAMMOCK, B. D., HUI, X., WESTER, R. C. & MAIBACH, H. I. 1999. HPLC-accelerator MS measurement of atrazine metabolites in human urine after dermal exposure. *Anal Chem,* 71**,** 3519-3525.

CAHN, A., HODGSON, S., WILSON, R., ROBERTSON, J., WATSON, J., BEERAHEE, M., HUGHES, S. C., YOUNG, G., GRAVES, R., HALL, D., VAN MARLE, S. & SOLARI, R. 2013. Safety, tolerability, pharmacokinetics and pharmacodynamics of GSK2239633, a CC-chemokine receptor 4 antagonist, in healthy male subjects: results from an open-label and from a randomised study. *BMC Pharmacol Toxicol,* 14**,** 14.

CANNADY, E. A., ABURUB, A., WARD, C., HINDS, C., CZESKIS, B., RUTERBORIES, K., SUICO, J. G., ROYALTY, J., ORTEGA, D., PACK, B. W., BEGUM, S. L., ANNES, W. F., LIN, Q. & SMALL, D. S. 2015. Absolute bioavailability of evacetrapib in healthy subjects determined by simultaneous administration of oral evacetrapib and intravenous [$^{13}C_8$]-evacetrapib as a tracer. *J Labelled Comp Radiopharm*, 59, 238-244..

CATAFAU, A. M., BULLICH, S., NUCCI, G., BURGESS, C., GRAY, F. & MERLO-PICH, E. 2011. Contribution of SPECT measurements of D2 and 5-HT2A occupancy to the clinical development of the antipsychotic SB-773812. *J Nucl Med,* 52**,** 526-534.

CHEN, J., GARNER, R. C., LEE, L. S., SEYMOUR, M., FUCHS, E. J., HUBBARD, W. C., PARSONS, T. L., PAKES, G. E., FLETCHER, C. V. & FLEXNER, C. 2010. Accelerator mass spectrometry measurement of intracellular concentrations of active drug metabolites in human target cells in vivo. *Clin Pharmacol Ther,* 88**,** 796-800.

CHU, X., BLEASBY, K. & EVERS, R. 2013. Species differences in drug transporters and implications for translating preclinical findings to humans. *Expert Opin Drug Metab Toxicol,* 9**,** 237-252.

CLIFFORD, A. J., ARJOMAND, A., DUEKER, S. R., SCHNEIDER, P. D., BUCHHOLZ, B. A. & VOGEL, J. S. 1998. The dynamics of folic acid metabolism in an adult given a small tracer dose of 14C-folic acid. *Adv Exp Med Biol,* 445**,** 239-251.

DALEY-YATES, P., NORRIS, V., AMBERY, C. & PREECE, A. Early Clinical Evaluation of a Novel 5-Lipoxygenase Activating Protein (FLAP) Inhibitor (GSK2190915A). Pharmacokinetics, Bioavailability and Dose Form Selection: Influence of Age, Food, Drug Interactions and Regional Absorption (LPA112071, LPA112362, LPA114604). Proceedings of the British Pharmacological Society, BPS Winter Meeting, 2012.

DAMGAARD, S. E. 1977. Tritium effect in peroxidation of ehtanol by liver catalase. *Biochem J,* 167**,** 77-86.

DAMON, P. E., DONAHUE, D. J., GORE, B. H., HATHEWAY, A. L., JULL, A. J. T., LINICK, T. W., SERCEL, P. J., TOOLIN, L. J., BRONK, C. R., HALL, E. T., HEDGES, R. E. M., HOUSLEY, R., LAW, I. A., PERRY, C., BONANI, G., TRUMBORE, S., WOELFLI, W., AMBERS, J. C., BOWMAN, S. G. E., LEESE, M. N. & TITE, M. S. 1989. Radiocarbon dating of the Shroud of Turin. *Nature,* 337**,** 611-615.

DANIEL, R., MORES, M., KITCHEN, R., SUNDQUIST, M., HAUSER, T., STODOLA, M., TANNENBAUM, S., SKIPPER, P., LIBERMAN, R., YOUNG, G., CORLESS, S. & TUCKER, M. 2013. Development of a commercial Automated Laser Gas Interface (ALGI) for AMS. *Nuclear Instruments and Methods in Physics Research Section B: Beam Interactions with Materials and Atoms,* 294**,** 291-295.

DAVE, M., NASH, M., YOUNG, G. C., ELLENS, H., MAGEE, M. H., ROBERTS, A. D., TAYLOR, M. A., GREENHILL, R. W. & BOYLE, G. W. 2014. Disposition and metabolism of darapladib, a lipoprotein-associated phospholipase A2 inhibitor, in humans. *Drug Metab Dispos,* 42**,** 415-430.

DAVIES, B. & MORRIS, T. 1993. Physiological parameters in laboratory animals and humans. *Pharm Res,* 10**,** 1093-1095.

DE VRIES, R., SMIT, J. W., HELLEMANS, P., JIAO, J., MURPHY, J., SKEE, D., SNOEYS, J., SUKBUNTHERNG, J., VLIEGEN, M., DE ZWART, L., MANNAERT, E. & DE JONG, J. 2016. Stable isotope-labelled intravenous microdose for absolute bioavailability and effect of grapefruit juice on ibrutinib in healthy adults. *Br J Clin Pharmacol,* 81**,** 235-245.

DEAR, G. J., ROBERTS, A. D., BEAUMONT, C. & NORTH, S. E. 2008. Evaluation of preparative high performance liquid chromatography and cryoprobe-nuclear magnetic resonance

spectroscopy for the early quantitative estimation of drug metabolites in human plasma. *J Chromatogr B Analyt Technol Biomed Life Sci,* 876**,** 182-190.

DENTON, C. L., MINTHORN, E., CARSON, S. W., YOUNG, G. C., RICHARDS-PETERSON, L. E., BOTBYL, J., HAN, C., MORRISON, R. A., BLACKMAN, S. C. & OUELLET, D. 2013. Concomitant Oral and Intravenous Pharmacokinetics of Dabrafenib, a BRAF Inhibitor, in Patients with BRAF V600 Mutation-Positive Solid Tumors. *The Journal of Clinical Pharmacology,* 53**,** 955-961.

DUFEK, M. B., BRIDGES, A. S. & THAKKER, D. R. 2013. Intestinal first-pass metabolism by cytochrome p450 and not p-glycoprotein is the major barrier to amprenavir absorption. *Drug Metab Dispos,* 41**,** 1695-1702.

EMA 2001. Note for Guidance on the Investigation of Bioavailability and Bioequivalence. *In:* (CPMP), C. F. P. M. P. (ed.). EMA Website www.ema.europa.eu.

EMA 2013. Guideline on the Investigation of Drug Interactions. *In:* (CHMP), C. F. H. M. P. (ed.). Website www.ema.europa.eu.

EMA 2015. Questions & Answers: positions on specific questions addressed to the Pharmacokinetics Working Party (PKWP). *In:* AGENCY, E. M. (ed.) *EMA/618604/2008 Rev. 12.* Website www.ema.europa.eu.

ERIKSSON, C. J., FUKUNAGA, T., SARKOLA, T., CHEN, W. J., CHEN, C. C., JU, J. M., CHENG, A. T., YAMAMOTO, H., KOHLENBERG-MULLER, K., KIMURA, M., MURAYAMA, M., MATSUSHITA, S., KASHIMA, H., HIGUCHI, S., CARR, L., VILJOEN, D., BROOKE, L., STEWART, T., FOROUD, T., SU, J., LI, T. K. & WHITFIELD, J. B. 2001. Functional relevance of human ADH polymorphism. *Alcohol Clin Exp Res,* 25**,** 157s-163s.

FAGERHOLM, U. 2008. Prediction of human pharmacokinetics-biliary and intestinal clearance and enterohepatic circulation. *J Pharm Pharmacol,* 60**,** 535-542.

FDA 2008. Guidance for Industry - Safety Testing of Drug Metabolites. *In:* ADMINISTRATION, U. F. A. D. (ed.). Website http://www.fda.gov/cder/guidance/index.htm.

FDA 2012. Guidance for Industry Drug Interaction Studies *In:* ADMINISTRATION, U. F. A. D. (ed.). Website http://www.fda.gov/Drugs/GuidanceComplianceRegulatoryInformation/Guidances/default.htm.

FDA 2015. Prescribing information for Trametinib. *In:* SERVICES, U. D. O. H. H. A. (ed.). FDA Website.

GARNER, R. C., BARKER, J., FLAVELL, C., GARNER, J. V., WHATTAM, M., YOUNG, G. C., CUSSANS, N., JEZEQUEL, S. & LEONG, D. 2000. A validation study comparing accelerator MS and liquid scintillation counting for analysis of 14C-labelled drugs in plasma, urine and faecal extracts. *J Pharm Biomed Anal,* 24**,** 197-209.

GARNER, R. C., GORIS, I., LAENEN, A. A., VANHOUTTE, E., MEULDERMANS, W., GREGORY, S., GARNER, J. V., LEONG, D., WHATTAM, M., CALAM, A. & SNEL, C. A. 2002. Evaluation of accelerator mass spectrometry in a human mass balance and pharmacokinetic study-experience with ^{14}C-labeled (R)-6-[amino(4- chlorophenyl)(1-methyl-1H-imidazol-5-yl)methyl]-4-(3-chlorophenyl)-1- methyl-2(1H)-quinolinone (R115777), a farnesyl transferase inhibitor. *Drug Metab Dispos,* 30**,** 823-830.

GARRISON, K. L., SAHIN, S. & BENET, L. Z. 2015. Few Drugs Display Flip-Flop Pharmacokinetics and These Are Primarily Associated with Classes 3 and 4 of the BDDCS. *J Pharm Sci,* 104**,** 3229-3235.

GHIM, J. L., PAIK, S. H., HASANUZZAMAN, M., CHI, Y. H., CHOI, H. K., KIM, D. H. & SHIN, J. G. 2016. Absolute bioavailability and pharmacokinetics of the angiotensin II receptor antagonist fimasartan in healthy subjects. *J Clin Pharmacol,* 56**,** 576-580.

GILMARTIN, A. G., BLEAM, M. R., GROY, A., MOSS, K. G., MINTHORN, E. A., KULKARNI, S. G., ROMINGER, C. M., ERSKINE, S., FISHER, K. E., YANG, J., ZAPPACOSTA, F., ANNAN, R., SUTTON, D. & LAQUERRE, S. G. 2011. GSK1120212 (JTP-74057) is an inhibitor of MEK activity and activation with favorable pharmacokinetic properties for sustained in vivo pathway inhibition. *Clin Cancer Res,* 17**,** 989-1000.

GSK. 2016. *GSK Clinical Trials Register* [Online]. http://www.gsk-clinicalstudyregister.com/compounds/vilanterol/all/1/#. Available: http://www.gsk-clinicalstudyregister.com/compounds/vilanterol/all/1/#.

GUINEY, W. J., BEAUMONT, C., THOMAS, S. R., ROBERTSON, D. C., MCHUGH, S. M., KOCH, A. & RICHARDS, D. 2011. Use of Entero-Test, a simple approach for non-invasive clinical evaluation of the biliary disposition of drugs. *Br J Clin Pharmacol,* 72**,** 133-142.

HARRELL, A. W., SIEDERER, S. K., BAL, J., PATEL, N. H., YOUNG, G. C., FELGATE, C. C., PEARCE, S. J., ROBERTS, A. D., BEAUMONT, C., EMMONS, A. J., PEREIRA, A. I. & KEMPSFORD, R. D. 2013. Metabolism and disposition of vilanterol, a long-acting β(2)-adrenoceptor agonist for inhalation use in humans. *Drug Metab Dispos,* 41**,** 89-100.

HAWKSWORTH, G., DRASAR, B. S. & HILL, M. J. 1971. Intestinal bacteria and the hydrolysis of glycosidic bonds. *J Med Microbiol,* 4**,** 451-459.

HEIKKINEN, H., SARAHEIMO, M., ANTILA, S., OTTOILA, P. & PENTIKAINEN, P. J. 2001. Pharmacokinetics of entacapone, a peripherally acting catechol-O-methyltransferase inhibitor, in man. A study using a stable isotope techique. *Eur J Clin Pharmacol,* 56**,** 821-826.

HEINEMEIER, K. M., SCHJERLING, P., HEINEMEIER, J., MAGNUSSON, S. P. & KJAER, M. 2013. Lack of tissue renewal in human adult Achilles tendon is revealed by nuclear bomb (14)C. *Faseb j,* 27**,** 2074-2079.

HIGTON, D., YOUNG, G., TIMMERMAN, P., ABBOTT, R., KNUTSSON, M. & SVENSSON, L. D. 2012. European Bioanalysis Forum recommendation: scientific validation of quantification by accelerator mass spectrometry. *Bioanalysis,* 4**,** 2669-2679.

HIROM, P. C., MILLBURN, P., SMITH, R. L. & WILLIAMS, R. T. 1972. Species variations in the threshold molecular-weight factor for the biliary excretion of organic anions. *Biochem J,* 129**,** 1071-1077.

HO, M. Y., MORRIS, M. J., PIRHALLA, J. L., BAUMAN, J. W., PENDRY, C. B., ORFORD, K. W., MORRISON, R. A. & COX, D. S. 2014. Trametinib, a first-in-class oral MEK inhibitor mass balance study with limited enrollment of two male subjects with advanced cancers. *Xenobiotica,* 44**,** 352-368.

HOFFMANN, E., WALD, J., LAVU, S., ROBERTS, J., BEAUMONT, C., HADDAD, J., ELLIOTT, P., WESTPHAL, C. & JACOBSON, E. 2013. Pharmacokinetics and tolerability of SRT2104, a first-in-class small molecule activator of SIRT1, after single and repeated oral administration in man. *British Journal of Clinical Pharmacology,* 75**,** 186-196.

HOP, C. E., WANG, Z., CHEN, Q. & KWEI, G. 1998. Plasma-pooling methods to increase throughput for in vivo pharmacokinetic screening. *J Pharm Sci,* 87**,** 901-903.

HUGHES, S. C., SHARDLOW, P. C., HOLLIS, F. J., SCOTT, R. J., MOTIVARAS, D. S., ALLEN, A. & ROUSELL, V. M. 2008. Metabolism and disposition of fluticasone furoate, an enhanced-affinity glucocorticoid, in humans. *Drug Metab Dispos,* 36**,** 2337-2344.

ICH 2009. Guidance on nonclinical safety studies for the conduct of human clinical trials and marketing authorization for pharmaceuticals *In:* USE, I. C. O. H. O. T. R. F. R. O. P. F. H. (ed.). Website http://www.ich.org/fileadmin/Public_Web_Site/ICH_Products/Guidelines/Multidisciplinary/M3_R2/Step4/M3_R2__Guideline.pdf.

ICH 2011. Guidance on genotoxicity testing and data interpretation for pharmaceuticals intended for human use. *In:* USE, I. C. O. H. O. T. R. F. R. O. P. F. H. (ed.). Website http://www.ich.org/fileadmin/Public_Web_Site/ICH_Products/Guidelines/Safety/S2_R1/Step4/S2R1_Step4.pdf.

ICRP 1992. Radiological Protection in Biomedical Research. *In:* ICRP (ed.) *Ann. ICRP 22 (3).* ICRP Website; http://www.icrp.org/publication.asp?id=ICRP Publication 62.

INFANTE, J. R., FECHER, L. A., FALCHOOK, G. S., NALLAPAREDDY, S., GORDON, M. S., BECERRA, C., DEMARINI, D. J., COX, D. S., XU, Y., MORRIS, S. R., PEDDAREDDIGARI, V. G., LE, N. T., HART, L., BENDELL, J. C., ECKHARDT, G., KURZROCK, R., FLAHERTY, K., BURRIS, H. A., 3RD & MESSERSMITH, W. A. 2012. Safety, pharmacokinetic, pharmacodynamic, and

efficacy data for the oral MEK inhibitor trametinib: a phase 1 dose-escalation trial. *Lancet Oncol,* 13**,** 773-781.

INGS, R. M. 2009. Microdosing: a valuable tool for accelerating drug development and the role of bioanalytical methods in meeting the challenge. *Bioanalysis,* 1**,** 1293-1305.

IONPLUS. 2016. *AGE 3 - Automated Graphitization System* [Online]. Available: http://www.ionplus.ch/products/age-3/.

IVERSON, S. & SMITH, D. A. 2016. *Metabolite Safety in Drug Development (Chapter 12),*, John Wiley & Sons.

IYER, G. R., PATEL, Y. & TEUSCHER, N. S. 2012. A Novel Study Using Accelerated Mass Spectrometry to Evaluate the Pharmacokinetics of Total 14C AL-8309 (Tandospirone) Following Topical Ocular Administration in Healthy Male Subjects. *Clinical Pharmacology in Drug Development,* 1**,** 4-13.

JIANG, H., ZENG, J., LI, W., BIFANO, M., GU, H., TITSCH, C., EASTER, J., BURRELL, R., KANDOUSSI, H., AUBRY, A. F. & ARNOLD, M. E. 2012. Practical and efficient strategy for evaluating oral absolute bioavailability with an intravenous microdose of a stable isotopically-labeled drug using a selected reaction monitoring mass spectrometry assay. *Anal Chem,* 84**,** 10031-10037.

JUSKO, W. J., KOUP, J. R. & ALVAN, G. 1976. Nonlinear assessment of phenytoin bioavailability. *J Pharmacokinet Biopharm,* 4**,** 327-336.

KAGAN, M., DAIN, J., PENG, L. & REYNOLDS, C. 2012. Metabolism and pharmacokinetics of indacaterol in humans. *Drug Metab Dispos,* 40**,** 1712-1722.

KAUFMANN, A. M. & KRISE, J. P. 2007. Lysosomal sequestration of amine-containing drugs: analysis and therapeutic implications. *J Pharm Sci,* 96**,** 729-746.

KAYE, B., GARNER, R. C., MAUTHE, R. J., FREEMAN, S. P. H. T. & TURTELTAUB, K. W. 1997. A preliminary evaluation of accelerator mass spectrometry in the biomedical field. *Journal of Pharmaceutical and Biomedical Analysis,* 16**,** 541-543.

KECK, B. D., OGNIBENE, T. & VOGEL, J. S. 2010. Analytical validation of accelerator mass spectrometry for pharmaceutical development. *Bioanalysis,* 2**,** 469-485.

KIM, S. H., CHUANG, J. C., KELLY, P. B. & CLIFFORD, A. J. 2011. Carbon isotopes profiles of human whole blood, plasma, red blood cells, urine and feces for biological/biomedical 14C-accelerator mass spectrometry applications. *Anal Chem,* 83**,** 3312-3318.

KLODY, G. M., SCHROEDER, J. B., NORTON, G. A., LOGER, R. L., KITCHEN, R. L. & SUNDQUIST, M. L. 2005. New results for single stage low energy carbon AMS. *Nuclear Instruments and Methods in Physics Research Section B: Beam Interactions with Materials and Atoms,* 240**,** 463-467.

KOSOGLOU, T., STATKEVICH, P., JOHNSON-LEVONAS, A. O., PAOLINI, J. F., BERGMAN, A. J. & ALTON, K. B. 2005. Ezetimibe: a review of its metabolism, pharmacokinetics and drug interactions. *Clin Pharmacokinet,* 44**,** 467-494.

KUTSCHERA, W. 2013. Applications of accelerator mass spectrometry. *International Journal of Mass Spectrometry,* 349–350**,** 203-218.

KWON, Y. 2001. *Metabolism, in Handbook of essential pharmacokinetics, pharmacodynamics and drug metabolism for industrial scientists,* New York, Springer-Verlag.

LAPPIN, G. 2015. A historical perspective on radioisotopic tracers in metabolism and biochemistry. *Bioanalysis,* 7**,** 531-540.

LAPPIN, G. 2016. Approaches to intravenous clinical pharmacokinetics: Recent developments with isotopic microtracers. *The Journal of Clinical Pharmacology,* 56**,** 11-23.

LAPPIN, G., BOYCE, M. J., MATZOW, T., LOCIURO, S., SEYMOUR, M. & WARRINGTON, S. J. 2013a. A microdose study of (^{14})C-AR-709 in healthy men: pharmacokinetics, absolute bioavailability and concentrations in key compartments of the lung. *Eur J Clin Pharmacol,* 69**,** 1673-1682.

LAPPIN, G. & GARNER, R. C. 2005. The use of accelerator mass spectrometry to obtain early human ADME/PK data. *Expert Opinion on Drug Metabolism & Toxicology,* 1**,** 23-31.

LAPPIN, G., GARNER, R. C., MEYERS, T., POWELL, J. & VARLEY, P. 2006. Novel use of accelerator mass spectrometry for the quantification of low levels of systemic therapeutic recombinant protein. *Journal of Pharmaceutical and Biomedical Analysis,* 41**,** 1299-1302.

LAPPIN, G., NOVECK, R. & BURT, T. 2013b. Microdosing and drug development: past, present and future. *Expert Opin Drug Metab Toxicol,* 9**,** 817-834.

LAPPIN, G., SIMPSON, M., SHISHIKURA, Y. & GARNER, C. 2008. High-performance liquid chromatography accelerator mass spectrometry: correcting for losses during analysis by internal standardization. *Anal Biochem,* 378**,** 93-95.

LAPPIN, G. & TEMPLE, S. 2006. *Radiotracers in Drug Development - Chapter 7*, CRC Press.

LEE, J. J., SERAJ, J., YOSHIDA, K., MIZUGUCHI, H., STRYCHOR, S., FIEJDASZ, J., FAULKNER, T., PARISE, R. A., FAWCETT, P., POLLICE, L., MASON, S., HAGUE, J., CROFT, M., NUGTEREN, J., TEDDER, C., SUN, W., CHU, E. & BEUMER, J. H. 2016. Human mass balance study of TAS-102 using 14C analyzed by accelerator mass spectrometry. *Cancer Chemotherapy and Pharmacology,* 77**,** 515-526.

LENNERNAS, H., AHRENSTEDT, O., HALLGREN, R., KNUTSON, L., RYDE, M. & PAALZOW, L. K. 1992. Regional jejunal perfusion, a new in vivo approach to study oral drug absorption in man. *Pharm Res,* 9**,** 1243-1251.

LEONOWENS, C., PENDRY, C., BAUMAN, J., YOUNG, G. C., HO, M., HENRIQUEZ, F., FANG, L., MORRISON, R. A., ORFORD, K. & OUELLET, D. 2014. Concomitant oral and intravenous pharmacokinetics of trametinib, a MEK inhibitor, in subjects with solid tumours. *British Journal of Clinical Pharmacology,* 78**,** 524-532.

MA, S. & CHOWDHURY, S. K. 2016. The use of stable isotope-labeled drug as microtracers with conventional LC–MS/MS to support human absolute bioavailability studies: are we there yet? *Bioanalysis,* 8**,** 731-733.

MAHAR, K. M., SEHON, C., TAI, G., HAWS, T., HOWE, D., YOUNG, G. & DANOFF, T. Comparison of a GSK706769 Microdose CYP3A4 Drug-Drug Interaction Study With a Previous Pharmacological Dose Study. 2012 American College of Clinical Pharmacology, Annual Meeting September 23rd-25th, 2012.

MAMARIL-FISHMAN, D., ZHU, J., LIN, M., FELGATE, C., JONES, L., STUMP, P., PIERRE, E., BOWEN, C., NADERER, O., DUMONT, E., PATEL, P., GORYCKI, P. D., WEN, B., CHEN, L. & DENG, Y. 2014. Investigation of metabolism and disposition of GSK1322322, a peptidase deformylase inhibitor, in healthy humans using the entero-test for biliary sampling. *Drug Metab Dispos,* 42**,** 1314-1325.

MENDES, R. E., ALLEY, M. R., SADER, H. S., BIEDENBACH, D. J. & JONES, R. N. 2013. Potency and spectrum of activity of AN3365, a novel boron-containing protein synthesis inhibitor, tested against clinical isolates of Enterobacteriaceae and nonfermentative Gram-negative bacilli. *Antimicrob Agents Chemother,* 57**,** 2849-2857.

MOOIJ, M. G., VAN DUIJN, E., KNIBBE, C. A., WINDHORST, A. D., HENDRIKSE, N. H., VAES, W. H., SPAANS, E., FABRIEK, B. O., SANDMAN, H., GROSSOUW, D., HANFF, L. M., JANSSEN, P. J., KOCH, B. C., TIBBOEL, D. & DE WILDT, S. N. 2014. Pediatric microdose study of [(14)C]paracetamol to study drug metabolism using accelerated mass spectrometry: proof of concept. *Clin Pharmacokinet,* 53**,** 1045-1051.

MOOK, W. G. & PLICHT VAN DER, J. 1999. Reporting 14C Activities and Concentrations. *Radiocarbon,* 41**,** 227-239.

MORCOS, P. N., YU, L., BOGMAN, K., SATO, M., KATSUKI, H., KAWASHIMA, K., MOORE, D. J., WHAYMAN, M., NIEFORTH, K., HEINIG, K., GUERINI, E., MURI, D., MARTIN-FACKLAM, M. & PHIPPS, A. 2016. Absorption, distribution, metabolism and excretion (ADME) of the ALK inhibitor alectinib: results from an absolute bioavailability and mass balance study in healthy subjects. *Xenobiotica***,** 1-13.

MORRIS, C. A., DUEKER, S. R., LOHSTROH, P. N., WANG, L. Q., FANG, X. P., JUNG, D., LOPEZ-LAZARO, L., BAKER, M., DUPARC, S., BORGHINI-FUHRER, I., POKORNY, R., SHIN, J. S. &

FLECKENSTEIN, L. 2015. Mass balance and metabolism of the antimalarial pyronaridine in healthy volunteers. *Eur J Drug Metab Pharmacokinet,* 40**,** 75-86.

NEGASH, K., ANDONIAN, C., FELGATE, C., CHEN, C., GOLJER, I., SQUILLACI, B., NGUYEN, D., PIRHALLA, J., LEV, M., SCHUBERT, E., TIFFANY, C., HOSSAIN, M. & HO, M. 2016. The metabolism and disposition of GSK2140944 in healthy human subjects. *Xenobiotica***,** 46, 683-702.

NEWMAN, S. P., PITCAIRN, G. R., HIRST, P. H. & RANKIN, L. 2003. Radionuclide imaging technologies and their use in evaluating asthma drug deposition in the lungs. *Adv Drug Deliv Rev,* 55**,** 851-867.

NIEMI, M., BACKMAN, J. T., FROMM, M. F., NEUVONEN, P. J. & KIVISTÖ, K. T. 2003. Pharmacokinetic Interactions with Rifampicin. *Clinical Pharmacokinetics,* 42**,** 819-850.

NILIUS, R. R. 1983. Aldehyde dehydrogenase (E.C. 1.2.1.3) in chronic alcoholic liver diseases. *Hepato-gastroenterology,* 30**,** 134-136.

NORRIS, V. & AMBERY, C. 2014. Use of propranolol blockade to explore the pharmacology of GSK961081, a bi-functional bronchodilator, in healthy volunteers: results from two randomized trials. *Drugs R D,* 14**,** 241-251.

PATRICK, J. E., KOSOGLOU, T., STAUBER, K. L., ALTON, K. B., MAXWELL, S. E., ZHU, Y., STATKEVICH, P., IANNUCCI, R., CHOWDHURY, S., AFFRIME, M. & CAYEN, M. N. 2002. Disposition of the selective cholesterol absorption inhibitor ezetimibe in healthy male subjects. *Drug Metab Dispos,* 30**,** 430-437.

PRESTON, S. L., DRUSANO, G. L., GLUE, P., NASH, J., GUPTA, S. K. & MCNAMARA, P. 1999. Pharmacokinetics and absolute bioavailability of ribavirin in healthy volunteers as determined by stable-isotope methodology. *Antimicrob Agents Chemother,* 43**,** 2451-2456.

RICKERT, D. E., DINGLEY, K., UBICK, E., DIX, K. J. & MOLINA, L. 2005. Determination of the tissue distribution and excretion by accelerator mass spectrometry of the nonadecapeptide ^{14}C-Moli1901 in beagle dogs after intratracheal instillation. *Chem Biol Interact,* 155**,** 55-61.

ROBERTS, M. L., VON REDEN, K. F., BURTON, J. R., MCINTYRE, C. P. & BEAUPRÉ, S. R. 2013. A gas-accepting ion source for Accelerator Mass Spectrometry: Progress and applications. *Nuclear Instruments and Methods in Physics Research Section B: Beam Interactions with Materials and Atoms,* 294**,** 296-299.

ROESKE, C. A. & O'LEARY, M. H. 1985. Carbon isotope effect on carboxylation of ribulose bisphosphate catalyzed by ribulosebisphosphate carboxylase from Rhodospirillum rubrum. *Biochemistry,* 24**,** 1603-1607.

ROFFEY, S. J., OBACH, R. S., GEDGE, J. I. & SMITH, D. A. 2007. What is the objective of the mass balance study? A retrospective analysis of data in animal and human excretion studies employing radiolabeled drugs. *Drug Metab Rev,* 39**,** 17-43.

ROWLAND, M., BENET, L. Z. & GRAHAM, G. G. 1973. Clearance concepts in pharmacokinetics. *J Pharmacokinet Biopharm,* 1**,** 123-136.

RUHM, W., CARROLL, K. L., EGBERT, S. D., FAESTERMANN, T., KNIE, K., KORSCHINEK, G., MARTINELLI, R. E., MARCHETTI, A. A., MCANINCH, J. E., RUGEL, G., STRAUME, T., WALLNER, A., WALLNER, C., FUJITA, S., HASAI, H., HOSHI, M. & SHIZUMA, K. 2007. Neutron-induced 63Ni in copper samples from Hiroshima and Nagasaki: a comprehensive presentation of results obtained at the Munich Maier-Leibnitz Laboratory. *Radiat Environ Biophys,* 46**,** 327-338.

SALEHPOUR, M., POSSNERT, G. & BRYHNI, H. 2008. Subattomole sensitivity in biological accelerator mass spectrometry. *Anal Chem,* 80**,** 3515-3521.

SCHWAB, D., PORTRON, A., BACKHOLER, Z., LAUSECKER, B. & KAWASHIMA, K. 2013. A novel double-tracer technique to characterize absorption, distribution, metabolism and excretion (ADME) of [^{14}C]tofogliflozin after oral administration and concomitant intravenous microdose administration of [^{13}C]tofogliflozin in humans. *Clin Pharmacokinet,* 52**,** 463-473.

SHAPIRO, S. D., ENDICOTT, S. K., PROVINCE, M. A., PIERCE, J. A. & CAMPBELL, E. J. 1991. Marked longevity of human lung parenchymal elastic fibers deduced from prevalence of D-aspartate and nuclear weapons-related radiocarbon. *J Clin Invest,* 87**,** 1828-1834.

SIMPSON, M., LAPPIN, G. & KEELY, B. J. 2010. Development of 2D chiral chromatography with accelerator mass spectrometry for quantification of (^{14})C-labeled R- and S-verapamil in plasma. *Bioanalysis,* 2**,** 397-405.

SMITH, D. A. 2011. The debate is over: accelerator MS provides the route to better drug-development paradigms/protocols. *Bioanalysis,* 3**,** 391-392.

STEWART, B. J., NAVID, A., TURTELTAUB, K. W. & BENCH, G. 2010. Yeast dynamic metabolic flux measurement in nutrient-rich media by HPLC and accelerator mass spectrometry. *Anal Chem,* 82**,** 9812-9817.

STRONG, J. M., DUTCHER, J. S., LEE, W.-K. & ATKINSON, A. J. 1975. Absolute bioavailability in man of N-acetylprocainamide determined by a novel stable isotope method. *Clinical Pharmacology & Therapeutics,* 18**,** 613-622.

SYNAL, H.-A. 2013. Developments in accelerator mass spectrometry. *International Journal of Mass Spectrometry,* 349–350**,** 192-202.

SYNAL, H. A., JACOB, S. & SUTER, M. 2000. New concepts for radiocarbon detection systems. *Nuclear Instruments and Methods in Physics Research Section B: Beam Interactions with Materials and Atoms,* 161–163**,** 29-36.

THOMAS, A. T., STEWART, B. J., OGNIBENE, T. J., TURTELTAUB, K. W. & BENCH, G. 2013. Directly coupled high-performance liquid chromatography-accelerator mass spectrometry measurement of chemically modified protein and peptides. *Anal Chem,* 85**,** 3644-3650.

THORSSON, L., KENYON, C., NEWMAN, S. P. & BORGSTRÖM, L. 1998. Lung deposition of budesonide in asthmatics: a comparison of different formulations. *International Journal of Pharmaceutics,* 168**,** 119-127.

TORRES, R., DRESSMAN, M. A., KRAMER, W. G. & BAROLDI, P. 2015. Absolute Bioavailability of Tasimelteon. *Am J Ther,* 22**,** 355-360.

TURSI, A. 2016. Diverticulosis today: unfashionable and still under-researched. *Therap Adv Gastroenterol,* 9**,** 213-228.

TURTELTAUB, K. W., MAUTHE, R. J., DINGLEY, K. H., VOGEL, J. S., FRANTZ, C. E., GARNER, R. C. & SHEN, N. 1997. MeIQx-DNA adduct formation in rodent and human tissues at low doses. *Mutat Res,* 376**,** 243-252.

VAN DUIJN, E., SANDMAN, H., GROSSOUW, D., MOCKING, J. A., COULIER, L. & VAES, W. H. 2014. Automated combustion accelerator mass spectrometry for the analysis of biomedical samples in the low attomole range. *Anal Chem,* 86**,** 7635-7641.

VLAMING, M. L. H., VAN DUIJN, E., DILLINGH, M. R., BRANDS, R., WINDHORST, A. D., HENDRIKSE, N. H., BOSGRA, S., BURGGRAAF, J., DE KONING, M. C., FIDDER, A., MOCKING, J. A. J., SANDMAN, H., DE LIGT, R. A. F., FABRIEK, B. O., PASMAN, W. J., SEINEN, W., ALVES, T., CARRONDO, M., PEIXOTO, C., PEETERS, P. A. M. & VAES, W. H. J. 2015. Microdosing of a Carbon-14 Labeled Protein in Healthy Volunteers Accurately Predicts Its Pharmacokinetics at Therapeutic Dosages. *Clinical Pharmacology & Therapeutics,* 98**,** 196-204.

VOGEL, J. S. 1992. Rapid production of graphite for biomedical AMS. *Radiocarbon,* 34**,** 344-350.

VOGEL, J. S., GIACOMO, J. A., SCHULZE-KONIG, T., KECK, B. D., LOHSTROH, P. & DUEKER, S. 2010. Accelerator mass spectrometry best practices for accuracy and precision in bioanalytical (^{14})C measurements. *Bioanalysis,* 2**,** 455-468.

VOGEL, J. S. & LOVE, A. H. 2005. Quantitating Isotopic Molecular Labels with Accelerator Mass Spectrometry. *Methods in Enzymology.* Academic Press.

WACKER, L., FAHRNI, S. M., HAJDAS, I., MOLNAR, M., SYNAL, H. A., SZIDAT, S. & ZHANG, Y. L. 2013. A versatile gas interface for routine radiocarbon analysis with a gas ion source. *Nuclear Instruments and Methods in Physics Research Section B: Beam Interactions with Materials and Atoms,* 294**,** 315-319.

WAGNER, C., SIMPSON, M., ZEITLINGER, M., BAUER, M., KARCH, R., ABRAHIM, A., FEURSTEIN, T., SCHÜTZ, M., KLETTER, K., MÜLLER, M., LAPPIN, G. & LANGER, O. 2011. A Combined Accelerator Mass Spectrometry-Positron Emission Tomography Human Microdose Study with 14C- and 11C-Labelled Verapamil. *Clinical Pharmacokinetics,* 50**,** 111-120.

WANG, B., JACKSON, G. S., YOKEL, R. A. & GRULKE, E. A. 2014. Applying accelerator mass spectrometry for low-level detection of complex engineered nanoparticles in biological media. *J Pharm Biomed Anal,* 97**,** 81-87.

WARD, K. W., HARDY, L. B., KEHLER, J. R., AZZARANO, L. M. & SMITH, B. R. 2004. Apparent absolute oral bioavailability in excess of 100% for a vitronectin receptor antagonist (SB-265123) in rat. II. Studies implicating transporter-mediated intestinal secretion. *Xenobiotica,* 34**,** 367-377.

WU, C. Y. & BENET, L. Z. 2005. Predicting drug disposition via application of BCS: transport/absorption/ elimination interplay and development of a biopharmaceutics drug disposition classification system. *Pharm Res,* 22**,** 11-23.

XU, H., O'GORMAN, M., BOUTROS, T., BREGA, N., KANTARIDIS, C., TAN, W. & BELLO, A. 2015. Evaluation of crizotinib absolute bioavailability, the bioequivalence of three oral formulations, and the effect of food on crizotinib pharmacokinetics in healthy subjects. *J Clin Pharmacol,* 55**,** 104-113.

XU, X. S., DUEKER, S. R., CHRISTOPHER, L. J., LOHSTROH, P. N., KEUNG, C. F., CAO, K. K., BONACORSI, S. J., COJOCARU, L., SHEN, J. X., HUMPHREYS, W. G., STOUFFER, B. & ARNOLD, M. E. 2012. Overcoming bioanalytical challenges in an Onglyza((R)) intravenous [(14)C]microdose absolute bioavailability study with accelerator MS. *Bioanalysis,* 4**,** 1855-1870.

XU, X. S., JIANG, H., CHRISTOPHER, L. J., SHEN, J. X., ZENG, J. & ARNOLD, M. E. 2014. Sensitivity-based analytical approaches to support human absolute bioavailability studies. *Bioanalysis,* 6**,** 497-504.

YANG, X. & LIU, K. 2016. P-gp Inhibition-Based Strategies for Modulating Pharmacokinetics of Anticancer Drugs: An Update. *Curr Drug Metab*, 17, 806-826.

YOUNG, G., ELLIS, W., AYRTON, J., HUSSEY, E. & ADAMKIEWICZ, B. 2001. Accelerator mass spectrometry (AMS): recent experience of its use in a clinical study and the potential future of the technique. *Xenobiotica,* 31**,** 619-632.

YOUNG, G. C., CORLESS, S., FELGATE, C. C. & COLTHUP, P. V. 2008. Comparison of a 250 kV single-stage accelerator mass spectrometer with a 5 MV tandem accelerator mass spectrometer--fitness for purpose in bioanalysis. *Rapid Commun Mass Spectrom,* 22**,** 4035-42.

YOUNG, G. C. & ELLIS, W. J. 2007. AMS in drug development at GSK. *Nuclear Instruments and Methods in Physics Research Section B: Beam Interactions with Materials and Atoms,* 259**,** 752-757.

YOUNG, G. C. & SEYMOUR, M. 2015. Application of (^{14})C-accelerator MS in pharmaceutical development. *Bioanalysis,* 7**,** 513-517.

YOUNG, G. C., SEYMOUR, M., DUEKER, S. R., TIMMERMAN, P., ARJOMAND, A. & NOZAWA, K. 2014. New frontiers-accelerator mass spectrometry (AMS): Recommendation for best practices and harmonization from Global Bioanalysis Consortium Harmonization Team. *Aaps j,* 16**,** 357-359.

YU, J., RITCHIE, T. K., MULGAONKAR, A. & RAGUENEAU-MAJLESSI, I. 2014. Drug disposition and drug-drug interaction data in 2013 FDA new drug applications: a systematic review. *Drug Metab Dispos,* 42**,** 1991-2001.

Appendices

Appendix 1 : Contribution to the field of AMS research

i) Works published – Listing of all peer-reviewed literature papers/articles/poster abstracts/book chapters published with Graeme C. Young as lead author or co-author: [Commentary papers included]

AMS Technique related:

1. Garner R.C., Barker J., Flavell C., Garner J.V., Whattam M., **Young G.C.,** Cussans N., Jezequel S. & Leong D. 2000. A validation study comparing accelerator MS and liquid scintillation counting for analysis of ^{14}C-labelled drugs in plasma, urine and faecal extracts., *J Pharm Biomed Anal,* 24: 197-209.

2. **Young GC**., Corless S., Felgate CC. & Colthup PV. 2008. Comparison of a 250 kV single-stage accelerator mass spectrometer with a 5 MV tandem accelerator mass spectrometer – fitness for purpose in Bioanalysis, *Rapid Commun Mass Spectrom*, 22: 4035-4042.

3. Garofolo F., Dumont I., Martinez S., Lowes S., Woolf E., van Amsterdam P., Bansal S., Barra A.C.G., Bauer R., Booth B.P., Carrasco-Triguero M., DeSilva B., Dunn J., Gallicano K., Gouty D., Ho S., Hucker R., Jemal M., Katoril N., Le Blaye O., Lee J., Li W., Michael S., Nehls C., Nicholson R., Ormsby E., Tang D., Viswanathan CT., Weiner R. & **Young G**. 2011. 2011 White Paper on Recent Issues in Bioanalysis and Regulatory Findings from Audits and Inspections, *Bioanalysis*, 3(18): 2081-2096.

4. Lappin G., Seymour M., **Young G.,** Higton D. & Hill H.M. 2011. AMS method validation for quantitation in pharmacokinetic studies with concomitant extravascular and intravenous administration, *Bioanalysis*, 3(4): 393-405.

5. Lappin G., Seymour M., **Young G.,** Higton D. & Hill H.M. 2011. An AMS method to determine analyte recovery from pharmacokinetic studies with concomitant extravascular and intravenous administration, *Bioanalysis*, 3(4): 407-410.

6. Dijksman J., Timmerman P., Abbott R., Barroso B., Kloeppel M.B., Companjen A., Golob M., Gordon B., Herling C., Knutsson M., Luedtke S., Rasmussen B. B., Stoellner D., Vieser E., **Young G.** & van Amsterdam P. 2012. Less is more; defining modern Bioanalysis. Conference report 4th EBF Open meeting., *Bioanalysis*, 4 (6): 633-642.

7. Higton D., **Young G.,** Timmerman P., Abbott R., Knutsson M. & Svensson L. 2012. EBF recommendation: scientific validation of quantification by accelerator mass spectrometry, *Bioanalysis*, 4(22), 2669-2679.

8. Daniel R., Mores M., Kitchen R., Sundquist M., Hauser T., Stodola M., Tannenbaum S., Skipper P., Liberman R., **Young G.,** Corless S. & Tucker M. 2013. Development of a commercial automated laser gas interface (ALGI) for AMS, *Nuclear Instruments and Methods in Physics Research Section B: Beam Interactions with Materials and Atoms,* 294: 291-295.

9. **Young GC.,** Seymour M., Dueker S., Timmerman P., Arjomand A. & Nozawa K. 2014. New Frontiers—Accelerator Mass Spectrometry (AMS): Recommendation for Best Practices and Harmonisation from Global Bioanalysis Consortium Harmonization Team, *Aaps j*, 16: 357-359.

10. Timmerman P., Blech S., White S., Green M., Delatour C., McDougall S., Mannens G., Smeraglia J., Williams S. & **Young G.** 2016. Best practices for metabolite quantification in drug development: updated recommendation from the European Bioanalysis Forum, *Bioanalysis*, 8(12):1297-1305.

<u>Clinical microdose study related</u>:

11. Cahn A., Hodgson S., Wilson R., Robertson J., Watson J., Beerahee M., Hughes SC., **Young G.**, Graves R., Hall D. & van Marle S. 2013. Safety, tolerability,

pharmacokinetics and pharmacodynamics of GSK2239633, a CC-chemokine receptor 4 antagonist, in healthy male subjects: results from an open-label and from a randomised study, BMC Pharmacol Toxicol, 14: 14.

12. Mahar K.M., Sehon C., Tai G., Haws T., Howe D., Nagilla R., **Young G**. & Danoff T. 2012. Comparison of a GSK706769 Microdose CYP3A4 Drug-Drug Interaction Study With a Previous Pharmacological Dose Study, 2012 American College of Clinical Pharmacology, Annual Meeting September 23rd-25th, San Diego, California, abstract #1393294.

Clinical intravenous microtracer study related:

13. Denton C.L., Minthorn E., Carson S.W., **Young G.C.,** Richards-Peterson L., Botbyl J., Han C., Morrison R.A., Blackman S.C. & Ouellet D. 2013. Concomitant Oral and Intravenous Pharmacokinetics of Dabrafenib, a BRAF Inhibitor, in Patients with BRAF V600 Mutation-Positive Solid Tumours, *J Clin Pharmacol,* 53(9): 955-961. **[Commentary paper 6]**

14. Leonowens C., Pendry C., Bauman J., **Young G.C.,** Ho M., Henriquez F., Fang L., Morrison R.A., Orford K. & Ouellet D. 2014. Concomitant oral and microdose intravenous pharmacokinetics of trametinib, a MEK inhibitor, in subjects with solid tumours, *Br J Clin Pharmacol,* 78(3), 524-532. **[Commentary paper 7]**

Human ADME study related:

15. **Young G**., Ellis W., Ayrton J., Hussey E. & Adamkiewicz B. 2001. Accelerator mass spectrometry (AMS) : recent experience of its use in a clinical study and the potential future of the technique, Xenobiotica, 31 (8/9): 619-632. **[Commentary paper 1]**

16. Harrell A.W., Siederer S.K., Bal J., Patel N.H., **Young G.C.,** Felgate C.C., Pearce S.J., Roberts A.D., Beaumont C., Emmons A.J., Pereira A.I. & Kempsford R.D. 2013. Metabolism and disposition of vilanterol, a long-acting β2-adrenoreceptor agonist for inhalation use in humans, *Drug Metab Dispos*, 41: 89-100. **[Commentary paper 4]**

17. Bowers GD., Tenero D., Patel P., Huynh P., Sigafoos J., O'Mara K., **Young GC.,** Dumont E., Cunningham E., Kurtinecz M., Stump P., Conde JJ., Chism JP., Reese MJ., Yueh YL. & Tomayko JF. 2013. Disposition and metabolism of GSK2251052 in humans: a novel boron-containing antibiotic, *Drug Metab and Dipos*, 41: 1070-1081. **[Commentary paper 3]**

18. Dave M., Nash M., **Young GC**., Ellens H., Magee MH., Roberts A., Taylor M.A., Greenhill R. & Boyle G.W. 2014. Disposition and Metabolism of Darapladib, a Lipoprotein-Associated Phospholipase A2 Inhibitor in Humans, *Drug Metab Dipos*, 42: 415-430. **[Commentary paper 5]**

Assorted AMS related:

19. **Young G.**, Ayrton J. & Pateman T., A Handbook of Bioanalysis and Drug Metabolism (Chapter 11 : Isotope Drug Studies in Man), CRC Press, 2004.

20. **Young G.C**. & Ellis W.J. 2007. AMS in drug development at GSK, *Nuclear Instruments and Methods in Physics Research Section B: Beam Interactions with Materials and Atoms*, 259: 752-757. **[Commentary paper 2]**

21. In the search for new drugs, diverging roads for microdosing, Chemical & Engineering News, 91 (3), (2013) 9-13. Part contribution by **Young G.**

22. Beaumont C., **Young GC**, Cavalier T. & Young M. 2014. Human absorption, distribution, metabolism and excretion properties of drug molecules: a plethora of approaches, *Br. J.Clin. Pharmacol.,* 78(6): 1185-1200.

23. **Young GC**. & Seymour M. 2015. Application of ^{14}C-Accelerator MS in pharmaceutical development, *Bioanalysis*, 7(5): 513-517.

24. Pene Dumitrescu T., Santos L., Hughes S.C., Pereira A., **Young G.**, Hussey E., Charlton P., Baptiste-Brown S., Stuart J.S., Vincent V., Van Marle S.P. & Schmith V.D. 2016. A

first in human study to characterize the pharmacokinetics following administration of ^{14}C-Umeclidinium (UMEC) to the axilla and palm of healthy male subjects, *Clin. Transl. Sci.,* 9**,** 183-191.

25. Bloomer J., Beaumont C., Dear G.J., North S. & **Young G**. 2016. Metabolite Safety in Drug Development (Chapter 12: Case Studies : GlaxosmithKline), John Wiley & Sons, Ed. Iverson S. & Smith D.A.

Additional papers utilising AMS (GSK Sponsored) where Graeme C. Young provided support/input:

26. Hoffmann, E., Wald, J., Lavu, S., Roberts, J., Beaumont, C., Haddad, J., Elliott, P., Westphal, C. & Jacobson, E. 2013. Pharmacokinetics and tolerability of SRT2104, a first-in-class small molecule activator of SIRT1, after single and repeated oral administration in man*, Br J Clin Pharmacol,* 75(1):186-196.

27. Daley-Yates P., Norris, V., Ambery, C. & Preece, A. 2012. Early Clinical Evaluation of a Novel 5-Lipoxygenase Activating Protein (FLAP) Inhibitor (GSK2190915A). Pharmacokinetics, Bioavailability and Dose Form Selection: Influence of Age, Food, Drug Interactions and Regional Absorption (LPA112071, LPA112362, LPA114604); *Proceedings of the British Pharmacological Society*, BPS Winter Meeting 2012.

28. Hughes, S. C., Shardlow, P. C., Hollis, F. J., Scott, R. J., Motivaras, D. S., Allen, A. & Rousell, V. M. 2008. Metabolism and Disposition of Fluticasone Furoate, an Enhanced-Affinity Glucocorticoid, in Humans, *Drug Metab Dispos,* 36: 2337-2344.

29. Mamaril-Fishman, D., Zhu, J., Lin, M., Felgate, C., Jones, L., Stump, P., Pierre, E., Bowen, C., Naderer, O., Dumont, E., Patel, P., Gorycki, P. D., Wen, B., Chen, L. & Deng, Y. 2014. Investigation of Metabolism and Disposition of GSK1322322, a PDF Inhibitor, in Healthy Humans Using Entero-Test® For Biliary Sampling, *Drug Metab Dipo*s, 42: 1314-1325.

30. Negash, K., Andonian, C., Felgate, C., Chen, C., Goljer, I., Squillaci, B., Nguyen, D., Pirhalla, J., Lev, M., Schubert, E., Tiffany, C., Hossain, M. & Ho, M. Nov 2015. The metabolism and disposition of GSK2140944 in healthy human subjects, *Xenobiotica*, 19: 1-20.

Clinical Trials.gov reference for the Human ADME study for GSK961081:

https://www.clinicaltrials.gov/ct2/show/NCT02663089?term=GSK961081&rank=1

ii) Invited speaker at International Conferences:

- Drug Development Conference, London, 2005
- AMS-10 (Accelerator Mass Spectrometry) Conference, San Francisco, USA, 2005
- CosMos (Conference on Small Molecules), San Diego, USA, 2006
- WW Pharmaceutical Congress, Philadelphia, USA, 2007
- NJDMD (New Jersey Drug Metabolism Discussion Group), New Jersey, USA, 2006
- AMS Webinars (Xceleron sponsored), 2008 and 2014
- APA Conference, Boston, USA, 2008
- DMDG (Drug Metabolism Discussion Group), Cambridge, UK, 2009
- **ASMS (American Society of Mass Spectrometry), Philadelphia, USA, 2009 – Plenary presenter and AMS Session Chair**
- AMS in Pharmaceutical Research, Lawrence Livermore Nat. Lab, California, USA, 2009
- CPSA , Philadelphia, 2010
- CVG (Calibration and Validation Group) conference, Montreal, Canada 2011
- EBF (European Bioanalysis Forum) Conference, Barcelona, Spain, 2011
- BioAMS Workshop, National Institute of Health, Maryland, USA, 2011
- BABE (Bioavailability and Bioequivalence), Beijing China, 2013
- EBF (European Bioanalysis Forum) Workshop **[co-organiser and session co-chair],** Brussels, Belgium, 2015
- ECDC (Exploratory Clinical Development Conference) London, 2007, 2010, 2012 and 2015

iii) Reviewer of multiple journal articles related to the field of biomedical ^{14}C AMS, including articles published in Clinical Pharmacokinetics, Journal of Clinical Pharmacology, and Bioanalysis

iv) Chair of cross-Pharmaceutical company and Contract Research Organisation AMS user group since 2013

v) Academic collaborations :

- Active collaboration with ETH University, Zurich in development of AMS instrumentation and sample introduction
- Historical collaboration on AMS interface development with Massachusetts Institute of Technology from ~2008-2012
- Historical collaboration with Lawrence Livermore National Laboratory (Dept. of Energy), USA since 1997.

Impact of published works demonstrated through h-Index = 11 ; i10-index = 12 ; 359 citations based on 19 publications in Google scholar, as of March 2016.

Appendix 2: Reproduced principal papers

See reproduced papers at the end of this commentary. Permissions granted as detailed below -

Paper 1) Reprinted with permission from **Young, G**., W. Ellis, J. Ayrton, E. Hussey and B. Adamkiewicz (2001). "Accelerator mass spectrometry (AMS): recent experience of its use in a clinical study and the potential future of the technique." Xenobiotica **31**(8-9): 619-632, Elsevier, Copyright 2001.

Paper 2) Reprinted with permission from **Young, G**. and W. J. Ellis (2007). "AMS in Drug Development at GSK." Nuclear Instruments and Methods in Physics Research **B 259**: 752-757, Copyright 2001.

Paper 3) Reprinted with permission of the American Society for Pharmacology and Experimental Therapeutics. All rights reserved. Bowers, G. D., D. Tenero, P. Patel, P. Huynh, J. Sigafoos, K. O'Mara, **G. C.Young**, E. Dumont, E. Cunningham, M. Kurtinecz, P. Stump, J. J. Conde, J. P. Chism, M. J. Reese, Y. L. Yueh and J. F. Tomayko (2013). "Disposition and metabolism of GSK2251052 in humans: a novel boron-containing antibiotic." Drug Metab Dispos **41**(5): 1070-1081

Paper 4) Reprinted with permission of the American Society for Pharmacology and Experimental Therapeutics. All rights reserved. Harrell, A. W., S. K. Siederer, J. Bal, N. H. Patel, **G. C. Young**, C. C. Felgate, S. J. Pearce, A. D. Roberts, C. Beaumont, A. J. Emmons, A. I. Pereira and R. D. Kempsford (2013). "Metabolism and disposition of vilanterol, a long-acting β(2)-adrenoceptor agonist for inhalation use in humans." Drug Metab Dispos **41**(1): 89-100

Paper 5) Reprinted with permission of the American Society for Pharmacology and Experimental Therapeutics. All rights reserved. Dave, M., M. Nash, **G. C. Young**, H. Ellens, M. H. Magee, A. D. Roberts, M. A. Taylor, R. W. Greenhill and G. W. Boyle (2014). "Disposition and metabolism of darapladib, a lipoprotein-associated phospholipase A2 inhibitor, in humans." Drug Metab Dispos **42**(3): 415-430

Paper 6) Reproduced with permission from Denton, C. L., E. Minthorn, S. W. Carson, **G. C. Young**, L. E. Richards- Peterson, J. Botbyl, C. Han, R. A. Morrison, S. C. Blackman and D. Ouellet (2013). "Concomitant oral and intravenous pharmacokinetics of dabrafenib, a BRAF inhibitor, in patients with BRAF V600 mutation-positive solid tumors." J Clin Pharmacol **53**(9): 955-961. John Wiley and Sons, Copyright 2013.

7) Reproduced with permission from Leonowens, C., C. Pendry, J. Bauman, **G. C. Young**, M. Ho, F. Henriquez, L. Fang, R. A. Morrison, K. Orford and D. Ouellet (2014). "Concomitant oral and intravenous pharmacokinetics of trametinib, a **MEK** inhibitor, in subjects with solid tumours." Br J Clin Pharmacol **78**(3): 524-532. John Wiley and Sons, Copyright 2014.

Appendix 3: Letters from lead authors and GSK Position on common practice for authorship

Provided here are letters from lead authors of the papers upon which this Commentary is based, confirming Graeme C. Young's input to these papers and the work which they report. These are for Commentary papers 3, 4, 5, 6 and 7; Graeme C. Young was lead author on papers 1 and 2.
Also included in this Appendix is a document to provide background to the GSK common practice for contribution to works and authorship of papers.

See reproduced documents at the end of this commentary.

Appendix 4: Summary of Contributions by Graeme C. Young to each of the Commentary papers

Commentary paper no.	Title	Contribution by Graeme. C. Young
1	Accelerator mass spectrometry (AMS): recent experience of its use in a clinical study and the potential future of the technique.	• Lead Author • Designed and conducted experiments • Provided analytical input to both studies described
2	AMS in Drug Development at GSK.	• Lead Author • Designed and conducted experiments • Champion of establishment of AMS Capability at GSK • Provided analytical input to all studies described
3	Disposition and metabolism of GSK2251052 in humans: a novel boron-containing antibiotic.	• Participated in research design • Provided analytical input and resources • Contributing author
4	Concomitant oral and intravenous pharmacokinetics of dabrafenib, a BRAF inhibitor, in patients with BRAF V600 mutation-positive solid tumors.	• Contributing author • Participated in research design • Provided analytical input and resources
5	Metabolism and disposition of vilanterol, a long-acting β(2)-adrenoceptor agonist for	• Contributing author • Participated in research design

	inhalation use in humans.	• Provided analytical input and resources • Performed data analysis
6	Disposition and metabolism of darapladib, a lipoprotein-associated phospholipase A2 inhibitor, in humans.	• Contributing author • Participated in research design • Provided analytical input and resources • Performed data analysis
7	Concomitant oral and intravenous pharmacokinetics of trametinib, a MEK inhibitor, in subjects with solid tumours.	• Contributing author Participated in research design • Provided analytical input and resources

Appendix 5: Summary of author's main contributions to the knowledge

Advancement	Detail	Outcome
Scientific and strategic:		
LC+AMS principle	This author first proposed the principle in 1999, when all discussion was of use of AMS for total ^{14}C and metabolite profiling applications – credit is due to others as outlined in this commentary for developing the microdose and microtracer principles, as well as specific methodologies such as the use of an IS	LC+AMS term coined by this author to highlight the offline nature of this procedure (i.e. distinct from a hyphenated approach such as LC-MS); the approach is now in common use within the AMS field of research
Harmonisation of validation procedures for LC+AMS assays	This author has lead the drive to harmonise validation principles for clinical LC+AMS assays through chair of the inter-company AMS service provider team	Ongoing collaborations and publication to support agreed principles [(Young et al., 2014)]
Entero-test human bile collection	GSK laboratory first to use AMS in human ADME studies and IV microtracer studies for analysis of drug and metabolites in human bile	Extremely insightful data produced on multiple studies showing routes of metabolism not detected by analysis of other matrices – now an approach being taken up across the industry

Novel design of combination human ADME with IV microtracer for an inhaled therapy	This author has proposed a design which incorporates the intravenous ^{14}C microtracer approach concomitant to an inhaled administration (at a supra-therapeutic dose) as one discrete phase of a human ADME study ; the second phase is a cross-over oral administration of ^{14}C-labelled drug	The study is in progress and the intent is to publish the outcomes

Technical advancements:		
Carbon carrier selection	Switched from Liquid Paraffin to Aq. Sodium benzoate	Provided advantages of reduction in data errors due to improved ease of handling (pipette volume increased from 1 µL of a highly viscous material, to 20 µL of aqueous)
Established frequency of chromatographic fractionation (12 seconds for HPLC flow rate of 1mL/min.) – others performed 30 second or even 1 minute fractions resulting in very poor resolution	Developed a good understanding of fractionation frequency which lead to some standardisation	Experiments are designed to maximise efficiency and scientific integrity – further increased frequency used where necessary to achieve chromatographic peak resolution (eg. as frequent as 3 second fractions)
Sensitivity enhancement through analyte chromatographic peak concentration	On occasions when AMS has been inadequately sensitive for metabolite profiles to be generated, our group has made up to 4 injections of the same extract onto the LC	So long as the chromatographic retention times are consistent enough to allow multiple repeat injections onto the LC, sensitivity improvements can be achieved
Multiple predose clinical samples	Championed the idea of taking three predose blood samples at screening visit, Day-1 and Day of dosing	Establishes good understanding of control endogenous background ^{14}C, in-study sample contamination and/or previous ^{14}C

		exposure of subjects
Re-use of non-disposable Y-piece for cryogenic transfer step of graphitisation	Common practice to use only disposable items during graphitisation due to concerns around cross-contamination	Investigations in our laboratory showed that no sample to sample carryover occurred with a metal re-usable Y-piece [improved science and resource saving]
Developed a novel approach to definition of the LoQ for radioactive drug related material in plasma (rather than eg. 2x background as is the accepted empirical based practice for LSC)	Defined LoQ based upon specific activity of the drug and statistical assessment of variability in endogenous background as well as measurement of ^{14}C above that level	LoQ can now be stated within limits of statistical confidence (as - x pg drug equivalents/mL)

Appendix 6: Ethics statement

GlaxoSmithKline Research
& Development Limited
Park Road
Ware
Hertfordshire
SG12 0DP
Tel. +44 (0)1920 469469
www.gsk.com

Ethics statements relating to PhD Commentary on Published Works by Graeme Charles Young:

All of the work sponsored or conducted by GlaxoSmithKline, detailed in the papers included in this Commentary, complied with the following:

All GSK-sponsored studies were conducted in accordance with the guiding principles of the Declaration of Helsinki and in compliance with good clinical practices and local regulatory guidelines. The protocols and informed consent forms were approved by an institutional review board or independent ethics committee at each study site before any subject was enrolled or study procedure performed. All human biological samples were sourced ethically and, where applicable, patient consent was obtained for their use for research. Additionally subject anonymity was maintained through use of study assignment randomisation codes.

All GSK-sponsored animal studies were conducted in accordance with the relevant GSK Policy on the Care, Welfare and Treatment of Laboratory Animals and were reviewed by the Institutional Animal Care and Use Committee (or similar at the time of conduct) either at GSK or by the ethical review process at the institution where the work was performed.

John Toso

------- ---------- -----March 21, 2016----------

Dr. John Toso, MD, Physician Director **Date**

GlaxoSmithKline Research and Development Ltd.

Registered in England & Wales
No. 835139
Registered office
980 Great West Road
Brentford, Middlesex. TW8 9GS

gsk.0014b

Appendix 7: AMS Instrumentation evolution

The technical evolution of AMS instrumentation has been significant over recent decades (Synal, 2013). Instruments have been simplified, the size and complexity reduced whilst their sensitivity has been honed to be applications driven. A good example being the GSK SSAMS which was designed and built specifically for analysis of carbon, whereas larger instruments can analyse a range of elemental isotopes by virtue of their higher energies. These developments have created wide spread use of AMS in modern research fields (Kutschera, 2013). Today, commercial high-performance instruments are in use in more than 100 AMS facilities around the world, although those conducting biomedical work are but a few.

Voltages less than about 2.5 MV were thought to be inadequate for dissociating molecular background interferences until the ETH Zurich group demonstrated low background carbon AMS with 0.5 MV tandem accelerators (Synal et al., 2000). This breakthrough lead to the development of the 250 kV SSAMS (Klody et al., 2005). The first carbon-dedicated AMS system was built and tested around 2003. The injector included two 40-sample ion sources, electrostatic and magnetic analysis, and fast sequential injection. The gas stripper, analysing magnet, electrostatic analyzer, and detector were on an open air 250 kV deck – this was a shift from the previous tandem higher voltage accelerators which had to have their charging chain housed in a tank which contained an inert gas (SF_6) to avoid discharge to the surrounding air. Both ^{12}C and ^{13}C currents were measured on the deck after the stripper, and a solid silicon barrier detector was used for ^{14}C ion incident counting. Injected ^{12}C and mass 13 (^{13}C and ^{12}CH) currents were also measured. Initial test results showed precision for $^{14}C/^{12}C$ ratios and backgrounds for unprocessed graphite that were compatible with the requirements of ^{14}C enriched biological sample measurements. From this prototype the 250 kV SSAMS emerged as a commercially viable instrument and the second of these (in the world) was brought into service at GSK.

The GSK instrument had additional safety features added to it, through our group's input, over and above the initial manufacturer design. These included automatic

earthing of the instrument upon any of the instrument cage doors being opened and x-ray detection system with automatic instrument shut-down in the event of spurious x-ray radiation being generated.

Since installation in 2005, there have also been instrumental improvements such as changes to the caesium focussing to improve beam currents, leading to reduction in analytical run times. Our instrument has also been enabled to accept gas, with successful production of ion beams from 5% CO_2 with helium as a carrier gas (based on research by ETH University, Zurich, Switzerland (Wacker et al., 2013).

Appendix 8: Toward a unique AMS capability

All of this work **(Commentary papers 1 and 2** in particular**)** demonstrated the confidence building approach i.e. start with non-clinical, lower "value" studies (animal and in vitro studies) and progress towards clinical work. GSK lead the field amongst pharmaceutical companies, with the author as the leading scientist behind these activities. The power of the technique over a range of applications (sensitivity and benefit of selectivity for ^{14}C-labelled drug analysis) was shown; both AMS targeted and what was termed "hybrid" study support. These latter designs are those where the intent was to use AMS in combination with, or as an adjunct to, other techniques such as LSC, for analysis of samples containing higher amounts of radiocarbon. The scientific impact of my work led to a justification for GSK to invest in the AMS technology. This resulted in the 250 kV SSAMS instrument being purchased and a complete in-house capability being established at a cost of >£3M, with an assortment of specialised sample preparation and instrument laboratory suites, in addition to allocation of dedicated staff, at the GSK, UK Ware site in 2004*. This was particularly important as no other pharmaceutical company had made such a move and in fact this is still the case, even though this author is aware that our laboratory are envied by our industry peers for our capability and experience level in that regard.

* GSK initially established two AMS facilities, one in the UK (at the Ware site) with the other being at a site in Philadelphia USA, but long term, without a local champion the capability in the USA was not deemed to be providing enough business value and thus was dissolved.

Appendix 9: Schematics of the GSK SSAMS and next generation AMS systems

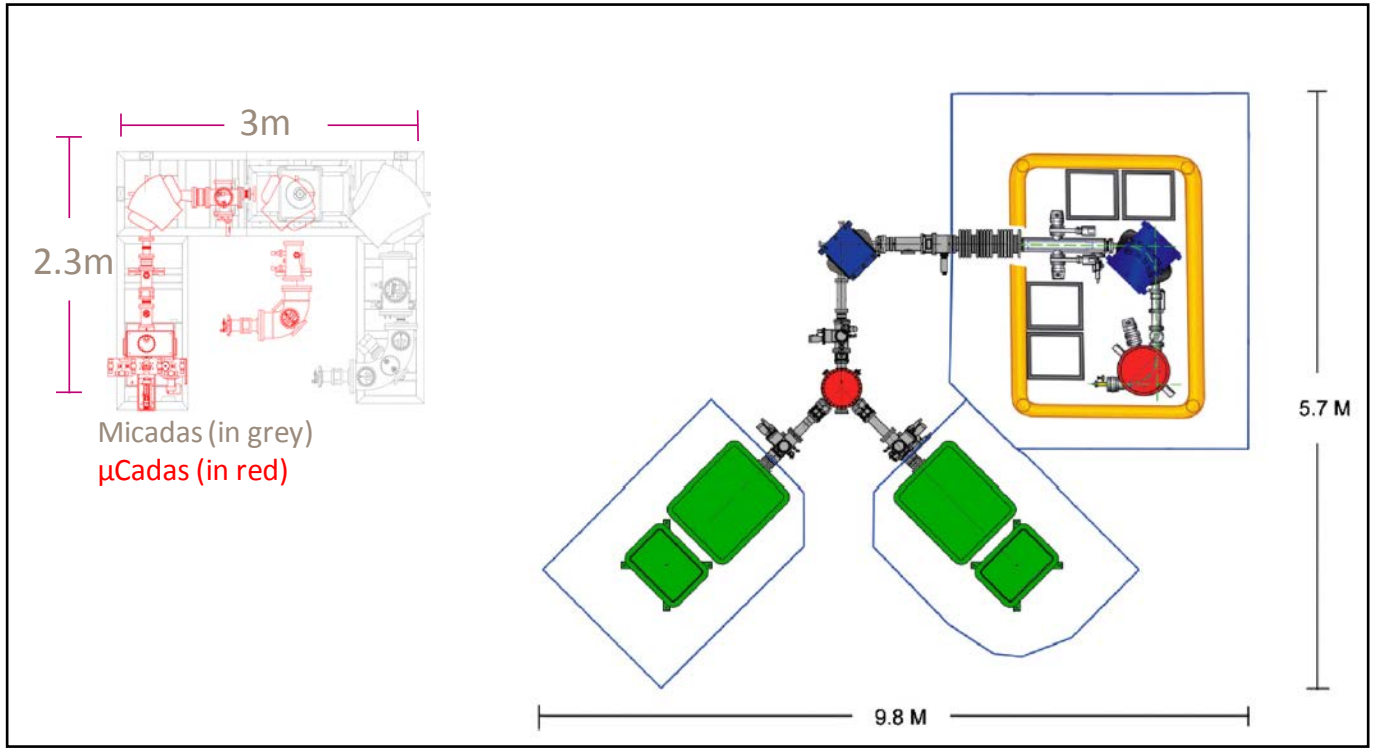

The Micadas and µCadas systems were designed and built by ETH, Zurich (Swiss Federal Institute of Technology)*.

The key breakthrough in the size reduction to the prototype µCadas system is the change from argon to helium as the stripper gas providing improved stripping efficiency (similar at 50kV for helium as at 250kV for argon) thus less acceleration is required, which allows the low energy magnet to be directly coupled to the molecular dissociator.

* Reproduced here by kind permission of ETH, Zurich. Schematic of the GSK SSAMS reproduced by kind permission of National Electrostatics Corp., WI, USA.

Appendix 10: Risks Associated with Ionising Radiations

ICRP (International Commission on Radiological Protection) 1992

Risk category	**Corresponding effective dose range (adults) (mSv)**	**Level of risk**	**Level of societal benefit**
Category I (~10^{-6} or less)	<0.1	Trivial	Minor
Category II IIa (~10^{-5} or less) IIb (~10^{-4} or less)	 0.1 - 1 1 – 10	Minor to intermediate	Intermediate to moderate
Category III (~10^{-3} or greater)	>10	Moderate	Substantial

XENOBIOTICA, 2001, VOL. 31, NO. 8/9, 619–632

Accelerator mass spectrometry (AMS): recent experience of its use in a clinical study and the potential future of the technique

G. YOUNG†*, W. ELLIS†, J. AYRTON†, E. HUSSEY‡ and B. ADAMKIEWICZ‡

† Division of Bioanalysis and Drug Metabolism, Glaxo Wellcome Research and Development Ltd, Park Road, Ware SG12 ODP, UK
‡ Division of Clinical Pharmacology, Glaxo Wellcome, Inc., Research Triangle Park, NC 27709, USA

Received 22 January 2001

1. The technique of accelerator mass spectrometry (AMS) is outlined.

2. The use of AMS in an initial validation study in animals is outlined. As part of the validation of the technique, samples from the animal study were analysed by both liquid scintillation counting (LSC) and, following dilution, by AMS. The results were similar.

3. The use of AMS in support of a clinical study is described. Six healthy male human volunteers were administered 2.7 mg [^{14}C]-GI1817771 (121 Bq; 3.3 nCi) to produce an exposure to ionizing radiation of 0.06 μSv. Mass balance in recovery of administered radioactivity was achieved and information about the presence of systemically circulating metabolites was gained.

4. The future potential of the technique of AMS is discussed.

Xenobiotica Downloaded from informahealthcare.com by GlaxoSmithKline (Active) on 03/15/11
For personal use only.

Introduction

Accelerator mass spectrometry (AMS) is a very sensitive nuclear physics technique that was developed in America in the 1970s. AMS has been used in the analysis of a wide range of elements and its use in measurement of radiocarbon (^{14}C) to date archaeological samples first appeared in the literature in the 1970s (Bennett *et al.* 1977, Nelson *et al.* 1977). AMS uses a tandem van de Graaff accelerator to provide the potential energy to strip off the valency electrons of negatively ionized atoms generating positively charged atoms which can then be separated using conventional mass spectrometry. In the measurement of carbon by AMS, the three isotopic species (i.e. ^{14}C, ^{13}C and ^{12}C) are separated from each other by virtue of their different energies and mass:charge ratios. AMS can measure radiocarbon concentrations down to 1000th of the natural levels found in living tissue and so is significantly more sensitive than liquid scintillation counting (LSC). AMS as an analytical tool for the pharmaceutical industry has been recently comprehensively reviewed (Garner 2000).

The use of AMS for analysis of drugs and metabolites in biological matrices has been discussed extensively but little original data have been presented in the literature. A short communication demonstrating the feasibility of using AMS for drug measurement has been published by Kaye *et al.* (1997), as has a paper detailing validation of AMS for analysis of radiocarbon in biomedical samples

*Author for correspondence; e-mail: gcy1283@glaxowellcome.co.uk

Xenobiotica ISSN 0049–8254 print/ISSN 1366–5928 online © 2001 Taylor &
http://www.tandf.co.uk/journals
DOI: 10.1080/00498250110052724

RIGHTSLINK

Figure 1. Accelerator mass spectrometry instrument at The Centre for Biomedical Accelerator Mass Spectrometry Ltd, Sand Hutton, York. Reproduced by kind permission of CBAMS Ltd.

Xenobiotica Downloaded from informahealthcare.com by GlaxoSmithKline (Active) on 03/15/11
For personal use only.

(Garner *et al.* 2000). The AMS instrument upon which the validation work described here was conducted (figure 1) was established at The Centre for Biomedical Accelerator Mass Spectrometry (CBAMS) Ltd, Sand Hutton, York, UK. CBAMS Ltd became operational in 1998 and was cofunded by a group of companies from the pharmaceutical industry, along with the UK Ministry of Agriculture, Fisheries and Food (Central Science Laboratory) and the University of York.

This paper describes the approach taken by Glaxo Wellcome Research and Development Ltd to using the technology of AMS in the establishment of a facility to handle samples that contain very low quantities of radiocarbon-labelled material in the initial validation study. The paper also describes a clinical study where only 121 Bq (3.3 nCi) of a radioactively labelled new chemical entity ([^{14}C]-GI181771) was administered by the oral route to six healthy male human volunteers to allow estimation of a mass balance of radioactivity of this compound in humans. The paper also discusses the potential future of AMS in biomedical applications and its possible impact on drug discovery and development in the pharmaceutical industry.

Validation of AMS

As part of the validation of the technique of AMS in biomedical use, we conducted an excretion balance and pharmacokinetics study in male Han Wistar rats using [^{14}C]-fluticasone propionate ((6α,11β,16α,17β)-6,9-difluoro-11-hydroxy-16-methyl-3-oxo-17-propionyloxy-androsta-1,4-diene-17-carbothioic acid *S*-fluoromethyl ester), a chemical in general medical use for the treatment of asthma and rhinitis. Samples of blood plasma and excreta from the animal study were analysed by both LSC and, following dilution, by AMS, and the results were similar. The design of the study and the results obtained are covered in detail in Garner *et al.* (2000). It should be noted that when handling the low levels of

RIGHTSLINK

radiocarbon in the samples destined for analysis by AMS, we took the approach of designating a laboratory area and isolating it, and the equipment in it, from all other routine use of radiocarbon. The laboratory was established in a temporary building with access limited to only those persons who were directly involved in work with very low level radiocarbon samples. 'Clean laboratory' techniques were employed to minimize further the risk of contamination from other laboratory areas. Following successful validation of the technique of AMS, from the perspective of Glaxo Wellcome Research and Development Ltd, using the animal study samples, the laboratory was equipped with everything that was required to support the preliminary preparation of samples generated from a small clinical study. This included sample storage, weighing, aliquotting, homogenizing, and separation of drugs and metabolites by high-performance liquid chromatography (HPLC) with fraction collection.

Xenobiotica Downloaded from informahealthcare.com by GlaxoSmithKline (Active) on 03/15/11
For personal use only.

Clinical study

Materials and methods

Radiolabelled compound. GI181771 was radiolabelled by introduction of a ^{14}C-atom in a position considered unlikely to be vulnerable to metabolic transformation. The radiolabelled drug (0.04 mg) was diluted with unlabelled GI181771 (3.03 g) to produce a specific activity of 44.65 Bq mg^{-1}. Radiochemical purity of the labelled drug prior to dilution with unlabelled drug was 99.8%. The chemical purity after dilution was 95.2% with the main impurities being water and solvents. The radiochemical purity was not rechecked following dilution due to the limitations in assaying drug of such low specific activity.

Stable isotopic-labelled compound. [$^{2}H_5$]-GI181771 was prepared for use as the internal standard for the assay of GI181771 by liquid chromatography with tandem mass spectrometric detection (LC-MS-MS). The chemical purity of this material was >98.6%.

Dosing and sample collection. Six healthy male human volunteers, aged 23–37 years, received a single oral administration of [^{14}C]-GI181771 at a mean dosage of 2.7 mg in 5 ml polyethylene glycol 400 (Union Carbide Corporation, Danbury, CT, USA). The radiolabel dose was to be limited to that which would produce an exposure to ionizing radiation of 1 μSv, which is equivalent to a 4-h exposure to environmental (background) ionizing radiation in the UK. This exposure is the limit below which one is exempt from requiring a certificate from the UK Department of Health's Administration of Radiolabelled Substance Advisory Committee (ARSAC) to administer radioactive medicinal products to human subjects in the UK. The initial target exposure was 0.9 μSv, but the actual average dose of radioactivity administered to each volunteer was 121 Bq, producing exposure to ionizing radiation of 0.06 μSv. The exposure was as low as this for specific logistical reasons, which arose during the planning of the study. The total dose to be administered was reduced from the initially planned target dose and the radioactive dose was also reduced as a direct result. It was felt that reliable data could still be obtained at this dose level and the study therefore proceeded using this lower total dose and resultant lowered exposure to ionizing radiation.

Blood samples were collected predose and at 0.25, 0.5, 0.75, 1, 1.5, 2, 2.5, 3, 4, 6, 8, 12, 16 and 24 h post-dose. After clotting and centrifugation, serum was transferred to polypropylene tubes and stored frozen. Urine samples were collected predose and 0–12, 12–24, 24–48, 48–72, 72–96 and 96–120 h post-dose. The weights of the collections were recorded and an aliquot stored frozen prior to analysis.

Faeces samples were collected predose and 0–24, 24–48, 48–72, 72–96 and 96–120 h post-dose. The complete collections were stored frozen and weights recorded prior to processing.

Preliminary preparation of faeces and urine samples for analysis by AMS. Faeces samples (50–180 g) were weighed into 1.2 litre containers and smaller samples were weighed into 250 ml containers. Making the assumption that 1 g faeces was equivalent to 1 ml, 3 vols methanol (Rathburn Chemicals Ltd, Walkerburn, UK) were added. Samples were thawed and homogenized with an Ultra Turrax homogenizer (Brunner Scientific, Unit 4C, Hunmanby, Filey, UK). The final homogenate appeared as a fine suspension and was stored at nominally −20°C. Triplicate aliquots were taken from different positions from within each resuspended homogenate and were sent on solid CO_2 to CBAMS Ltd for

RIGHTSLINK

analysis by AMS. Aliquots of neat urine were sent frozen to CBAMS Ltd for analysis by AMS. Samples sent to CBAMS Ltd could be shipped as non-radioactive due to the extremely low quantities of radioactivity involved, with consequent reductions in costs and bureaucracy.

Serum sample preparation for analysis by AMS. Aliquots of neat serum were sent frozen to CBAMS Ltd for analysis by AMS. This method of analysis could not distinguish the very low concentrations of radioactivity present in serum samples against the endogenous background radiocarbon in neat serum, following administration of such a low dose of radioactivity. In an attempt to enhance the signal:noise ratio, the endogenous radioactivity was reduced through removal of carbon-containing components by precipitation of the serum proteins prior to analysis by AMS. An aliquot (400 µl) of each serum sample was vortex mixed with 800 µl acetonitrile (Rathburn Chemicals). After centrifugation, 800 µl of the supernatant was subjected to analysis by AMS.

Faecal extracts: preparation prior to fraction collection from HPLC. To allow metabolic profiling of the faecal samples, selected predose and 0–48 h post-dose collection faecal samples were extracted and fractionated by HPLC. Twenty millilitres of faecal homogenate from each sample was centrifuged. The supernatant was concentrated by evaporation under a stream of nitrogen to a final volume of up to 2 ml. Aliquots (100 µl) were fractionated by HPLC and sent to CBAMS Ltd for analysis by AMS. Radiochromatograms were constructed from the radioactivity in the HPLC fractions.

Serum samples: preparation prior to fraction collection from HPLC. Serum samples from all of the volunteers were combined into three pools according to times after dosing: 0.5–0.75, 2–6 and 12–16 h. This resulted in up to 2 ml serum from each of these times after dosing. Acetonitrile (2 vols) was added to each pooled sample, vortex mixed and centrifuged. The supernatant was concentrated by evaporation under a stream of nitrogen and reconstituted in ~150 µl 50% acetonitrile:50% water (v/v). An aliquot (100 µl) was fractionated by HPLC and the fractions were sent to CBAMS Ltd for analysis by AMS.

HPLC fractionation and metabolite profiling of serum and faeces. Aliquots (100 µl) of the sample of precipitated serum or faecal extract were injected on to an Inertsil ODS2 (250 × 4.6 mm i.d., 5 µm) analytical column, which was eluted under gradient conditions at a flow rate of 1 ml min^{-1}. Mobile phase A was 0.1% v/v trifluoroacetic acid in water and mobile phase B was 95% v/v acetonitrile in 0.1% v/v trifluoroacetic acid (in water). The mobile phase was a linear gradient which started at 75% A and 25% B, rose to 90% B over 30 min and returned to the starting conditions from 35 to 45 min. The column was maintained at ambient temperature. The column eluant was monitored at $A_{240\,nm}$. Column eluant fractions were collected every 0.5 min from 5 to 6 and from 14 to 30 min from the point of injection. A Gilson 233XL Fraction Collector (Anachem Ltd, Luton, UK) run from Unipoint v.1.02 was used. On this system, the retention times of GI181771 and its glucuronide were 24 and 20 min respectively. The column eluant fractions (0.5 ml) were sent frozen on solid carbon dioxide to CBAMS Ltd for analysis by AMS.

Graphitization of samples. In order to measure the ^{14}C content of samples by AMS, the carbon in the samples was first converted to graphite by CBAMS Ltd using a previously described method (Vogel 1992). In instances where insufficient carbon was present in samples, a carrier of known total carbon content and carbon isotope inventory was added. The carrier used was usually tributyrin (1,2,3-tributyrylglycerol; Sigma-Aldrich Company Ltd, Poole, UK).

C,H,N analysis. C,H,N analysis was conducted by CBAMS Ltd on samples submitted for analysis by AMS. It was necessary to determine the percentage carbon content in samples so as to assess the volume or mass of sample required to produce good graphite. The determination also allowed conversion of the results output from the AMS which was expressed as $^{14}C\,mg^{-1}$ carbon, to total ^{14}C $sample^{-1}$ and subsequent conversion to the commonly used units of radioactivity of dpm ml^{-1} or dpm g^{-1} of sample. Following sample addition and any pretreatment, tin capsules were closed and pressed prior to being loaded into the autosampler of a C,H,N analyser (Model NA2100 Brew Analyser, Elemental MicroAnalysis, Okehampton, UK). Pretreatment of samples included drying for faecal homogenates and serum extracts. A calibration curve of urea standards was prepared and used to determine the carbon content of each sample.

AMS analysis. The AMS sample wheel into which graphite-containing cathodes were placed was inserted into the ion source of the AMS instrument (5 MV 15SDH-2 Pelletron AMS system, National Electrostatics Corporation, Middleton, WI, USA) at CBAMS Ltd. The multicathode negative-ion source generated a caesium (Cs^+) ion beam that was accelerated onto each cathode's graphite surface in sequence. The resulting negative carbon ion beam contained $^{12}C^-$, $^{13}C^-$ and $^{14}C^-$ and other ions such as $^{16}O^-$.

Xenobiotica Downloaded from informahealthcare.com by GlaxoSmithKline (Active) on 03/15/11
For personal use only.

RIGHTSLINK

Xenobiotica Downloaded from informahealthcare.com by GlaxoSmithKline (Active) on 03/15/11
For personal use only.

The carbon ion beam was pre-accelerated, passed through a spherical electrostatic analyser and then progressed towards the injection magnet. Output of $^{12}C^-$ was typically 1–100 μA. The magnet was set to inject $^{12}C^-$ (150 μs), $^{13}C^-$ (600 μs) and $^{14}C^-$ (0.1 s) ions sequentially normally at 68 keV; one combined measurement on each isotope in turn corresponded to one cycle. The carbon ion beam was accelerated towards the positive centre terminal of the tandem Pelletron accelerator through an Einzel lens. The terminal voltage used for this series of analyses was 4.5 MV with a particle energy of ~22.5 MeV. At the central terminal, electrons were stripped from the carbon atom in an argon gas collision cell to yield positively charged carbon ions ($^{12,13,14}C^{+1\text{ to }+6}$). C^{4+} ions were selected for measurement as these were the most abundant at this energy. These ions were accelerated away from the positive centre terminal and onwards towards the electrostatic quadrupole triplet and analysing magnet.

Immediately past the post-analysing magnet, $^{12}C^{4+}$ and $^{13}C^{4+}$ ions were measured as an ion current in offset Faraday cups. $^{14}C^{4+}$ ions were passed down the high-energy beam line, through an electrostatic quadrupole doublet and a cylindrical electrostatic analyser. From here, the ions entered a gas ionization detector where they were collected on anodes (four in total), which measured the energy loss and total energy of each ion. Other interfering non-$^{14}C^{4+}$ ions were generally prevented from entering the gas ionization detector by the combinations of electrostatic analysers, magnets, slits and charge state separation. Vacuum pressures of ~10^{-9} Torr were maintained in the beam line and 10^{-6} Torr in the ion source. Ion transmission through the instrument was between 30 and 60%. A schematic of the AMS instrument is shown in figure 2.

Overall time for analysis of each sample ranged from 5 to 25 min consisting of a burn-in time of 600 cycles (60.4 s) and sample analysis of 500–5000 cycles (50.4–504 s) conducted a minimum of three times and a maximum of five. In some instances long analysis times were required to improve the precision of the data from samples, such as serum and serum extracts, containing very low levels of radiocarbon against relatively high background levels.

For each AMS run, in addition to cathodes containing graphitized samples, cathodes containing standards or blanks were included as quality controls.

Determination of limit of quantification (LOQ) for analysis by AMS. The determination of LOQ for analysis of samples by AMS was of critical importance since all samples analysed contained measurable background levels of radiocarbon. Analysis of controls and predose samples were used to estimate contributions of radiocarbon present as background and those values were subtracted from the post-dose sample results.

Limits of quantification for faeces, urine, neat serum and precipitated serum extracts were calculated from an analysis of variance of the predose controls and final sample equivalents measured in dpm ml^{-1} or dpm g^{-1}. Two background readings per subject, deemed to be ideally required in the calculation of the LOQ, were not available from samples generated from within the study. Samples from collections at the latest time points after dosing were thus considered to be equivalent to predose samples since by this time the levels of radioactivity appeared to have returned to predose levels. Limits of quantification, for

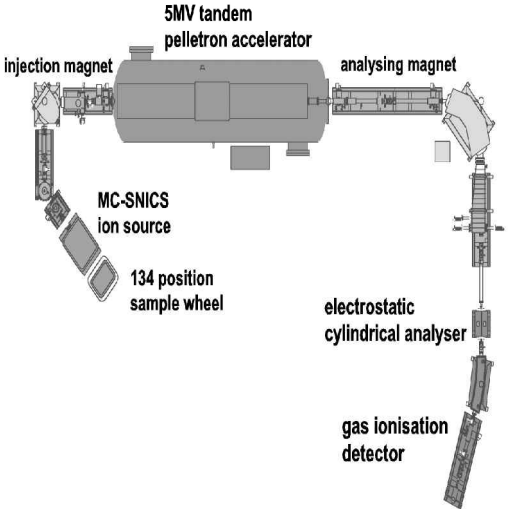

Figure 2. Schematic of the AMS instrument at The Centre for Biomedical Accelerator Mass Spectrometry Ltd. Reproduced by kind permission of CBAMS Ltd.

RIGHTSLINK

reconstructed radiochromatograms of HPLC fractions, were calculated from an analysis of variance of the fractions contained within defined background regions of interest, in dpm per fraction.

Two components of variance were calculated: between-subject variation and within-subject variation of predose or backgrounds. Both contributed to the overall variation associated with the LOQ.

A pooled estimated standard deviation was calculated as follows:

$$\sigma = \sqrt{\sigma_B^2 + \sigma_W^2}$$

where σ_B^2 is between-subject predose or background variance and σ_W^2 is within-subject predose or background variance.

Using criteria as defined in a Glaxo Wellcome Research and Development internal policy (based on the International Committee on Harmonization (ICH) Guideline 1996) for faeces, urine, neat serum and precipitated serum extracts, the limit of quantification was estimated using the increase above the background readings (5σ), whereas for HPLC fractions the LOQ determination included background (5σ + mean background). 95% confidence intervals of the limits of quantification were also calculated.

LC-MS-MS analysis of GI181771. Serum samples were prepared for analysis of GI181771 by liquid-chromatography with detection by tandem mass spectrometry. Calibration standards of GI181771 in human serum were prepared over the range 10–1500 pg ml^{-1}. All samples and standards were extracted by solid-phase extraction on a Packard MultiPROBE (Packard Instruments Ltd, Pangbourne, UK). Extraction was carried out on 50 mg Varian C18 Microlute II SPE 96-well blocks (Porvair Sciences Ltd, Shepperton, UK). The blocks were conditioned with 0.5 ml methanol (Fisher Scientific, Loughborough, UK) followed by 0.5 ml water. The blocks were loaded with 0.5 ml serum sample diluted with 0.5 ml internal standard in 20% v/v formic acid (BDH, Poole, UK) in water. The blocks were washed sequentially with 0.5 ml 20% v/v formic acid then 0.5 ml 40% v/v methanol and analytes of interest were then eluted with 0.75 ml ethyl acetate (Fisher Scientific). The resulting extracts were evaporated to dryness under a stream of nitrogen (nominally heated to 37°C) and reconstituted in 100 µl 50% mobile phase A, 50% mobile phase B prior to analysis by liquid chromatography with tandem mass spectrometric detection (LC-MS-MS). Mobile phase A was 0.01% formic acid in water:methanol (95:5 v/v) and mobile phase B was 0.01% formic acid in water:methanol (5:95 v/v). The serum extracts (50 µl) were analysed on a Perkin-Elmer Sciex API 3000 mass spectrometer (PE Sciex, Foster City, CA, USA) using TurboIonspray and selected ion monitoring. The liquid chromatography was performed on a 50 × 2 mm i.d. Phenomenex Luna C18 (5 µm) analytical column maintained at nominally 40°C. The mobile phase was a linear gradient which started at 50% A and 50% B, rose to 80% B over 2 min and returned to the starting conditions from 3.1 to 4 min, at a flow rate of 0.8 ml min^{-1}. The transitions of the protonated molecule, m/z 606.2 to the fragment ion m/z 443.2 were monitored for GI181771 and transitions of the protonated molecule m/z 611.2 to the fragment ion m/z 448.2 were monitored for the internal standard [$^2H_5$]-GI181771. The method was validated and quality control acceptance criteria were applied to indicate inaccuracy of the method to be <15%.

Results

The recovery of the administered radioactive dose in faeces from six human volunteers over 5 days was determined (table 1). The majority of the dose, >59%, was excreted in the faeces within the first 48 h. After 5 days, a mean total of 92% of the dose could be accounted for in the faeces. Volunteer 64 was excluded from calculation of the means, as collection of faeces from this volunteer was incomplete. In four of the six volunteers an average of 99.2% of the dose was recovered in the faeces over the 5 days.

The recovery of the administered dose in urine from six human volunteers over the first 2 days after dose was determined (table 2). All of the values obtained from urine were below LOQ. The mean total recovery in urine was <6.5% of the dose with LOQ from 0.4 to 3.8% of the dose.

Animal studies with oral administration of [^{14}C]-GI181771 showed low recovery of radiocarbon in the urine suggesting that <1% of the dose was absorbed (unpublished data). The results in this study in human volunteers indicate similarly low urinary excretion of drug-related material in humans.

Xenobiotica Downloaded from informahealthcare.com by GlaxoSmithKline (Active) on 03/15/11
For personal use only.

RIGHTSLINK

Table 1. Percent recovery of radiocarbon in faeces following oral administration of 2.7 mg [^{14}C]-GI181771 to male human volunteers.

Collection time (h)	Volunteer number						Mean (%)	SD (%)
	61	62	63	64*	65	66		
0–24	11.8	<6.3	34.0	38.0	43.6	103	38.5	38.9
24–48	85.5	44.6	53.4	n.s.	15.8	<6.0	39.9	28.7
48–72	1.2	19.2	8.7	n.s.	40.3	<5.8	13.9	16.1
72–96	<6.2	<7.4	<2.2	n.s.	<3.3	<6.4	<5.1	n.c.
96–120	n.s.	<3.7	<3.2	<5.2	<6.4	<8.9	<5.5	n.c.
Total	98.5	63.8	96.1	38*	99.7	103	92.2	16.1

*Excluded from mean calculations.
n.c., Not calculated: n.s., no sample.

Table 2. Percent recovery of radiocarbon in urine following oral administration of 2.7 mg [^{14}C]-GI181771 to male human volunteers.

Collection time (h)	Volunteer number						Mean (%)
	61	62	63	64	65	66	
0–12	<3.7	<2.4	<1.4	<0.4	<1.3	<3.7	<2.2
12–24	<2.7	<1.5	<1.4	<1.8	<1.4	<0.9	<1.6
24–48	<3.8	<3.2	<2.5	<1.6	<2.0	<3.1	<2.7
Total	<10.2	<7.1	<5.3	<3.8	<4.7	<7.7	<6.5

Selected neat serum samples, those taken at 0.25–1.5 h after dose, were initially analysed directly by AMS to produce the concentration of radioactivity in ng GI181771 equivalents ml^{-1} serum. All concentrations were below the LOQ of 161 ng ml^{-1}. The parent drug concentrations at these times, analysed separately, rose to ~3 ng ml^{-1}. The sensitivity of the AMS assay was such that the serum concentration of radiocarbon could not be compared with the concentrations of parent drug.

Subsequent sample preparation of all serum samples by protein precipitation resulted in an improvement in sensitivity. Removal of the majority of carbon in the sample, not derived from the dose, lead to reduction in the background signal. Results were corrected for recovery of radioactivity based on the known extraction efficiency of 105% for [^{14}C]-GI181771 by serum protein precipitation (table 3). This, >100% recovery, indicated exclusion of [^{14}C]-GI181771 from the pellet such that the apparent concentration measured in the extract supernatant was an overestimate of the true concentration. The assumption was made that the [^{14}C]-GI181771 related compounds found in the serum of dosed volunteers showed the same degree of recovery as [^{14}C]-GI181771. The radiocarbon present in the precipitated serum samples was expressed as ng equivalents of GI181771 ml^{-1} after subtraction of the predose levels. Over 25% of the values were quantifiable, above the LOQ of ~2.0 ng ml^{-1}, with concentrations ranging up to ~9.6 ng ml^{-1}.

An example of the data produced, for serum samples, by AMS and LC-MS-MS is shown in figure 3. The profiles obtained indicated that the concentration of radioactive drug-related material in serum was generally higher than concentra-

Xenobiotica Downloaded from informahealthcare.com by GlaxoSmithKline (Active) on 03/15/11
For personal use only.

RIGHTSLINK

Table 3. Concentration of radioactivity in extracted serum (ng equivalents GI181771 ml^{-1}) following oral administration of 2.7 mg [^{14}C]-GI181771 to male human volunteers.

Sampling time (h)	Volunteer number					
	61	62	63	64	65	66
Predose	0.00	0.00	0.00	0.00	0.00	0.00
0.25	<2.02	<2.02	2.66	<2.02	<2.02	<2.02
0.5	2.97	3.95	9.55	<2.02	2.46	<2.02
0.75	3.28	3.97	8.92	<2.02	2.49	3.97
1	<2.02	2.48	7.45	<2.02	<2.02	4.71
1.5	<2.02	<2.02	5.38	<2.02	<2.02	2.66
2	n.s.	<2.02	3.56	<2.02	<2.02	<2.02
2.5	<2.02	n.s.	4.31	<2.02	<2.02	<2.02
3	<2.02	<2.02	3.79	<2.02	<2.02	<2.02
4	2.63	<2.02	3.25	n.s.	<2.02	<2.02
6	3.85	<2.02	<2.02	<2.02	<2.02	<2.02
8	<2.02	<2.02	<2.02	<2.02	<2.02	<2.02
12	n.s.	<2.02	<2.02	<2.02	<2.02	<2.02
16	<2.02	<2.02	<2.02	<2.02	<2.02	<2.02
24	<2.02	<2.02	<2.02	<2.02	<2.02	<2.02

n.s., No sample.

Xenobiotica Downloaded from informahealthcare.com by GlaxoSmithKline (Active) on 03/15/11
For personal use only.

tions of parent drug. Although there were insufficient data to allow for a calculation of areas under the serum radiocarbon:time curve (AUC), peak concentrations of radiocarbon may be up to eight times higher than concentrations of parent drug in serum of some volunteers.

A trend was evident indicating that the volunteers with the higher radiocarbon concentrations in serum also had the higher concentrations of GI181771 in serum, adding confidence that the data obtained were reliable.

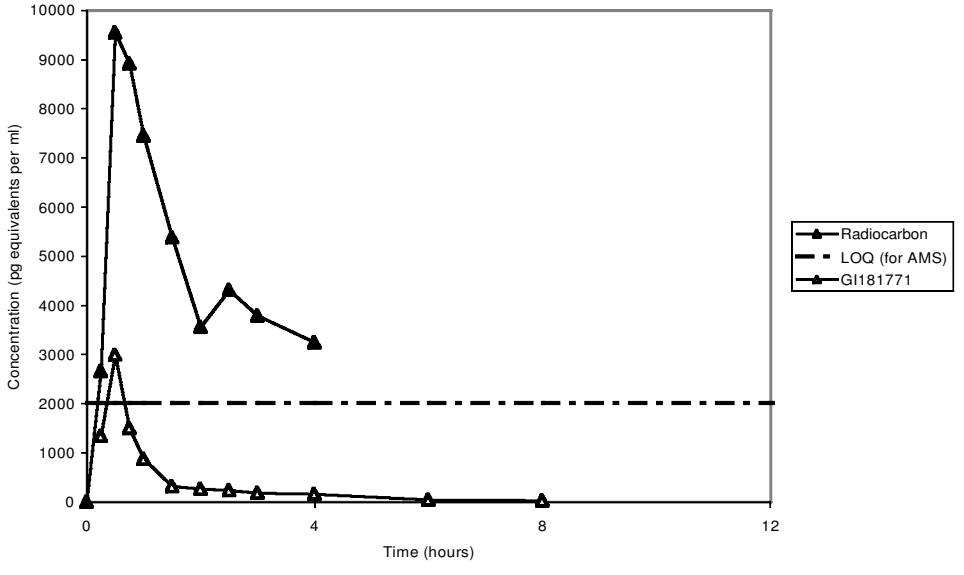

Figure 3. Example profiles of concentrations of radiocarbon due to drug-related material and concentrations of GI181771 in serum from a human male volunteer (no. 63) following oral administration of 2.7 mg [^{14}C]-GI181771.

RIGHTSLINK

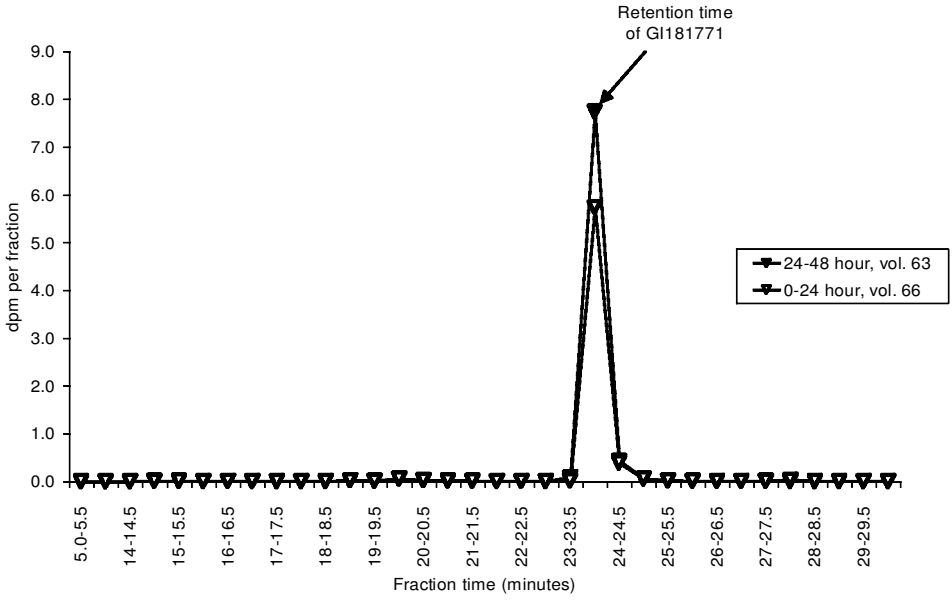

Figure 4. Reconstructed radiochromatograms (AMS results) of HPLC separation of faecal extracts from volunteers 63 and 66 following oral administration of 2.7 mg [^{14}C]-GI181771.

Xenobiotica Downloaded from informahealthcare.com by GlaxoSmithKline (Active) on 03/15/11
For personal use only.

A reconstructed radiochromatogram of HPLC separations from 10 times concentrated faecal extracts taken from selected predose and post-dose samples is shown in figure 4. The data indicated that radioactive material was mostly excreted as unchanged GI181771. The same data are shown in figure 5 using a magnified scale and they indicate that ~0.2% of the radioactivity detected corresponds to the retention time of a metabolite previously observed in rat bile and in human, rat and cynomolgus monkey liver preparations (unpublished data).

Results from the HPLC fractions of the pooled serum extracts showed no obvious drug-related components. These samples had been converted to graphite using an alternative to tributyrin as the carbon carrier, which contained minimal radiocarbon, to reduce the background and improve sensitivity. Unfortunately due to the very low levels of radioactivity (<0.01 dpm ml^{-1}) in all of the fractions, background regions of interest could not be defined, the limit of quantification could not be calculated and therefore drug-related radioactivity could not be determined.

In this study, LOQ for a range of biological matrices was determined (table 4). Serum samples obtained from a placebo group dosed orally with the same dosing vehicle (polyethylene glycol 400) as used in this study were processed to help further the determination of LOQ. To provide an estimate of LOQ for each of the matrices, a statistical analysis of background results was carried out. HPLC fractions coinciding with background regions of interest were treated as background measurements for this purpose. LOQ was taken as five times the pooled standard deviation of the background measurements derived from the between- and within-subject variations. LOQ was ~0.9 dpm g^{-1} for faeces homogenate, 0.4 dpm ml^{-1} for neat serum and 0.2 dpm ml^{-1} for neat urine. LOQ were lower for

RIGHTSLINK

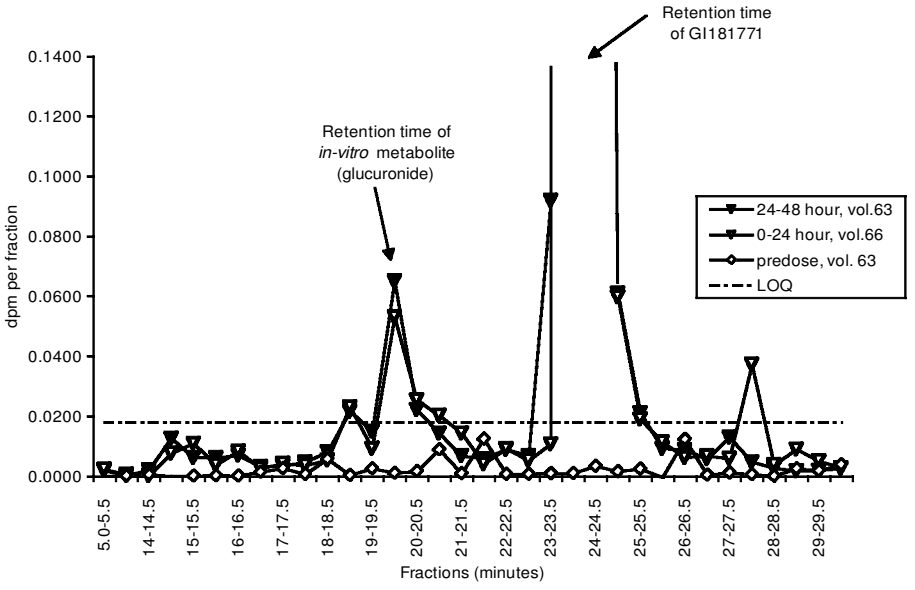

Figure 5. Reconstructed radiochromatograms (AMS results) of HPLC separation of faecal extracts from volunteers 63 and 66 following oral administration of 2.7 mg [^{14}C]-GI181771 – expanded *y*-axis.

Table 4. Limits of quantification for analysis of biomedical matrices by AMS, as defined for this study within Glaxo Wellcome Research and Development Ltd.

			dpm g^{-1}, dpm ml^{-1} or dpm/fraction				
						LOQ after predose of background has been subtracted	
Sample description	Matrix	Volume or weight analysed	Mean predose or background	SD (pooled)	CV (%)	Best estimate	95% Confidence interval
Faeces	homogenate	50 mg	0.60	0.17	28	0.86	0.58–1.97
Urine	neat	200 µl	0.11	0.040	36	0.20	0.15–0.37
Serum	neat	60 µl	0.57	0.087	15	0.43	0.28–0.96
Serum extract[1]	supernatant	800 µl	0.021	0.0011	5	0.005	0.004–0.011
Serum extract[2]	supernatant	800 µl	0.025	0.0042	17	0.021	0.017–0.026
						LOQ including background	
HPLC fraction of faecal extract[3]	mobile phase	100 µl	0.0027	0.0030	111	0.018	0.014–0.025
HPLC fraction of serum extract[4]	mobile phase	150 µl	0.0011	0.0016	145	0.009	0.008–0.012

[1] Volunteer 63 was excluded, through application of a statistical test, as an outlier from the LOQ calculation.

[2] Data generated from serum samples from subjects administered only with dosing vehicle (PEG 400). Calculation assumes 100% recovery after precipitation.

[3] Pre- and post-dose fractions, contained within the defined background regions of interest (5–6, 14–18 and 28–30 min), were used in calculation of LOQ.

[4] Fractions were converted to graphite using an older (undisclosed) carbon source than Tributyrin. As background regions of interest could not be defined all fractions were used in calculation of LOQ.

Xenobiotica Downloaded from informahealthcare.com by GlaxoSmithKline (Active) on 03/15/11
For personal use only.

RIGHTSLINK

samples that were processed further such that LOQ for serum extracts ranged from 0.02 to 0.005 dpm ml^{-1}. Fractions from HPLC of faecal extracts produced an LOQ = 0.02 dpm ml^{-1} and for serum extracts LOQ = 0.009 dpm ml^{-1}. As expected, samples containing either the least amount of total carbon or naturally occurring radiocarbon have the least variation in background and have the lowest LOQ for radiocarbon determinations. The data shown here represent a crude estimation of the LOQ that may be found in these matrices. The values are based on limited predose samples and approximations to predose samples, which were analysed in triplicate for a set period: 100–500 s.

Xenobiotica Downloaded from informahealthcare.com by GlaxoSmithKline (Active) on 03/15/11
For personal use only.

Discussion

AMS is now recognized as a useful addition to the tools available to those involved in drug discovery and development. Glaxo Wellcome Research and Development Ltd has been involved in the validation of AMS for biomedical use through the conduct of studies in animals and has established a dedicated laboratory for the preliminary sample handling involved. In the pilot clinical study described, it has been successfully demonstrated that AMS can be used as a tool for determining routes of excretion following administration of a very low dosage of radiocarbon-labelled drug. Throughout the conduct of the work on the clinical study and samples generated, contamination of samples with radiocarbon was not encountered and this may well endorse the contamination containment precautions taken by all involved. The approach taken by Glaxo Wellcome Research and Development Ltd with regard to contamination containment was that of minimizing risk and may have been overcautious, i.e. a specialized laboratory may not be required so long as appropriate precautions are taken.

A mean dose of 2.7 mg, 121 Bq (3.3 nCi) [^{14}C]-GI181771 was administered to six healthy human male volunteers and mass balance was achieved between administered and recovered radiocarbon. The mean faecal recovery of radiocarbon was 92% of the dose, mostly recovered in the first 48 h in the form of unchanged drug. Radiocarbon was not detected in any of the samples of urine implying that urine collected in the first 48 h following dosing contained no more than 6.5% of the dose. Concentrations of radioactivity in serum were measured using a precipitation step to increase sensitivity and contained up to 10 ng GI181771 equivalents ml^{-1}. Comparison with parent drug levels indicated the presence of systemically circulating metabolites.

It is clear that the LOQ for analysis of biomedical samples by AMS is improved when 'cleaner' samples (those containing lowered levels of endogenous material) are analysed as the impact of background radiocarbon is reduced. Signal:noise ratios and hence limits of detection were improved significantly (ranging from 20- to 80-fold) by use of protein precipitation to 'clean-up' the serum prior to analysis. The assumption was made that a high recovery of radioactive drug-related components was achieved through this sample preparation procedure. The estimate for LOQ obtained for serum extracts from the dosed subjects, after excluding an outlier from the calculation, was 0.005 dpm ml^{-1}, with a coefficient of variation (CV) = 5%. This LOQ was used in calculating the results for precipitated serum samples from the subjects dosed with drug. The LOQ determined from the placebo-dosed subjects in a separate study was 0.021 dpm ml^{-1}, with CV = 17%. This value was similar to that obtained

RIGHTSLINK

from subjects dosed with drug, with the outlier included (0.020 dpm ml^{-1}) and may be a more typical value. The background level of radiocarbon in extracts of serum may vary from one particular group of subjects to another, possibly due to dietary differences and thus result in a different LOQ being determined for each individual study. It is likely that the use of plasma rather than serum may reduce variability by removal of the variable protein recoveries associated with the clotting process and leading to lower LOQ. Indeed CBAMS Ltd has determined LOQ = 0.01 dpm ml^{-1} for neat plasma from studies conducted for other sponsors (unpublished data). There is an intention to assess the variability in background levels of radiocarbon in plasma from human volunteers in an AMS study, with a view to recommending that plasma is used rather than serum in all future AMS studies, conducted within Glaxo Wellcome Research and Development Ltd.

With regard to the LOQ determined in this study, precision would be improved by increasing the AMS analysis time, but the time constraints encountered when processing hundreds of biomedical samples would need to be borne in mind. A further study to examine specifically the limits of quantification for various matrices is, in our opinion, warranted.

Valuable lessons have been learned during the conduct of this study, which will aid in the design of future studies where AMS is used. Administration of a dose of radiolabel that produces the maximum exposure to ionizing radiation of 1 μSv, where no certification is required from ARSAC, would likely improve sensitivity ~17-fold over that observed in this study, where the exposure was only 0.06 μSv. A robust determination of limits of quantification for each matrix requires at least two predose samples per subject, ideally taken several hours apart. These extra predose samples would need to be included in any future study design. If concentrations of drug-related radioactivity in serum equating to <0.4 dpm ml^{-1} are expected, then a precipitation step may be required to provide adequate sensitivity, involving both an estimation of recovery and carbon analysis of the supernatant.

Future potential of AMS

AMS has the potential to provide supplemental information in studies where conventional doses have been administered and sensitivity becomes an issue, for example at later time-point sample collections, or to enable conduct of studies that are currently not possible. The inherent sensitivity of this technique could be harnessed to enable monitoring of drug-related analytes following administration of very low doses. Such low dose studies, which have been termed 'microdosing' studies, may be of interest to the pharmaceutical industry. Through the use of sample separation techniques coupled with AMS for off-line detection, as shown here, pharmacokinetics of both parent drug molecule and total drug-related material (drug and metabolites), could be elucidated. With the use of high specific activity radiocarbon labelled drugs incorporated into a small, perhaps low μg or even sub-μg, total dose it is envisaged that sensitivities in the high fg ml^{-1} range may be achievable. It is possible that the administration of such a small dose may not require very much in the way of supporting safety information from toxicology and ADME (absorption, distribution, metabolism and elimination) studies, thereby speeding up the progression from drug discovery to first clinical investigation. There may well be many caveats placed upon information obtained from

Xenobiotica Downloaded from informahealthcare.com by GlaxoSmithKline (Active) on 03/15/11
For personal use only.

RIGHTSLINK

microdosing studies, but should there be a desire to rank compounds according to their pharmacokinetics or susceptibility to metabolism then this could be achieved in human subjects earlier in a drug development programme than is currently the norm. The authors believe that this type of approach, and its pros and cons, is under consideration in a number of companies within the pharmaceutical industry.

AMS could also be of use in the reduction of numbers of animals used in drug discovery pharmacokinetic and excretion balance studies. The small sample size required for analysis by AMS, as low as 5 µl for plasma or serum, means that serial blood sampling from small animals such as rodents is viable and the need for composite study designs is reduced with consequent reduction in the number of animals required.

One of the biggest drawbacks to the use of AMS in early drug discovery is potentially the requirement for incorporation of the radioisotopic label within the molecule of interest. If the technique is ever to be used as part of a screening strategy for drug discovery candidates then incorporation of, for example, radiocarbon would need to be higher in throughput than is currently the case.

With the advent of the use of AMS in the pharmaceutical industry, the way is opened to reducing the use of relatively high levels of radioactivity for drug discovery and development. Reduction in levels of radioactivity handled brings with it not only ethical advantages associated with clinical use, but also a reduction in the environmental issues involved in the handling and disposing of radioactivity.

This paper has focussed on the use of AMS for the measurement of radiocarbon, but it should be noted that other elemental isotopes may well be of interest, for example ^{41}Ca and ^{129}I, both of which can be analysed using this technique. ^{41}Ca has been used to label human bones in studies to measure bone turnover (Freeman *et al.* 1997). ^{131}I and ^{125}I are frequently used in radioimmunoassays and AMS provides the alternative of using the more radiologically safe ^{129}I. Labelling of proteins or antibodies with ^{129}I and subsequent analysis by AMS could be of use in developing new therapies or diagnostic reagents.

AMS will no doubt be more widely used in biomedical investigations in the future. The rate-limiting step in the analysis of samples is the sample preparation which for radiocarbon involves the technically challenging combustion and graphitization steps. It is envisaged that advances will be sought in interfacing the AMS with some sort of on-line chromatography system for increased sample throughput and improved ease of use. At present there is only one commercial AMS facility in the UK for analysis of biomedical samples, but it may be that as the technique matures in the biomedical area and as AMS instrument size and cost potentially reduce, more will become available.

Xenobiotica Downloaded from informahealthcare.com by GlaxoSmithKline (Active) on 03/15/11
For personal use only.

Acknowledgements

The authors are grateful for the analytical service and input to study design provided by Professor Colin Garner, Sally Gregory and staff at The Centre for Biomedical Accelerator Mass Spectrometry (CBAMS) Ltd, Sand Hutton, York. The authors acknowledge staff at the Glaxo Wellcome Clinical Pharmacology Unit, Northwick Park Hospital, London, for conducting the clinical study and they also thank the staff of the Lawrence Livermore National Laboratory, Livermore, CA, for assistance in the early days. The authors also acknowledge

RIGHTSLINK

the assistance of Michael Aylott, Statistical Services at Glaxo Wellcome Research and Development Ltd.

References

ARSAC, Application for Certificate to Administer Radioactive Medicinal Products; obtained from ARSAC Support Unit, National Radiological Protection Board, Chilton, Didcot, UK.

Bennett, C. L., Beukens, R. P., Clover, M. R., Gove, H. E., Liebert, R. B., Litherland, A. E., Purser, K. H. and Sondheim, W. E., 1977, Radiocarbon dating using electrostatic accelerators: negative ions provide the key. *Science*, **198**, 508–510.

Freeman, S. P. H. T., King, J. C., Vieira, N. E., Woodhouse, L. R. and Yergey, A. L., 1997, Human calcium metabolism including bone resorption measured with ^{41}Ca tracer. *Nuclear Instruments and Methods in Physics Research*, **B123**, 266–270.

Garner, R. C., 2000, Accelerator mass spectrometry in pharmaceutical research and development – a new ultrasensitive analytical method for isotope measurement. *Current Drug Metabolism*, **1**, 205–213.

Garner, R. C., Barker, J., Flavell, C., Garner, J. V., Whattam, M., Young, G. C., Cussans, N., Jezequel, S. and Leong, D., 2000, A validation study comparing accelerator mass spectrometry and liquid scintillation counting for analysis of [^{14}C]-labelled drugs in plasma, urine and faecal extracts. *Journal of Pharmaceutical and Biomedical Analysis*, **24**, 197–209.

ICH Guideline 1996, *The International Conference on Harmonisation of Technical Requirements for Registration of Pharmaceuticals for Human Use (ICH) Guideline, 1996, Q2B Validation of Analytical Procedures: Methodology*.

Kaye, B., Garner, R. C., Mauthe, R. J., Freeman, S. P. H. T. and Turteltaub, K. W., 1997, A preliminary evaluation of accelerator mass spectrometry in the biomedical field. *Journal of Pharmaceutical and Biomedical Analysis*, **16**, 541–543.

Nelson, D. E., Korteling, R. G. and Scott, W. R., 1977, Carbon-14: direct detection at natural concentrations. *Science*, **198**, 507–508.

Vogel, J. S., 1992, Rapid production of graphite without contamination for biomedical AMS. *Radiocarbon*, **34**, 344–350.

Xenobiotica Downloaded from informahealthcare.com by GlaxoSmithKline (Active) on 03/15/11
For personal use only.

RIGHTSLINK

Available online at www.sciencedirect.com
ScienceDirect
Nuclear Instruments and Methods in Physics Research B 259 (2007) 752–757
NIM B
Beam Interactions with Materials & Atoms
www.elsevier.com/locate/nimb

AMS in drug development at GSK

G.C. Young *, W.J. Ellis

DMPK, GlaxoSmithKline Research and Development Ltd., Park Road, Ware, Herts, SG12 0DP, UK

Available online 3 February 2007

Abstract

A history of the use of AMS in GSK studies spanning the last 8 years (1998–2005) is presented, including use in pilot studies through to clinical, animal and in vitro studies. A brief summary of the status of GSK's in-house AMS capability is outlined and views on the future of AMS in GSK are presented, including potential impact on drug development and potential advances in AMS technology.
© 2007 Elsevier B.V. All rights reserved.

PACS: 82.80.Ms; 87.66.Ff

Keywords: Radiocarbon; Accelerator mass spectrometry; Pilot; Clinical; Drug; GlaxoSmithKline

1. Introduction

Accelerator mass spectrometry (AMS) has been used in GSK since 1998. All of the studies conducted to date have been supported by Xceleron Ltd. (formerly CBAMS Ltd.) with some sample preparation conducted at GlaxoSmithKline (GSK) Research and Development, including activities such as fraction collection following HPLC. Dedicated laboratories have been used throughout to minimise the risk of contamination of samples destined for analysis by AMS, although for a period a conventional laboratory used previously for handling higher levels of radiocarbon labelled samples was converted for use as an AMS sample preparation area. At the time of writing this article (late 2005), GSK is in the process of establishing a new dedicated sample preparation suite for AMS.

AMS has been used for atypical drug development projects to date, largely due to constraints such as the high cost of AMS analysis under contract and sample throughput limitations. The studies that have been conducted have fallen into two fairly distinct categories: ''true'' AMS studies and ''hybrid'' studies. In the context of GSK experience, AMS studies are those where the level of radiocarbon dosed was very limited. Studies have been categorised as an AMS study when dosimetry limitations have occurred due to tissue retention or protracted elimination of drug-related material in non-clinical species. AMS study categorisation has also occurred where a potent pharmacophore has been dosed and so insufficient radiocarbon could be administered due to the low chemical dose of drug utilised. Hybrid studies are those where conventional doses of radioactivity have been administered but some of the samples generated from the study were particularly low in radiocarbon. Studies have been categorised as a ''hybrid study'' when compounds have had very limited absorption, resulting in low levels of radioactivity in the samples or when investigation of late post-dose plasma sample timepoints was desired and again these were too low in activity to be analysed with more conventional techniques such as liquid scintillation counting (LSC).

The studies have been of a variety of designs and for a variety of purposes including studies in animals and humans, and in vitro studies. The studies have been both investigative in nature and in some instances have been key decision making studies to enable further progression of a new chemical entity (NCE).

This paper provides outline details of these studies for the purpose of highlighting uses of AMS for GSK, rather

* Corresponding author. Tel.: +44 1920 882391; fax: +44 1920 884374.
E-mail address: Graeme.C.Young@gsk.com (G.C. Young).

0168-583X/$ - see front matter © 2007 Elsevier B.V. All rights reserved.
doi:10.1016/j.nimb.2007.01.212

than providing all relevant experimental methods and results.

GSK has started to establish a capability for conducting AMS studies in-house and brief mention of this is described below. Additionally, views are expressed regarding the potential impact of AMS on drug development in GSK and potential advances in the technology are discussed.

2. Studies at GSK using AMS

2.1. Pilot rat excretion balance study

Conducted in 1998, a pilot rat excretion balance study was the first study to be carried out by GSK using AMS as the detection method. This work has been published previously [1] and so the details will not be discussed further but it is mentioned here to provide a more complete picture of the uses to which AMS has been put in GSK.

2.2. Pilot low radioactive dose clinical study

Conducted in 1999, a pilot low radioactive dose clinical study was the first use of AMS for GSK in support of a clinical study. As for the rat study above, this work has been published previously [2], but again is mentioned here for completeness.

2.3. Serum metabolite profiling for ''conventional dose'' clinical study

Conducted in 2001, metabolite profiling for a conventional dose clinical study was carried out, in Phase 2 of clinical development, and involved the oral administration to humans of a NCE at a dose of 84 μCi per subject i.e. a ''hybrid'' type study. Most of the study support was conducted using LSC, but levels of radioactivity in late time-point serum samples were too low to allow metabolite profiling by conventional means such as HPLC with radiochemical detection. In contrast, the levels of radioactivity were too high for AMS and the samples were diluted by a factor of 25 to bring them into the acceptable range. Sample profiling was conducted by HPLC with fraction collection then subsequent analysis of each fraction by AMS. The amount of radioactivity injected onto the HPLC ranged from 10 dpm down to 0.2 dpm and resulted in successful assignment of major metabolites by co-chromatography. Fig. 1 shows reconstructed chromatograms of serum samples taken predose, 1 h (7.9 dpm on column) and 12 h (3.4 dpm on column) after dose with assignments of many of the radioactive peaks observed (metabolites indicated using arbitrary ''M'' numbers). This study provided extremely useful experience in profiling with AMS at comparatively low levels and provided information on the nature of the drug-related material present in serum following administration of this new drug candidate.

2.4. In vitro blood cell binding study

Conducted in 2001, an in vitro blood cell binding study was carried out to investigate the extent of blood cell binding of a potent primary sulphonamide NCE. Prior work, not reported here, had been conducted at elevated concentrations far above the anticipated therapeutic range for this compound and it was decided to conduct a study at more relevant concentrations, using AMS as the detection method. Fig. 2 shows a bar chart indicating the degree of binding determined and the degree of displacement which occurred when the NCE was co-incubated at various concentrations in the presence and absence of potentially

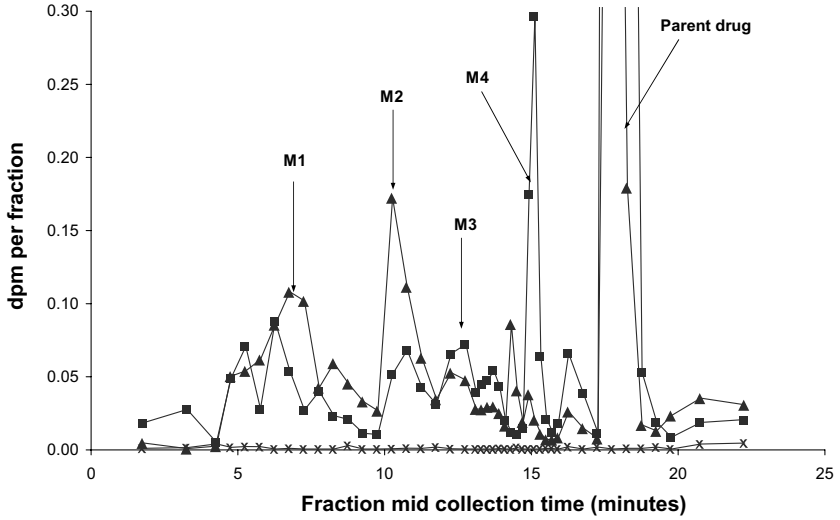

Fig. 1. Reconstructed radiochromatogram showing retention times of known metabolites in serum following administration of a NCE to human volunteers. ''M'' numbers are used to assign many of the radioactive peaks observed to known metabolites. Key: Pre-dose serum (×), 1 h post-dose serum (square), 12 h post-dose serum (triangle).

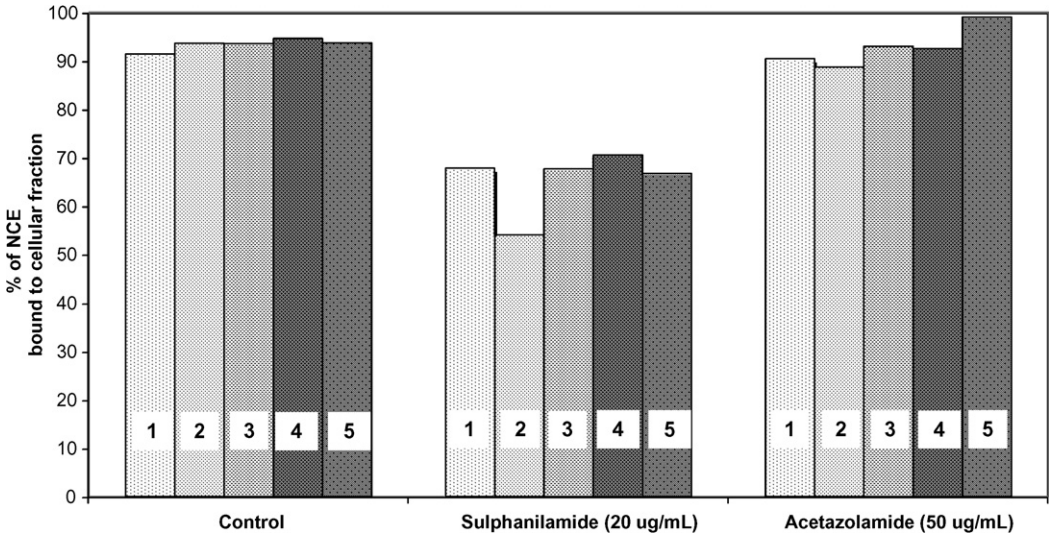

Fig. 2. In vitro blood cell binding and displacement of a NCE. The vertical bars represent data from experiments conducted using either LSC or AMS as the detection technique. Key: Concentrations of NCE at 0.01 (Bar 1; AMS), 0.1 (Bar 2; AMS), 1 (Bar 3; AMS), 100 (Bar 4; LSC) and 1000 ng/mL (Bar 5; LSC).

co-administered compounds (sulphanilamide and acetazolamide). The lower concentrations of NCE (0.01, 0.1 and 1 ng/mL) were analysed by AMS and the higher concentrations (100 and 5000 ng/mL) were analysed by LSC. The data generated showed that generally very similar results were obtained at the elevated and the anticipated therapeutic concentrations of the NCE, thus the use of AMS detection had "validated" the work carried out at supra-therapeutic concentrations.

2.5. Non-clinical study: excretion balance study in dogs

Conducted in 2003, a study in dogs involved the intravenous administration of 1 μg/kg, delivering only 1 μCi to the dogs, for the purpose of assessing routes of excretion, mass balance and metabolite profiling for a NCE. The excretion balance was successfully assessed using LSC with confirmation of some lower level samples using AMS, and metabolite profiling was achieved for urine and plasma samples using HPLC fractionation followed by AMS analysis.

2.6. Low radioactive dose clinical study

Conducted in 2004, a low radioactive dose clinical study was used in making a decision on the progression of development for a NCE, in Phase 1 of clinical development. The study was a true AMS study with administration of only 500 nCi to each human volunteer. The dose used was necessitated by predicted protracted elimination based upon animal data for this NCE. Excreta and blood collections were made over several weeks following dose administration and all samples were analysed by AMS, for excretion balance and total radiocarbon in blood/plasma. Fig. 3 shows the cumulative excretion of radiolabelled drug-related material with time. Periodic collections of excreta were used to allow an extended collection period without having to keep the volunteers in the clinic for longer than 15 days. The cumulative recovery obtained was achieved by extrapolations based on plots of amount excreted per day versus time. The mean total recovery from excreta obtained, using this extrapolation method, was >85%. Fig. 4 shows the total radiocarbon in plasma after dosing. Both sets of data highlight the expected, protracted elimination of drug-related material in humans and fully justify the approach of using AMS and severely limiting the radiocarbon dose administered versus a conventional human ADME study where circa 100 μCi may be administered.

2.7. Metabolite profiling of samples from a low radioactive dose clinical study

Conducted in 2004, using samples generated from the study mentioned (in Section 2.6) above, for investigations of metabolite profiles in urine and plasma. Samples were prepared and fractionated by HPLC and the fractions subsequently analysed by AMS. The amounts of radioactivity injected onto the HPLC column ranged from 5 dpm down to 0.02 dpm. Fig. 5 shows the reconstructed radiochromatogram of a post-dose plasma sample, 0.06 dpm on column, and indicates that most major peaks observed were attributable to known metabolites.

3. GSK's in-house AMS capability

GSK ordered two 250 kV single stage accelerator mass spectrometers (SSAMS) systems from National Electrostatics Corp. (NEC), Wisconsin; one for a GSK site in the UK and one for a site in the USA. Fig. 6 shows a schematic of the GSK systems. The instruments have two ion

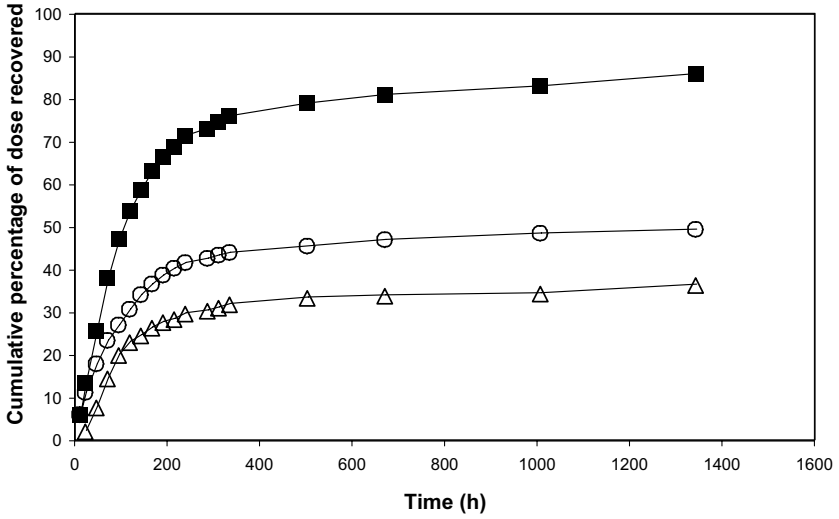

Fig. 3. Plots of cumulative excretion of radiolabelled drug-related material with time following oral administration of a NCE (500 nCi) to healthy human volunteers. Key: Faeces (triangle), urine (circle), total (square).

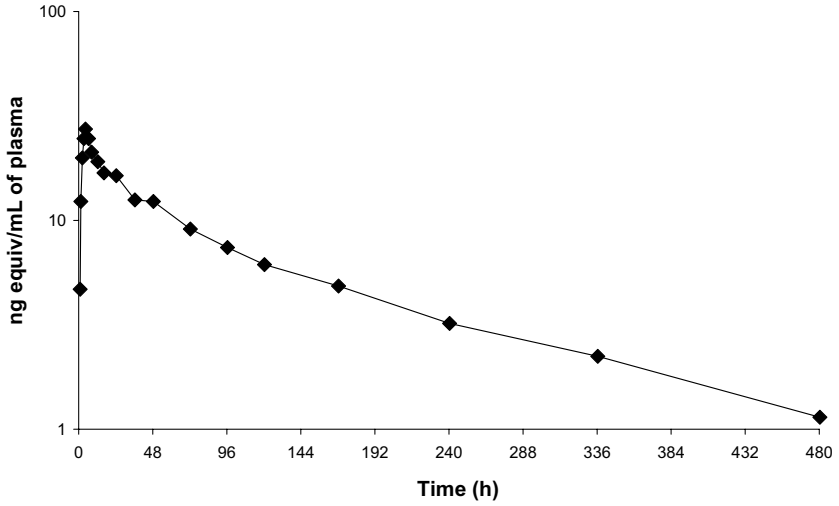

Fig. 4. Plot of total radiolabelled drug-related material in plasma with time following oral administration of a NCE (500 nCi) to healthy human volunteers.

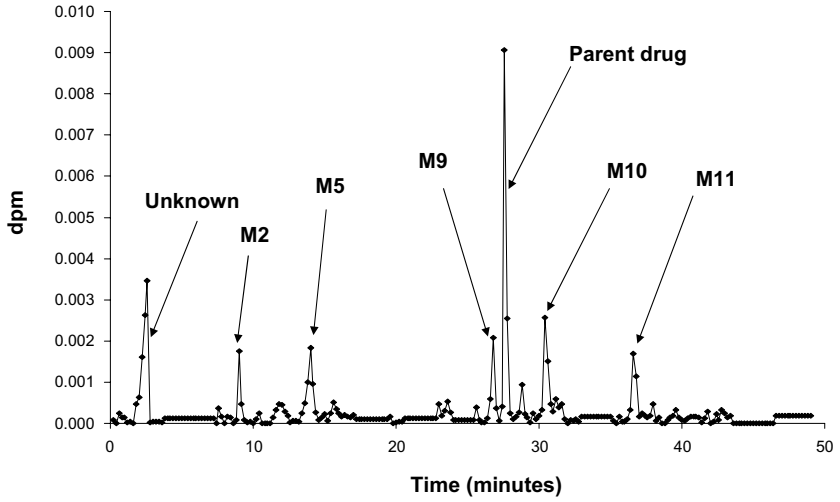

Fig. 5. Reconstructed radiochromatogram of a plasma sample taken following oral administration of a NCE (500 nCi) to healthy human volunteers (0.06 dpm on column).

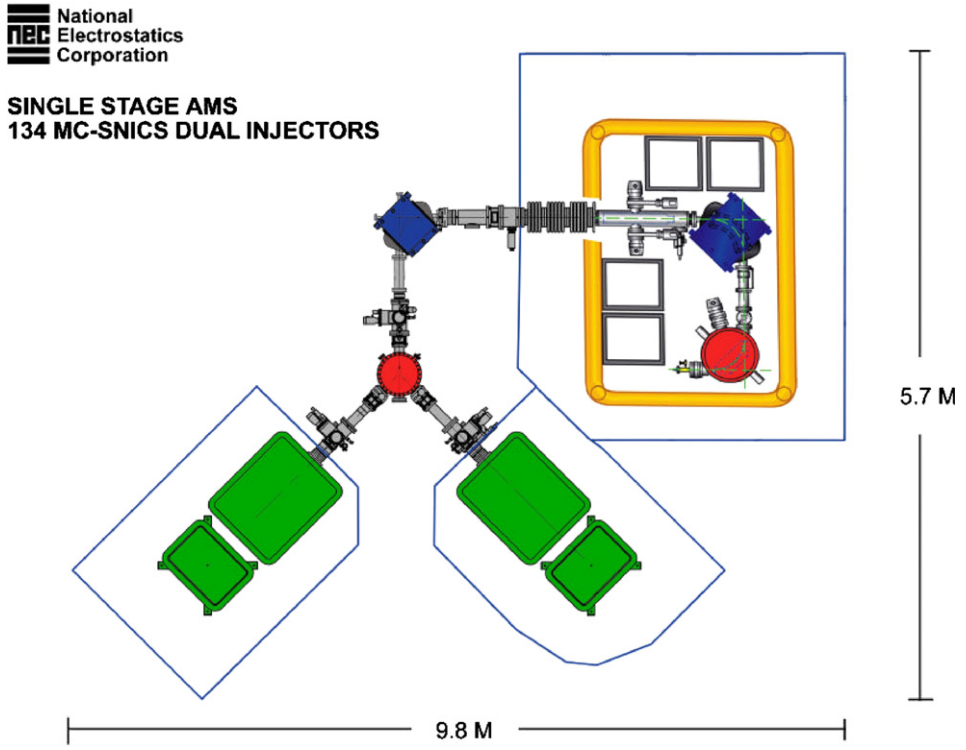

Fig. 6. Schematic of single stage AMS with dual 134 sample MC-SNICS. Reproduced by kind permission of NEC (National Electrostatics Corporation, Wisconsin, USA).

sources, each capable of holding a 134 sample wheel for graphite samples. Specialised sample preparation laboratories and instrument laboratories are being constructed at the GSK sites and staff are receiving training in sample preparation and AMS operation. At the time of writing it was envisaged that the GSK AMS systems will support real studies from 2006.

4. Future of AMS in GSK

4.1. Potential impact on drug development

AMS in itself provides no direct structural identification and the information provided by the instrument needs to be coupled with information from mass spectrometry and/or nuclear magnetic resonance spectroscopy for full structural identification of the components detected. This is only achievable if the doses selected, in the case of an in vivo study are sufficiently high in terms of chemical mass of drug to allow application of the other techniques mentioned to be of value. Use of AMS for metabolite profiling requires very robust chromatography since assignment of peaks to parent or metabolites is often dependent on co-chromatography for which standards of metabolites as markers is often advantageous, as are other data such as non-clinical metabolic pathway information. It is felt by some that since there may be a heavy reliance on the robustness of the chromatography used for separation of components subsequently quantified by AMS, the use of a second confirmatory chromatography method may be of use. It should also be noted that many clinical AMS studies may not be low enough in radiocarbon dose level to be categorised as exempt studies (as categorised by ARSAC the Administration of Radioactive Substances Advisory Committee, UK), but this is likely to be compound and study objective dependent. The current situation in GSK is that AMS is focussed on use in support of human ADME studies. Drug candidates administered by the inhaled, intranasal and dermal routes tend to produce low systemic exposures and so AMS is required due to its sensitivity advantages in dealing with samples generated from such studies. Additionally, low dose (potent) oral compounds and poorly absorbed compounds also produce analytical challenges in terms of sensitivity which may be addressed using AMS.

In the short term future, GSK is likely to harness the sensitivity of AMS to impact on relevant clinical study designs and perhaps use the technique in a wider range of non-clinical studies. The in-house availability and accessibility of AMS may well open up more opportunities for use of AMS including those beyond the types of applications highlighted in the past use of AMS in GSK, above. It is envisaged that conventional human ADME studies will still be conducted in the short term, but that early clinical AMS studies may be conducted, which will add value to the conventional human ADME study and reduce risk of surprises, later in development. Use of AMS early in development may help with understanding the metabolism

of NCEs in humans earlier in development and to "validate" the selected toxicology species early on, thus providing a greater understanding of the safety of the NCE and bringing value to the package of information used in submissions to regulatory authorities.

In the longer term, AMS is likely to be applied to typical as well as to atypical drugs in development, particularly in supporting early profiling and quantification of circulating metabolites following administration of NCEs to humans. There has been much talk about clinical microdosing of late; the concept of using very low doses as a surrogate for what is likely to occur at therapeutic doses, with potential use of AMS as the analytical tool. The authors are aware of some of the potential advantages of microdosing in relation to drug candidate selection, or de-selection, definition of intravenous pharmacokinetics in cases where drug solubility is dose limiting and so on. The authors believe that GSK will remain open to the possibilities of such applications of AMS and also in the potential advantages to be gained in reducing the levels of radiocarbon used in other studies, such as animal ADME studies. The technique does provide the sensitivity to enable alternatives to the conventional approaches in drug development. It should be borne in mind that conducting more detailed studies earlier in development can create difficulties in carrying on the progression of NCEs, as well as potentially assisting progression. It is entirely possible, for example, that an early clinical AMS study could highlight the presence of a metabolite that is unique to humans or for which there is insufficient safety cover in the animal toxicology species and this may cause difficulties in the continuation of clinical trials. Many seem agreed though that it is better to have this information earlier, rather than later in a new drug candidate's development.

4.2. Potential advances in technology

GSK is interested in making advances in sample preparation for AMS such as automation of the graphitisation process or identification of an alternative process to that being put in place at GSK, since sample preparation is currently the limiting step in throughput. The authors are aware that others are looking into interfacing of the AMS to achieve either off-line or on-line coupling to HPLC, CHN analyser or gas chromatograph and certainly would encourage such activities. GSK recognises that the instruments that it has purchased, are a first step towards bringing AMS into the mainstream of techniques in use in drug development. These instruments really need to be adapted or even replaced with "next generation" instruments in order to move AMS forward significantly.

5. Summary

AMS has been used in GSK with increasing frequency and in an ever widening range of applications, including clinical, animal and in vitro for both true AMS and hybrid studies. The cost of future contract research support for AMS studies was predicted to be high for GSK and so the company has made the move into establishing an in-house AMS capability. The main objective for GSK in regard to AMS is to use it as one of a range of techniques to aid in elucidating metabolism of new drug candidates in humans, early in development. AMS technology appears to be evolving quickly, so we can probably expect to see big changes, in a relatively short timeframe, certainly the authors believe that GSK will be taking an active interest in the development of AMS, particularly in regard to sample preparation and interfacing with HPLC.

Acknowledgements

We are grateful to Xceleron Ltd. (formerly CBAMS Ltd.) for their support in providing sample analysis by AMS for all of the studies detailed in this paper. We would also like to acknowledge GSK management for their support and encouragement, especially in regard to making the groundbreaking move towards investment in our own AMS capability.

References

[1] R.C. Garner, J. Barker, C. Flavell, J.V. Garner, M. Whattam, G.C. Young, N. Cussans, S. Jezequel, D. Leong, J. Pharm. Biomed. Anal. 24 (2000) 197.
[2] G.C. Young, W.J. Ellis, J. Ayrton, E. Hussey, B. Adamkiewicz, Xenobiotica 31 (8/9) (2001) 619.

Supplemental material to this article can be found at:
http://dmd.aspetjournals.org/content/suppl/2013/02/25/dmd.112.050153.DC1.html

1521-009X/41/5/1070–1081$25.00
DRUG METABOLISM AND DISPOSITION
Copyright © 2013 by The American Society for Pharmacology and Experimental Therapeutics
http://dx.doi.org/10.1124/dmd.112.050153
Drug Metab Dispos 41:1070–1081, May 2013

Disposition and Metabolism of GSK2251052 in Humans: A Novel Boron-Containing Antibiotic[S]

Gary D. Bowers, David Tenero, Parul Patel, Phuong Huynh, James Sigafoos, Kathryn O'Mara, Graeme C. Young, Etienne Dumont, Elizabeth Cunningham, Milena Kurtinecz, Patrick Stump, J. J. Conde, John P. Chism, Melinda J. Reese, Yun Lan Yueh, and John F. Tomayko

Department of Drug Metabolism and Pharmacokinetics (G.D.B., P.H., J.S., K.O., J.P.C., M.J.R., Y.L.Y.), and Infectious Diseases Therapeutic Area (P.P.), GlaxoSmithKline, Research Triangle Park, North Carolina; Department of Drug Metabolism and Pharmacokinetics, GlaxoSmithKline, Ware, UK (G.C.Y.); Department of Clinical Pharmacology, Modeling and Simulation (D.T.), API Chemistry and Analysis (J.J.C.), and Projects, Clinical Platforms and Sciences (E.C., P.S.), GlaxoSmithKline, King of Prussia, Pennsylvania; and Clinical Statistics (M.K.) and Infectious Diseases Therapeutic Area (E.D., J.F.T.), GlaxoSmithKline, Collegeville, Pennsylvania

Received November 16, 2012; accepted February 25, 2013

Downloaded from dmd.aspetjournals.org at ASPET Journals on November 8, 2015

ABSTRACT

(S)-3-(Aminomethyl)-7-(3-hydroxypropoxy)-1-hydroxy-1,3-dihydro-2,1-benzoxaborole (GSK2251052) is a novel boron-containing antibiotic that inhibits bacterial leucyl tRNA synthetase, and that has been in development for the treatment of serious Gram-negative infections. In this study, six healthy adult male subjects received a single i.v. dose of [^{14}C]GSK2251052, 1500 mg infused over 1 hour. Blood, urine, and feces were collected over an extended period of 14 days, and accelerator mass spectrometry was used to quantify low levels of radioactivity in plasma at later time points to supplement the less-sensitive liquid scintillation counting technique. An excellent mass balance recovery was achieved representing a mean total of 98.2% of the dose, including 90.5% recovered in the urine. Pharmacokinetic analysis demonstrated that radioactivity was moderately associated with the blood cellular components, and together with GSK2251052, both were highly distributed into tissues. The parent compound had a much shorter half-life than total radioactivity in plasma, approximately 11.6 hours compared with 96 hours. GSK2251052 and its major metabolite M3, which resulted from oxidation of the propanol side chain to the corresponding carboxylic acid, comprised the majority of the plasma radioactivity, 37 and 53% of the area under the plasma versus time concentration curve from time zero to infinity, respectively. Additionally, M3 was eliminated renally, and was demonstrated to be responsible for the long plasma radioactivity elimination half-life. A combination of in vitro metabolism experiments and a pharmacokinetic study in monkeys with the inhibitor 4-methylpyrazole provided strong evidence that alcohol dehydrogenase, potentially in association with aldehyde dehydrogenase, is the primary enzyme involved in the formation of the M3 metabolite.

Introduction

GSK2251052 [(S)-3-(aminomethyl)-7-(3-hydroxypropoxy)-1-hydroxy-1,3-dihydro-2,1-benzoxaborole hydrochloride], also known as AN3365, is an antibacterial compound that has been in development for the treatment of serious Gram-negative infections. Leucyl tRNA synthetase (LeuRS) is an essential bacterial enzyme that catalyzes the coupling of the amino acid leucine onto its corresponding leucine transfer ribonucleic acid (tRNA^{Leu}), which is used by the ribosome for protein synthesis. Inhibition of LeuRS prevents protein synthesis and stops growth of the bacteria. Through the unique chemical binding properties of the boron atom, GSK2251052 binds to the editing active site of bacterial LeuRS and forms a boron adduct with the 3′ terminus of tRNA^{Leu} which locks the tRNA^{Leu} to LeuRS in an unproductive state.

GSK2251052 has good in vitro activity against *Enterobacteriaceae* and *Pseudomonas aeruginosa*, and was not affected by any of the tested resistance mechanisms, including major efflux pumps, extended-spectrum β-lactamase, *Klebsiella pneumoniae* carbapenemase, and class C β-lactamase, which are known to be important contributors to the resistance of Gram-negative bacteria (Schweizer, 2012). It is acknowledged that there is a critical need for new antibiotics to treat Gram-negative bacterial infections (Spellberg et al., 2008), and GSK2251052 is one of several new compounds being developed that target protein synthesis as a mechanism of action (Sutcliffe, 2011).

dx.doi.org/10.1124/dmd.112.050153.
[S]This article has supplemental material available at dmd.aspetjournals.org.

ABBREVIATIONS: ADH, alcohol dehydrogenase; AE, adverse event; ALDH, aldehyde dehydrogenase; AMS, accelerator mass spectrometry; API, active pharmaceutical ingredient; $AUC_{(0-t)}$, area under the plasma versus time concentration curve from time zero to time of the measured concentration; $AUC_{(0-\infty)}$, area under the plasma versus time concentration curve from time zero to infinity; Cb, blood concentration; CL_p, plasma clearance; Cp, plasma concentration; GSK2251052, (S)-3-(aminomethyl)-7-(3-hydroxypropoxy)-1-hydroxy-1,3-dihydro-2,1-benzoxaborole; HPLC, high-performance liquid chromatography; LC/MS/MS, liquid chromatography-tandem mass spectrometry; LeuRS, leucyl tRNA synthetase; LLQ, lower limit of quantification; LSC, liquid scintillation counting; metabolite M3, (S)-3-(aminomethyl)-7-(carboxyethoxy)-1-hydroxy-1,3-dihydro-2,1-benzoxaborole; 4-MP, 4-methylpyrazole; MRT, mean residence time; *m/z*, mass-to-charge ratio; S9, homogenate fraction obtained from centrifugation at 9000*g*; tRNA^{Leu}, leucine transfer ribonucleic acid; Vss, volume of distribution at steady state; λ_z, terminal elimination rate constant.

In this article, we describe the pharmacokinetics, metabolism, and elimination of [^{14}C]GSK2251052 in humans following a single i.v. administration, which was one of the intended therapeutic routes of administration. Sampling of blood, urine, and feces allowed the evaluation of mass balance, route(s) of elimination (renal or metabolic), identification of primary metabolites, and a comparison of the exposure and half-lives of both parent compound and total radioactivity, which included metabolites. Additionally, the enzyme(s) responsible for the metabolism of GSK2251052 was investigated by conducting in vitro experiments and a nonclinical pharmacokinetic study.

Materials and Methods

Chemicals and Reagents

[^{14}C]GSK2251052 hydrochloride (specific activity of 0.00865 μCi/mg, stated radiochemical purity of 99.4%) (Fig. 1), GSK2251052 hydrochloride salt, [$^{2}H_2{}^{13}$C]GSK2251052, and [$^{2}H_2{}^{13}$C]M3 [(S)-3-(aminomethyl)-7-(carboxyethoxy)-1-hydroxy-1,3-dihydro-2,1-benzoxaborole] were supplied by GlaxoSmithKline Active Pharmaceutical Ingredient (API) Chemistry and Analysis (Stevenage, UK). Metabolite M3 was supplied by GlaxoSmithKline API Chemistry and Analysis (Upper Merion, PA). Scintillation cocktails, Ultima Gold and Ultima-Flo M, and Deepwell LumaPlate 96-well plates were obtained from PerkinElmer (Boston, MA). For in vitro experiments, all subcellular fractions (cynomolgus monkey and human) were supplied by Xenotech (Lenexa, KS). All human subcellular fractions were supplied pooled of mixed gender, and the monkey fractions were supplied pooled from male animals.

Formulated Drug

GlaxoSmithKline supplied nonsterile GSK2251052 hydrochloride salt powder containing [^{14}C]GSK2251052 hydrochloride, and the clinical site prepared sterile GSK2251052 containing [^{14}C]GSK2251052 solution for infusion. Powder was dissolved in sterile water for injection to a concentration of 125 mg/ml and was sterilized via filtration. Then 12 ml of solution, equivalent to 1500 mg of GSK2251052, was diluted to 250 ml with 0.9% NaCl injection prior to infusion.

Synthesis of Metabolite M3

The synthesis of metabolite M3 is depicted in Fig. 2. GSK2251052 (hydrochloride) was neutralized with di-isopropylethylamine, and then the corresponding free base was treated with benzyl bromide in methanol, in the presence of potassium carbonate, to give the desired dibenzylamino protected compound, which was then submitted to standard oxidation conditions using chromium (VI) oxide (CrO_3) in a mixture of acetic acid and acetone. The corresponding carboxylic acid was isolated as the sodium salt after basic workup. Hydrogenolysis of the *N*-benzyl groups using 5% palladium on carbon as the catalyst in a mixture of tetrahydrofuran and aqueous HCl produced the expected metabolite M3 as the hydrochloride salt.

Clinical Mass Balance Study

A phase I, open-label, nonrandomized, single-dose, single-center, mass balance study was conducted to investigate the recovery, excretion, and pharmacokinetics of GSK2251052 after i.v. administration. The study (NCI 01475695) was conducted according to principles of good clinical practice, applicable regulatory requirements, and the Declaration of Helsinki. The in-life portion of this study was conducted at PRA International, Stationsweg 163, 9471 GP (Zuidlaren, The Netherlands). Following Independent Ethics Committee approval by the Stichting Beoordeling Ethiek Biomedisch Onderzoek (Assen, The Netherlands) and collection of written informed consent, all subjects underwent an initial screening assessment within 30 days prior to the first dose. The screening included a medical history, physical evaluation, and clinical laboratory tests. Exclusion criteria included regular use of tobacco or nicotine-containing products (within 6 months prior to screening), a positive drug or alcohol test, recent participation in another research trial with an investigational product (i.e., within 30 days prior to screening), participation in a clinical trial involving a ^{14}C-labeled compound (within the last 12 months), and any pre-existing conditions that would interfere with normal gastrointestinal anatomy, motility, or hepatic or renal function which could interfere with the absorption, metabolism, and/or excretion of the study drug. Use of vitamins, dietary and herbal supplements, antacids, any prescription drugs, or grapefruit-containing products within 7 days prior to the start of the dosing through to the follow-up visit was prohibited. Six healthy adult male volunteers with a mean age of 42.2 years (S.D. 8.28 years), mean body weight of 83.1 kg (S.D. 3.41 kg), and mean body mass index of 25.5 kg/m^2 (S.D. 1.38 kg/m^2) were enrolled in this study. Five subjects were Caucasian and one subject was of Arabic/North-African heritage.

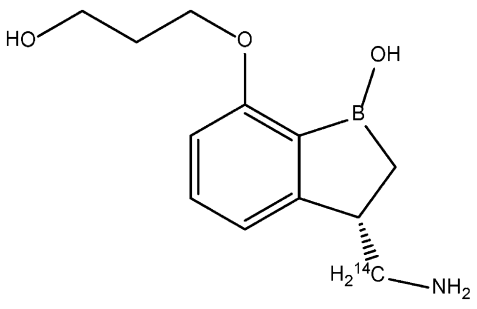

Fig. 1. Chemical structure of [^{14}C]GSK2251052 showing location of the radiolabel.

The radiolabeled dose was calculated in accordance with the 1990 Recommendations of the International Commission on Radiologic Protection (ICRP Publication 60; http://www.icrp.org/publication.asp?id=ICRP%20Publication%2060) as implemented in the 1999 Ionizing Radiations Regulations. The calculation was based on [^{14}C]GSK2251052 data obtained from a quantitative tissue distribution study conducted in rats. It was determined that, to comply with the International Commission on Radiological Protection guidance limit of 100 μSv (microsievert), the maximum activity would be 0.69 MBq (18.8 μCi). To ensure that this limit was not exceeded, a target dose of 15 μCi was chosen. All subjects enrolled who met eligibility criteria were fasted at least 10 hours prior to receiving a single radiolabeled i.v. dose of 1500 mg of [^{14}C]GSK2251052 (15 μCi, 0.56 MBq) infused at a constant rate over 1 hour. Following dosing, serial and intermittent whole-blood (including blood for plasma), urine, and fecal samples were collected for a minimum of 336 hours (14 days) postdose for study assessments (recovery, excretion, and pharmacokinetic). Safety was monitored throughout the study.

Venous blood samples were collected into tubes containing K_2 EDTA as the anticoagulant. All collection times listed are from the start of the 1-hour infusion. Blood samples (6 ml) for the pharmacokinetic analysis of blood and plasma radioactivity were collected predose and at 0.5, 1, 1.083, 1.25, 1.5, 2, 3, 4, 5, 6, 8, 12, 16, 24, 36, 48, 60, 72, 96, 120, 144, 168, 192, 240, 288, and 336 hours. Blood samples (2 ml) to prepare plasma for the pharmacokinetic analysis of GSK2251052 and metabolite M3 were collected predose and at 1, 1.5, 2, 2.5, 3, 4, 6, 8, 12, 16, 24, 36, 48, and 72 hours. Additional blood samples (4 ml) were collected at 1, 6, and 12 hours to prepare plasma, which was acidified with equal volumes of 50 mM citrate buffer (pH 4.0) and used to examine the stability of a hypothetical acyl glucuronide metabolite of M3. Blood samples (15 ml) to provide plasma for metabolite profiling were collected predose and at 1, 6, 12, 24, 48, 96, 144, and 336 hours. The 96-, 144-, and 336-hour plasma samples were subsequently used for the pharmacokinetic analysis of GSK2251052 and M3. Urine was collected predose and at 0–6, 6–12, and 12–24 hours, and thereafter at 24-hour intervals through 336 hours, while feces were collected predose and at 24-hour intervals through 336 hours.

Quantification of Radioactivity

Radioactivity in blood, plasma, urine, and feces were quantified at PRA International by liquid scintillation counting (LSC) using a Packard 3100TR liquid scintillation counter (Packard Instrument Company, Downers Grove, IL) with low-level count mode. Aliquots of plasma (0.25–1 ml) and urine (1 ml) were mixed directly with appropriate amounts of Ultima Gold scintillation cocktail prior to analysis. Whole blood (0.5 ml) was incubated with 1 ml of Solvable (PerkinElmer) for 1 hour at 60°C, and cooled prior to the addition of 0.1 M EDTA (100 μl). The samples were decolorized by the addition of

Downloaded from dmd.aspetjournals.org at ASPET Journals on November 8, 2015

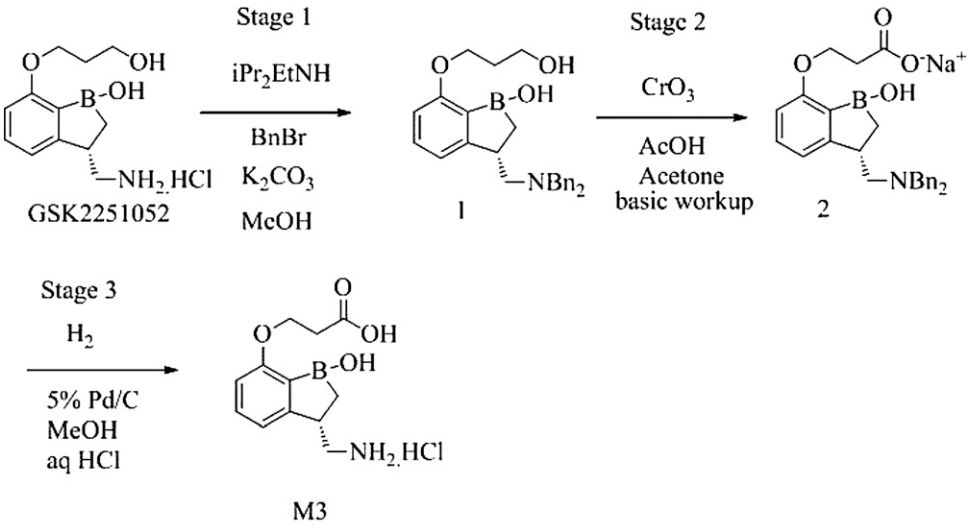

Fig. 2. The synthesis of metabolite M3.

hydrogen peroxide (4 × 100 μl) followed by a 30-minute incubation at room temperature, 20-minute incubation at 45°C, and 1-hour incubation at 60°C. Ultima Gold scintillation cocktail was added to the cooled samples, which were allowed to sit for at least 12 hours in the dark prior to analysis by LSC. Feces were mixed with water (1–2 times the sample weight) and homogenized prior to combustion of duplicate aliquots (0.5 g) using a PerkinElmer Model 307 sample oxidizer. The resulting $^{14}CO_2$ was trapped in Carbo-Sorb, mixed with Permafluor scintillation cocktail, and analyzed by LSC.

Accelerator Mass Spectrometry Analyses

Initially, plasma samples were analyzed for radioactivity using liquid scintillation counting as described previously. Samples in which concentrations were determined to be below the lower limit of quantification (LLQ; 870 ng equivalents/ml, 20 dpm/ml) were reanalyzed by accelerator mass spectrometry (AMS; LLQ 2.0 ng equivalents/ml, ~0.05 dpm/ml) at GlaxoSmithKline (Ware, Hertfordshire, UK). Analysis by AMS requires conversion of samples via a two-step process of oxidation to CO_2 and then reduction to graphite (Vogel, 1992). The AMS provides an isotope ratio of [^{14}C]:[^{12}C] from which ^{14}C per milligram of carbon is derived (Klody et al., 2005). A carbon content of control plasma of 4.38%, previously established using a Costech Carbon Analyzer (Valencia, CA), was used as the basis for the carbon content of all plasma samples analyzed. Untreated plasma sample aliquots (60 μl) were dried together with copper oxide, sealed into evacuated quartz tubes, and heated at 900°C for 2 hours. The CO_2 thus formed was cryogenically transferred into evacuated tubes containing zinc powder, titanium hydride, and cobalt catalyst, and the tubes were sealed. The reduction tubes were heated to 500°C for 4 hours, followed by 550°C for 6 hours to complete the graphitization process. Carbon as graphite, deposited on the cobalt, was pressed into aluminum cathodes and analyzed by AMS on a National Electrostatics Corp. (Middleton, WI) 250-kV single-stage accelerator mass spectrometer (Young et al., 2008). Control samples, including Australian National University (Acton, ACT, Australia) sugar and sodium benzoate, were processed with the analytical run. Instrument standards of pooled Australian National University and synthetic graphite were used to normalize the data and check suitability of instrumental background, respectively. The data from the AMS and carbon content analyses were combined to provide radiocarbon levels for each sample, with background subtraction of predose plasma concentration data as appropriate.

Sample Preparation for Metabolite Profiling

Urine. Urine was pooled across sampling times (0–120 hours) on a total sample weight basis to produce a representative pool for each subject containing ≥90% of the radioactivity excreted in the urine (90.2% of the dose). Additionally, 120–336-hour urine samples from each subject were pooled in the same manner, and equal volumes of each pool were combined to produce a single composite sample. The pooled urine was centrifuged at ~21,000*g* for 10 minutes, and a portion of each supernatant (500–1500 μl) was profiled using high-performance liquid chromatography (HPLC) with radiochemical detection. Triplicate-weighed aliquots of urine (200–2000 μl) were assayed using LSC before and after centrifugation to determine the recovery of radioactivity.

Feces. Feces were pooled across sampling times (0–120 hours) on a total sample weight basis to produce a representative pool for each subject containing ≥90% of the radioactivity excreted in the feces (6.0% of the dose). Due to the low levels of radioactivity in fecal samples, two sets of fecal homogenates were extracted in parallel. One set was used to monitor the recovery of radioactivity, and the second set was used for profiling. The homogenates (~1 g) were extracted twice by the addition of 4 volumes of acetonitrile:methanol:water:formic acid (50%:25%:25%:1%, v/v/v/v) followed by sonication for 20 minutes. Following each extraction, samples were centrifuged at 1620*g* for 10 minutes at 25°C, and the supernatants were combined in tared tubes. The total weights of the supernatants were determined, and triplicate-weighed aliquots (100–1500 μl) were assayed using LSC to determine the recovery of radioactivity. The supernatants were evaporated to dryness under a stream of nitrogen and reconstituted in 500 μl of water:methanol (90:10, v/v) before they were sonicated and centrifuged at 1620*g* for 10 minutes. The supernatants were transferred to microcentrifuge tubes and centrifuged at 21,000*g* for 5 minutes. To increase the recovery of radioactivity, the residual pellets were rinsed with 100 μl of water. Following centrifugation, the rinses were combined with the corresponding extracts. The total weights of the

Downloaded from dmd.aspetjournals.org at ASPET Journals on November 8, 2015

extracts were determined, and triplicate-weighed portions (10–100 μl) were analyzed using LSC to determine the recovery of radioactivity upon reconstitution. Portions (400 μl) of each fecal extract were profiled using HPLC with radiochemical detection.

Metabolite Profiling and Identification

Urine and fecal samples were analyzed using an Agilent-1260 HPLC system (Hewlett Packard, Palo Alto, CA) and a Waters Atlantis T_3 column (4.6 × 250 mm, 5 μm; Waters Corporation, Milford, MA). Mobile phase A consisted of 100 mM ammonium acetate (pH 4.5, pH adjusted with 100 mM acetic acid)/water (10:90, v/v), and mobile phase B consisted of 100 mM ammonium acetate (pH 4.5)/methanol (10:90, v/v). The gradient was held at starting conditions (10% B) from 0 to 10 minutes and increased linearly to 70% B from 10 to 55 minutes, and then to 95% B from 55 to 55.1 minutes. The gradient was held at 95% B from 55.1 to 60 minutes and returned to starting conditions at 60.1 minutes and held for a further 5 minutes. The column was allowed to equilibrate for an additional 10 minutes between injections. The analyses were performed at 30°C and a flow rate of 1 ml/min. The HPLC effluent was split, with 80% of the sample collected into deep-well LumaPlate-96 solid scintillant microplates (PerkinElmer; 0.2 minutes/well) and the remaining 20% directed to a Thermo Finnigan LTQ-Orbitrap Hybrid mass spectrometer equipped with an ElectroSpray Ionization source (Thermo Scientific, San Jose, CA) for metabolite identification. The LumaPlates, containing dimethylsulfoxide (10 μl/well) to reduce nonspecific binding of drug-related material, were dried on SPE Dry 96 Dual plate driers (Argonaut Technologies, Foster City, CA) under a stream of heated nitrogen and analyzed using a PerkinElmer TopCount NXT microplate scintillation counter (PerkinElmer Life Sciences, Downers Grove, IL). Data from the TopCount NXT were imported into Laura software (version 3.4.11; LabLogic Systems, Inc., Sheffield, UK), and the chromatograms were manually integrated. The lower limits of radiochemical detection (defined as peak height) were determined based on the proposal by Currie (1968) for the measurement of paired radioactivity, and calculated using counting time (30 minutes) and instrument background. Integrated peak areas of less than 3 times background are reported as <LLQ. Background was assigned for each run by selecting representative regions at the beginning and end of each chromatogram. The radioactive drug-related components in feces and urine are reported as a percentage of the administered dose, and as a percentage of the radioactivity in the matrix (to 1 decimal place). Results were corrected for the recovery of radioactivity following centrifugation (urine) or extraction and reconstitution (feces).

Metabolites were characterized using a ThermoFinnigan Orbitrap XL (Thermo Scientific) mass spectrometer in the positive mode based on accurate mass measurements from full-scan MS data [*m/z* (mas-to-charge ratio) 100–700 at 30,000 resolution]. Mass spectral data obtained from metabolites identified in the preclinical species (unpublished observations) were also used in the assignment of metabolite structures.

Monkey Pharmacokinetic Study with 4-Methylpyrazole

GSK2251052 was administered to cynomolgus monkeys (3 per sex per group) as a single constant rate i.v. infusion over 1 hour at a dose level of 35 mg/kg, either alone or 1 hour after an oral gavage administration of the alcohol dehydrogenase (ADH) inhibitor 4-methylpyrazole (4-MP) (Sigma-Aldrich, St. Louis, MO). GSK2251052 was formulated at 7 mg/ml as a solution in 0.9% sodium chloride injection, USP (saline), pH 5, and administered at a dose volume of 5 ml/kg/h. 4-MP was formulated as a solution at 8.75 mg/ml in purified water and administered to cynomolgus monkeys at a dose volume of 4 ml/kg. Venous blood samples (0.5 ml) for the plasma pharmacokinetic analysis of GSK2251052 and M3 were collected into tubes containing K_2 EDTA as the anticoagulant predose and at 0.5, 0.92, 1.08, 1.25, 1.5, 2, 3, 5, 9, 24, 48, 72, 96, and 120 hours. All times listed are from the start of the 1-hour infusion.

Quantification of GSK2251052 and Metabolite M3 in Monkey and Human Plasma

The plasma concentrations of GSK2251052 and metabolite M3 were measured using validated methods based on protein precipitation followed by liquid chromatography-tandem mass spectrometry (LC/MS/MS) analysis. Briefly, a 50-μl (human) or 15-μl (monkey) aliquot of plasma was added to 250 μl (human) or 100 μl (monkey) of methanol containing formic acid (0.1% v/v), [$^2H_2{}^{13}C$]-GSK2251052, and [$^2H_2{}^{13}C$]-M3 (100 ng/ml each) in 96-deep-well plates and vortex mixed for 10 minutes. The samples were then centrifuged at 3000*g* for 5 minutes. For human samples, 225 μl of the supernatants were transferred to clean 96-deep-well plates and dried under warm nitrogen before reconstitution in 60 μl, 0.1% formic acid (v/v) in water. Monkey plasma sample supernatants were diluted by adding 25–150 μl of 0.1% formic acid. Between 1- and 5-μl aliquots of the reconstituted or diluted samples were injected into an LC/MS/MS system consisting of a Waters Acquity ultra high-pressure liquid chromatography (Waters Corporation), a Waters HSS T_3 column (50 × 2.1 mm, 1.8 μm) at 50°C, and an MDS Sciex 4000 API-4000 mass spectrometer (Applied Biosystems/MDS Sciex, Concord, ON, Canada). Mobile phase A consisted of water containing 0.1% formic acid (v/v), and mobile phase B consisted of methanol: water:formic acid (50%:50%:0.1%, v/v/v). The compounds were eluted from the column at a flow rate of 0.7 ml/min and for human samples with a gradient starting at 22% B, which increased linearly to 30% B from 0.5 to 1.51 minutes and returned to 22% B from 1.51 to 1.6 minutes. For monkey samples, the column was eluted isocratically, with 85% mobile phase A and 15% B. Tandem mass spectrometry analyses were performed using a TurboIonSpray interface (Applied Biosystems/MDS Sciex) operated in the positive mode and a probe temperature of 400°C. The analytes were measured by multiple reaction monitoring of the following $[M+H]^+$ transitions: GSK2251052 *m/z* 238 → 202 and metabolite M3 *m/z* 252 → 162. The transitions monitored for the internal standards were 3 mass units higher than the corresponding analyte. Data collection and integration were performed using Analyst software (version 1.4.2; Applied Biosystems/MDS Sciex). Quantification was based on analyte/internal standard peak area ratios and calculated using a weighted $1/x^2$ linear regression model within SMS2000 (version 2.3; GlaxoSmithKline, Research Triangle Park, NC). The operating range of the assays for both analytes, GSK2251052 and M3, was 5–10,000 ng/ml in human plasma and 100–200,000 ng/ml in monkey plasma.

Pharmacokinetic Analysis

The plasma pharmacokinetic parameters were estimated by noncompartmental methods with either WinNonlin Professional Edition version 5.2 (Pharsight, Mountain View, CA) using actual pharmacokinetic sampling times

TABLE 1

Summary of human pharmacokinetic parameters of GSK2251052, M3, and total radioactivity after a single i.v. infusion dose of [^{14}C]GSK2251052 (1500 mg)

Matrix	Analyte	$AUC_{(0\text{-}t)}$ [a]	$AUC_{(0\text{-}\infty)}$ [a]	C_{max} [a]	CL [a]	Vss [a]	$T_{1/2}$ [b]	T_{max} [b]
		μg · h/ml	*μg.h/ml*	*μg/ml*	*l/h*	*l*	*h*	*h*
Plasma	GSK2251052	72.3 (7.34)	72.5 (7.41)	24.6 (14.5)	20.7 (7.41)	197 (8.87)	11.6 (9.96–12.1)	0.917 (0.50–0.92)
	M3	101 (12.1)	103 (12.1)	1.77 (9.77)	NA	NA	77.3 (68.1–78.5)	7.00 (5.00–24.0)
	Radioactivity	191 (10.0)	195 (9.90)	24.3 (16.1)	7.70 (9.90)	348 (12.6)	96.0 (86.2–117)	0.917 (0.92–0.92)
Whole blood	Radioactivity	141 (20.8)	193 (21.1)	43.7 (10.2)	7.79 (21.1)	116 (17.8)	14.3 (7.28–16.1)	0.917 (0.92–0.92)

%CV, % coefficient of variation; NA, not applicable.
[a] Geometric mean (%CV).
[b] Median (range).

Downloaded from dmd.aspetjournals.org at ASPET Journals on November 8, 2015

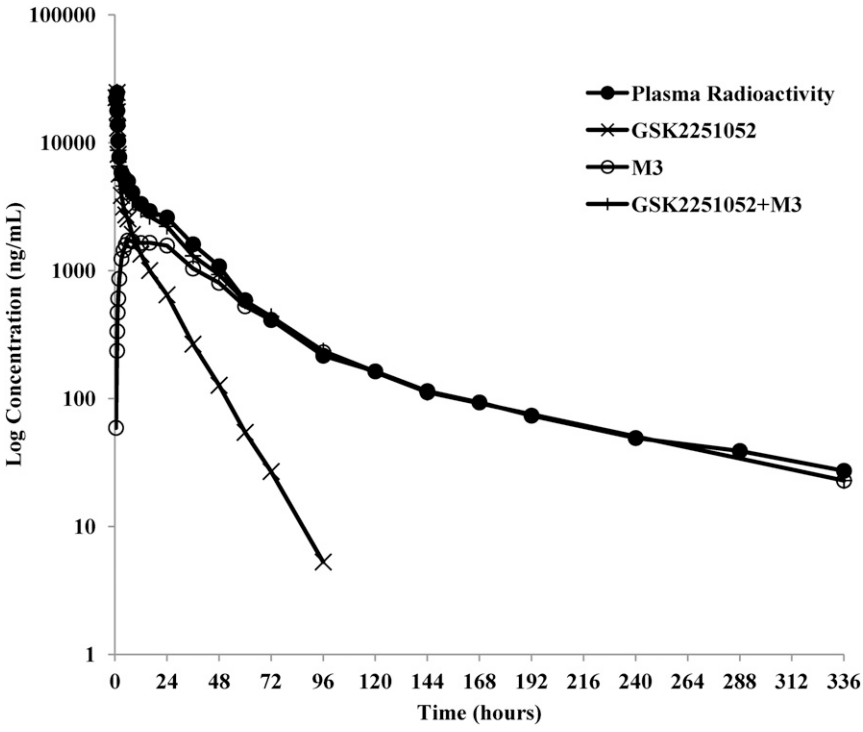

Fig. 3. Concentration-time plot: mean (n = 6) plasma concentrations of GSK2251052 (×, ng/ml), M3 (○, ng/ml), GSK2251052 + M3 (+, ng/ml), and total radioactivity (●, ng equivalents/ml) obtained from a combination of LSC, AMS, and LC/MS/MS analyses.

(human study), or WinNonlin Enterprise Edition version 4.1 using the nominal sampling times (monkey study). The maximum observed plasma concentration (C_{max}), the time at which C_{max} was observed, and the time to the last measurable concentration were determined directly from the raw concentration-time data or using WinNonlin. The area under the concentration-time curve from time zero to the last quantifiable time point [$AUC_{(0\text{-}t)}$] and the area from time zero to infinity [$AUC_{(0\text{-}\infty)}$] were calculated using the linear up/logarithmic down trapezoidal method. The $AUC_{(0\text{-}\infty)}$ was estimated as the sum of $AUC_{(0\text{-}t)}$ plus $C_{last}/\lambda z$, where C_{last} is the concentration at the last quantifiable time point. The terminal elimination rate constant (λ_z) was estimated from linear regression analysis of the log-transformed concentration-time profile. The number of points included in the terminal phase was determined by visual inspection of the semilog plots of the concentration-time profiles. The associated apparent terminal elimination half-life ($t_{1/2}$) was calculated as $\ln 2/\lambda_z$. Clearance was calculated as dose/$AUC_{(0\text{-}\infty)}$, and the volume of distribution at steady state was calculated as CL * mean residence time (MRT), where MRT is the mean residence time after i.v. administration.

For human samples, the percentage of radioactivity associated with blood cells was calculated according to the equation 100 – [(Cp)(1 − Hct)/(Cb) × 100], where Cp and Cb are the concentrations of radioactivity in plasma and blood, respectively, and Hct is the hematocrit. The blood:plasma ratio was calculated as Cb/Cp.

Investigations to Generate M3 Using In Vitro Systems

S9 and Microsomal Incubations. For incubations with NADP, [^{14}C]GSK2251052 (50 and 500 μM) was incubated with 4 mg/ml of monkey S9 (homogenate fraction obtained from centrifugation at 9000g; liver, lung, and kidney) or liver microsomes (monkey and human) in 50 mM potassium phosphate buffer at pH 7.4 containing 5.5 mM glucose-6-phosphate, 0.44 mM NADP, and 1.12 units/ml glucose-6-phosphate dehydrogenase. For incubations with NAD^+, [^{14}C]GSK2251052 (500 μM) was incubated with 4 mg/ml S9 (monkey liver, lung, kidney, and human liver S9 only) or liver microsomes (monkey and human) and 7.5 mM NAD^+ in 30 mM sodium pyrophosphate buffer at pH 7.4, or in 23 mM sodium pyrophosphate buffer at pH 8.4 or 8.8.

Incubations containing no NADP, NAD^+, or S9 were used as negative controls, whereas incubations containing 250 μM 7-ethoxycoumarin served as positive controls. Where appropriate, 4-MP was added to incubations to yield a final concentration of 0.6 mM.

Cytosol Incubations. [^{14}C]GSK2251052 (500 μM) was incubated with 4 mg/ml of liver cytosol (monkey and human) containing 7.5 mM NAD^+ in 30 mM sodium pyrophosphate buffer at pH 7.4 or 23 mM sodium pyrophosphate buffer at pH 8.4. Incubations without NAD^+ or liver cytosol were used as negative controls. Where appropriate, 4-MP was added to incubations to yield a final concentration of 0.6 mM. To verify ADH in the preparations of liver cytosol, human and monkey liver cytosol (4 mg/ml) was incubated with 7.5 mM NAD^+, ethanol (0.1%), and 30 mM sodium pyrophosphate buffer at pH 7.4. Incubations in the absence of ethanol or in the presence of 4-MP (0.6 mM) were performed in parallel as controls. To assess the concentration-dependent inhibitory effect of GSK2251052 on its own metabolism, [^{14}C]GSK2251052 (1–50 μM) was incubated with human liver cytosol (1.5 mg/ml) in phosphate buffer, pH 7.4, containing 7.5 mM NAD^+ for up to 20 hours.

In Vitro Sample Preparation and Analysis. All samples from in vitro incubations, except positive controls with ethanol, were run in triplicate for 1 or 3 hours in a shaking water bath set to 37°C and 100 rpm. Following incubation, individual samples were quenched with acetonitrile such that the ratio of acetonitrile was 45%. Samples were then centrifuged at approximately 21,000g for 5 minutes to remove protein precipitate, and the supernatant was removed to

TABLE 2

Mean percentage of cumulative radioactivity recovered from six healthy male subjects after a single 1500 mg i.v. infusion dose of [^{14}C]GSK2251052

Time Period	Urine	Feces	Total
h	*% dose*	*% dose*	*% dose*
0–24	51.2	0.1	51.3
0–48	69.2	1.3	70.5
0–72	76.9	4.3	81.2
0–96	81.1	6.4	87.5
0–120	83.4	7.3	90.7
0–144	85.1	7.5	92.6
0–168	86.4	7.6	94.0
0–192	87.4	7.6	95.0
0–216	88.2	7.6	95.8
0–240	88.8	7.6	96.4
0–264	89.3	7.6	97.0
0–288	89.8	7.6	97.4
0–312	90.2	7.6	97.8
0–336	90.5	7.6	98.2

Downloaded from dmd.aspetjournals.org at ASPET Journals on November 8, 2015

a fresh vial. An aliquot (10 μl) of each supernatant, except 7-ethoxycoumarin, was mixed with 5.0 ml Ultima Gold scintillation cocktail and analyzed using liquid scintillation counting. Data obtained from liquid scintillation counting were used to assess the recovery of radiocarbon in sample extracts.

Portions of the replicates were then pooled using equal volumes to produce a single representative sample for each incubation condition. The pooled portions were diluted with water 10-fold prior to analysis using HPLC as described previously in the *Metabolite Profiling and Identification* section, except that radiochemical detection was performed by a PerkinElmer Radiomatic 625TR series flow scintillation analyzer with Laura version 3.4.11 software and Ultima Flo M scintillation fluid (3 ml/min).

Experiments to Assess the Formation of NADH. GSK2251052 (final concentrations of 0.001, 0.01, 0.1, 1.0, and 10 mM) was incubated with human liver cytosol (1.5 mg/ml), NAD^+ (0.22 mM), and sodium pyrophosphate buffer, pH 8.8 (22 mM), or potassium phosphate buffer, pH 7.4 (50 mM), at room temperature. The incubations, in triplicate, were conducted in a 96-well plate with the reactions started by addition of GSK2251052. The NADH produced during GSK2251052 oxidation in the incubations was measured at an absorbance of 340 nm using a SpectraMax spectrophotometer (Molecular Devices, Sunnyvale, CA). Incubations with the ADH inhibitor 4-MP (0.6 mM) were included as positive inhibitor controls. Incubations without enzyme, NAD^+, or GSK2251052 were included as negative controls. Incubations containing ethanol in the absence of GSK2251052 were conducted to confirm metabolic activity of the enzyme preparations. Cytosolic and purified ADH incubation samples were analyzed by UV absorbance detection at 340 nm as a function of time (every 60 seconds for1 hour, or every 2 minutes for 120 minutes). Rates of NADH formation were calculated by monitoring the decrease in NADH formation, and were expressed as the rate (slope).

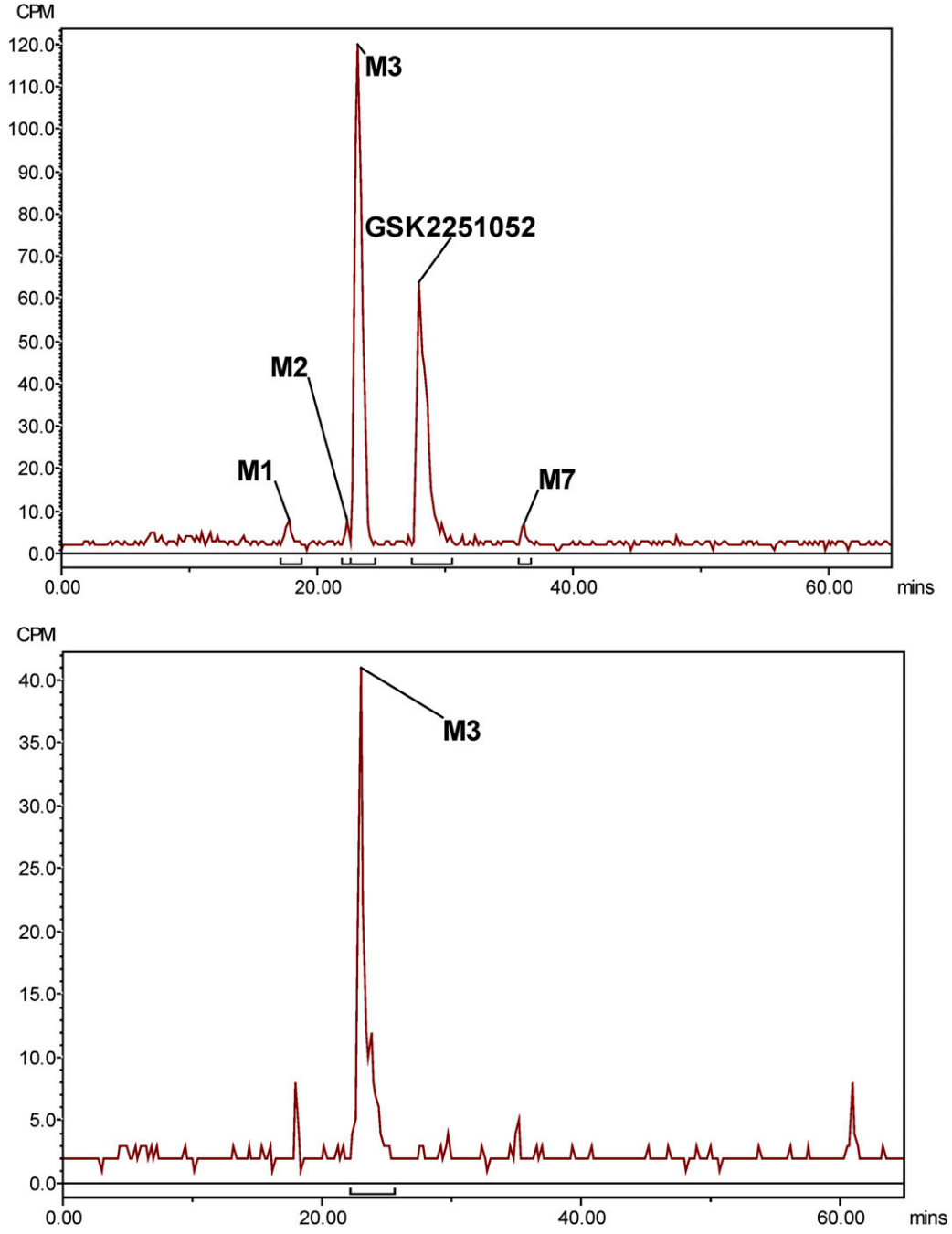

Fig. 4. Representative HPLC radiochromatogram of pooled urine [0–120 hours (top) and 120–336 hours (bottom)] following a single 1500-mg i.v. infusion of GSK2251052 in humans. CPM, counts per minute.

Downloaded from dmd.aspetjournals.org at ASPET Journals on November 8, 2015

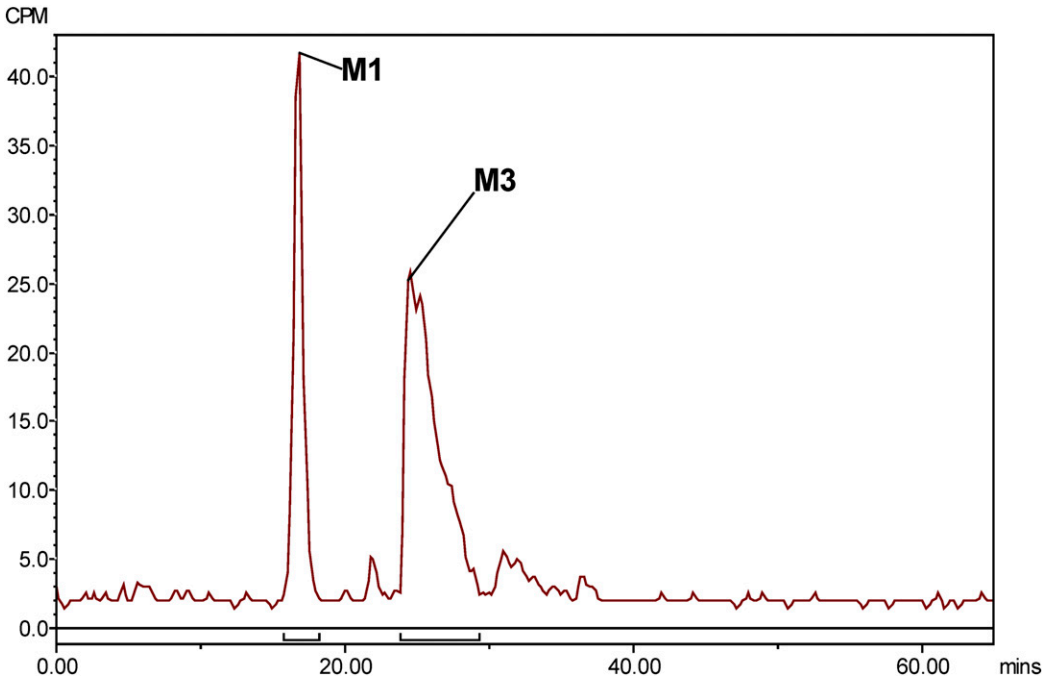

Fig. 5. Representative HPLC radiochromatogram of pooled feces (0–120 hours) following a single 1500-mg i.v. infusion of GSK2251052 in humans. CPM, counts per minute.

GSK2251052 (final concentrations of 1 and 10 μM) was incubated with purified ADH (0.025 units/ml), NAD^+ (7.5 mM), and potassium phosphate buffer, pH 7.4 (50 mM), at room temperature, and samples were analyzed by UV detection as described previously.

Results

Clinical Safety and Tolerability Data. All subjects completed the study as planned and received the correct treatment in the fasting state. The treatments were well tolerated with no deaths, serious adverse events, or withdrawals due to adverse events (AEs) reported. Three subjects (50%) reported AEs, all of which were mild in intensity (headache, diarrhea, infrequent bowel movements, and insomnia) and resolved during the study without treatment or intervention. Two subjects experienced multiple AEs (infrequent bowel movements and headache; insomnia and headache). None of the AEs were considered to be related to the study drug.

TABLE 3

Individual percentage of GSK2251052-related components in human excreta (0-120 hours) after a single i.v. dose of 1500 mg of [^{14}C]GSK2251052

Metabolite	% Administered Dose Recovered in Each Subject						
	101	102	103	104	105	106	Mean ± S.D.
Urine[a]							
GSK2251052	27.8	31.6	32.4	23.3	27.9	30.4	28.9 ± 3.0
M1	BQL	BQL	BQL	BQL	BQL	BQL	BQL ± NC
M2	BQL	BQL	BQL	BQL	BQL	BQL	BQL ± NC
M3[b]	44.7	42.6	43.8	41.0	39.3	51.6	43.8 ± 3.9
M7	BQL	BQL	BQL	BQL	BQL	BQL	BQL ± NC
Total quantified	72.5	74.2	76.2	64.4	67.3	82.0	72.8 ± 5.8
Total radioactivity	84.1	83.2	86.6	80.8	77.4	86.4	83.1 ± 3.2
Feces							
M1	1.2	1.3	1.1	2.3	0.8	1.8	1.4 ± 0.5
M3	2.6	4.7	2.7	3.3	3.1	3.3	3.3 ± 0.7
Total quantified	3.9	6.0	3.8	5.5	3.9	5.1	4.7 ± 0.9
Total radioactivity	4.7	7.4	5.4	6.9	5.7	5.9	6.0 ± 0.9

BQL, below quantification limit; NC, not calculated.
[a]120–336-hour urine samples from each subject were pooled proportionally by sample weight, and equal volumes of each pool were combined to produce a single composite sample.
[b]M3 (5.9% of dose) was the only component detected in the composite sample.

Clinical Pharmacokinetic Results. Six healthy fasted males received a single i.v. dose of 1500 mg of [^{14}C]GSK2251052 (15 μCi) infused over 1 hour. The pharmacokinetic parameters for whole blood and plasma radioactivity, GSK2251052, and M3 are presented in Table 1, and the concentration-time profiles for plasma radioactivity are shown in Fig. 3. The bioanalytical method was robust and performed well, with quality control samples for both GSK2251052 and M3 demonstrating accuracy and precision in the range of 0.0–6.2% and 1.5–6.6%, respectively, during analysis of the study samples. The half-life of radioactivity (96 hours) was notably longer than that observed for the parent compound (11.6 hours). The plasma concentration for M3 peaked at 7 hours, and the elimination half-life was 77.3 hours, approaching that observed for total plasma radioactivity. The plasma $AUC_{(0-\infty)}$ values for GSK2251052 and M3 were 37 and 53% of the radioactivity $AUC_{(0-\infty)}$ value, respectively. Relative to total body water [42 l (Davies and Morris, 1993)], total radioactivity and GSK2251052 were both highly distributed in tissues with volume of distribution at steady state (Vss) values of 348 and 197 l, respectively, and plasma clearance (CL_p) for GSK2251052 was 20.7 l/h. Blood-to-plasma-concentration ratios ranged from 1.03 to 2.03 through 24 hours postdose, and the calculated percentage of radioactivity associated with red blood cells ranged from 44 to 71.9% through 24 hours postdose. The $AUC_{(0-\infty)}$ of radioactivity in plasma and whole blood were generally similar (2% difference).

Mass Balance and Excretion in Urine and Feces. The mean total recovery of radioactivity was 98.2% (range of 92.7–99.9%) (Table 2), with the majority of the dose (90.5%) excreted in the urine and fecal elimination representing a minor route of elimination (7.6% of the dose). Approximately 80% of the dose was recovered during the first 72 hours, and by 192 hours, 95% of the administered dose had been recovered. Excretion of residual radioactivity into the urine continued throughout the 336-hour collection period, which is consistent with the long plasma half-life of M3.

Downloaded from dmd.aspetjournals.org at ASPET Journals on November 8, 2015

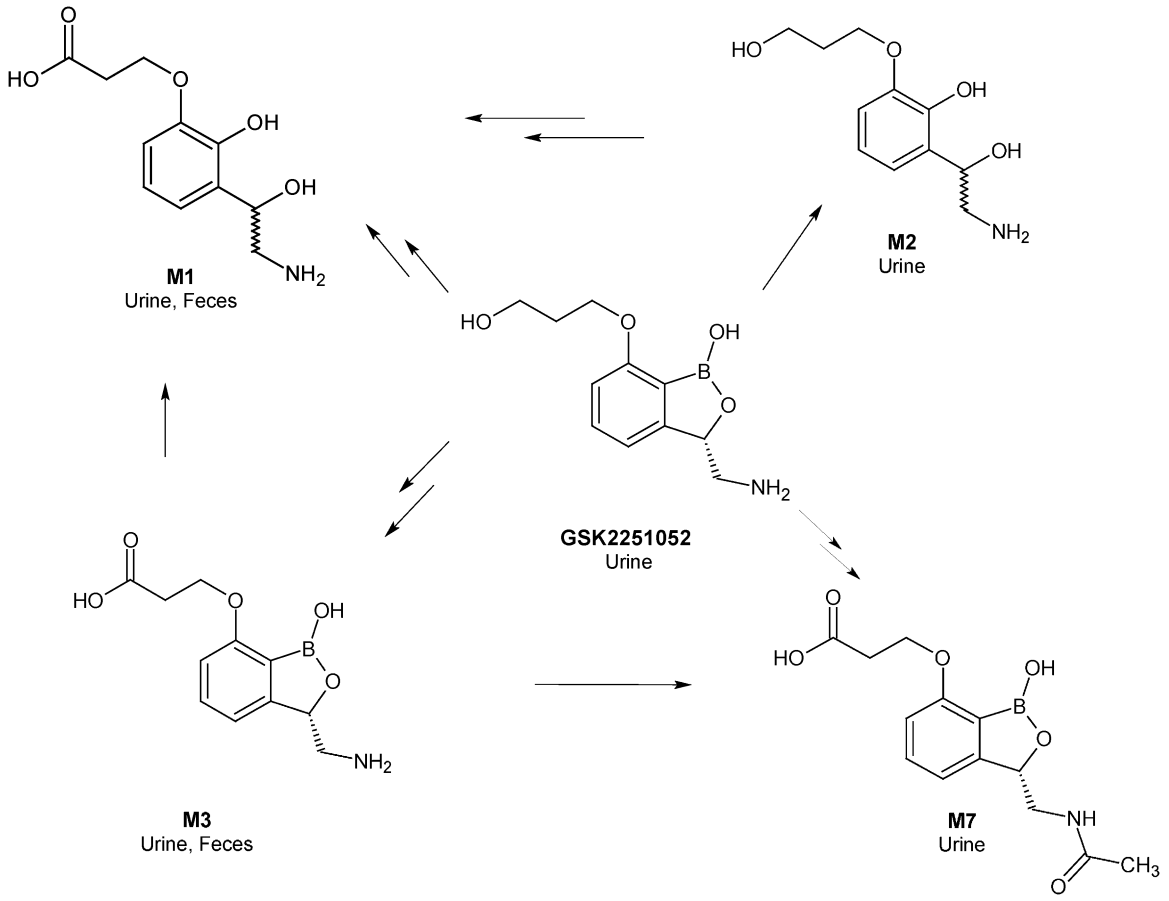

Fig. 6. Proposed metabolites of GSK2251052 in humans.

Metabolite Profiling and Characterization. Low levels of radioactivity present in plasma precluded metabolite profiling analysis of this particular matrix using conventional approaches. Representative HPLC radiochromatograms of pooled urine (0–120 and 120–336 hours) and fecal extracts (0–120 hours) are shown in Figs. 4 and 5. Individual and mean quantitative data for metabolites from the six subjects are presented in Table 3. GSK2251052 and metabolite M3 represented a mean of 28.9 and 49.7% of the administered dose, respectively, through 336 hours postdose in urine. Three minor metabolites were also detected in urine and identified by mass spectrometry (Supplemental Table 1), but were below the LLQ: M1 (deboronation, oxidation), M2 (deboronation), and M7 (*N*-acetylated M3). The proposed metabolic scheme for GSK22520152 in humans is shown in Fig. 6.

TABLE 4

Percentage of GSK2251052 and M3 following 3-hour incubations of [^{14}C]GSK2251052 (500 μM) with NAD$^+$ (7.5 mM) at pH 7.4, 8.4, and 8.8 in monkey liver S9, cytosol, and microsomes

Peak	Percentage of Total Radioactivity (Peak Area)					
	S9			Cytosol		Microsomes
	pH 7.4	pH 8.4	pH 8.8	pH 7.4	pH 8.4	pH 7.4
M3	7.7	6.7	4.3	1.7	0.9	2.5
GSK2251052	87.8	85.6	89.0	88.7	97.7	87.9
Total	95.5	92.3	93.3	90.4	98.6	90.4

Mean combined extraction and reconstitution efficiencies of radioactivity from the fecal homogenates were 94.8%. The principal components in feces were metabolites M3 and M1, which represented a mean of 3.3 and 1.4% of the dose through 120 hours postdose, respectively. Unchanged GSK2251052 was not detected in feces. Overall, at least 83% of the administered radioactivity was identified in urine and feces.

In Vitro Investigations of the Enzyme Responsible for the Formation of M3. The in vitro metabolism of [^{14}C]GSK2251052 and the formation of the oxidative metabolite M3 were investigated in selected tissue subcellular fractions from cynomolgus monkey (liver S9, cytosol, microsomes, as well as, lung and kidney S9) and human (liver S9, cytosol, and microsomes). No metabolism of [^{14}C]GSK2251052 or formation of metabolite M3 was observed in monkey liver, lung, or kidney S9, or human liver microsomes in the presence of an NADPH regeneration system (unpublished data). In contrast, in the presence of NAD$^+$, low ($\leq$10%) but detectable metabolism of [^{14}C]GSK2251052 and the formation of M3 was observed in monkey liver S9, cytosol, and microsomes (Table 4), but not in monkey lung and kidney S9, or in human liver S9, cytosol, or microsomes (unpublished data). Additionally, M3 was not observed in monkey liver S9 or cytosol containing NAD$^+$ cofactor following incubation in the presence of the ADH inhibitor 4-MP.

Although M3 was not observed in human liver cytosolic and purified ADH enzyme incubations, ADH involvement in GSK2251052 metabolism was further assessed by spectrophotometric measurement of NADH produced in the incubations as a result of oxidation to an aldehyde intermediate of M3. In human liver cytosol and purified ADH enzyme incubations with GSK2251052, a time-dependent

Downloaded from dmd.aspetjournals.org at ASPET Journals on November 8, 2015

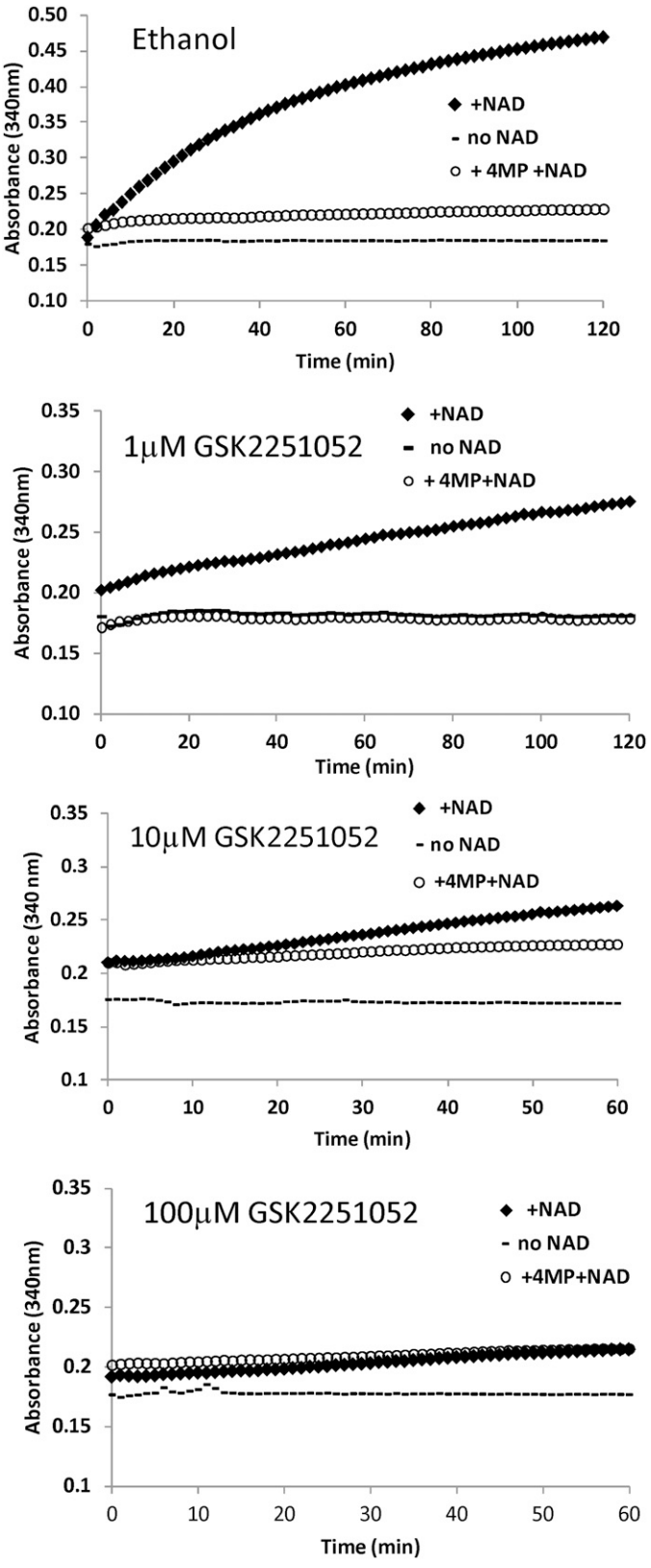

Fig. 7. NADH formation (absorbance at 340 nm) in human liver cytosolic incubations with the ADH probe substrate, ethanol, or GSK2251052 (1, 10, or 100 μM) for 60 or 120 minutes at pH 7.4.

increase in absorbance at 340 nm was observed. This increase in absorbance was dependent on the ADH cofactor, NAD^+, and was not observed in the presence of the ADH inhibitor, 4-MP (Fig. 7).

Pharmacokinetics of GSK2251052 in Monkeys Administered 4-MP. During a single 1-hour infusion of GSK2251052, following an oral dose of 4-MP, a 53–63% decrease in the mean CL_P of GSK2251052 was observed (Table 5). This decrease in plasma clearance resulted in a 2.0- to 2.7-fold increase in the mean $AUC_{(0-\infty)}$ values of GSK2252015 and an associated 79–91% decrease in systemic exposure (mean plasma C_{max} and $AUC_{(0-t)}$ values) of M3. The ratio of the AUC values for M3 to GSK2251052 ranged from 0.49 to 1.3 when GSK2251052 was dosed alone; the ratio ranged from 0.04 to 0.09 when 4-MP was dosed with GSK2251052. However, the impact of 4-MP on the mean GSK2251052 C_{max} values was minimal. The mean plasma half-life ($t_{1/2}$) and MRT of GSK2251052 increased 55–70% and 2.2- to 2.3-fold, respectively, in the presence of 4-MP. There was no impact of 4-MP on the mean Vss for GSK2251052. As there were no significant differences in the pharmacokinetics between male and female animals, for brevity, only data from male animals are described in this paper.

Discussion

GSK2251052 is a novel, boron-containing antibiotic that inhibits bacterial LeuRS and has been in development for the treatment of serious Gram-negative infections. This investigation evaluated the pharmacokinetics, metabolism, and excretion of GSK2251052 in humans after a single i.v. dose (1500 mg) of [^{14}C]GSK2251052 administered as an infusion over 1 hour. Additionally, the enzyme believed to be responsible for the metabolism of GSK2251052 was studied by conducting in vitro experiments and a nonclinical pharmacokinetic study with the ADH inhibitor 4-MP. In the clinical study, GSK2251052 was well tolerated with only mild adverse events reported. This clinical study was designed with an extended collection period (minimum of 14 days postdose) to provide the best opportunity for complete recovery. The result was that mass balance was achieved, with a large proportion of the radioactivity (mean 81.1%) recovered in urine within 5 days following i.v. administration, and essentially complete recovery (98.2%) in urine and feces by 14 days.

Total radioactivity and GSK2251052 were both highly distributed in tissues with Vss values of 348 and 197 l, respectively, far exceeding total body water (42 l) for a typical 70-kg male (Davies and Morris, 1993). On average, CL_p was 20.7 l/h for GSK2251052. Since approximately 70% of GSK2251052 systemic CL_p is nonrenal (unpublished observations) and based on a blood:plasma ratio of 1.5, the average hepatic blood CL is 9.7 l/h, indicating that GSK2251052 is a low-clearance compound relative to a hepatic blood flow of 87 l/h (Davies and Morris, 1993). The mean $AUC_{(0-\infty)}$ values of radioactivity in plasma and whole blood were generally similar (2% difference), indicating that radioactivity was moderately associated with red blood cells.

LC/MS/MS quantification and subsequent pharmacokinetic analysis of GSK2251052 and metabolite M3 demonstrated that the metabolite had a significantly longer elimination half-life: 77.3 hours compared with 11.6 hours for the parent compound. Consistent with these data, plasma concentrations of metabolite M3 were measurable at the last sampling time point, 336 hours (Fig. 3), in contrast to GSK2251052, which was only measurable up to 96 hours. Using LSC, it was only possible to quantify plasma radioactivity up to the 96-hour time point due to the lack of sensitivity of this particular analytical approach. Using AMS as a significantly more sensitive technique to determine plasma radioactivity at later time points allowed construction of the complete plasma concentration-time profile. It was then possible to demonstrate that the combined GSK2251052 and metabolite M3 plasma exposure (mean $AUC_{(0-\infty)}$ of 37 and 53%, respectively)

Downloaded from dmd.aspetjournals.org at ASPET Journals on November 8, 2015

TABLE 5

Summary of pharmacokinetic parameters of GSK2251052 and M3 after a single i.v. infusion of GSK2251052 (35 mg/kg) alone or with a single oral gavage dose of 4-MP (35 mg/kg) in male monkeys

Analyte	Treatment[a]	$AUC_{(0-\infty)}$ [b,c]	C_{max} [b]	CL [b]	Vss [b]	MRT [b]	$T_{1/2}$ [b]	T_{max} [b]
		h · μg/ml	*μg/ml*	*l/h/kg*	*l/kg*	*h*	*h*	*h*
GSK2251052	Alone	60.7 (51.3–76.7)	46.0 (17.3–99.1)	0.60 (0.46–0.68)	3.04 (1.66–3.97)	4.9 (3.6–5.8)	5.4 (4.8–5.9)	0.92 (0.92–0.92)
	Plus 4-MP	161 (148–18)	68.6 (21.9–161)	0.22 (0.19–0.24)	2.53 (1.99–2.88)	11 (10–12)	9.2 (8.6–9.7)	0.92 (0.92–0.92)
M3	Alone	52.3 (42.8–67.0)	4.15 (3.49–4.54)	NA	NA	NA	NA	3.0 (3.0–3.0)
	Plus 4-MP	11.0 (9.49–13.0)	0.36 (0.32–0.42)	NA	NA	NA	NA	9.0 (9.0–48)

NA, not applicable.
[a]N = 3/treatment, and data from males shown only for brevity.
[b]Values are the mean and (range), except for T_{max}, which is shown as the median (range).
[c]For M3, AUC_{0-t}.

represented the significant majority of the plasma radioactivity $AUC_{(0-\infty)}$. Additionally, the elimination half-life of M3 (77.3 hours) approached that of plasma radioactivity, 96 hours. Although an acyl glucuronide conjugate of M3 had not been previously observed in other metabolism studies (unpublished data), analysis of acidified plasma from this clinical study provided confirmation that such a conjugate, if

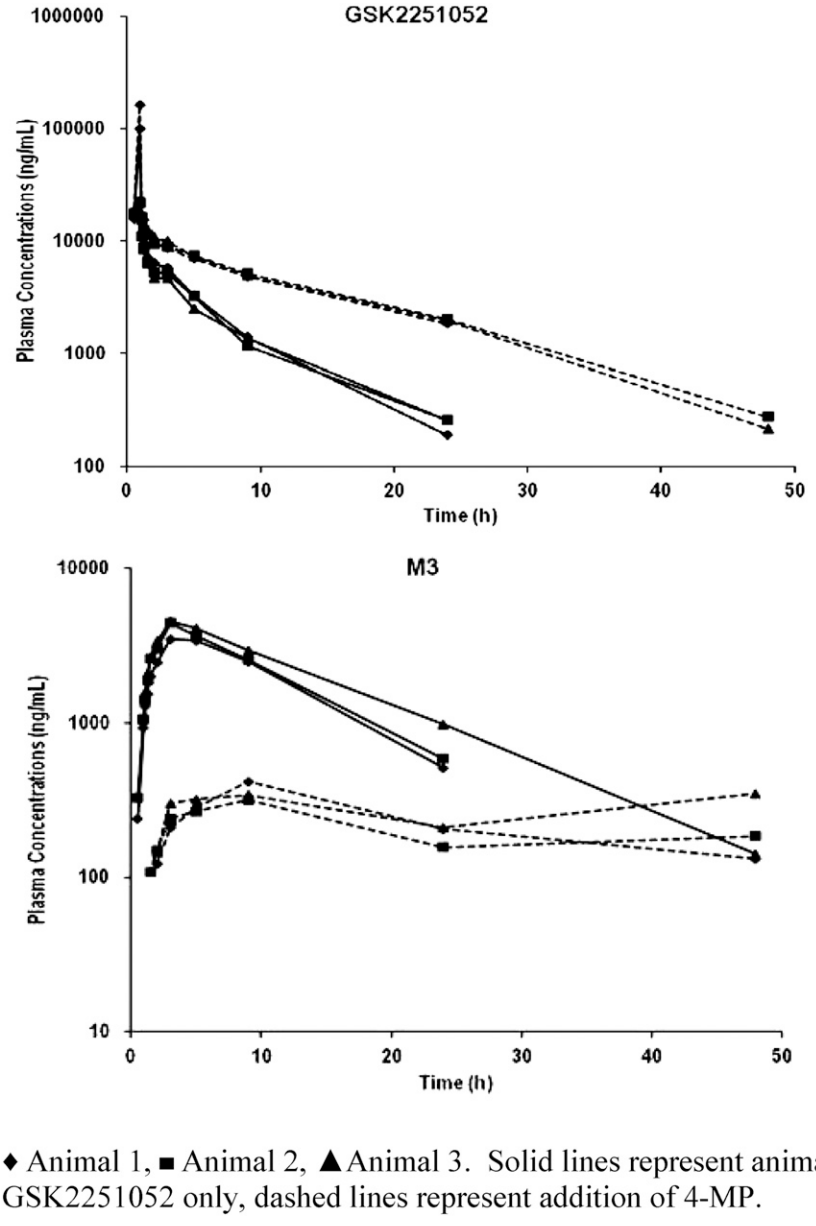

Fig. 8. Individual plasma concentration-time profiles of GSK2251052 and M3 from LC/MS/MS analyses following a single i.v. infusion administration of GSK2251052 at 35 mg/kg alone or in combination with 4-MP at 35 mg/kg to male monkeys.

Downloaded from dmd.aspetjournals.org at ASPET Journals on November 8, 2015

present in plasma, would not hydrolyze and interfere with the quantitative assessment of M3.

Consistent with the plasma pharmacokinetic data, analysis of urine demonstrated that metabolite M3 was a significant pathway of clearance for GSK2251052, consisting of approximately 50% of the dose recovered in that matrix. M3 was considered major as it represented greater than 10% of drug-related exposure, and therefore, according to the International Conference on Harmonization (Non-Clinical Safety Studies for the Conduct of Human Clinical Trials for Pharmaceuticals, International Conference on Harmonization Guidance M3(R2), 2009; http://www.emea.europa.eu/pdfs/human/ich/028695en.pdf), was investigated further in the relevant toxicity species (unpublished data). In addition to M3, three other minor metabolites of GSK2251052 were also identified in this study. Metabolite M1, which results from deboronation and oxidation of the propanol side chain, represented 1.4% of the dose recovered in the feces. M1 was also detected in urine but below quantifiable levels, similar to the two other minor metabolites, M2 and M7. Metabolite M3 results from a simple oxidation of the propanol side chain to the corresponding carboxylic acid derivative; however, it has been determined previously that the metabolite does not appear to have significant antibacterial activity (Peter DeMarsh, internal communication).

To assess the enzyme responsible for the formation of M3, a series of in vitro studies were conducted using both human and monkey hepatic and nonhepatic tissue subcellular fractions. The limited formation of M3 in these experiments in the presence of NADPH suggested that the metabolism of [^{14}C]GSK2251052 was likely not mediated by cytochrome P450 enzymes. Additionally, the low ($\leq$10%), but detectable, formation of M3 observed in monkey liver S9 in the presence of NAD^+ was eliminated in the presence of 4-MP, a known inhibitor of monkey liver ADH (Makar and Tephly, 1975). Although M3 was not detected in human liver cytosolic or purified ADH incubations fortified with NAD^+, the NADH produced during GSK2251052 oxidation could be assessed by the UV spectrophotometric measurement of the conversion of NAD^+ to NADH, which results in a time-dependent increase in absorbance at 340 nm. The NADH formation in these enzyme preparations was dependent on the ADH cofactor, NAD^+, and was not observed in the presence of the ADH inhibitor 4-MP. Class I ADH enzymes (ADH1A, 1B, and 1C) are highly sensitive to 4-MP, and demonstrate substrate inhibition at high concentrations (Riveros-Rosas et al., 1997). Indeed, a concentration-dependent inhibitory effect of GSK2251052 on its own metabolism was observed as noted by the overlapping 340-nm absorbance spectra at the highest concentration of GSK2251052 (100 μM) in the presence of NAD^+ compared with that observed in the presence of the ADH inhibitor, 4-MP. In contrast, at a substrate concentration of 1 μM, time-dependent absorbance changes were only observed with incubations containing NAD^+, and the absorbance spectrum was identical in the absence or presence of cofactor and the ADH inhibitor 4-MP. Taken together with consideration that M3 resulted from oxidation of the propanol side chain to the corresponding carboxylic acid, the in vitro data indicated that ADH may be involved in metabolism of [^{14}C]GSK2251052. To test this hypothesis, a pharmacokinetic interaction study was designed and conducted in monkeys with GSK2251052 and 4-MP. An i.v. administration of GSK2251052 to monkeys, in combination with an oral dose of 4-MP, markedly decreased the plasma clearance of GSK2251052. The resultant increase in GSK2251052 plasma exposure was observed with a concordant reduction in M3 exposure (Fig. 8). Additionally, the terminal half-life and MRT of GSK2251052 were markedly increased in the presence of 4-MP, with no impact on Vss. Collectively, these experiments provide strong evidence that ADH, potentially in association with aldehyde dehydrogenase (ALDH), is the enzyme(s) involved in the metabolism of GSK2251052 and formation of M3. Both ADH and ALDH are polymorphic enzymes and critical players in ethanol metabolism; ADH1B catalyzes the oxidation of ethanol to acetaldehyde, and ALDH2 catalyzes the oxidation of acetaldehyde to acetate. Functional polymorphisms in the ADH1B and ALDH2 genes (Agarwal, 2001) have a significant influence on the activities of both enzymes, and are stratified by race, with the ADH1B*2 (increased catalytic activity) and ALDH2*2 (reduced catalytic activity) alleles being common in East Asians and virtually absent in Caucasians (Eriksson et al., 2001).

Downloaded from dmd.aspetjournals.org at ASPET Journals on November 8, 2015

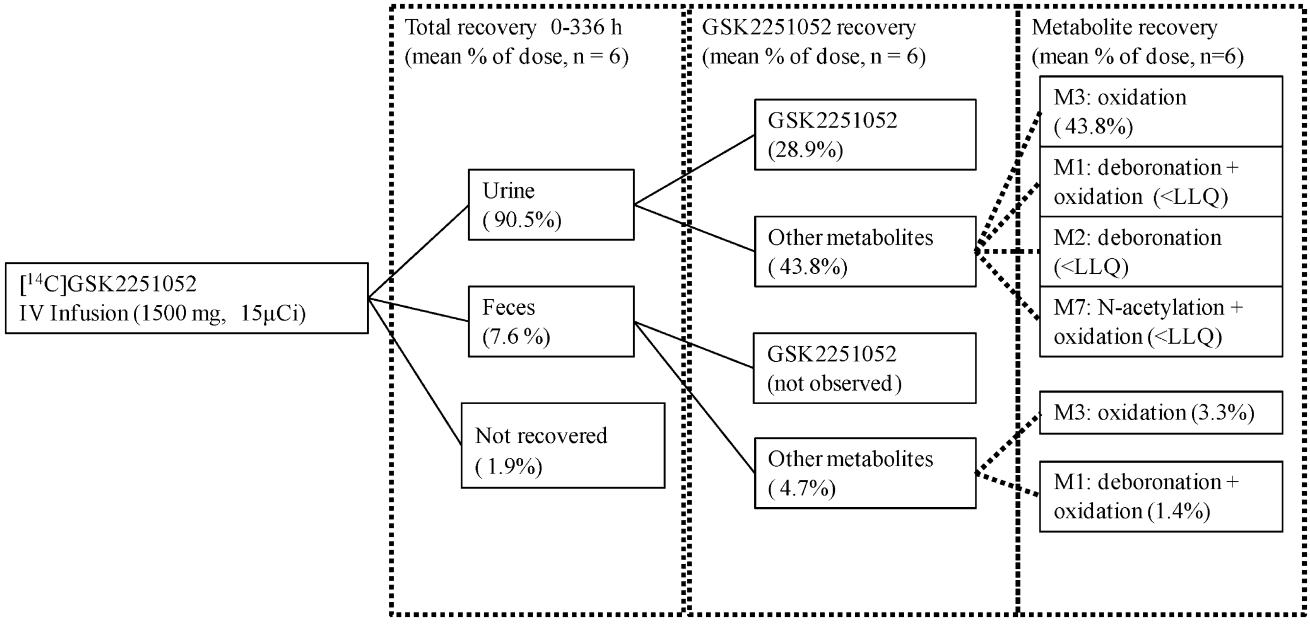

Fig. 9. Summary of the routes of elimination of GSK2251052-related components in humans.

Theoretically, subjects with increased or rapid ADH activity may quickly metabolize GSK2251052, leading to lower parent concentrations, which in turn may impact efficacy. Subjects with reduced or inactive ALDH activity may slowly or ineffectively metabolize the aldehyde intermediate to the acid (M3).

In conclusion, following i.v. administration, the recovery of [^{14}C]GSK2251052 and related components from urine and feces was essentially complete, with urine being the principal route of excretion (Fig. 9). Metabolite M3, a product of oxidation of the propanol side chain, was the primary metabolite of GSK2251052 and the predominant circulating component in plasma. Our data suggest that M3 is formed by ADH, potentially in association with ALDH. These are polymorphic enzymes, and therefore, the clinical exposure of GSK2251052 and M3 may vary between certain ethnic populations (Enomoto et al., 1991; Chen et al., 2009).

Acknowledgments

The authors acknowledge PRA International, The Netherlands, for conduct of the clinical mass balance study; Steve Corless and Clive Felgate, GlaxoSmithKline, for conducting the AMS analyses, and Igor Goljer for spectroscopic analysis of the metabolites; The Anacor Medicinal Chemistry group for advice on chemical synthesis; Amanda Culp, Mark deSerres, Grant Generaux, and Dwayne Lavoie for scientific conduct and advice for the in vitro metabolism and nonclinical pharmacokinetic experiments; and Zhengyu Xue and Justin Rubio for scientific discussions regarding ADH and ALDH genetic polymorphism.

Authorship Contributions

Participated in research design: Bowers, Young, Chism, Sigafoos, Reese, Cunningham, Tomayko, Tenero, Kurtinecz, Patel, Dumont.

Conducted experiments: Yueh, Huynh, Reese.

Contributed new reagents or analytic tools: Conde.

Performed data analysis: Bowers, Chism, O'Mara, Yueh, Huynh, Reese, Tenero, Kurtinecz.

Wrote or contributed to the writing of the manuscript: Bowers, Young, Chism, O'Mara, Sigafoos, Yueh, Huynh, Reese, Cunningham, Tomayko, Stump, Tenero, Kurtinecz, Patel, Dumont.

References

Agarwal DP (2001) Genetic polymorphisms of alcohol metabolizing enzymes. *Pathol Biol (Paris)* **49**:703–709.

Chen YC, Peng GS, Wang MF, Tsao TP, and Yin SJ (2009) Polymorphism of ethanol-metabolism genes and alcoholism: correlation of allelic variations with the pharmacokinetic and pharmacodynamic consequences. *Chem Biol Interact* **178**:2–7.

Currie LA (1968) Limits for qualitative detection and quantitative determination. Application to radiochemistry. *Anal Chem* **40**:586–593.

Davies B and Morris T (1993) Physiological parameters in laboratory animals and humans. *Pharm Res* **10**:1093–1095.

Enomoto N, Takase S, Yasuhara M, and Takada A (1991) Acetaldehyde metabolism in different aldehyde dehydrogenase-2 genotypes. *Alcohol Clin Exp Res* **15**:141–144.

Eriksson CJ, Fukunaga T, Sarkola T, Chen WJ, Chen CC, Ju JM, Cheng AT, Yamamoto H, Kohlenberg-Müller K, and Kimura M, et al. (2001) Functional relevance of human adh polymorphism. *Alcohol Clin Exp Res* **25**(5, Suppl ISBRA)157S–163S.

Klody GM, Schroeder JB, Norton GA, Loger RL, Kitchen RL, and Sundquist ML (2005) New results for single stage low energy carbon AMS. *Nucl Instrum Methods Phys Res B* **240**: 463–467.

Makar AB and Tephly TR (1975) Inhibition of monkey liver alcohol dehydrogenase by 4-methylpyrazole. *Biochem Med* **13**:334–342.

Riveros-Rosas H, Julian-Sanchez A, and Piñā E (1997) Enzymology of ethanol and acetaldehyde metabolism in mammals. *Arch Med Res* **28**:453–471.

Schweizer HP (2012) Understanding efflux in Gram-negative bacteria: opportunities for drug discovery. *Expert Opin Drug Discov* **7**:633–642.

Spellberg B, Guidos R, Gilbert D, Bradley J, Boucher HW, Scheld WM, Bartlett JG, and Edwards J, Jr Infectious Diseases Society of America (2008) The epidemic of antibiotic-resistant infections: a call to action for the medical community from the Infectious Diseases Society of America. *Clin Infect Dis* **46**:155–164.

Sutcliffe JA (2011) Antibiotics in development targeting protein synthesis. *Ann N Y Acad Sci* **1241**:122–152.

Vogel JS (1992) Rapid production of graphite without contamination for biomedical AMS. *Radiocarbon* **34**:344–350.

Young GC, Corless S, Felgate CC, and Colthup PV (2008) Comparison of a 250 kV single-stage accelerator mass spectrometer with a 5 MV tandem accelerator mass spectrometer—fitness for purpose in bioanalysis. *Rapid Commun Mass Spectrom* **22**:4035–4042.

Address correspondence to: Gary D. Bowers, Department of Drug Metabolism and Pharmacokinetics, GlaxoSmithKline, 5 Moore Drive, Research Triangle Park, NC 27709. E-mail: gary.d.bowers@gsk.com

Downloaded from dmd.aspetjournals.org at ASPET Journals on November 8, 2015

1521-009X/41/1/89–100$25.00
DRUG METABOLISM AND DISPOSITION
http://dx.doi.org/10.1124/dmd.112.048603
Drug Metab Dispos 41:89–100, January 2013
Copyright © 2013 by The American Society for Pharmacology and Experimental Therapeutics

Metabolism and Disposition of Vilanterol, a Long-Acting β_2-Adrenoceptor Agonist for Inhalation Use in Humans

Andrew W. Harrell, Sarah K. Siederer, Jo Bal, Nainesh H. Patel, Graeme C. Young, Clive C. Felgate, Sebastian J. Pearce, Andy D. Roberts, Claire Beaumont, Amanda J. Emmons, Adrian I. Pereira, and Rodger D. Kempsford

Drug Metabolism and Pharmacokinetics, GlaxoSmithKline Research and Development, Ware, Hertfordshire, United Kingdom (A.W.H., N.H.P., G.C.Y., C.C.F., S.J.P., A.D.R., C.B., A.I.P.); Clinical Pharmacology or Medicines Discovery Research, GlaxoSmithKline Research and Development Ltd., Stevenage, Hertfordshire, United Kingdom (A.J.E., S.K.S., R.D.K.); and Medicines Discovery and Development, GlaxoSmithKline Research and Development, Stockley Park, Middlesex, United Kingdom (J.B.)

Received August 30, 2012; accepted October 4, 2012

ABSTRACT

The metabolism and disposition of vilanterol, a novel long-acting β_2-adrenoceptor agonist (LABA) for inhalation use, was investigated after oral administration in humans. Single oral administrations of up to 500 μg of vilanterol were shown to be safe and well tolerated in two clinical studies in healthy men. In a human radiolabel study, six healthy men received a single oral dose of 200 μg of [^{14}C]vilanterol (74 kBq). Plasma, urine, and feces were collected up to 168 hours after the dose and were analyzed for vilanterol, metabolites, and radioactivity. At least 50% of the radioactive dose was orally absorbed. The primary route of excretion of drug-related material was via *O*-dealkylation to metabolites, which were mainly excreted in urine. Vilanterol represented a very small percentage (<0.5%) of the total drug-related material in plasma, indicative of extensive first-pass metabolism. Circulating metabolites resulted mainly from *O*-dealkylation and exhibited negligible pharmacologic activity. The therapeutic dose level for vilanterol is 25 μg by the inhalation route. At this low-dose level, the likelihood of pharmacologically inactive metabolites causing unexpected toxicity is negligible. In addition to providing an assessment of the disposition of vilanterol in human, this work highlights a number of complexities associated with determining human absorption, distribution, metabolism, and excretion (ADME) for inhaled molecules—mainly related to the low chemical doses and complications associated with the inhalation route of administration.

Introduction

Vilanterol, GW642444, or 4-[(1*R*)-2-[(6-{2-[(2,6-dichlorophenyl) methoxy]ethoxy}hexyl)amino]-1-hydroxyethyl]-2-(hydroxyl methyl) phenol, is a novel long-acting β_2-agonist (LABA) with inherent 24-hour activity for once-daily clinical treatment of chronic obstructive pulmonary disease (COPD) and asthma in combination with the inhaled novel corticosteroid fluticasone furoate, also active for 24 hours (Hanania et al., 2012; Lotvall et al., 2012). This publication describes in vitro and clinical studies conducted to determine the metabolism and disposition of vilanterol in humans. This information is used to provide reassurance on the metabolite safety of vilanterol, to assess any metabolite contribution to the pharmacology, and to define the mechanisms of disposition and elimination that might be susceptible to drug interactions or relevant to special patient populations.

Traditionally, the metabolism and disposition of a molecule is determined after administration of a radioactive drug analog by the intended clinical route and includes aspects such as radioactive recovery in excreta, identification of metabolites, and quantitative radiometabolite profiles, usually in plasma and excreta. This study is commonly referred to as the human radiolabel study (HRS). There are many challenges associated with the design and conduct of an HRS for low-dose inhalation molecules such as vilanterol where the clinical dose is only 25 μg. These, as described here, considerably impacted the approaches used to determine the metabolism and disposition of vilanterol.

Although precedent exists for dosing radiolabel by the inhalation route (Affrime et al., 2000), for some molecules the inhalation route is not necessarily the best or most feasible approach, especially if the

This work was funded by GlaxoSmithKline R&D, UK, as part of the development program for vilanterol as a novel therapeutic agent. Data in this manuscript correspond with clinical study numbers B2C106180 (GSK company report GM2009/00020/00) and B2C106181 (GSK company report YM2010/00088/00) with metabolite identifications reported in study number 10DMW020 (GSK company report 2011N115614). Hepatocyte incubations were reported in GSK company report WD2006/02574/00. Pharmacologic activities of metabolites were reported in GSK company report HR2008/00016/00. All authors were employees of GlaxoSmithKline Research and Development Ltd. at the time of conducting the work.

Primary Laboratory of Origin: Drug Metabolism and Pharmacokinetics Division, GlaxoSmithKline Research and Development Ltd., Park Road, Ware, United Kingdom

dx.doi.org/10.1124/dmd.112.048603.

ABBREVIATIONS: ADME, absorption, distribution, metabolism, and excretion; AMS, accelerator mass spectrometry; $AUC_{(0-t)}$, area under the curve to last sample time where drug was measurable; COPD, chronic obstructive pulmonary disease; CRC, concentration–response curve; DMSO, dimethyl sulfoxide; DRM, drug-related material; GSK, GlaxoSmithKline; HMR, Hammersmith Medicines Research Centre; HPLC, high-performance liquid chromatography; HRS, human radiolabel study; LABA, long-acting β-agonist; LLQ, lower limit of quantification; LSC, liquid scintillation counting; MS, mass spectrometry; NMR, nuclear magnetic resonance spectroscopy; NQ, nonquantifiable; PRA, Pharmaceutical Research Associates; TR-FRET, time-resolved fluorescence resonance energy transfer.

inhalation device and formulation are complex. Re-creating the commercial physical form of a radioactive drug analog in its intended device is difficult; thus, the quantitative information after inhalation of a radioactive analog is not usually representative of the clinical situation. Exhalation of radioactive drug after inhalation administration not only creates safety and containment considerations but also makes it very difficult to reliably quantify the administered radioactivity that is needed to fully interpret excretion and metabolism data. Other challenges arise due to the low chemical dose level of inhaled drugs, which limits the radioactive dose and leads to biologic samples containing very low concentrations of both metabolite chemical mass and radioactivity, thereby impairing our ability to measure and identify metabolites. The inhalation route provides few opportunities to adjust chemical and radioactive doses to avoid these technical problems.

Further complications, specific to [^{14}C]vilanterol, included radiolysis of the [^{14}C] isotope, which meant that it was unstable over the periods required to support manufacture and release of either intravenous or inhalation formulations, effectively ruling out these routes of administration. Radiolysis limited the [^{14}C]vilanterol specific activity to 370 kBq/mg, also restricting the amount of radioactivity that could be administered. The vilanterol HRS was, therefore, conducted by the oral route using a dose level of 200 μg containing only 74 kBq radioactivity. The oral dose level of 200 μg of [^{14}C] vilanterol was selected because it was higher than the inhaled clinical dose of 25 μg, allowing sufficient administered radioactivity to generate radioactive metabolite profiles for plasma, urine, and feces using accelerator mass spectrometry (AMS) as a highly sensitive radioactivity counter. The chemical structure of [^{14}C]vilanterol showing the position of the [^{14}C] label is shown in Fig. 1. A preceding clinical study (hereafter referred to as the tolerability study) established the safety and tolerability of oral administrations up to 500 μg of unlabeled vilanterol.

The emergence of AMS as a very low level radioactivity counter has enabled radioactive metabolite profiles to be generated in samples containing very low levels of radioactivity. The radioactive dose of 74 kBq permitted traditional liquid scintillation counting (LSC) to be used for some aspects of the study (e.g., radioactivity in urine and feces), but AMS was essential for determining concentrations of radioactivity in plasma and for metabolite profile work. Although AMS is an excellent technique for low-level radioactivity measurement, it

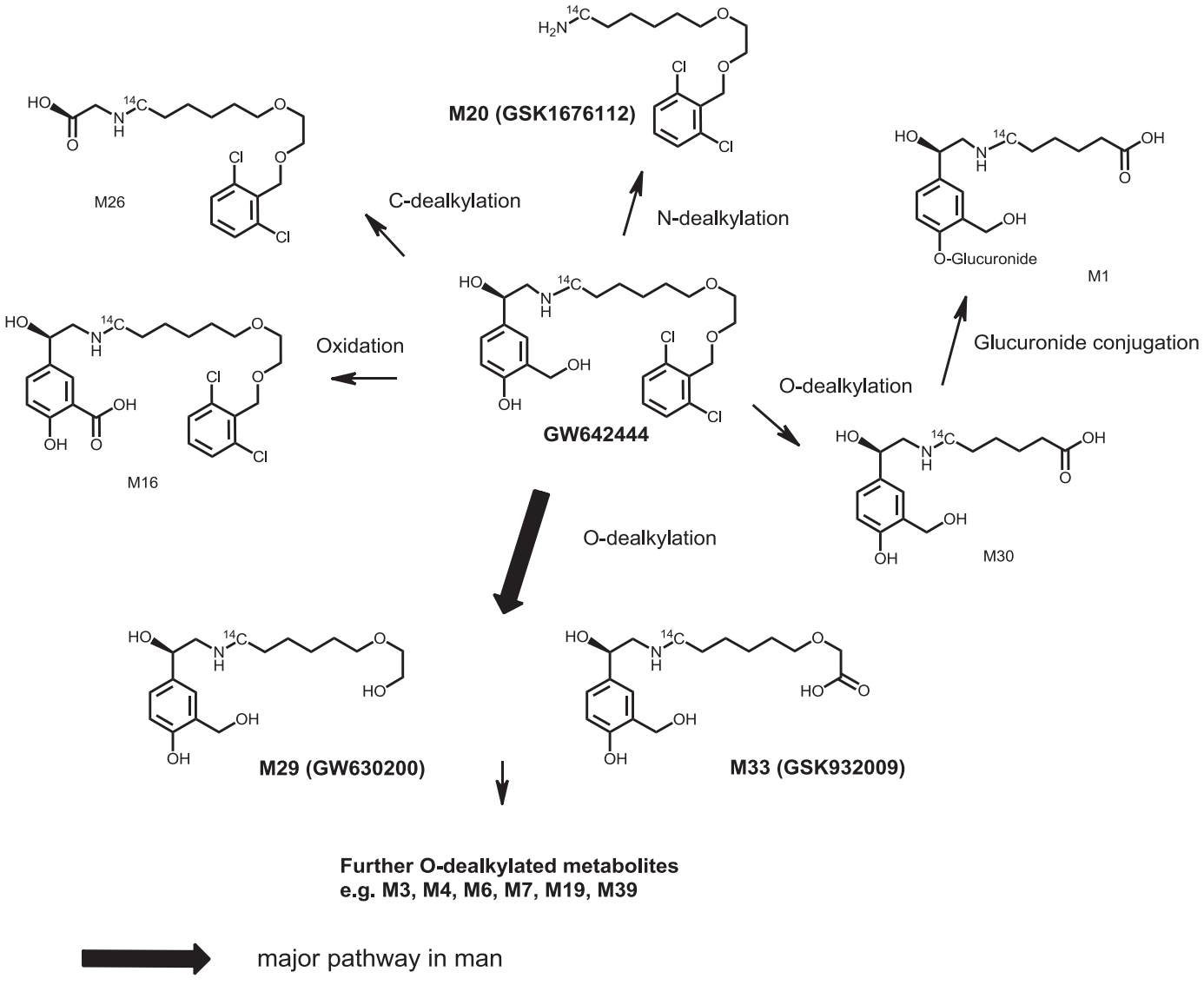

Fig. 1. Metabolic scheme for vilanterol in humans. Chemical structures are shown for vilanterol and important human metabolites. ^{14}C indicates the position of labeled carbon.

does not directly provide structural information to assist with metabolite identification. The chemical dose level used here (200 μg) allowed limited application of high-performance liquid chromatography–mass spectrometry (HPLC-MS) to provide structural information on some metabolites. The majority of human metabolite structures were, however, assigned by chromatographic retention time comparison with metabolites whose full identification was achieved in other samples containing greater chemical mass (e.g., in vitro/in situ experiments or animal studies). Thus, in vitro incubations conducted using mouse, rat, dog, rabbit, and human hepatocytes that were the primary source of metabolite structures are also described.

Materials and Methods

Vilanterol, [^{14}C]vilanterol, and four potential metabolites (GW630200, GSK167112, GW853734, and GSK932009) were supplied by Chemical Development, GlaxoSmithKline (GSK) R&D, Stevenage, United Kingdom. The specific activity of vilanterol was 370 kBq/mg. All other solvents and reagents were of analytical grade and were purchased from commercial suppliers.

Clinical Study Design, Study Centers, and Subjects The tolerability study was an ascending-dose, single-center, open-label study in nine healthy men conducted at Hammersmith Medicines Research Centre (HMR), London, United Kingdom, between October 21, 2008 and December 17, 2008 (last sample last visit). The HRS was a single-center, open-label study in six healthy male volunteers conducted at Pharmaceutical Research Associates (PRA), Zuidlaren, the Netherlands between May 18, 2010 and July 9, 2010. All subjects provided written informed consent before participation, and the protocols were approved by the investigational centers' ethics committees. The men were in good health as shown by medical examination, clinical chemistry, hematology, and urine analysis. They were nonsmokers with no history of drug or alcohol abuse, were taking no other medication at the time of each study, and had taken no prescribed medication within 14 days of each study commencing. The target radioactive dose of 74 kBq corresponds to an effective radioactive dose of 20 μSv, which is considerably lower than the upper limit for both the World Health Organization ($<$500 μSv) and International Commission on Radiologic Protection ($<$100 μSv) category I exposures which are considered variations in natural background radiation with a minimal risk. The effective radioactive dose was calculated by the United Kingdom Health Protection Agency according to the recommendations of the International Commission on Radiologic Protection (ICRP, 1991).

Dose Formulation and Administration Vilanterol and [^{14}C]vilanterol were supplied to the study centers by GSK, Ware, UK, as sterile solutions. For the tolerability study, a solution (5% ethanol in water) containing 50 μg/ml vilanterol was supplied to HMR. The subjects received a single oral dose of either 4 ml or 10 ml of this solution containing 200 or 500 μg of vilanterol, respectively. For the HRS, a solution (80% ethanol in water) containing 200 μg/ml [^{14}C]vilanterol (74 kBq/ml radioactivity) was supplied to PRA. For each volunteer, the solution was diluted 1 in 20 with water by PRA. All subjects received a single 20 ml oral dose containing 200 μg of [^{14}C]vilanterol (74 kBq radioactivity) administered via syringe. After administration of each vilanterol solution, water (2 $\times$ 20 ml) was administered to the subject using the same syringe to ensure that the complete dose was given. A third volume of water (20 ml) was drawn up into the syringe (HRS only) then dispensed into a suitable container, and residual radioactivity was determined by liquid scintillation counting (LSC). The total residual radioactivity was deducted from the dispensed radioactivity to determine the overall administered radioactive dose.

Sample Collection Blood samples (2 ml in the tolerability study; 6 ml in the HRS) were collected at predefined times up to 7 days after dosing via either an indwelling cannula or by direct venipuncture into EDTA-containing polypropylene tubes. These were used for plasma measurement of vilanterol (both studies) and radioactivity (HRS only). Additional blood (18 ml, HRS only) was collected at 0.5, 3.5, and 24 hours after dosing and used for metabolic investigations. Blood was placed on crushed ice before centrifugation in a refrigerated centrifuge at approximately 1500*g* for 10 minutes to yield plasma, which was then stored frozen at nominally $-$20°C. All urine and feces (HRS only) were collected at 24-hour intervals up to at least 7 days after the dose administration. The fecal and urine samples were stored frozen at $-$20°C or less before analysis.

In Vitro Incubations [^{14}C]Vilanterol was incubated at a concentration of 10 μM in the presence of mouse, rat, dog, rabbit, and human cryopreserved hepatocytes (In Vitro Technologies Inc., Baltimore, MD) using Williams Medium E incubation media supplemented with antibiotics, at 37°C for 24 hours. After incubation, methanol (1.2 ml) was added to all hepatocyte incubations (0.6 ml), the precipitate was centrifuged at 7500*g* at ambient temperature for 5 minutes, and the supernatant was removed for further analysis.

Assay for Total Radioactivity (HRS Only) After measurement of the volume of urine or weight of stool, the levels of radioactivity were determined by LSC (Beckman LS series, Bucks, UK, or PerkinElmer Life Sciences, Bucks, UK) with quench correction performed by an automatic external standard ratio method, which was established using sealed ^{14}C standards. Aliquots of liquid samples (e.g., urine and dose dilutions) or extracts of samples were mixed with scintillation fluid. Fecal samples were homogenized with a minimal amount of water and reweighed. Aliquots of homogenized fecal material were combusted using a Packard model 307 oxidizer (Canberra Packard, Didcot, UK) before the radioassay. In some urine and feces samples, the levels of radioactivity were too low to be determined by LSC. After their combustion to graphite, the levels of radioactivity in these samples were determined via AMS (a 5 MV tandem accelerator mass spectrometer) at Xceleron Ltd. (York, UK). The analysis of plasma was conducted at GSK using AMS (a 250-kV single-stage accelerator mass spectrometer; Young et al., 2008). The lower limit of quantitation (LLQ) was previously established as 10% above endogenous background levels of total radioactivity in human plasma with greater than 95% confidence limit (data not shown). Based on the predose plasma values for the six men in the human ADME study and the specific activity administered, this corresponded to 2.45 pg equivalents of vilanterol/ml.

Determination of Radiochemical Purity (HRS Only) The radiochemical purity of [^{14}C]vilanterol solution was determined using the HPLC system described here for metabolite analysis. The radiochemical purity of the administered [^{14}C]vilanterol determined on the day of dosing was 99.4%.

Quantification of Vilanterol in Plasma (Tolerability Study and HRS) Concentrations of vilanterol in human plasma samples were determined using analytical methods validated to GSK worldwide standard operating procedures, which are based on guidelines set out by the US Food and Drug Administration. The extraction method for vilanterol used solid-phase extraction to achieve a low limit of quantitation (LLQ) of 10 pg/ml from a 200-μl aliquot of plasma where [$^{2}H_{12}$]vilanterol was added as an isotopically labeled internal standard. Extracts were analyzed using HPLC (Waters Acquity System; Waters, Milford, MA) and tandem mass spectrometry (HPLC-MS/MS). The mass spectrometer used was an API-4000 triple quadrupole using a TurboIonSpray interface (AB Sciex, Framingham, MA) in positive mode with multiple reaction monitoring. The mass transitions were 486 to 159 and 498 to 159 for vilanterol and [$^{2}H_{12}$] vilanterol, respectively.

Quantification and Profiling of Metabolites An equal volume of plasma from each man was pooled to produce a single discrete representative sample per time point. A single discrete pooled human urine sample was prepared by mixing proportional volumes of 0- to 24-hour urine collected from each volunteer, which individually represented $>$95% of the radioactivity excreted by this route. Representative fecal homogenates were obtained by pooling across sampling times on a total sample weight basis to generate a discrete pool containing 80% or greater of the radioactivity excreted in feces for each man. These were subsequently pooled across individuals to obtain a single feces homogenate sample representative of the whole study. Radioactive material was extracted from plasma and feces samples by vortex-mixing successive aliquots of acetonitrile. The extracts were evaporated to near dryness under a stream of nitrogen before reconstitution in small volumes of ammonium formate buffer (50 mM, pH 2.5) and acetonitrile. Plasma and feces extracts and human urine were spiked with dimethyl sulfoxide (DMSO) solutions containing authentic reference standards of vilanterol, GW630200, and GSK932009 as chromatographic UV retention time markers. The spiked plasma, urine, and feces samples were subsequently analyzed by HPLC with UV detection and radiometric detection by offline AMS analysis. The supernatants from the hepatocyte incubations were analyzed with no further treatment by use of HPLC with offline radio detection by microtiter plate scintillation counting and HPLC-MS.

The chromatographic instrumentation consisted of an Agilent system (South Queensferry, Scotland, UK), comprising a 1100 binary pump, column oven (25°C), UV detector (λ 275 nm), and autosampler, which was linked to a fraction collector (Gilson, Luton, UK). A Luna Phenyl Hexyl RP column (250 × 4.6 mm, 5-micron particle size) was used. The mobile phase consisted of 50 mM ammonium formate, pH 2.5 (solvent A), and acetonitrile (solvent B; supplied by Thermo Fisher Scientific, Loughborough, Leicestershire, UK) at a flow rate of 1 ml/min. A linear gradient was used as follows: 10 to 37% B over 13 minutes; 37 to 52% B by 14 minutes; 52% B to 64% B by 35 minutes; 64% B to 90% B by 40 minutes; conditions were held at 90% B until 45 minutes. The column was re-equilibrated for a minimum of 6 minutes after each injection. Fractions from the HRS samples were collected into quartz glass tubes (York Glassware Services, York, UK) every 30 seconds for offline radiodetection by AMS. For hepatocyte samples, the HPLC fractions were collected into 96-deep-well microtiter plates containing yttrium silicate solid scintillant (PerkinElmer Life and Analytical Sciences) every 12 seconds. Each HPLC eluate was evaporated to dryness in a drying oven overnight, and the dried plates were sealed using a microplate heat sealing film (PerkinElmer Life and Analytical Sciences). Radioactivity in each well was subsequently counted using a TopCount NXT counter (PerkinElmer Life and Analytical Sciences).

Structural Identification of Metabolites Structural characterization was performed on selected HRS samples by HPLC-MS using an Accela autosampler and HPLC system coupled to an Orbitrap XL mass spectrometer with Xcalibur software (Thermo Fisher Scientific, Hemel Hempstead, UK). The majority of human metabolites were identified through chromatographic comparisons to metabolites identified in other samples, such as the hepatocyte incubations. Metabolites in the hepatocyte incubations were characterized using an Agilent HP1100 autosampler and HPLC system coupled to a Micromass Quattro Micro triple quadrupole mass spectrometer with MassLynx software (Waters MS Technologies, Manchester, UK) or a ThermoFinnigan LTQ linear trap mass spectrometer with Xcalibur software (Thermo Fisher Scientific). All mass spectrometric analyses employed electrospray ionization in the positive and negative ion modes. The flow was split 1:2 (Orbitrap) or 1:20 (Quattro and LCT) between the mass spectrometers and fraction collector (CTC Analytics HTX PAL).

Metabolites in human hepatocyte supernatant were also separated by preparative HPLC using an Agilent series 1100 Preparative-LC system (Waldbronn, Germany) for characterization by nuclear magnetic resonance spectroscopy (NMR). Separations were performed on a Luna Phenyl Hexyl HPLC column (250 × 10 mm i.d., 5-micron particle size) at ambient temperature with a mobile phase of 50 mM ammonium formate (pH 2.5, solvent A) and acetonitrile/methanol (20:80 v/v, solvent B) at a constant flow rate of 4 ml/min with an initial gradient of 10% B increasing linearly to 37% B at 13 minutes, then to 52% B at 14 minutes, 64% B at 25 minutes, and 90% B at 40 minutes where it was held for a further 5 minutes. The HPLC eluent was collected into fractions, in a time-slice mode, into two 96-deep-well plates using a frequency of 15 seconds per fraction. This resulted in 180 fractions, each containing 1 ml of column eluent. The flow was split 100:1 into a Micromass ZQ mass spectrometer (Waters MS Technologies) that was fitted with an electrospray source operated in the positive ionization mode. System control was mediated through MassLynx and FractionLynx (Waters, Milford, MA).

The fractions were taken to dryness under nitrogen at 37°C within the 96-deep-well plates using a Micro DS96 dry down station (Porvair Scientific Ltd., Shepperton, UK) and then reconstituted in approximately 0.6 ml of deuterium oxide/acetonitrile (1:1) before being transferred to 5 mm NMR tubes. We performed 1D proton NMR experiments on all 180 fractions using a Bruker 600 MHz spectrometer equipped with an inverse 5 mm TXI Cryo-Probe (1H/13C/15N) operating at 600.13 MHz under the control of TopSpin software (Bruker, Rheinstetten, Germany).

Accelerator Mass Spectrometry The ^{14}C content of human plasma, fecal homogenates, urine, plasma extracts, and HPLC fractions was measured by AMS, which measures the radiocarbon content in a sample through separation of the isotopes of carbon present by their different mass-to-charge ratios. Before analysis by AMS, the samples were graphitized via a two-step process of oxidation and reduction (Young et al., 2008). The graphite, containing a cobalt catalyst, was packed into an aluminum cathode and loaded into a sample wheel that was then placed into the ion source of the AMS instrument (either NEC 5 MV tandem or 250 KV single-stage AMS system; National Electrostatics Corporation, Middleton, WI). A generic value of 4.14%, based on GSK historical data, for the carbon content of plasma was used for any neat plasma samples analyzed, and the values were adjusted appropriately to allow for any dilution.

For fecal homogenates, the carbon content for each sample was measured independently using an elemental analyzer (NA2100 Brewanalyser; CE Instruments, Wigan, UK). The carbon content for the HPLC fractions and for urine was deemed to be insignificant, so only the carbon content of the carbon carrier was used in calculations to determine the ^{14}C content based on the determined ^{14}C to ^{12}C ratio in the samples. The AMS data, which are expressed as the percentage of modern carbon, were used to calculate the dpm/ml sample, where 100% modern carbon equals 0.01356 dpm/mg carbon.

Pharmacokinetic Calculations Pharmacokinetic analyses of plasma vilanterol concentration–time data (tolerability study only) and ^{14}C radioactivity concentration–time data (HRS only) were conducted using the non-compartmental Model 200 (for extra vascular administration) of WinNonLin Professional Edition version 5.2 (Pharsight Corporation, Cary, NC). Values for the following pharmacokinetic parameters were estimated: the maximum observed plasma concentration (C_{max}), the first time to reach C_{max} (t_{max}), the concentration at last measurable time point (Ct), and the time of the last observed plasma concentration (t_{last}). Where possible, the terminal plasma elimination rate-constant (λz) was estimated from a log-linear regression analysis of the terminal phase of the plasma concentration–time profile. The area under the plasma concentration–time curve from time zero to the last quantifiable time point (AUC_{0-t}) and extrapolated to infinity ($AUC_{0-\infty}$) were calculated by a combination of linear and logarithmic trapezoidal methods.

In Vitro Pharmacologic Activity of Metabolites The β_1 and β_2 activities of vilanterol, GW630200 (M29), GSK932009 (M33), GSK167112 (M20), and GW853734 (a potential metabolite of vilanterol undetected in animals or human) were determined via cAMP TR-FRET LANCE (Time Resolved Fluorescence Energy Transfer; PerkinElmer Life and Analytical Sciences) agonist assays. These were either metabolites or potential metabolites of vilanterol that were selected to represent routes of human metabolism. The compounds were dissolved in DMSO at a concentration of 10 mM and serially diluted in DMSO using a 1 in 4 dilution step to provide 11-point concentration–response curves (CRCs). Chinese hamster ovary cells stably expressing either recombinant β_1- or β_2-receptor were thawed at 37°C, diluted in phosphate buffered saline, and centrifuged at 1500*g* for 5 minutes. Cells were resuspended (2 million cells/ml) in a stimulation buffer (Hanks' balanced salt solution containing 0.01% bovine serum albumin, 500 μM 3-isobutyl-1-methylxanthine, 5 mM HEPES final assay concentration, pH 7.4, with potassium hydroxide).

The in vitro activity against either β_1 and β_2 was measured by adding CRCs of compound or controls, 100 nl/well to a white Greiner polypropylene low-volume 384-well plate, to which the relevant cell suspension (10,000 cells/well at 5μl addition) and antibody solution (stimulation buffer containing Alexia Fluor 647at 5 μl/well) were added. Plates were incubated for 30 minutes at room temperature, then the detection mixture was added (kit components: detection buffer, europium W8044-labeled streptavidin, and biotin cAMP at 10 μl/well). Plates were covered and incubated at room temperature for 4 hours before being analyzed on a Viewlux Microplate Imager (PerkinElmer Life and Analytical Sciences).

Results

Demographic, Safety, and Tolerability Data Nine and six healthy men were enrolled into the tolerability and HRS studies, respectively. The demographic data from the tolerability study and HRS are shown in Table 1. Vilanterol was safe and well tolerated after oral administrations up to 500 μg, with no drug-related adverse events or clinically significant changes in vital signs (including heart rate and electrocardiogram interval) observed. No concomitant medication was reported for any subject during the studies.

Pharmacokinetics of Vilanterol and Radioactivity Pharmacokinetic data for vilanterol and ^{14}C radioactivity in both studies are summarized in Table 2. Plasma concentrations of vilanterol after oral administration of 200 or 500 μg of vilanterol in the tolerability study

TABLE 1

Summary of subject disposition and demographic characteristics after oral administration of 200 or 500 μg of vilanterol or 200 μg of [^{14}C]vilanterol to men

Subject disposition and demographic characteristics are summarized from two clinical studies. In the first tolerability study subjects received 200 or 500 μg of vilanterol. In the subsequent human radiolabel study, the subjects received 200 μg of [^{14}C]vilanterol containing 74 kBq radioactivity.

Characteristics	Tolerability Study GSK Study B2C106180	Human Radiolabel Study GSK Study B2C106181
Number of subjects completed: *n*	9	6
Oral administration	200 or 500 μg of vilanterol	200 μg of [^{14}C]vilanterol
Age (yr): mean (range)	33.1 (19–47)	43.3 (35–53)
Race, *n* (%)		
White/Caucasian/European	7 (78)	6 (100)
Asian	1 (11)	
African American	1 (11)	
Ethnicity, *n* (%)		
Not Hispanic or Latino	9 (100)	6 (100)
Body mass index (kg/m^2): mean (range)	24.8 (21.3–29.0)	26.2 (21.8–28.8)
Height (cm): mean (range)	178 (166–186)	179 (163–189)
Weight (kg): mean (range)	78.5 (66.9–90.8)	83.9 (57.8–102)

were low (≤24 and 65 pg/ml, respectively) and could only be quantified up to 0.8 hours (median T_{last}) after administration of 200 μg and up to 2.8 hours (median T_{last}) after the 500-μg dose. In the HRS, vilanterol was only quantified in plasma (LLQ 10 pg/ml) in a single individual (n = 1 of 6; subject 102) at 0.5 hours (14 pg/ml) and 3.0 hours (15 pg/ml) after the dose; at all other sampling times, vilanterol concentrations were nonquantifiable (NQ). Because two NQ values occurred in succession after the quantifiable concentration at 0.5 hours, the profile was deemed to have terminated at the first NQ value, and the subsequent quantifiable concentration at 3.0 hours was omitted from the pharmacokinetic calculations.

In contrast, the plasma concentrations of ^{14}C radioactivity (total drug-related material or DRM, representing vilanterol and its metabolites) were substantially higher than the vilanterol concentrations (Fig. 2; Table 2). For subject 102 (Table 2), the vilanterol C_{max} (14 pg/ml) represented a very small percentage (<0.5%) of the drug-related material (DRM) where C_{max} was 3148 pg vilanterol equivalents/ml (data not shown). For the other subjects, where vilanterol concentrations were not quantifiable, vilanterol C_{max} was <10 pg/ml (the limit of quantitation for the assay), which also corresponded to <0.5% of the DRM C_{max} (2060 pg equivalents/ml), indicating that vilanterol represented a small proportion (<0.5%) of the total drug-related material in plasma.

Excretion of [^{14}C]Vilanterol Drug-Related Material The cumulative percentage recovery of administered radioactivity in urine and feces is depicted in Fig. 3. DRM was mainly excreted in urine (50% administered radioactivity or 70% of the recovered radioactivity). Fecal excretion accounted for a further 21% of the administered radioactivity (or 30% of the recovered radioactivity). Absorption of vilanterol was at least 50% based on urinary recovery. The total recoveries of radioactivity were relatively low (72% of the administered radioactivity). Excretion of radioactivity was essentially complete by the end of day 4 (>99% of recovered radioactivity), with <0.3% of administered radioactivity being recovered, in total, between days 5 and 7 after dosing.

Metabolite Profiles Radiochromatograms of separated metabolites were generated from HPLC eluate fractions using AMS as a highly sensitive offline radiodetector. Representative radiochromatograms for human plasma, urine, and feces are shown in Fig. 4, with each radioactive peak given an alphabetical assignment (A to M). Solvent extraction efficiencies were 64% for the 0.5-hour plasma (where metabolites were quantified) and 75% from feces homogenates. The solvent extraction efficiency from the 24-hour plasma sample was very low, at <10%. Low chemical mass precluded the generation of interpretable MS spectra for all but a few metabolites. The majority of metabolites were thus assigned by comparison of chromatographic retention times to either authentic reference material or to metabolites identified in other nonclinical studies (Table 3) where higher amounts of metabolite had facilitated more detailed identifications. Characterized metabolites were given a numerical designation preceded by the letter M

TABLE 2

Pharmacokinetic parameters in human plasma for vilanterol and [^{14}C] radioactivity after oral administration of 200 or 500 μg of vilanterol and 200 μg of [^{14}C]vilanterol

Plasma $AUC_{(0-t)}$, C_{max}, and T_{max} of vilanterol and ^{14}C radioactivity in plasma are shown after single oral administrations to healthy men in two clinical studies. For the tolerability study, the parameters are presented for two dose levels after specific assay analysis for vilanterol. For the human radiolabel study, the parameters are presented from a single dose level and are calculated from the mean specific assay data for vilanterol in all subjects, the specific assay data for vilanterol in subject 102 (the only subject with measurable concentrations), and the mean radioactivity measurements (DRM) in all subjects presented as picogram equivalents of vilanterol per milliliter.

	Tolerability Study (200 or 500 μg of Vilanterol)						Human Radiolabel Study (200 μg of [^{14}C]Vilanterol)						
	200 μg	*n*	n^1	500 μg	*n*	n^1	Vilanterol	Vilanterol[a]	*n*	n^1	Radioactivity	*n*	n^1
$AUC_{(0-t)}$ (95% CI), pg·h/ml	21.8 (NC)	3	1	62.6 (25, 156)	6	0	NC	NC	0	6	66,000 (52,000, 84,000)[b]	6	0
C_{max} (95% CI, pg/ml	18.5 (10, 33)	3	0	44.5 (32, 62)	6	0	NC	14	1	5	2060 (1580, 2700)[b]	6	0
T_{max} median [range], h	0.5 [0.25–0.5]	3	0	0.5 [0.25–1.0]	6	0	NC	0.5	1	5	3.0 [2.5–4.0]	6	0
T_{last} median [range], h	0.8 [0.5–3.0]	3	0	2.8 [1.0–8.0]	6	0	NC	0.5	1	5	168 [168–168]	6	0

[a] Data are presented separately for subject 102 in whom there was a single quantifiable concentration of 14 pg/ml at 0.5 hours after dosing.

[b] Radioactivity concentrations are expressed in terms of picogram equivalents of vilanterol per milliliter.

CI, confidence interval; *n*, number of subjects with non-missing observations, including inputted NC values for AUC and C_{max}; n^1, number of subjects for whom parameters cannot be derived because of nonquantifiable concentrations; NC, not calculable due to insufficient data or concentrations below lower limit of quantification (10 pg/ml).

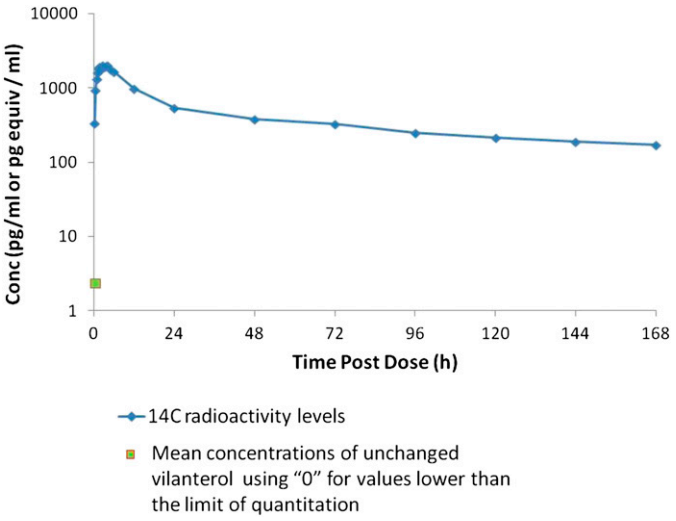

Fig. 2. Mean concentrations of vilanterol and radioactivity in plasma after oral administration of [^{14}C]vilanterol to humans The difference in mean plasma concentrations of radioactivity (pg equivalents DRM /ml) and concentrations of unchanged vilanterol (pg/ml) are highlighted on this concentration–time semi-log plot generated using data collected after a single oral administration of 200 μg of [^{14}C]vilanterol containing 74 kBq radioactivity.

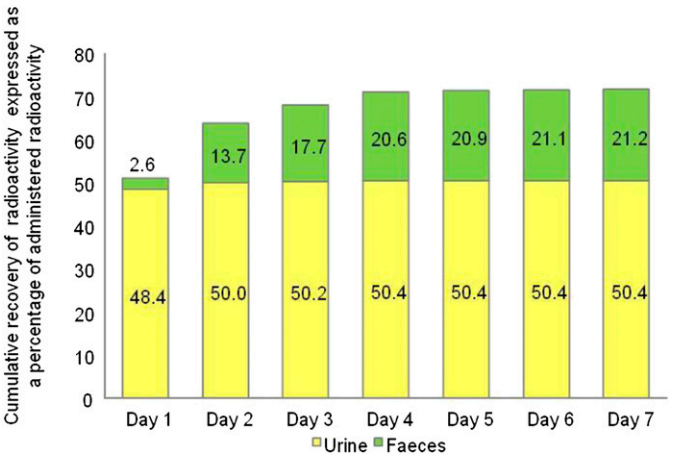

Fig. 3. Mean percentage cumulative recovery of radioactivity in urine and feces (expressed as % administered radioactivity) after oral administration of [^{14}C] vilanterol (74 kBq) to humans. Cumulative recovery of radioactivity is shown in urine and feces collected for up to 7 days after a single oral administration of 200 μg of [^{14}C]vilanterol containing 74 kBq radioactivity. Mean data from six subjects is presented.

(e.g., M1), each number representing a distinct metabolite structure. Metabolite structures assigned to each radioactive peak, along with supporting evidence from other studies, are shown in Table 3.

Plasma Metabolites HPLC radiochromatograms of human plasma extracts from samples taken at 0.5 and 3.5 hours after dosing are shown in Fig. 4. Radioactive peaks from the 0.5-hour sample time (C_{max} of vilanterol in plasma) are quantified in Table 4. The largest radioactive peaks (F and G) were assigned as a mixture of *O*-dealkylated metabolites (including M33/GSK932009 and M29/GW630200). These metabolites represented approximately 33% of plasma radioactivity in the 0.5-hour plasma extract. Peak J2 (assigned as M26, a *C*-dealkylated metabolite) and peak B (M1, an

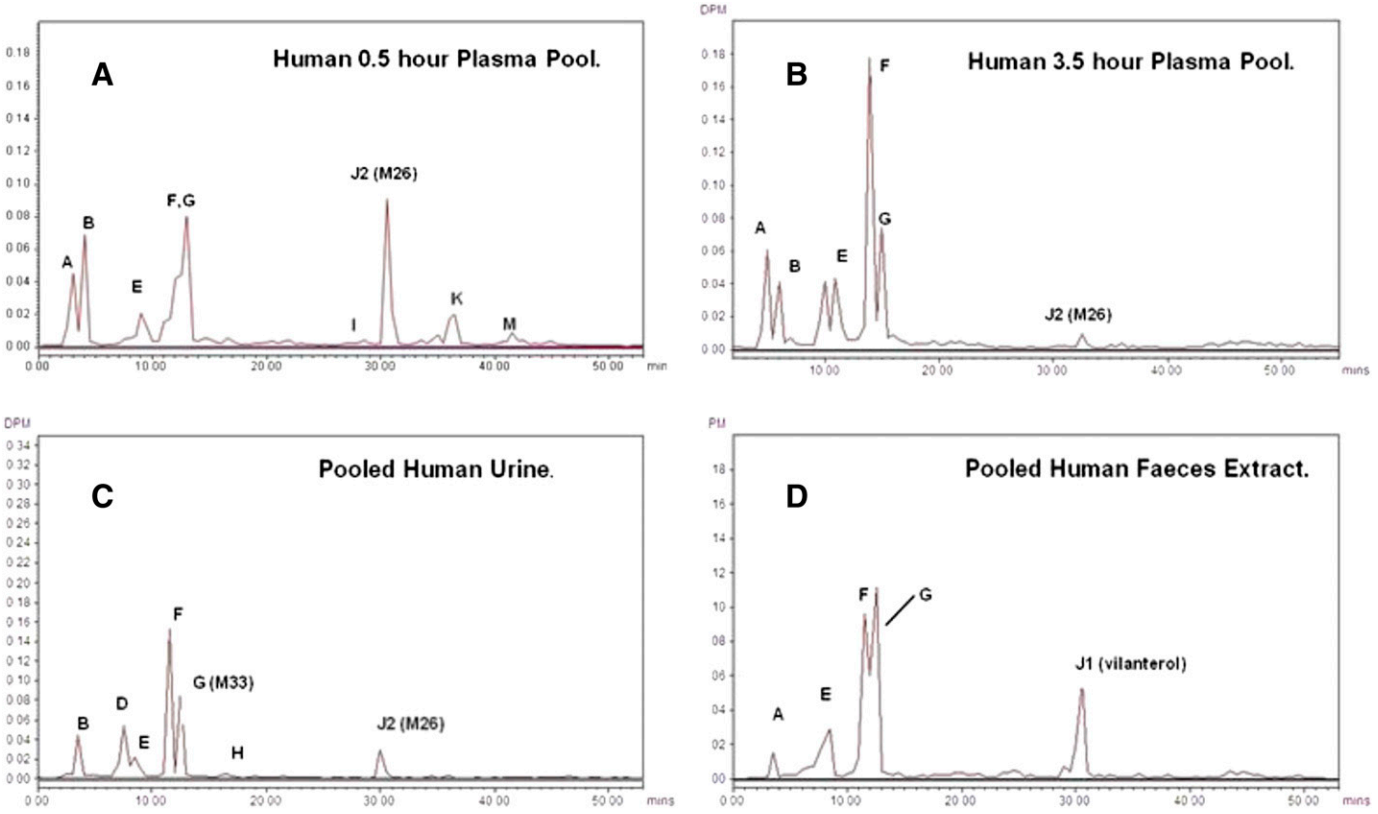

Fig. 4. HPLC radiochromatograms of plasma, urine, and feces after oral administration of [^{14}C]vilanterol to humans. Representative HPLC radiochromatograms are presented after analysis of human plasma (0.5 and 3.5 hours: A and B) extracts, human urine (C), and human feces (D) extracts obtained after a single oral administration of 200 μg of [^{14}C]vilanterol containing 74 kBq radioactivity. Structures assigned to peaks are depicted in Table 3.

TABLE 3

A summary of the metabolite structures assigned to radiochromatographic peaks in human urine, feces, and plasma after a single oral administration of 200 μg of [^{14}C]vilanterol

Chemical structures and supporting evidence from in vitro samples for metabolites assigned to radiochromatographic peaks detected in human urine, feces, and plasma obtained after a single oral administration of 200 μg of [^{14}C]vilanterol containing 74 kBq of radioactivity.

Peak	Numerical Assignment	Proposed Structure	Parent Ion $[M+H]^+$ *MS/MS Product Ions*[a]	^{1}H NMR Chemical Shifts	Evidence Supporting Structural Assignment
			m/z	*ppm*	
A	Void volume	Not applicable	Not applicable	Not applicable	Not applicable
B	M1 (*O*-dealkylation, oxidation and *O*-glucuronidation)	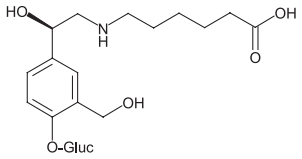	476 *440, 300, 282, 264, 246*	No NMR from in vitro samples[b]	Peak B assigned as M1 based on chromatographic retention time comparison with mouse and rat hepatocyte incubations
D, E	M3 (*O*-dealkylation and *O*-glucuronidation)	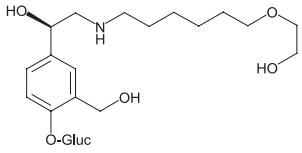	506[b]	No NMR from in vitro samples[b]	Peaks D and E assigned as a mixture of M3, M4, and M30 based on chromatographic retention time comparisons to mouse, rat, rabbit, dog, and human hepatocyte incubations.
	M4 (*O*-dealkylation, oxidation and *O*-glucuronidation)	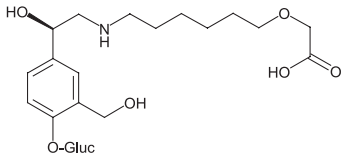	520 *484, 344, 326, 308, 250, 232*	No NMR from in vitro samples[b]	
	M30 (*O*-dealkylation and oxidation)	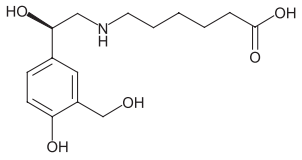	330 *282, 264, 246, 228*	δ ppm 7.26 (d, J = 1.6, 1H), 7.16 (dd, J = 8.3, 1.6, 1H), 6.84 (d, J = 8.3, 1H), 4.86 (t, J = 6.5, 1H), 4.59 (s, 2H), 3.14 (d, J = 6.5, 2H), 3.00 (t, J = 7.9, 2H), 1.49–1.67 (m, 6H)	
F	M6 (*O*-dealkylation and oxidation)	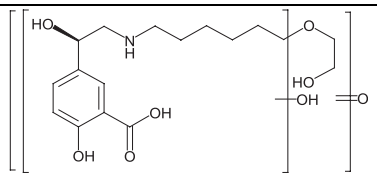	No MS[b]	No NMR	Peak F assigned as a mixture of *O*-dealkylated metabolites based on chromatographic retention time comparisons to metabolites indentified in other studies. M6 and M19 assigned based on chromatographic comparisons to rat bile (data not shown).
	M7 (*O*-dealkylation and oxidation)	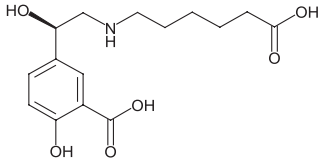	314 *296, 278*	δ ppm 7.76 (d, J = 2.3, 1H), 7.36 (dd, J = 8.5, 2.3, 1H), 6.87 (d, J = 8.5, 1H), 4.89 (t, J = 7.1, 1H), 3.03 (t, J = 7.9, 2H), 2.27 (m, 2H) 1.64–1.70 (m, 4H), 1.33 (m, 2H)	M7 assigned based on chromatographic comparison with human hepatocyte incubations.
	M19 and M39 (*O*-dealkylation and oxidation)	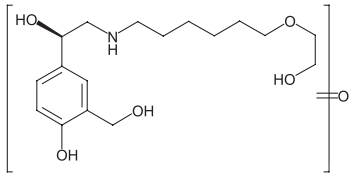	M19: No MS[b] M39: 344 *308, 250, 232*	No NMR	M39, a metabolite identified in human hepatocyte incubations (Fig. 4) was detected by HPLC-MS in human urine.

(*continued*)

TABLE 3—*Continued*

Peak	Numerical Assignment	Proposed Structure	Parent Ion $[M+H]^+$ *MS/MS Product Ions*[a]	^{1}H NMR Chemical Shifts	Evidence Supporting Structural Assignment
			m/z	*ppm*	
	M29 (GW630200, *O*-dealkylation)	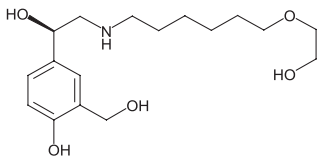	330 *294, 250, 232*	δ ppm 7.26 (d, J = 1.8, 1H), 7.15 (dd, J = 8.1, 1.8, 1H), 6.84 (d, J = 8.1, 1H), 4.86 (t, J = 6.8, 1H), 4.59 (s, 2H), 3.61 (t, J = 5.1, 2H), 3.48 (t, J = 5.1, 2H), 3.45 (t, J = 6.7, 2H), 3.13 (d, J = 6.5, 2H), 2.99 (t, J = 8.3, 2H), 1.64 (m, 2H), 1.53 (m, 4H), 1.32 (m, 2H)	M29 was a major component in incubations with human hepatocytes (Fig. 4) and human liver microsomes (data not shown). Despite the availability of reference standard (GW630200), the presence of this metabolite could not be confirmed by HPLC-MS in human urine.
G	M33 (GSK932009, *O*-dealkylation and oxidation)	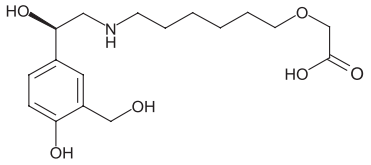	344 308, 250, 232	δ ppm 7.26 (d, J = 2.2, 1H) 7.15 (dd, J = 8.3, 2.2, 1H), 6.84 (d, J = 8.3, 1H), 4.86 (t, J = 6.7, 1H), 4.59 (s, 2H), 3.79 (s, 2H), 3.43 (t, J = 6.6, 2H), 3.14 (d, J = 6.7, 2H), 3.00 (t, J = 7.9, 2H), 1.64 (m, 4H), 1.54 (m, 2H), 1.33 (m, 2H)	Peak G assigned as M33 based on chromatographic retention time comparisons to standard GSK932009. M33 was detected by HPLC-MS in human urine.
I	M20 (GSK1676112, *N*-dealkylation)	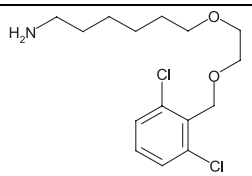	322 *159*	No NMR from in vitro samples[b]	Peak I assigned as M20 based on chromatographic retention time comparison with standard GSK1676112.
J	Vilanterol	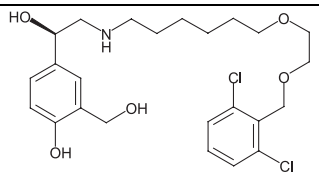	488 470, 452, 250, 234, 232, 159	δ ppm 7.40 (d, J = 8.2, 2H), 7.30 (t, J = 8.2, 1H), 4.59 (s, 2H), 7.25 (d, J = 2.3, 1H), 7.13 (dd, J = 8.2, 2.3), 6.82 (d, J = 8.2, 1H), 4.79 (dd, J = 9.1, 4.4, 1H), 4.77 (2, 2H), 3.66 (m, 2H), 3.56 (m, 2H), 3.42 (t, J = 6.6, 2H), 3.00 (m, 2H), 2.84 (d, J = 7.6, 2H), 1.56 (m, 2H), 1.49 (m, 2H), 1.28 (m, 4H)	Peak J assigned as a mixture of unchanged vilanterol and M26 based on chromatographic retention time comparisons to vilanterol reference material and M26 in rabbit and dog hepatocyte incubations. M26 was detected by HPLC-MS in human urine.
	M26 (*C*-dealkylation: oxidative cleavage of the salicyl alcohol moiety)	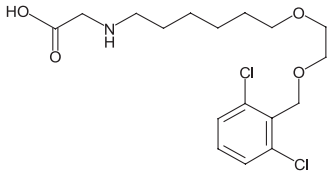	380 *334, 234, 204, 176, 159*	δ ppm 7.42 (d, J = 8.0, 2H), 7.31 (t, J = 8.0, 1H), 3.66 (m, 2H), 3.56 (m, 2H), 3.42 (t, J = 6.7, 2H), 3.45 (s, 2H), 2.92 (m, 2H), 4.77 (s, 2H)	Using a second HPLC system (data not shown) and specific assays developed for vilanterol, M26 was assigned as the major component of peak J in human urine and plasma, and vilanterol was assigned as the major component of peak J in human fecal extracts.
K	M16 (oxidation)	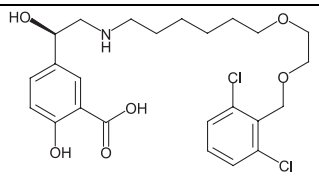	502 *466, 264, 246*	δ ppm 7.75 (d, J = 2.3, 1H), 7.38 (dd, J = 8.6, 2.3, 1H), 7.35 (d, J = 8.1, 2H), 7.24 (t, J = 8.1, 1H), 6.90 (d, J = 8.6, 1H), 4.91 (t, J = 6.8, 1H), 4.83 (s, 2H), 3.73 (m, 2H), 3.61 (m, 2H), 3.46 (t, J = 6.8, 2H), 3.18 (d, J = 6.8, 2H), 2.99 (t, J = 7.9, 2H)	Peak K assigned as M16 based on chromatographic retention time comparison with rabbit and dog hepatocyte incubations.
C, H	Unassigned	Not applicable	No MS	No NMR	No metabolite structures could be assigned to these peaks.

[a] The *m/z* values are presented for the ^{14}C isotope (major isotope for in vitro incubations).
[b] Additional nuclear magnetic resonance spectroscopy (NMR) and/or mass spectrometry (MS) data available from in situ or in vivo rat study to allow structural characterization of metabolite (data not shown).

O-dealkylated glucuronide conjugate) represented 18% and 13% of plasma radioactivity in the 0.5-hour sample. No other radioactive peak represented greater than 10% plasma drug-related material. All systemically circulating metabolites, with the exception of peak K (M16, an oxidative metabolite), were the products of *O*- or *C*-dealkylation.

Urine and Feces Metabolites HPLC radiochromatograms of pooled human urine and feces extracts are shown in Fig. 4 and are quantified in Table 4. The largest radioactive peaks in human urine and feces, as in plasma, were peaks F and G, assigned as a mixture of *O*-dealkylated metabolites. Peaks F and G accounted for 50% of urinary radioactivity, 35% of fecal radioactivity, and a combined 51% of the recovered dose. Peaks B, D, and E (assigned as M1, M3, M4, and M30) were also associated with *O*-dealkylation pathways and represented a combined total of 32% urinary radioactivity, 14% fecal radioactivity, or a combined 27% recovered radioactive dose. M26 was a minor urinary component. Unchanged vilanterol was not detected in human urine but represented about 15% fecal radioactivity (5% of the recovered dose).

In Vitro Metabolites HPLC radiochromatograms of mouse, rat, dog, rabbit, and human hepatocyte incubations are shown in Fig. 5. The main route of metabolism of vilanterol in human hepatocyte incubations was *O*-dealkylation to yield M29 (GW630200) with subsequent oxidation to M33 (GSK932009), M30, and M39. *O*-dealkylation was also a notable route of metabolism in all animal species except for the mouse, where direct glucuronidation of vilanterol to yield M12 was the major pathway. *O*-glucuronidation with *O*-dealkylation to M3 was a major pathway in the rat (M3). *C*-Dealkylation of the salicyl alcohol moiety to M26 was a major pathway in dog and rabbit hepatocytes.

Pharmacologic Activity of Metabolites The pharmacologic activity of potential metabolites using human β_1 and β_2 cAMP LANCE assays are shown in Table 5 along with their chemical structures. Tested metabolites were representative of the main routes of human metabolism. M29 (GW630200) and M33 (GSK932009) were major in vitro pathways representing *O*-dealkylation. M20 (GSK1676112) and GW853734 were investigated to understand the effect of N-dealkylation (both halves of the molecule) on its pharmacologic activity. All the cleaved structures tested were ≥2500 times less potent compared with vilanterol on the β_2–receptor, indicating that metabolic cleavage largely removes the β_2-agonist pharmacology associated with vilanterol. Similarly, the metabolites and cleaved analogs of vilanterol were either inactive against β_1 or were of such low potency that β-agonist-related effects would be unlikely in humans.

Discussion

The results we describe provide an understanding of the metabolism and disposition of vilanterol in humans. The oral route of administration represents the swallowed portion of an inhaled dose; based on urinary recovery of radioactivity (Fig. 3), at least 50% of the vilanterol oral dose solution was absorbed. Metabolite profiles, however, indicated that <5% of the administered radioactivity was associated with unchanged vilanterol in feces, potentially reflecting the percentage of unabsorbed drug (Table 4). Therefore, oral absorption of vilanterol is probably higher than the estimate based on urinary excretion alone and is likely virtually complete. Systemic exposure to vilanterol represented a very small proportion (<0.5%) of DRM in plasma (Fig. 2) and, together with the presence of several circulating metabolites, was indicative of extensive first-pass metabolism of vilanterol. Considered together, systemic vilanterol concentrations measured after inhalation administration thus are attributed to absorption through the lung with little or no contribution from the swallowed portion of the dose, which is well absorbed but undergoes extensive first-pass metabolism.

The total recovery of radioactivity was relatively low (71.6% of the administered radioactivity), and the precise cause is unknown but is most likely attributed to technical reasons related to the low radioactive dose (74 kBq; 25- to 50-fold lower than that used in more traditionally designed studies) and the low vilanterol chemical mass administered (200 μg). This results in excreta containing very low mass concentrations, where the measurement of radioactivity would be sensitive to very low levels of nonspecific binding to any apparatus used. The mixed methods used for radioactivity measurement may also have contributed to the low radioactive recovery.

Any concerns about the slow release of DRM from a depot within the body or loss due to exhalation of radioactivity were not supported by the data. By 4 days after dosing, elimination of radioactivity was essentially complete (>99% of the recovered radioactivity detected in urine or feces collections) with only <0.3% of radioactivity recovered within the next 3 days, and there was little evidence for substantial metabolism associated with atoms close to the [^{14}C] isotope to easily explain exhalation of radioactivity as carbon dioxide. A retrospective

TABLE 4

Summary of vilanterol metabolites in human plasma, urine, and feces after oral administration of 200 μg of vilanterol

Metabolites of vilanterol are quantified in pooled plasma, urine, and feces obtained after a single oral administration of 200 μg of [^{14}C] vilanterol.

Peak ID	% Radioactivity in 0.5-Hour Human Plasma	% Radioactivity in Urine and Fecal Extracts (% recovered dose)	
		Pooled Urine	Pooled Feces
A	8.7	ND	2.8 (0.8)
B (M1)	12.8	9.4 (6.6)	ND
D (M3)	ND	13.5 (9.5)	ND
E (M30, M4)	7.3	9.0 (6.3)	13.8 (4.1)
F (M6, M7, M19, M29, M39)	32.5	31.0 (21.7)	21.5 (6.4)
G (M33)		19.3 (13.5)	33.9 (10.2)
H	ND	2.0 (1.4)	ND
I (M20)	<1	ND	1.3 (0.4)
J1, GW642444 (P)	ND	ND	15.4 (4.6)
J2 (M26)	17.7	6.5 (4.6)	ND
K (M16)	6.0	ND	ND

ND, not detected. Peak J was assigned as unchanged vilanterol in feces (J1) and M26 in plasma and urine (J2).

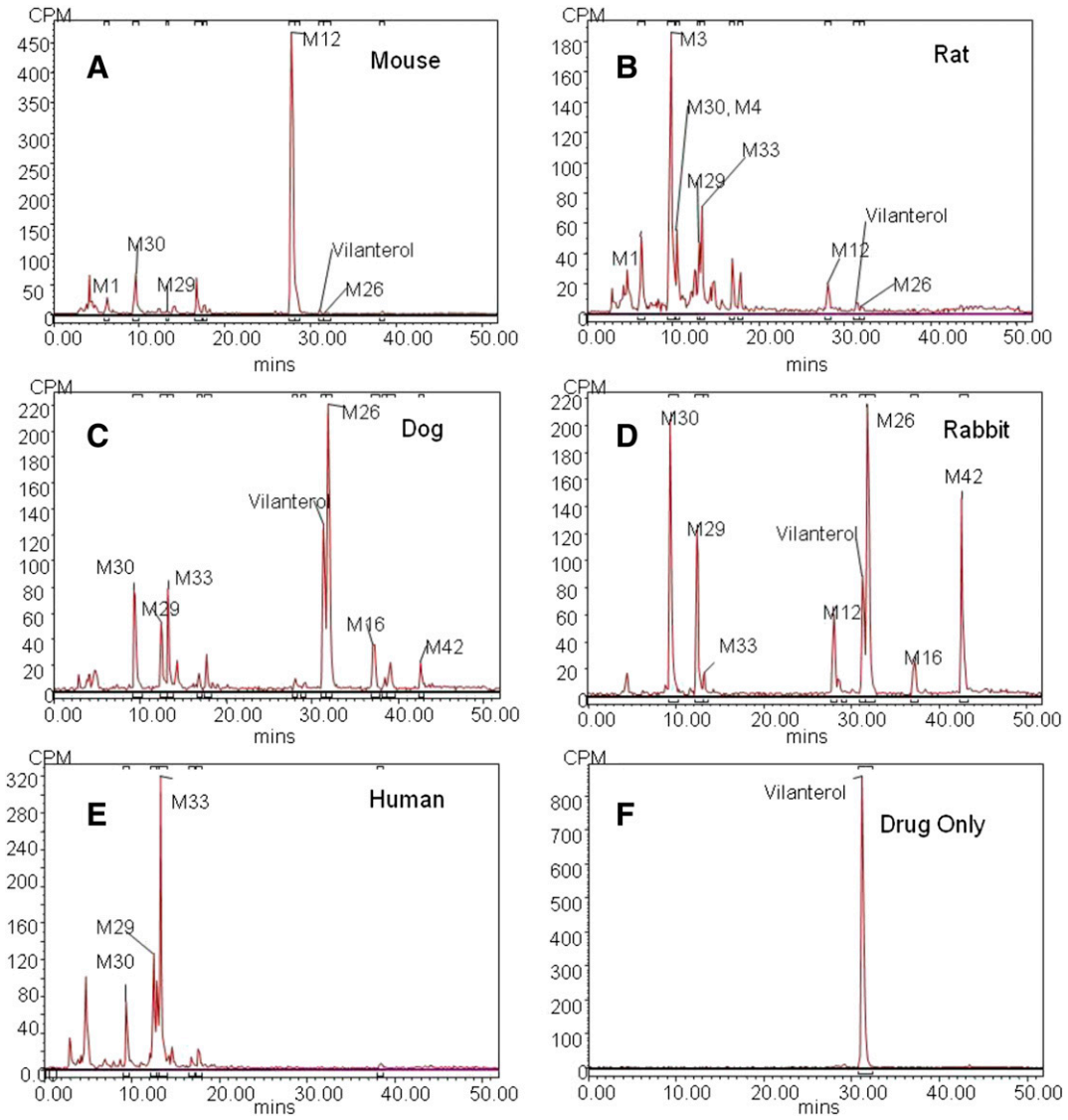

Fig. 5. HPLC radiochromatograms of mouse, rat, dog, rabbit, human, and control hepatocyte incubations with [^{14}C]vilanterol. Representative HPLC radiochromatograms are presented after analysis of incubations of [^{14}C]vilanterol with mouse- (A), rat- (B), dog- (C), rabbit- (D), and human- (E) cryopreserved hepatocytes. A control incubation without hepatocytes (drug-only) is included for comparison (F).

analysis of mass balance data (Roffey et al., 2007) suggests that total radioactive recovery in humans, using routine methodology, should normally be 80% or greater. Roffey et al. conclude that a low mass balance is more likely due to technical limitations, which often confound the generation of a full mass balance and should not be regarded as tissue sequestration per se.

The plasma half-life of radioactivity was very long (see Fig. 2), and the low extraction efficiencies (<10% extracted at 24 hours after dosing) were consistent with tight or covalent binding of DRM to plasma protein rather than slow release of DRM from a depot. This binding phenomenon, which occurs in many metabolism studies, is accentuated when using the very high sensitivity conferred by AMS when compared with traditional LSC counting.

The human metabolic profiles in human plasma, urine, and feces (Fig. 4) were broadly similar to that observed using human hepatocytes (Fig. 5). Elimination of vilanterol was mainly by metabolism (Fig. 4; Table 4) followed by excretion of metabolites in urine (70% of recovered radioactivity) and feces (30% of recovered radioactivity). Direct secretion or direct conjugation of vilanterol were not major routes of elimination, with less than 5% of the administered dose associated with unchanged vilanterol. The major route of metabolism (Fig. 1) was via *O*-dealkylation, with up to 78% of the recovered dose (in all human excreta) eliminated as *O*-dealkylated metabolites (Tables 3 and 4). *N*-Dealkylation and *C*-dealkylation were minor pathways, representing a combined 5% of the recovered dose. Although *C*-dealkylation is uncommon, it has been described elsewhere as a route of metabolism for indacaterol, another β-agonist (Kagan et al., 2012) that shares the same (amino-hydroxyethyl) phenol moiety with vilanterol. Kagan et al. tentatively propose two mechanisms for this carbon–carbon cleavage: one initiated by a one-electron oxidation of the oxygen in the phenol moiety followed by a β-scission reaction, and the other initiated by phenolic hydroxylation, subsequent keto/enol tautomerism, followed by a retro-Aldol reaction. Both mechanisms are also feasible for the *C*-dealkylation of vilanterol.

The proposed commercial dose for vilanterol is 25 μg, once daily, by the inhalation route. All identified routes of metabolism for vilanterol are associated with innocuous (as opposed to reactive)

TABLE 5

Pharmacologic activity of selected human metabolites of vilanterol tested using human β_1 and β_2 cAMP LANCE assays

Pharmacologic activity is shown in terms of mean pEC_{50} for vilanterol, four human metabolites, and one potential metabolite.

Metabolite	Mean pEC_{50} (n = 7–24)	
	β_1	β_2
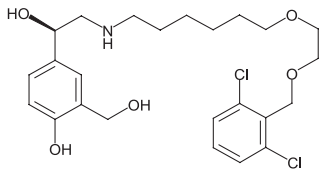 Vilanterol	7.0	10.4
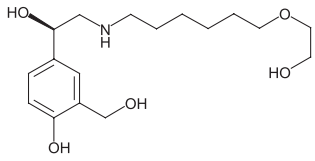 GW630200 (M29)	5.7	7.0
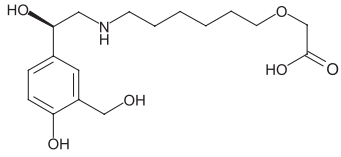 GSK932009 (M33)	5.0	6.9
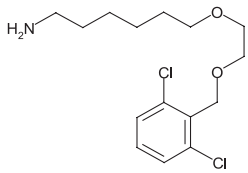 GSK1676112 (M20)	<4.5	5.0
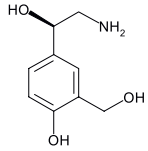 GW853734 (potential metabolite – not detected in animals or human)	5.3	5.4

chemical mechanisms. The maximum daily body burden to any metabolite does not exceed the vilanterol dose level of 25 μg/day, which is negligible when compared with the 10-mg daily threshold for clinical adverse drug reactions mediated by reactive metabolite mechanisms proposed by a number of key opinion leaders (Uetrecht, 1999; Smith, 2005). In addition, at this low-dose level, the likelihood of a metabolite causing new unexpected toxicity, unrelated to its β-agonist pharmacology, is negligible. As a result, a major focus of the metabolism work for vilanterol was to establish whether any metabolites possessed β-agonist pharmacologic activity that could result in unwanted systemic effects. First, after oral administration of vilanterol at up to 500 μg, plasma concentrations of metabolites were significantly higher than unchanged vilanterol as well as being significantly greater than metabolite concentrations produced after an inhaled administration at the lower therapeutic dose of 25 μg. Despite the higher metabolite concentrations, there were no changes in measured vital signs or heart rate in either clinical study, indicating a lack of metabolite β-adrenergic activity. Second, synthesized metabolites, representative of the major human metabolic routes, were $\geq$2500 times less potent against β_2-receptors compared with vilanterol (Table 5). The synthesized metabolites were either inactive against β_1-receptors or of such low potency that no β_1-agonist-related effects would be seen in human after the human daily dose. The metabolites tested represented both halves of the molecule after cleavage metabolism and demonstrate how *O*- or *N*-dealkylation considerably reduces potency against both β_1- and β_2-receptors. The lack of potency associated with GW853734 demonstrates that *N*-dealkylation to metabolites where the [^{14}C] radioisotope label might be lost will also dramatically reduce pharmacologic activity.

The metabolites detected in human matrices were also present in the species used for toxicology assessment (data not shown), demonstrating their relevance to the assessment of safety for vilanterol in humans. Additionally, all major routes of metabolism in human hepatocytes were also shown in mouse, rat, dog, and rabbit hepatocyte incubations. The largest radioactive chromatographic peaks in human plasma after oral administration were peak G (M33/GSK932009) and peak F [several *O*-dealkylated and oxidized metabolites including GW630200, peak J2 (M26), and peak B (M1)] (see Fig. 4; Table 4). These radioactive peaks each represented >10% plasma DRM (the threshold for further investigation as recommended by ICH M3[R2]), 0.5 hours after an oral administration of vilanterol. It should be noted, however, that the proposed commercial dose of vilanterol (25 μg) is considerably lower than the 10-mg threshold proposed in ICH M3(R2) guidance (International Committee on Harmonisation, 2009), below which a more lenient threshold than 10% plasma DRM is deemed appropriate. Concentrations of M33 (GSK932009) and M29 (GW630200) were measured in plasma from asthma and COPD patients dosed up to 50 μg of vilanterol by the inhalation route and were generally lower than the quantification limit (180 and 90 pg/ml, respectively, data not shown). Both metabolites circulated at higher concentrations in mice, rats, and dogs compared with humans, when measured as part of the inhalation toxicology studies.

In summary, oral vilanterol is well absorbed in humans and is subject to extensive first-pass metabolism to metabolites, with negligible β-agonist pharmacologic activity. The metabolism of vilanterol is mainly by *O*-dealkylation, and metabolites are excreted both via feces and urine. To a large extent, the low dose levels often associated with inhalation molecules (25 μg in this case) mitigate any metabolite or metabolism safety concerns.

Acknowledgments

The authors thank Dr. Geoff Badman (Chemical Development, GSK R&D, Stevenage, UK) for the synthesis and supply of [^{14}C]vilanterol and the metabolite standards, Dr. Michael Butler and staff at Xceleron Ltd., York, UK, for the accelerator mass spectrometry analysis of fecal homogenates, Dr. Gordon Dear for the metabolite identification work from hepatocyte incubations, and Steve Corless for AMS analysis of GSK graphites.

Authorship Contributions

Participated in research design: Harrell, Siederer, Bal, Young, Kempsford.

Conducted experiments: Patel, Felgate, Pearce, Roberts, Beaumont, Emmons, Pereira.

Performed data analysis: Harrell, Siederer, Patel, Young, Felgate, Pearce, Beaumont, Emmons.

Wrote or contributed to the writing of the manuscript: Harrell, Siederer, Young, Roberts, Beaumont, Kempsford.

References

Affrime MB, Cuss F, Padhi D, Wirth M, Pai S, Clement RP, Lim J, Kantesaria B, Alton K, and Cayen MN (2000) Bioavailability and metabolism of mometasone furoate following administration by metered-dose and dry-powder inhalers in healthy human volunteers. *J Clin Pharmacol* **40**:1227–1236.

Hanania NA, Feldman G, Zachgo W, Shim JJ, Crim C, Sanford L, Lettis S, Barnhart F, and Haumann B (2012) The efficacy and safety of the novel long-acting β2 agonist vilanterol in patients with COPD: a randomized placebo-controlled trial. *Chest* **142**:119–127.

International Committee on Harmonisation (2009). Guidance on nonclinical safety studies for the conduct of human clinical trials and marketing authorization for pharmaceuticals. Nonclinical Safety Studies M3(R2), http://www.ich.org/products/guidelines/safety/safety-single/article/guidance-on-nonclinical-safety-studies-for-the-conduct-of-human-clinical-trials-and-marketing-author.html.

International Committee on Radiological Protection (1991) 1990 Recommendations of the international commission on radiological protection. ICRP Publication 60. *Ann ICRP* **21**(1–3).

Kagan M, Dain J, Peng L, and Reynolds C (2012) Metabolism and pharmacokinetics of indacaterol in humans. *Drug Metab Dispos* **40**:1712–1722.

Lotvall J, Bateman ED, Bleecker ER, Busse WW, Woodcocks A, Follows R, Lim J, Stone S, Jacques L, and Haumann B (2012) 24-h duration of the novel LABA vilanterol trifenatate in asthma patients treated with inhaled corticosteroids. *Eur Respir J* **40**:570–579.

Roffey SJ, Obach RS, Gedge JI, and Smith DA (2007) What is the objective of the mass balance study? A retrospective analysis of data in animal and human excretion studies employing radiolabeled drugs. *Drug Metab Rev* **39**:17–43.

Smith DA and Obach RS (2005) Seeing through the MIST: abundance versus percentage. Commentary on metabolites in safety testing. *Drug Metab Dispos* **33**:1409–1417.

Uetrecht JP (1999) New concepts in immunology relevant to idiosyncratic drug reactions: the "danger hypothesis" and innate immune system. *Chem Res Toxicol* **12**:387–395.

Young G, Corless S, Felgate C, and Colthup P (2008) Comparison of a 250 kV single-stage accelerator mass spectrometer with a 5 MV tandem accelerator mass spectrometer—fitness for purpose in bioanalysis. *Rapid Commun Mass Spectrom* **22**:4035–4042.

Address correspondence to: Andrew W. Harrell, Division of Drug Metabolism and Pharmacokinetics, GlaxoSmithKline R&D, Park Road, Ware, Hertfordshire, SG12 0DP, United Kingdom. E-mail: andrew.w.harrell@gsk.com

1521-009X/42/3/415–430$25.00
Drug Metabolism and Disposition
Copyright © 2014 by The American Society for Pharmacology and Experimental Therapeutics
http://dx.doi.org/10.1124/dmd.113.054486
Drug Metab Dispos 42:415–430, March 2014

Disposition and Metabolism of Darapladib, a Lipoprotein-Associated Phospholipase A2 Inhibitor, in Humans

Mehul Dave, Mike Nash, Graeme C. Young, Harma Ellens, Mindy H. Magee, Andrew D. Roberts, Maxine A. Taylor, Robert W. Greenhill, and Gary W. Boyle

Department of Drug Metabolism and Pharmacokinetics (M.D., M.N., G.C.Y., A.D.R., M.A.T., G.W.B.) and Department of Safety Assessment (R.W.G.), GlaxoSmithKline Research & Development, Ware, United Kingdom, and Department of Drug Metabolism and Pharmacokinetics (H.E.) and Clinical Pharmacology, Modeling and Simulation (M.H.M.), GlaxoSmithKline Research & Development, Upper Merion, Philadelphia

Received September 6, 2013; accepted December 30, 2013

ABSTRACT

The absorption, metabolism, and excretion of darapladib, a novel inhibitor of lipoprotein-associated phospholipase A_2, was investigated in healthy male subjects using [^{14}C]-radiolabeled material in a bespoke study design. Disposition of darapladib was compared following single i.v. and both single and repeated oral administrations. The anticipated presence of low circulating concentrations of drug-related material required the use of accelerator mass spectrometry as a sensitive radiodetector. Blood, urine, and feces were collected up to 21 days post radioactive dose, and analyzed for drug-related material. The principal circulating drug-related component was unchanged darapladib. No notable metabolites were observed in plasma post-i.v. dosing; however, metabolites resulting from hydroxylation (M3) and N-deethylation (M4) were observed (at 4%–6% of plasma radioactivity) following oral dosing, indicative of some first-pass metabolism. In addition, an acid-catalyzed degradant (M10) resulting from presystemic hydrolysis was also detected in plasma at similar levels of ~5% of radioactivity post oral dosing. Systemic exposure to radioactive material was reduced within the repeat dose regimen, consistent with the notion of time-dependent pharmacokinetics resulting from enhanced clearance or reduced absorption. Elimination of drug-related material occurred predominantly via the feces, with unchanged darapladib representing 43%–53% of the radioactive dose, and metabolites M3 and M4 also notably accounting for ~9% and 19% of the dose, respectively. The enhanced study design has provided an increased understanding of the absorption, distribution, metabolism and excretion (ADME) properties of darapladib in humans, and substantially influenced future work on the compound.

Introduction

Despite contemporary multidrug therapies (treatment with statins, antiplatelet therapy, renin-angiotensin aldosterone system, and/or β adrenergic blockade and diabetes control), there is still a large unmet medical need to develop new strategies for the treatment of atherosclerotic vascular disease. Lipoprotein-associated phospholipase A_2 (Lp-PLA_2) has been identified as a risk marker in atherosclerosis (Thompson et al., 2010) and is therefore a target for therapeutic intervention. Darapladib (SB-480848 or *N*-[2-(diethylamino)ethyl]-2-(2-{[(4-fluorophenyl)methyl]thio}-4-oxo-4,5,6,7-tetrahydro-1*H*-cyclopenta[*d*]pyrimidin-1-yl)-*N*-{[4'-(trifluoromethyl)-4-biphenylyl]methyl}acetamide) is a novel, selective, orally active inhibitor of Lp-PLA_2, and is in late-phase clinical development as a potential antiatherosclerotic agent when administered in combination with current standard of care treatment of patients with acute coronary syndrome or coronary heart disease (Mohler et al., 2008; Serruys et al., 2008). It has been generally safe and well tolerated in clinical studies completed to date. A dose of 160 mg produced significant and sustained inhibition of plasma Lp-PLA_2 activity and halted necrotic core progression, a key determinant of plaque vulnerability (Serruys et al., 2008). This dose was therefore selected for the ongoing pivotal outcomes studies.

The current study was designed to characterize the disposition and metabolism of darapladib in healthy adult male volunteers following single doses of i.v. as well as oral [^{14}C]darapladib (Fig. 1). Early in preclinical development, an N-desethyl metabolite (M4; SB-553253)

dx.doi.org/10.1124/dmd.113.054486.

ABBREVIATIONS: AMS, accelerator mass spectrometry; $AUC_{(0\text{-}t)}$, area under the curve from time zero to time of last measured timepoint; AUC(0-τ), area under the curve from time zero to the next dosing interval; $AUC_{(0\text{-}inf)}$, area under the curve from time zero to infinity; darapladib (SB-480848), *N*-[2-(diethylamino)ethyl]-2-(2-{[(4-fluorophenyl)methyl]thio}-4-oxo-4,5,6,7-tetrahydro-1*H*-cyclopenta[*d*]pyrimidin-1-yl)-*N*-{[4'-(trifluoromethyl)-4-biphenylyl]methyl}acetamide; HLM, human liver microsome; HPLC, high-performance liquid chromatography; LLQ, lower limit of quantification; Lp-PLA_2, lipoprotein-associated phospholipase A_2; LSC, liquid scintillation counting; M3 (SB-823094), *N*-[2-(diethylamino)ethyl]-2-(2-{[(4-fluorophenyl)methyl]thio}-5-hydroxy-4-oxo-4,5,6,7-tetrahydro-1*H*-cyclopenta[*d*]pyrimidin-1-yl)-*N*-{[4'-(trifluoromethyl)-4-biphenylyl]methyl}acetamide; M4 (SB-553253), *N*-[2-(ethylamino)ethyl]-2-(2-{[(4-fluorophenyl)methyl]thio}-4-oxo-4,5,6,7-tetrahydro-1*H*-cyclopenta[*d*]pyrimidin-1-yl)-*N*-{[4'-(trifluoromethyl)-4-biphenylyl]methyl}acetamide; M7 (SB-735258), *N*-[2-(diethylamino)ethyl]-2-[2-(methyloxy)-4-oxo-4,5,6,7-tetrahydro-1*H*-cyclopenta[*d*]pyrimidin-1-yl]-*N*-{[4'-(trifluoromethyl)-4-biphenylyl]methyl}acetamide; M10 (SB-554008), *N*-[2-(diethylamino)ethyl]-2-(2,4-dioxo-2,3,4,5,6,7-hexahydro-1*H*-cyclopenta[*d*]pyrimidin-1-yl)-*N*-{[4'-(trifluoromethyl)-4-biphenylyl]methyl}acetamide; M11 (GSK219147), *N*-[2-(diethylamino)ethyl]-2-(4-oxo-2-thioxo-2,3,4,5,6,7-hexahydro-1*H*-cyclopenta[*d*]pyrimidin-1-yl)-*N*-{[4'-(trifluoromethyl)-4-biphenylyl]methyl}acetamide; MS, mass spectrometry; MS/MS, tandem mass spectrometry; NEC, National Electrostatics Corp.; NMR, nuclear magnetic resonance; PgP, P-glycoprotein; QC, quality control; T_{max}, time of C_{max}; λz, terminal plasma elimination rate constant.

Downloaded from dmd.aspetjournals.org at ASPET Journals on November 7, 2015

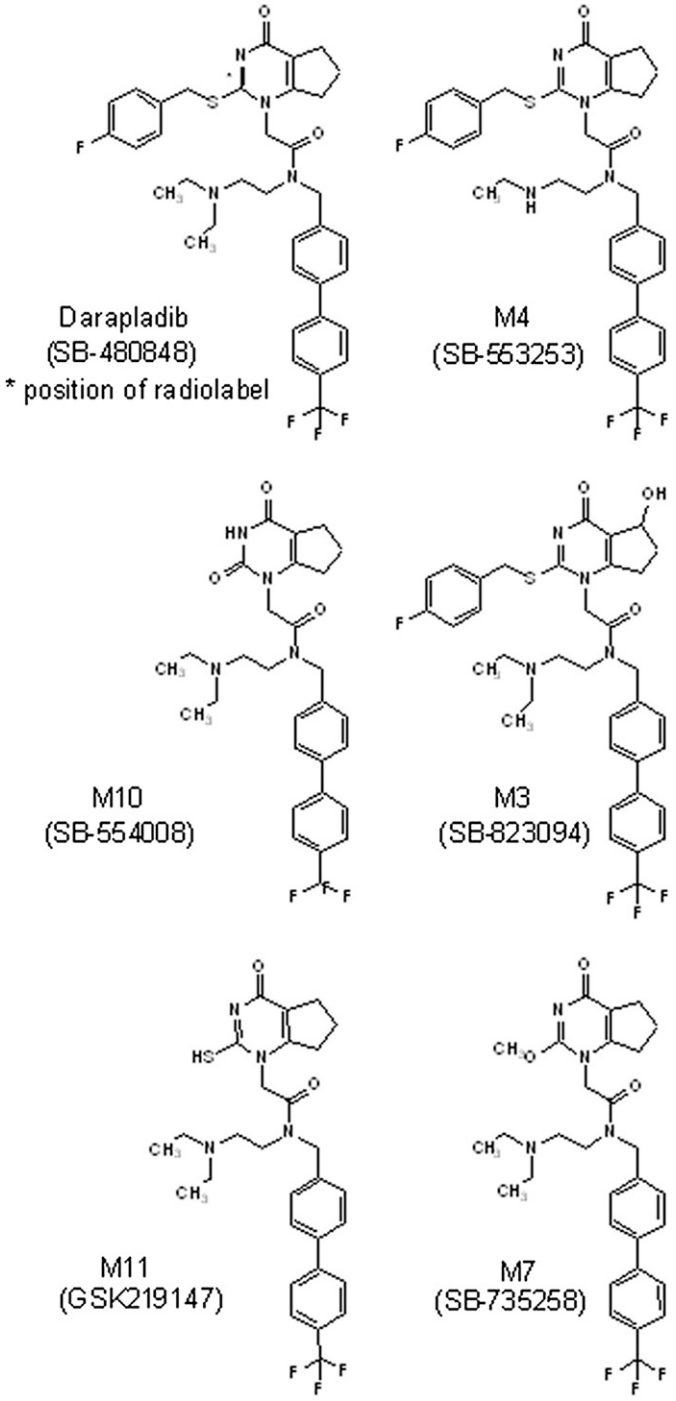

Fig. 1. Structure of [^{14}C]darapladib and synthetic metabolites.

was identified and found to be pharmacologically active, and this metabolite has been assayed in all subsequent work, including the current study.

Preclinical excretion and metabolism studies in rats and dogs estimated that darapladib absorption, based on the sum of biliary secretion and urinary excretion of radioactive drug-related material, was relatively low at approximately 4% of the dose, with the majority of the dose eliminated apparently as unabsorbed drug via the feces (M. Dave et al., data on file). The major route of elimination of absorbed drug was via biliary secretion of metabolites (resulting predominantly from N-deethylation and oxidation) and unchanged darapladib, whereas direct intestinal secretion of darapladib (post i.v. dosing) was also observed. Darapladib recovered in feces following an oral dose in humans may therefore represent both biliary and/or intestinal secretion, or simply unabsorbed drug. Administration of the i.v. dose in this current study facilitates elucidation of the processes involved in excretion, i.e., the extent to which darapladib is eliminated in feces and urine as parent or metabolites.

In early clinical studies, it was noted that darapladib accumulates (at 30%–60%) in the systemic circulation after multiple oral doses. However, this was less than predicted from the single-dose pharmacokinetics (PK) data which suggested accumulation of 130%–200%. The ideal way to investigate the reasons for this would be to administer radiolabeled darapladib until steady-state conditions are achieved (10 days) and compare the results to that following a single dose. Nonetheless, radioactive exposure following this dosing regimen and utilizing conventional radioactive doses would have been unacceptable. Therefore, nonradiolabeled darapladib was administered for 10 days, and on day 11, a single oral dose of [^{14}C]darapladib was administered, followed by three more doses of nonradiolabeled darapladib. This allowed examination of the relative metabolic profile of [^{14}C]darapladib at steady-state compared with that following a single dose.

Dose levels of 8 mg (i.v. infusion), 80 mg (radiolabeled oral solution), and 160 mg (nonradiolabeled enteric tablet) were selected based on each providing similar systemic exposure. Accelerator mass spectrometry (AMS) was used to determine levels of total radioactivity in plasma samples (post oral administration) and plasma metabolite profiles from all phases due to the very low levels of radioactivity in these samples.

Materials and Methods

Chemicals

[^{14}C]Darapladib, darapladib, [$^{13}C_6$]darapladib (stable labeled in the phenyl ring), and a number of synthetic standards were supplied by Chemical Development, GlaxoSmithKline Research and Development Ltd. (Stevenage, UK). Metabolite standards were as follows: *N*-[2-(diethylamino)ethyl]-2-(2-{[(4-fluorophenyl)methyl]thio}-5-hydroxy-4-oxo-4,5,6,7-tetrahydro-1*H*-cyclopenta[*d*]pyrimidin-1-yl)-*N*-{[4'-(trifluoromethyl)-4-biphenylyl]methyl}acetamide (coded M3, SB-823094); *N*-[2-(ethylamino)ethyl]-2-(2-{[(4-fluorophenyl)methyl]thio}-4-oxo-4,5,6,7-tetrahydro-1*H*-cyclopenta[*d*]pyrimidin-1-yl)-*N*-{[4'-(trifluoromethyl)-4-biphenylyl]methyl}acetamide (coded M4, SB-553253) and [$^{13}C_6$]SB-553253 (stable labeled in the phenyl ring); *N*-[2-(diethylamino)ethyl]-2-[2-(methyloxy)-4-oxo-4,5,6,7-tetrahydro-1*H*-cyclopenta[*d*]pyrimidin-1-yl]-*N*-{[4'-(trifluoromethyl)-4-biphenylyl]methyl}acetamide (coded as M7, SB-735258); *N*-[2-(diethylamino)ethyl]-2-(2,4-dioxo-2,3,4,5,6,7-hexahydro-1*H*-cyclopenta[*d*]pyrimidin-1-yl)-*N*-{[4'-(trifluoromethyl)-4-biphenylyl]methyl}acetamide (coded as M10, SB-554008); and *N*-[2-(diethylamino)ethyl]-2-(4-oxo-2-thioxo-2,3,4,5,6,7-hexahydro-1*H*-cyclopenta[*d*]pyrimidin-1-yl)-*N*-{[4'-(trifluoromethyl)-4-biphenylyl]methyl}acetamide (coded as M11, GSK219147). All of these materials were used as chromatographic, mass spectrometric, and/or nuclear magnetic resonance (NMR) spectroscopy standards during the study (Fig. 1). Commercially obtained chemicals and solvents were of high-performance liquid chromatography (HPLC) or analytical grade. Liquid scintillation cocktails were obtained from PerkinElmer LAS (UK) Ltd. (Beaconsfield, UK).

Sucrose (IAEA-C6) standard (certificated value = 1.506 times modern), from the International Atomic Energy Agency (Vienna, Austria), was used as the source of graphite (6.5 mg of sugar for each graphite produced) for use as the AMS instrument normalization and process control standard.

Synthetic graphite 200 mesh (99.9999%), from Alfa Aesar (Heysham, UK), was used as the AMS instrument background determination standard. All of the reagents used in preparation of samples to graphite prior to analysis by AMS were supplied by Sigma-Aldrich Company Ltd., Gillingham, UK.

Darapladib Formulations

The i.v. dose was prepared by taking 8 ml of [^{14}C]darapladib (at 1 mg/ml; 6.25 μCi/ml) and diluting to 40 ml with normal saline to give a final i.v. dose of 8 mg of darapladib. The 40-ml i.v. solution was subsequently infused over a period

Downloaded from dmd.aspetjournals.org at ASPET Journals on November 7, 2015

of 3 hours. The radiolabeled oral dose was prepared by mixing 3.2 ml of [^{14}C]darapladib (1 mg/ml; 6.25 μCi/ml) injection solution with 76.8 ml of non-radiolabeled darapladib (1 mg/ml solution) to give a final oral solution dose of 80 mg of darapladib. Radiochemical purity determination of the dose formulations was conducted and was >98% for the i.v. dose and >99% for each oral radiolabeled dose. Nonradiolabeled darapladib (micronized) was supplied as enteric-coated 160-mg white tablets.

Study Design and Subjects

The clinical study (GlaxoSmithKline SB-480848/015) was performed at Covance Laboratories Inc. in conjunction with the Covance Clinical Research Unit (Madison, WI) in accordance with Good Clinical Practice and the guiding principles of the 1996 version of the Declaration of Helsinki. The protocol including the proposed radioactive dose was reviewed by the GlaxoSmithKline Global Safety Board and by the Covance Clinical Research Unit Institutional Review Board. The total radioactive dose of 90 μCi was estimated using rat whole-body autoradiography and excretion balance data and corresponded to an effective dose of ≤1 mSv, which is approximately one-third of the annual average background effective dose and within risk category IIa, in accordance with the International Commission on Radiologic Protection. The amount of radioactivity used for each phase also incorporated the anticipated analytical requirements and study objectives. Written consent was obtained from all subjects before any protocol-specific procedures were conducted.

Eight healthy male subjects (four white, three African American, one mixed race), between 30 and 44 years of age, bodyweight >50 kg, and with a body mass index between 19 and 32 kg/m^2, were enrolled in this study with seven completing all sessions (one subject was excluded from the final session due to low recovery of radioactivity in the previous session). The study design was an open-label, nonrandomized, three-session study in which darapladib was administered to each subject over three sessions in the following order: a single radiolabeled i.v. dose (session 1), a single radiolabeled oral dose (session 2), and a series of nonradiolabeled repeat oral doses with a radiolabeled oral dose administered on day 11 of 14 days of dosing (session 3). There was a minimum 21-day washout period between radioactive doses in each session. Subjects were in good health, with no history of drug or alcohol abuse, and were taking no other medication at the time of the study, with no prescribed medication within 7 days (or 5 half-lives, whichever was longer) of the study commencing.

Study Procedures

On the morning of day 1 for session 1, all subjects received a single i.v. infusion at a target dose of 8 mg (approximately 50 μCi) of [^{14}C]darapladib in 40 ml of normal saline over 3 hours. After a washout period, on the morning of day 1 for session 2, all subjects received a single oral administration at a target dose of 80 mg (approximately 20 μCi) of [^{14}C]darapladib as an 80-ml solution, and were instructed to rinse their mouth with a further 100 ml of water and swallow the water. After a further washout period, on the morning of day 1 for session 3, seven subjects received a 160-mg dose of an enteric-coated darapladib tablet, and subsequently received daily doses of a 160-mg enteric-coated darapladib tablet on days 2–10. On the morning of day 11, subjects received a single oral administration at a target dose of 80 mg (approximately 20 μCi) of [^{14}C]darapladib as an 80-ml solution, with a further 100 ml of water. Daily dosing of a 160-mg enteric-coated darapladib tablet continued on days 12–14.

After i.v. administration, blood samples (7 ml) for plasma total radioactivity, unchanged darapladib, and SB-553253 analysis were collected into EDTA tubes at predose and 0.5, 1, 2, 3 (immediately prior to termination of infusion), 3.5, 4, 5, 6, 7, 9, 12, 18, 24, 32, 48, 72, and 96 hours after the start of infusion. Following oral administration in session 2 and on day 11 of session 3, blood samples (7 ml) were collected at predose and 0.5, 1, 2, 3, 4, 6, 9, 12, 18, 24, 32, 48, 72, and 96 hours postdose. Additional samples (30 ml) were also collected for metabolite analysis from subjects at 3, 12, 24, and 48 hours post start of i.v. infusion or after oral administration (session 2 or following dosing on day 11 of session 3). Blood samples were mixed, immediately chilled on crushed ice, and centrifuged for 15 minutes at 1500*g* at approximately 4°C to obtain plasma. Total radioactivity was measured using aliquots of plasma (0.06–0.5 ml); the remaining plasma was stored at −70°C or less before the assay for darapladib and SB-553253, or metabolite profiling by HPLC.

Urine samples from all three sessions were collected predose and between 0 and 6, 6 and 12, and 12 and 24 hours after drug administration and then at 24-hour intervals until 504 hours post i.v. infusion (session 1), 216 hours post single oral dose (session 2), and 264 hours post day 11 dosing (session 3). For each collection period, after thorough mixing, the weight and pH were measured and recorded. A single subsample (50 ml) was removed from the bulk sample and set aside for metabolite profiling and identification and stored at −20°C. Total radioactivity was measured using triplicate aliquots (approximately 1 ml) of urine.

Feces samples for all three sessions were collected quantitatively predose and at 24-hour intervals for the same time periods described for urine. Feces from each collection interval were weighed, mixed with deionized water (approximately 1:1), and the total weight of the sample recorded prior to homogenization. Total radioactivity was measured using triplicate aliquots (0.3 g) of each feces homogenate. A single subsample (30 g) was removed from the bulk sample and set aside for metabolite profiling and identification and stored at −20°C.

Assay of Total Radioactivity by Liquid Scintillation Counting

Aliquots (0.5 ml) of plasma samples from session 1 were mixed with Ultima Gold scintillation fluid [PerkinElmer LAS (UK) Ltd.] and analyzed by liquid scintillation counting (LSC) using a low level scintillation counter [PerkinElmer LAS (UK) Ltd.]. The lower limit of quantification (LLQ) was 1.0 darapladib nanogram equivalents per milliliter. Triplicate aliquots (1 ml) of urine were also subjected to LSC following mixing with Ultima Gold scintillation fluid. Triplicate aliquots (0.3 g) of feces homogenates were weighed into Combustocones containing Combustopads for oxidation using a Packard 307 automatic sample oxidizer [PerkinElmer LAS (UK) Ltd.]. The $^{14}CO_2$ generated was collected by absorption in CarboSorb (8 ml) to which Permafluor was added [PerkinElmer LAS (UK) Ltd.]. Radioactivity from urine and feces was quantified using a liquid scintillation counter (Packard Instrument Company, Downers Grove, IL) with automatic quench correction using an external standard method (Botta et al., 1985). Prior to calculation of individual results, a background count rate was determined and subtracted from each sample count rate. The LLQ for liquid scintillation counting of urine samples or those derived from feces was 4–110 ng of darapladib.

Assay of Total Radioactivity by AMS

Aliquots (0.06 ml) of plasma from session 2 and 3 samples were analyzed by AMS and were first prepared so that the carbon within the samples was harvested and converted to graphite. This involved a two-stage process of sample combustion (oxidation) followed by graphitization (reduction) as detailed in a previously published method (Young et al., 2008).

The carbon analysis was carried out using a Costech (Valencia, CA) Elemental Combustion System (model 4010) CHNS-O Analyzer, supplied by Pelican Scientific Ltd. (Chester, UK). The AMS instrument was manufactured by National Electrostatics Corp. (NEC; Middleton, WI). The AMS instrument was a 250 kV single stage accelerator mass spectrometer, and was operated via NEC proprietary "AccelNET" software on a Linux operating system. Post acquisition data processing was performed using the NEC software "abc." Further details of the operating conditions have been previously published (Young et al., 2008).

The predose samples from session 1 were also analyzed by AMS and used as background values for samples from sessions 2 and 3 (LLQ was 0.1 darapladib nanogram equivalents per milliliter).

Darapladib and SB-553253 (M4) Quantification

Plasma concentrations of darapladib and SB-553253 were quantified using a validated analytical method based on protein precipitation with acetonitrile-ammonium formate pH 3.0, followed by HPLC–tandem mass spectrometry (MS/MS) analysis. The LLQ for darapladib and SB-553253 was 0.1 and 0.25 ng/ml, respectively, using a 50-μl aliquot of human plasma with a higher limit of quantification of 50 ng/ml for both compounds. Acetonitrile-ammonium acetate pH 3.0 (75:25, v/v) containing internal standards ([$^{13}C_6$]darapladib and [$^{13}C_6$]SB-553253, at concentrations of 2 and 5 ng/ml, respectively) was added to the plasma samples. After vortex mixing, the

Downloaded from dmd.aspetjournals.org at ASPET Journals on November 7, 2015

deproteinized samples were centrifuged for 20 minutes at approximately 6800*g*. The supernatant was analyzed using a TurboIonSpray Interface (Applied Biosciences, Ontario, Canada) and multiple reaction monitoring. The chromatography was performed using a 50 × 2.0 mm i.d. Mac Mod ACE C18 (3 μ) column (Chadds Ford, PA) and eluted at a flow rate of 0.75 ml/min. The isocratic mobile phase consisted of 30% 2 mM ammonium formate (to pH 3.0 with formic acid), 55% acetonitrile, and 15% water. The mass spectrometer used was a Sciex API-4000 triple quadrupole mass spectrometer (Applied Biosciences, Ontario, Canada) operated in positive ion mode. The temperature of the probe was maintained at 650°C with a curtain gas setting of 20 and collision gas setting of 12. Darapladib and SB-553253 were monitored by multiple reaction monitoring of 667–391 and 639–235, respectively. [$^{13}C_6$]Darapladib and [$^{13}C_6$]SB-553253 were monitored by multiple reaction monitoring of 673–397 and 645–241, respectively.

The concentrations of darapladib and SB-553253 in plasma samples were calculated from calibration plots, constructed from analysis of calibration standards prepared at known concentrations of darapladib and SB-553253 in human plasma. A weighted $1/x^2$ linear regression was applied in each case over the range 0.1–50 ng/ml for darapladib and 0.25–50 ng/ml for SB-553253.

Quality control (QC) samples, prepared at three different analyte concentrations and stored with study samples, were analyzed with each batch of samples against separately prepared calibration standards. QC samples and calibration standards were prepared using independently prepared stock solutions of darapladib and SB-553253 reference materials. For the analysis to be acceptable, no more than one-third of the QC results were to deviate from the nominal concentration by more than 15%, and at least 50% of the results from each QC concentration were to be within 15% of nominal.

Quantification and Profiling of Metabolites in Plasma, Urine, and Feces

Plasma samples taken at 3, 12, and 24 hours post dose were pooled using volumes in proportion to the time interval between individual samples to provide a single pool of plasma, representative of the pharmacokinetic area under the curve (AUC) described by these time points, for each volunteer and for each dose session (according to the method described by Hop et al., 1998). Plasma samples at 48 hours post dose were not examined due to the very low levels of radioactivity present. Representative samples of feces were pooled by total weight ratio for each volunteer, to obtain a pool containing 90% or greater of the radioactivity excreted via that route. For session 1 (i.v. dosing), this ranged between 0- to 72-hour and 0- to 240-hour collections; for session 2 (single oral dose), this ranged between 0- to 72-hour and 0- to 240-hour collections; and for session 3 (following dosing on day 11), this ranged between 0- to 96-hour and 0- to 120-hour collections. Urine was not analyzed from any session due to the very low levels of drug-related material excreted in this matrix.

All plasma sample pools were analyzed following dilution, rather than solvent extraction, prior to HPLC-AMS analysis. Each pooled plasma sample was diluted 20-fold [plasma–50 mM ammonium acetate (native pH)–10% methanol (aqueous), 1:18:1, v/v) incorporating authentic nonradiolabeled standards each at concentrations of 10 μg/ml. Each diluted plasma sample was individually fractionated at a frequency of 0.2 minutes by HPLC, a carbon carrier (2.6 μl of liquid paraffin; a source of carbon essentially containing no ^{14}C) added to each fraction, followed by conversion to graphite and analysis of radioactivity by AMS.

Fecal homogenates (approximately 2 g) were extracted by vortex mixing for 1 minute then rotary mixing for 30 minutes with 6 ml of methanol. After centrifugation, the supernatant was removed, and the process was repeated. Weighed aliquots were taken from the individual supernatants and assayed by LSC. The two extracts for each sample were subsequently combined, and the residual pellets were oxidized to determine the extent of any unextracted radioactivity. Prior to radio-HPLC analysis, aliquots (0.5 ml) of each pooled fecal extract were diluted 1:1 with 50 mM ammonium acetate (native pH). All spiked control and blank control samples were subjected to the same methods of pretreatment as detailed for test samples.

HPLC Method. The chromatographic instrument used consisted of an Agilent 1100 series binary pump and column oven (40°C) (Agilent Technologies, Santa Clara, CA), with an autosampler (CTC Analysis LC PAL; CTC Analytics AG, Zwingen, Switzerland) using a Waters Symmetry Shield RP8 column (25 cm × 4.6 mm, 5μ; Waters Corporation, Milford, MA). The mobile phase consisted of 50 mM ammonium acetate (native pH) (solvent A) and acetonitrile (solvent B) at a flow rate of 1 ml/min. A gradient was used, starting at 5% B and held for 5 minutes, then additional linear changes to 35% B by 10 minutes, to 50% by 35 minutes, and to 95% by 45 minutes, with these conditions being maintained for an additional 5 minutes.

HPLC column recoveries were determined on selected plasma samples only using AMS through comparison of precolumn injectates with total radioactivity of all fractions, and recoveries were 95% or greater in all cases.

Radio-HPLC data were captured off-line (Bruin et al., 2006) with chromatographic fractions collected using a Gilson 222XL fraction collector into 96 deep-well microtiter LUMAPLATES containing yttrium silicate solid scintillant [PerkinElmer LAS (UK) Ltd.]. Radioactivity determination was performed by scintillation counting using a Packard Topcount NXT counter [PerkinElmer LAS (UK) Ltd.]. HPLC-AMS data analysis was captured as previously described.

Metabolites of interest were isolated by preparative HPLC (Agilent 1100 autosampler, UV detector, and binary pump; Agilent Technologies) with a Zorbax SB C18 column (5 cm × 21.2 mm, 5 μ; Agilent Technologies). The mobile phase consisted of 50 mM ammonium acetate (native pH) (solvent A) and acetonitrile (solvent B) at a flow rate of 20 ml/min. A gradient was used, starting at 5% B and held for 5 minutes, then additional linear changes to 35% B by 10 minutes, to 50% by 35 minutes and held for 10 minutes, to 95% by 49.5 minutes, with these conditions being maintained for an additional 0.5 minute. Metabolite-containing fractions were taken to dryness and reconstituted in 1:1 acetonitrile:D_2O before being submitted for NMR analysis.

Structural Identification of Metabolites

Structural characterization was performed on selected samples by HPLC-mass spectrometry (MS) using triple quadrupole Quattro Ultima and hybrid quadrupole/time-of-flight Q-TOF Premier mass spectrometers (Waters MS Technologies, Manchester, UK). Electrospray ionization, in the positive ion mode, was used. The HPLC flow was split (1:3) between mass spectrometer and waste or fraction collector.

Metabolites were identified based on charged molecular ions, mass accuracy, and their collision-induced dissociation fragmentation (Oliveira and Watson, 2000). Authentic standards, when available, were used to compare chromatographic retention times (in particular for drug-related material in plasma) and fragmentation patterns. Supporting data from preclinical studies were also used in the assignment of metabolite structures. For many metabolites, confirmation of the structure has been obtained by ^1H-NMR using a Bruker DRX-600 spectrometer (Bruker, Rheinstetten, Germany) equipped with an inverse 5-mm TCI Cryo-Probe (Bruker) ($^1H/^{13}C/^{15}N$) operating at 600.40 MHz under the control of Topspin v1.3 (Bruker). ^1H-NMR spectra were acquired using a standard nuclear overhauser effect spectroscopy with presaturation (NOESYPRESAT) pulse sequence with spoil gradients for solvent suppression with time-shared double presaturation of the water and acetonitrile frequencies. In these experiments, typically 256 transients were acquired into 65,536 data points over a spectral width of 12,019 Hz (20 ppm) with an interscan delay of 2.4 seconds giving a pulse repetition time of 5 seconds. Acquisition time was extended up to 4096 transients for some metabolites to improve signal to noise. Fully characterized metabolites were designated by the letter M followed by a number; where a synthetic standard was available, a GSK (or SB) code number was assigned.

Pharmacokinetic Analysis

Actual blood collection times and the actual dose administered were used for all pharmacokinetic calculations. Analysis of plasma total radioactivity, darapladib, and SB-553253 concentration-time data was conducted using the noncompartmental models 200 and 202 of WinNonlin Professional Edition versions 4.1 and 5.2 (Pharsight Corporation, Mountain View, CA). Maximum plasma concentration (C_{max}) and time of C_{max} (T_{max}) were taken directly from the pharmacokinetic concentration-time data. Where data permit, the terminal plasma elimination rate constant (λz) was estimated from log-linear regression analysis of the terminal phase of the plasma concentration-time profile. The number of points included in the terminal phase was determined by visual inspection of the semilog plots of the plasma concentration-time profiles. The

Downloaded from dmd.aspetjournals.org at ASPET Journals on November 7, 2015

associated elimination half-life was calculated as ln2/ λz. Values of area under the curve from time zero to last measured timepoint (AUC_{0-t}) and area under the curve from time zero to infinity (AUC_{0-inf}) were calculated using linear trapezoidal method for each incremental trapezoid and the logarithmic trapezoidal method for each decremental trapezoid. After i.v. administration only, systemic clearance was calculated as dose divided by AUC_{0-inf}, and the volume of distribution was the product of systemic clearance and the mean residence time as determined by moment analysis. Concentration units for radioactivity are expressed as nanogram equivalents of darapladib/milliliter and as dpm/ml.

Due to the relatively long plasma half-life of total radioactivity and the sensitivity of the AMS analysis, many predose plasma samples contained total radioactivity concentrations that were above the LLQ (0.1 darapladib nanogram equivalents per milliliter). In many cases, the predose plasma radioactive concentrations (in dpm/ml) were >5% of the observed maximum plasma concentration in the same profile, thus correction was made for each individual plasma total radioactivity concentration-time profile to subtract, at each sampling time, the residual plasma total radioactivity concentrations resulting from the previous dose. The correction process involved initial determination of the terminal elimination rate constant (λz) of total radioactivity in the plasma profile from the previous dose period (i.e., from the plasma profile before the profile to be corrected). Thus, pharmacokinetics calculations were first performed using the original, uncorrected plasma concentration-time profiles to determine the required λz values. This initial λz value was then used to calculate a plasma concentration decay profile from the predose total radioactivity concentration (above the LLQ) for each plasma profile using the following equation:

$$C_{ti} = C_{t0} \bullet e^{(-\lambda z \bullet ti)}$$

where C_{ti} is the concentration at the i^{th} sampling time, with C_{t0} as the predose (time zero) concentration. The corrected plasma concentration-time profile was then calculated by subtracting the residual concentration at each time point (per decay curve) from the original concentration.

In Vitro Reaction Phenotyping

[^{14}C]Darapladib was incubated at 5 and 50 μM with human liver microsomes (HLMs), at 2 mg/ml microsomal protein and 37°C, in phosphate buffer (50 mM, pH 7.4). Reactions were started by the addition of prewarmed cofactor solution [a NADPH regenerating system containing 1.7 mg of NADP, 7.8 mg of glucose-6-phosphate, and 6 units of glucose-6-phosphate dehydrogenase per milliliter of 2% (w/v) sodium hydrogen carbonate] and performed in the presence and absence of the selective cytochrome P450 inhibitors: furafylline (CYP1A2), quercetin (CYP2C8), sulphaphenazole (CYP2C9), quinidine (CYP2D6), and ketoconazole (CYP3A). [^{14}C]Darapladib was also incubated with Supersomes (BD Gentest, Woburn, MA), overexpressing individual cytochrome P450 enzymes 1A2, 2C8, 2C9, 2C19, 2D6, or 3A4. All incubations were terminated by addition of acetonitrile and were centrifuged (at approximately 13,000*g*), and supernatants removed for analysis by HPLC-MS.

In Vitro Bacterial Incubations

[^{14}C]Darapladib was incubated at a concentration of 5 μM in an anaerobic environment at 37°C for 72 hours in the presence of individually cultured bacteria: *Enterococcus faecalis, Escherichia coli, Bifidus adolenscetis, Bifidobacterium longum, Lactobacillus casei, Bacteroides vulgatus*, and *Bacteroides thetaiotaomicron*. These bacteria were selected based on their known presence in the human gastrointestinal tract and their availability. After the incubations, an equal volume of acetonitrile was added to each, and the resultant samples were centrifuged (at approximately 3300*g*) and the supernatants removed for analysis by HPLC-MS.

In Vitro Bacterial Mutation Assay

Both darapladib and SB-554008 (M10) were assessed in the bacterial mutation assay (or Ames test). Genetically modified strains of *Salmonella typhimurium* (TA98, TA100, TA1535, and TA1537) and *Escherichia coli* (WP2 pKM101 and WP2 uvra pKM101) were used, in the presence and absence of an exogenous mammalian oxidative metabolism system (Aroclor or phenobarbital-induced rat liver post mitochondrial S9 fraction) using established methodologies (Ames et al., 1973; Maron and Ames, 1983; Green, 1984). The final volume of the S9 mix used was 500 μl/plate, with darapladib tested up to 5000 μg/plate and SB-554008 tested up to 500 μg/plate (concentration limited by precipitation). An additional assessment of drug-related components present under the conditions of the darapladib Ames test was conducted, using a mammalian oxidative metabolism system comparable to that described earlier, to assess the metabolism of darapladib (at concentrations of 25 and 100 μM).

Results

Demographic, Safety, and Tolerability Data

Eight healthy male subjects (four white, three African American, one mixed race) were entered into the study, and seven subjects completed all three sessions with one individual excluded due to lack of compliance with sample collection during session 2. Following all three sessions, the compound was regarded as generally safe and well tolerated, and any adverse events reported were typically mild in nature (e.g., diarrhea, flatulence, dizziness, etc.).

Mass Balance of Total Radioactivity

The actual doses of i.v. and oral [^{14}C]darapladib administered ranged from 6.62 to 7.91 mg (41.4– 49.5 μCi, session 1), 75.3 to 78.8 mg (18.6–19.9 μCi, session 2), and 79.2 to 79.4 mg (19.2–20.0 μCi, session 3), respectively. Mean cumulative excretion balance data obtained from up to eight healthy male subjects following doses of [^{14}C]darapladib (i.v. and oral routes) are detailed in Table 1.

Following both i.v. and oral administration, total radioactivity was eliminated almost exclusively in the feces, accounting for 85% of the dose post i.v. infusion and 93%–95% following oral administration. Total radioactivity recovered in urine was negligible (<1%) following all dosing regimens over the respective collection periods (up to 216 or 504 hours post dose). Mean recoveries of approximately 90%–94% of the radioactive dose were reached by 120 hours post oral administration, with the remaining radioactivity recovered up to 216 or 264 hours post dose. Slower elimination of total radioactivity was observed post i.v. administration, with only approximately 62% recovered by 120 hours post dose and collections continuing to 504 hours, recovering 86% of the dose.

Pharmacokinetics

A summary of the plasma pharmacokinetic parameters for darapladib, SB-553253 (M4), and total radioactivity after a single i.v. dose, a single oral dose, and repeat dose oral administration is presented in Table 2. Due to the relatively long half-life of total radioactivity, many predose plasma samples in sessions 2 and 3 still contained levels of radioactivity indicating that a small amount of circulating radioactivity remained after the i.v. dose. Subtraction of the residual plasma radioactivity was performed (as described in the *Materials and Methods* section), and resulting parameters are summarized in Table 2. Mean (± S.D.) plasma concentrations of darapladib, SB-553253, and total radioactivity are shown in Fig. 2. After i.v. administration, maximum darapladib concentrations were achieved, as expected, at the end of the 3-hour infusion, with volume of distribution estimated at >800 l and low plasma clearance of 17 l/h. After i.v. and single oral dose administration, the terminal half-life of darapladib was similar, and relatively long at ~40 hours. After single- and repeat-dose oral administrations, darapladib solutions were absorbed slowly, with a median T_{max} of 5 hours (single dose) and 6 hours (repeat dose). The absolute bioavailability of darapladib solution was 12%, on average, comparing dose normalized exposures following single-dose i.v. and single-dose oral administration. Due to the study design, no estimate of oral bioavailability of the tablet was conducted within this study. The mean area under the curve from time zero to next dosing

Downloaded from dmd.aspetjournals.org at ASPET Journals on November 7, 2015

TABLE 1

Mean cumulative total radioactivity excreted in urine and feces (percentage of dose) after i.v. and oral administration of [^{14}C]darapladib to healthy volunteers

All urine and fecal radioactivity was determined using LSC

Elapsed Time from Dose (h)	Intravenous				Single Oral				Repeat Dose Oral			
	n	Urine	Feces	Total	*n*[a]	Urine	Feces	Total	*n*[b]	Urine	Feces	Total
Predose		0.00	0.00	0.00								
0–24	8	0.4	8.0	8.4	8	0.1	11.7	11.8	7	0.1	7.7	7.8
0–48	8	0.5	21.9	22.4	8	0.2	37.1	37.3	7	0.1	51.7	51.8
0–72	8	0.6	37.5	38.1	8	0.2	73.8	74.0	7	0.1	84.2	84.3
0–96	8	0.7	57.8	58.5	8	0.2	84.8	85.0	7	0.1	86.9	87.0
0–120	8	0.7	61.5	62.2	8	0.2	90.1	90.3	7	0.1	94.3	94.4
0–144	8	0.8	69.1	69.9	8	0.2	92.4	92.6	7	0.1	94.9	95.0
0–168	8	0.8	74.2	75.0	8	0.2	93.0	93.2	7	0.1	95.0	95.1
0–192	8	0.8	74.8	75.6	8	0.2	93.2	93.4	7	0.1	95.0	95.1
0–216	8	0.8	77.9	78.7	8	0.2	93.2	93.4	7	0.1	95.1	95.2
0–240	8	0.9	79.7	80.6	8	0.2	93.2	93.4	7	0.1	95.1	95.2
0–504[c]	8	0.9	85.5	86.4	8	0.2	93.2	93.4	7	0.1	95.2	95.3

[a]Fecal data from subject 101 have been excluded from the calculation of fecal mean due to low balance recovery during single oral dose regimen.
[b]Subject 101 excluded from this regimen due to low balance recovery during single oral administration regimen.
[c]Intravenous group samples collected for 504 hours, both single and repeat oral dose final sampling point was 264 hours post (radioactive) dose.

interval [AUC(0-τ)] following repeat oral dosing was approximately 50% greater than AUC(0-τ) following a single oral dose, indicating accumulation; however, this degree of accumulation was less than expected from single-dose exposure data [approximately 270% accumulation was predicted from AUC(0-inf)/AUC(0-τ) following single-dose oral data]. This less than expected accumulation was consistent with results observed from previous pharmacokinetic studies in healthy volunteers (data on file).

The metabolite SB-553253 was rapidly formed following both i.v. and oral administration of darapladib, with a T_{max} similar to that of the parent compound, although plasma concentrations of SB-553253 were much lower, with exposure of SB-553253 (as estimated by the AUC) being 0.2%, 1%, and 5% of parent darapladib following single i.v., single oral, and repeat oral administration, respectively.

$AUC_{(0\text{-inf})}$ and half-life parameters for total radioactivity were not reported, as the sampling duration of 96 hours was too short relative to the approximated half-life of radioactivity to adequately describe the terminal elimination phase of plasma total radioactivity resulting in a large extrapolation area. Pharmacokinetic parameters for total radioactivity (nanogram equivalents) following repeat oral dosing could not be generated due to the unknown dilution effect of nonradiolabeled darapladib from dosing on days 1–10.

Metabolite Profiles

Plasma. Representative reconstructed radiochromatogram profiles of individual time-adjusted pooled plasma samples from each dose regimen are shown in Fig. 3. Quantification of drug-related material in plasma from each dose regimen is summarized in Table 3.

Following i.v. infusion of [^{14}C]darapladib, the predominant component in plasma across all volunteers was unchanged darapladib, which represented a mean of 89% of plasma radioactivity. The only other radiolabeled component detected was SB-553253 (M4), which accounted for approximately 1% of plasma radioactivity.

Following single oral administration of [^{14}C]darapladib, unchanged darapladib was again the principal radiolabeled component in plasma, representing a mean of 75% of plasma radioactivity. Circulating

TABLE 2

Geometric mean coefficient of variation (%) [CV%] pharmacokinetic parameters of total radioactivity, darapladib, and SB-553253 in plasma after i.v. and oral administration of [^{14}C]darapladib to healthy volunteers

Total radioactivity post i.v. administration was determined using LSC; total radioactivity post oral dosing was determined using AMS.

Parameter	Single-Dose Intravenous (*n* = 8)			Single-Dose Oral (*n* = 8)			Repeat-Dose Oral (*n* = 7)		
	Total Radioactivity	Darapladib	SB-553253	Total Radioactivity[a]	Darapladib	SB-553253	Total Radioactivity[a,b]	Darapladib	SB-553253
$AUC_{(0\text{-inf})}$ (ng.h/ml)		491 (17.7)			603 (18.8)				
$AUC_{(0\text{-t})}$[c] (ng.h/ml)	567 (16.1)	405 (17.2)	0.614[d] (9.22)	1025 (20.0)	510 (17.4)	6.24 (31.4)			
$AUC_{(0\text{-}\tau)}$ (ng.h/ml)		200 (13.8)			222 (14.2)			335 (18.5)	16.8 (19.1)
C_{max}[e] (ng/ml)	34.9 (20.6)	25.3 (12.4)	0.296 (11.0)	25.2 (17.9)	15.4 (16.7)	1.37 (14.9)		22.2 (17.4)	1.76 (33.2)
T_{max} (h)[f]	2.98 (2 - 5)	2.97 (2–3.53)	2.98 (2–3.5)	6 (3–6.02)	5.04 (4–6.02)	5.04 (3.02–6.02)	6 (4–6.03)	6 (2 – 6.03)	6 (3–6.03)
$T_{1/2}$ (h)		40.9 (8.74)			40.4 (6.8)				
CL (l/h)	11.2 (17.1)	17.3 (16.3)							
Vss (l)	632.3 (19.1)	833 (17.7)							

CL, systemic clearance; $T_{1/2}$, elimination half-life; Vss, volume of distribution at steady-state.
[a]AUC and C_{max} corrected for predose concentration (see detail in *Materials and Methods* section).
[b]Relative mean radioactive exposure (i.e., dpm only) was 320 dpm.h/ml on day 11 (compared with 420 dpm.h/ml on day 1).
[c]Parameter units for total radioactivity are ng equiv.h/ml for all regimens.
[d]*n* = 2.
[e]Parameter units for total radioactivity are ng equiv./ml for all regimens.
[f]Median (range).

Downloaded from dmd.aspetjournals.org at ASPET Journals on November 7, 2015

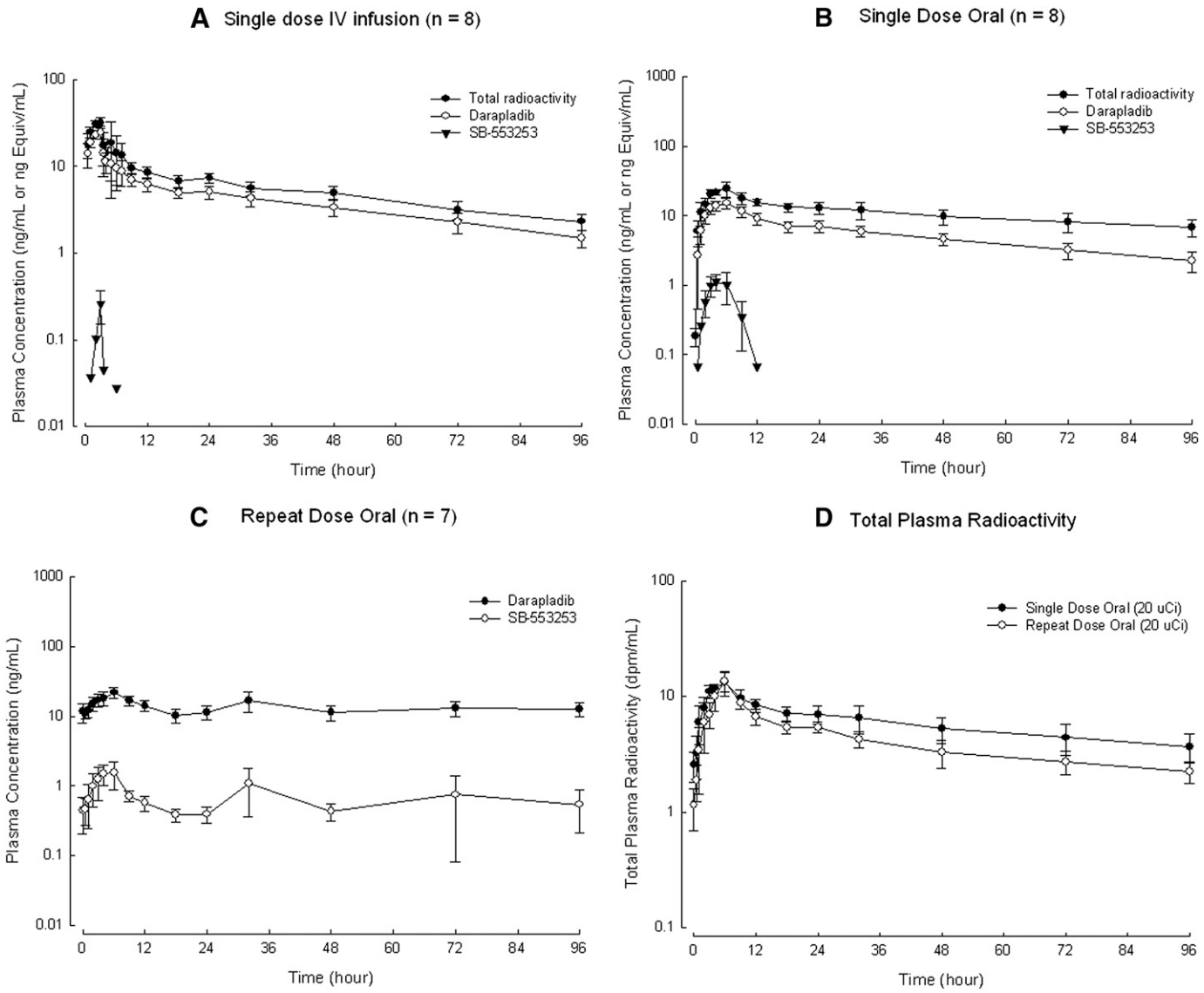

Fig. 2. Mean (± S.D.) concentrations of total radioactivity, darapladib, and SB-553253 following single i.v. (A), single oral (B), and repeat dose oral administration (C) of [^{14}C]darapladib to human volunteers, and comparative total radioactivity profiles following single and repeat oral dose of [^{14}C]darapladib to human volunteers (D).

metabolites were more notable and included: M3 (SB-823094), resulting from hydroxylation of the cyclopenta pyrimidinone moiety; SB-553253; M10 (SB-554008), a uracil derivative formed following removal of the fluorobenzylthiol group; and a hydroxylated N-desethyl metabolite (M16), each of which accounted for approximately 4%–5% of plasma radioactivity. Any remaining metabolites each accounted for <1% of plasma radioactivity.

The principal radiolabeled component in plasma samples obtained following repeat oral administration was unchanged darapladib, which represented a mean of 64% of plasma radioactivity. Circulating metabolites observed included SB-823094 (M3), SB-553253, and SB-554008 (M10), which individually accounted for means of 4%–6% of plasma radioactivity. Other metabolites were observed, each accounting for 1% or less of the plasma radioactivity. Proposed structures and supporting spectral data are shown in Table 4.

Urine. Negligible amounts (1% or less of the dose) were recovered in urine across all three regimens, and therefore this matrix was not examined further.

Feces. Radio-HPLC analyses of fecal extracts from i.v. and oral administration of [^{14}C]darapladib were similar. Representative radiochromatograms of pooled fecal extracts are shown in Fig. 4. Quantification of drug-related material in feces from each dose regimen is summarized in Table 3.

For the three dose regimens, mean recovery of radioactive material from feces following solvent extraction ranged from 96% to 99%. Radio-HPLC analysis of fecal extracts from all dose regimens revealed the predominant radiolabeled component was unchanged darapladib, although several other drug-related peaks were also evident. Following i.v. administration, unchanged darapladib represented a mean of approximately 55% of the fecal radioactivity (43% of the dose). The predominant metabolites observed across all subjects were SB-553253 (M4) and SB-823094 (M3), accounting for means of 23% and 11% of the fecal radioactivity (18% and 9% of the administered dose, respectively). Following both single- and repeat-dose oral administration, unchanged darapladib accounted for a mean of 53% of the radioactive dose administered. As for i.v. administration, the predominant metabolites post oral dosing were SB-553253 and SB-823094, accounting for

Downloaded from dmd.aspetjournals.org at ASPET Journals on November 7, 2015

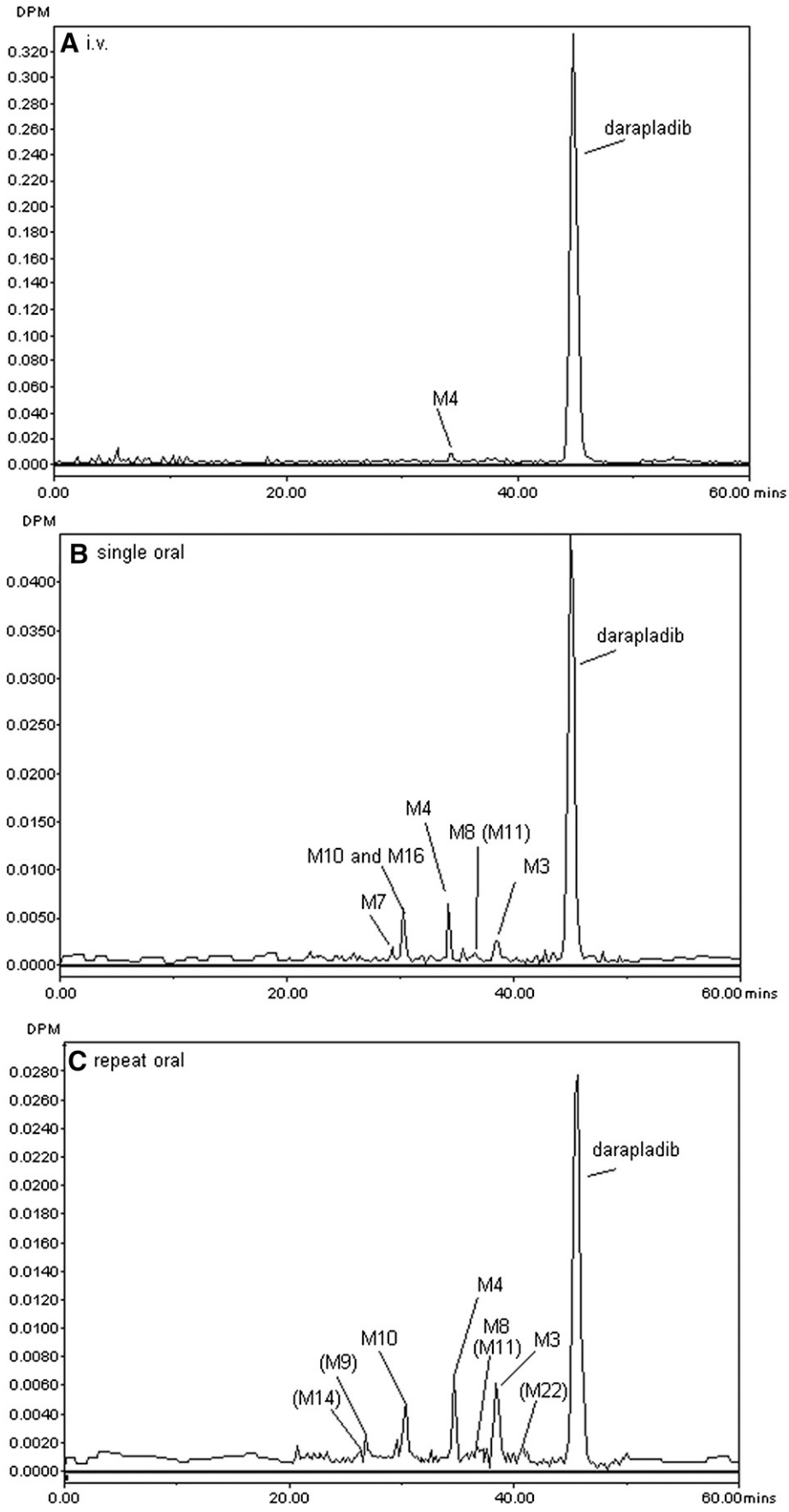

Fig. 3. Representative radiochromatograms of human plasma following single i.v. (A), single oral (B), and repeat dose oral administration (C) of [^{14}C]darapladib to human volunteers.

Downloaded from dmd.aspetjournals.org at ASPET Journals on November 7, 2015

TABLE 3

Mean percentage of radioactivity of darapladib and its metabolites in human plasma and feces after i.v. and oral administration of [^{14}C]darapladib to healthy volunteers

Several metabolites, including M2, M6, M12, M21, and M22, observed in fecal extracts were detected by mass spectrometry only. Plasma profiles were determined using HPLC AMS, whereas fecal profiles used off-line radio-HPLC.

Peak identification	Mean Percentage Plasma Radioactivity			Mean % Matrix Radioactivity (mean % dose)		
	Plasma			Feces		
	i.v.	Single Oral	Repeat Oral[e]	i.v.	Single Oral	Repeat Oral[e]
Darapladib	89.2	75.3	64.2	54.5 (42.8)	57.5 (52.7)	55.8 (52.7)
M3 (SB-823094)	ND	4.3	4.8	11.0 (8.6)	12.2 (11.1)	11.5 (10.8)
SB-553253 (M4)	1.2	4.1	4.0	23.3 (18.2)	20.4 (18.6)	18.5 (17.2)
SB-735258 (M7)	ND	0.6	ND	1.3 (1.0)	1.2 (1.1)	1.2 (1.1)
M8	ND	ND	ND	ND	2.1 (1.9)	1.8[b] (1.7)
M9	ND	ND	0.7	ND	BLQ	0.6[a] (0.5)
GSK219147 (M11) or M8	ND	0.6	1.0	2.1 (1.6)	ND	1.8[b] (1.7)
SB-554008 (M10)	ND	4.5[c]	5.7	5.0[d] (3.9)	4.2[d] (3.9)	4.3[d] (4.0)
M14	ND	ND	0.4	BLQ	BLQ	0.6[a] (0.5)
M16	ND	4.5[c]	ND	5.0[d] (3.9)	4.2[d] (3.9)	4.3[d] (4.0)
M19	ND	ND	ND	5.0[d] (3.9)	4.2[d] (3.9)	4.3[d] (4.0)

BLQ, below limit of quantification; ND, not detected.
[a]Metabolites M9 and M14 coelute.
[b]Metabolites M8 and M11 coelute.
[c]Metabolites M10 and M16 coelute.
[d]Metabolites M10, M16, and M19 coelute (on a few occasions, some of these peaks were resolved but have been quantified as a coeluting peak for consistency).
[e]The repeat oral dose results–% dose results refers to only the radioactive dose administered on day 11.

approximately 18% and 11% of the administered radioactive dose. A number of minor metabolites were also observed across the dose regimens representing <4% of the dose and included SB-735258 (M7), SB-554008 (M10), M16 (hydroxylated SB-553253), and M19 (N-oxide). Proposed structures and supporting spectral data are shown in Table 4.

In Vitro Incubations

Reaction Phenotyping. Incubations of [^{14}C]darapladib with HLMs showed NADPH-dependent metabolism to several metabolites, including SB-553253 (M4) and SB-823094 (M3). Ketoconazole, a CYP3A inhibitor, caused marked inhibition of darapladib metabolism, whereas other cytochrome P450 inhibitors had no or minimal effects. Metabolism of darapladib with expressed enzymes showed extensive metabolism (up to 85% of parent metabolized) with CYP3A4, with minor turnover in other expression enzymes, most notably CYP2C8.

Bacterial Incubations. Incubations of darapladib with various human gut bacteria under anaerobic conditions produced no evidence of metabolism with any of the strains used.

Ames Bacterial Mutation Assay. Darapladib did not induce point (gene) mutation in *Salmonella typhimurium* (TA98, TA100, TA1535, TA1537), either in the presence or absence of metabolic activation, when tested up to 200 μg/plate (as limited by toxicity). Darapladib did not induce point (gene) mutation in *Escherichia coli* (WP2 pKM101 and WP2 *uvra* pKM101), either in the presence or absence of metabolic activation, when tested up to 5000 μg/plate. Similarly, SB-554008 (M10) showed no increases in the numbers of revertant colonies observed at any of the concentrations tested (up to 500 μg/plate), in either the presence or absence of metabolic activation. The metabolite SB-823094 was identified under the incubation and metabolic activation conditions of the Ames assay of darapladib and was not genotoxic.

Discussion

Following i.v. and oral administration of [^{14}C]darapladib to humans, total radioactivity was eliminated almost exclusively in the feces (86%–95% of the dose). Recovery of the dose was considered complete (Roffey et al., 2007) across all regimens (86%–95% of the administered dose) but elimination was somewhat protracted, especially following i.v. administration. Following oral dosing, between 90% and 94% of the dose had been recovered by 120 hours post dose, whereas recovery of the i.v. dose was only around 62% at this time, with notable amounts of dose continuing to be eliminated slowly thereafter. The volume of distribution in humans was very high (>800 l), suggesting notable tissue distribution. With a pK_a of 8.4 (tertiary amine) and a log $P > 3.4$, darapladib is a cationic amphiphilic drug, a common feature of which is sequestration in lysosomes by a mechanism called pH partitioning (Funk and Krise, 2012). As a result, cationic amphiphilic drugs often have a large volume of distribution, protracted elimination, and inhibit lysosomal lipid metabolism resulting in phospholipidosis (Reasor and Kacew, 2001), which was observed in rats and mice following dosing of darapladib at toxicological doses. It is therefore considered that the slower elimination of a proportion of the radioactive dose post i.v. dosing may represent more widespread tissue exposure to darapladib via direct administration into the blood, when compared with oral dosing where a large proportion of the dose is either unabsorbed or removed via first-pass metabolism or elimination of the parent compound prior to entering the systemic bloodstream (consistent with the low absolute bioavailability of 12%). The plasma elimination half-lives of darapladib post i.v. and oral dosing were consistent with prolonged elimination, each around 40 hours.

The principal radiolabeled component observed in human plasma following both i.v. and oral solution dosing of radiolabeled compound was unchanged darapladib. The only metabolite observed in plasma following i.v. dosing was SB-553253 (M4), albeit at very low levels (1% of plasma radioactivity). Following oral administration, circulating metabolites were more evident, including SB-823094 (M3), SB-553253, and SB-554008 (M10), each of which were present at mean concentrations of around 5% of plasma radioactivity, and at low absolute concentrations of less than 2 nanogram equivalents/milliliter. The fact that metabolites are more prevalent in the circulation after oral than after i.v. administration is indicative of first-pass metabolism, and is consistent with the notable difference (50%–60%) in plasma

Downloaded from dmd.aspetjournals.org at ASPET Journals on November 7, 2015

TABLE 4

Structural information on darapladib and its notable metabolites following administration of [^{14}C]darapladib to human volunteers

Matrix	Proposed Structure	$[M+H]^+$ Ion and MS-MS Product Ions	^{1}H-NMR (600 Mhz, 1:1 ACN:D_2O) (Where Available)
PL,FE	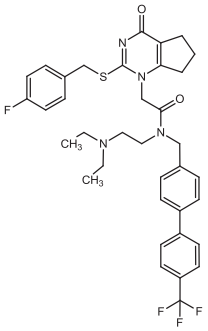 Darapladib	Accurate mass $[M+H]^+$ Observed: 667.2728 Calculated: 667.2730 594, 486, 391, 351, 317, 235, 109	7.75 (d, 2H), 7.67 (d, 2H), 7.53 (d, 2H), 7.38 (d, 2H), 7.30 (dd, 2H), 6.90 (t, 2H), 4.79 (s, 2H), 4.65 (s, 2H), 4.30 (s, 2H), 3.67 (brt, 2H), 2.91 (t, 2H), 2.84 (q, 4H), 2.77 (t, 2H), 2.68 (t, 2H), 2.05 (m, 2H), 1.07 (t, 6H) Mixture of rotamers, major rotamer assigned
FE[1]	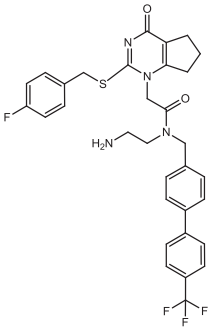 M2	Accurate mass $[M+H]^+$ Observed: 611.2112 Calculated: 611.2104	No NMR
PL[1],FE	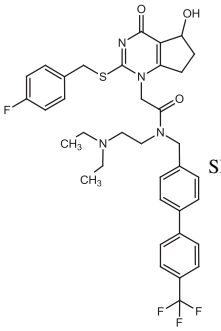 SB-823094 (M3)	Accurate mass $[M+H]^+$ Observed: 683.2681 Calculated: 683.2679 610, 557, 502, 484, 391, 351, 333, 315, 235, 207, 109	7.83 (d, 2H), 7.81 (d, 2H), 7.62 (d, 2H), 7.49 (d, 2H), 7.40 (dd, 2H), 7.08 (t, 2H), 5.18 (brm, 1H), 5.08 (s, 2H), 4.69 (s, 2H), 4.48 (s, 2H), 3.35 (t, 2H), 2.91 (ddd, 1H), 2.68 (ddd, 1H), 2.60 (t, 2H), 2.53 (q, 4H), 2.51 (m, 1H), 2.40 (m, 1H), 0.99 (t, 6H) Mixture of rotamers, major rotamer assigned
PL,FE	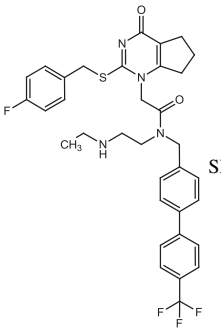 SB-553253 (M4)	Accurate mass $[M+H]^+$ Observed: 639.2408 Calculated: 639.2417 486, 431, 363, 323, 317, 235, 109	7.78 (d, 2H), 7.67 (d, 2H), 7.50 (d, 2H), 7.37 (d, 2H), 7.27 (dd, 2H), 6.88 (t, 2H), 4.67 (s, 2H), 4.59 (s, 2H), 4.27 (s, 2H), 3.77 (brt, 2H), 3.12 (t, 2H), 2.96 (q, 2H), 2.81 (t, 2H), 2.70 (t, 2H), 2.08 (m, 2H), 1.16 (t, 3H) Mixture of rotamers, major rotamer assigned
FE[1]	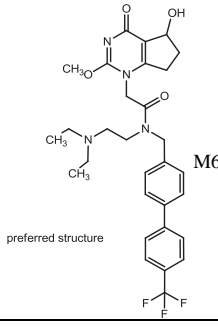 M6 preferred structure	Accurate mass $[M+H]^+$ Observed: 573.2689 Calculated: 573.2692 391, 235, 205	No NMR

(*continued*)

Downloaded from dmd.aspetjournals.org at ASPET Journals on November 7, 2015

TABLE 4—*Continued*

Matrix	Proposed Structure	[M+H]$^+$ Ion and MS-MS Product Ions	^{1}H-NMR (600 Mhz, 1:1 ACN:D_2O) (Where Available)
PL[1],FE	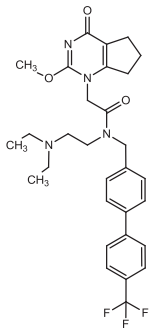 SB-735258 (M7)	Accurate mass [M+H]$^+$ Observed: 557.2751 Calculated: 557.2740 484, 391, 361, 351, 347, 235, 207, 127	7.85 (d, 2H), 7.79 (d, 2H), 7.79, (d, 2H), 7.41 (d, 2H), 4.78 (s, 2H), 4.70, (s, 2H), 3.91 (s, 3H), 2.76 (t, 2H), 2.68 (t, 2H), 1.05 (t, 6H) Some resonances obscured
PL[1],FE[1]	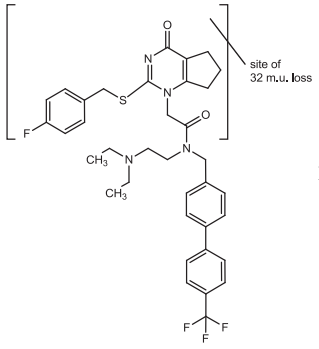 M8	635 [M+H]$^+$ 562, 235	No NMR
FE[1]	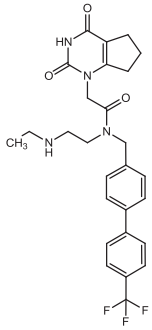 M9	Accurate mass [M+H]$^+$ Observed: 515.2263 Calculated: 515.2270	No NMR
PL,FE	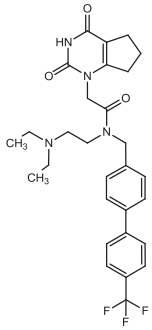 SB-554008 (M10)	Accurate mass [M+H]$^+$ Observed: 543.2554 Calculated: 543.2583 470, 235	7.84 (d, 2H), 7.78 (d, 2H), 7.75, (d, 2H), 7.45 (d, 2H), 4.68 (s, 2H), 4.65, (s, 2H), 3.52 (t, 2H), 2.62 (t, 4H), 0.99 (t, 6H) Some resonances obscured
PL,FE	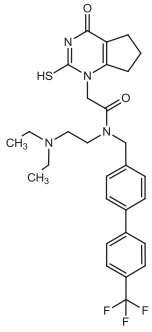 GSK219147 (M11)	Accurate mass [M+H]$^+$ Observed: 559.2349 Calculated: 559.2355 486, 351, 235, 209	7.84 (d, 2H), 7.79 (d, 2H), 7.76, (d, 2H), 7.56 (d, 2H) remaining resonances obscured

(*continued*)

Downloaded from dmd.aspetjournals.org at ASPET Journals on November 7, 2015

TABLE 4—*Continued*

Matrix	Proposed Structure	$[M+H]^+$ Ion and MS-MS Product Ions	^{1}H-NMR (600 Mhz, 1:1 ACN:D_2O) (Where Available)
FE[1]	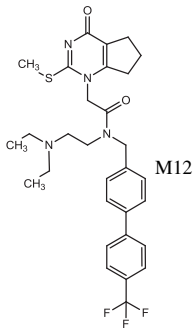 M12	Accurate mass $[M+H]^+$ Observed: 573..2511 Calculated: 573.2511 391, 309, 223, 209	No NMR
PL[1], FE	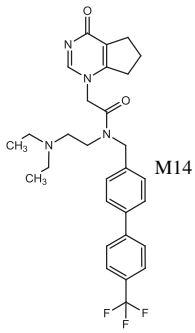 M14	Accurate mass $[M+H]^+$ Observed: 527.2634 Calculated: 527.2634	8.12 (s, 1H), 7.85 (d, 2H), 7.79 (d, 2H), 7.78 (d, 2H), 7.44 (d, 2H), 4.96 (s, 2H), 4.71, (s, 2H) remaining resonances obscured
PL[1],FE	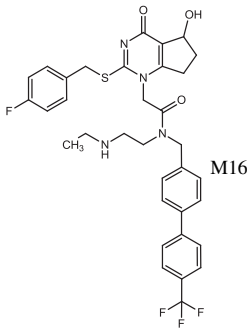 M16	Accurate mass $[M+H]^+$ Observed: 655.2363 Calculated: 655.2366 637, 529, 484, 363, 323, 315, 235, 207	7.79 (d, 2H), 7.67 (d, 2H), 7.51 (d, 2H), 7.37 (d, 2H), 7.29 (dd, 2H), 6.90 (t, 2H), 5.16 (dd, 1H), 4.80 (s, 2H), 4.71 (s, 2H) Mixture of rotamers, major rotamer assigned, remaining signals obscured
FE	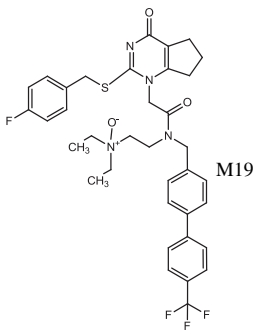 M19	Accurate mass $[M+H]^+$ Observed: 683.2712 Calculated: 683.2679 594	7.78 (d, 2H), 7.68 (d, 2H), 7.53 (d, 2H), 7.40 (d, 2H), 7.29 (dd, 2H), 6.89 (t, 2H), 4.79 (s, 2H), 4.65 (s, 2H), 3.21 (t, 2H) Mixture of rotamers, major rotamer assigned, remaining signals obscured
FE[1]	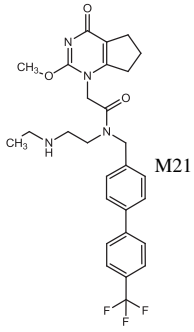 M21	Accurate mass $[M+H]^+$ Observed: 529.2424 Calculated: 529.2427	No NMR

(*continued*)

Downloaded from dmd.aspetjournals.org at ASPET Journals on November 7, 2015

TABLE 4—*Continued*

Matrix	Proposed Structure	[M+H]$^+$ Ion and MS-MS Product Ions	^{1}H-NMR (600 Mhz, 1:1 ACN:D_2O) (Where Available)
FE[1]	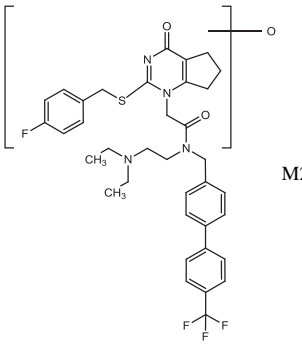 M22	Accurate mass [M+H]$^+$ Observed: 683.2683 Calculated: 683.2679 391,351,333,235	No NMR

ACN, acetonitrile; FE, seen in feces; PL, seen in plasma; PL[1]/FE[1], only seen in oral matrix.

AUC and C_{max} for total radioactivity compared with unchanged darapladib. Incubations with HLMs showed that CYP3A is the main enzyme responsible for darapladib metabolism, which is consistent with intestinal and/or hepatic first-pass metabolism. Notably, SB-554008 was not detected in any in vitro incubations using HLMs, but is the major acid degradant of darapladib (e.g., dosed in solution) in vivo. Moreover, the clinical formulation of darapladib has been developed as an enteric coated tablet to minimize acid hydrolysis in the stomach to SB-554008. Nonetheless, because of the nature and objectives of this study, and the technical issues of developing a protected radiolabeled formulation, [^{14}C]darapladib was formulated as a solution, and administered with food to minimize any acid degradation. Since SB-554008 was seen in plasma following a single oral dose but not post i.v. administration, it is inferred that a proportion of SB-554008 is being generated presystemically. Bacterial incubations with darapladib showed negligible metabolism, and therefore SB-554008 observed post oral dosing of [^{14}C]darapladib solution is likely the result of acid hydrolysis in the stomach and is greater than would be expected following administration of an enterically coated darapladib tablet.

Whereas SB-553253 (M4) was quantified in plasma in preclinical toxicology and clinical studies, SB-554008 had not been previously observed in preclinical species in either plasma or excreta, and SB-823094 (M3) had not been previously quantified in plasma, preclinically or clinically. Therefore, SB-554008 (M10) was potentially human specific and SB-823094 potentially disproportionate (i.e., present at higher plasma concentrations in humans than in preclinical species), albeit present at very low levels in plasma. Both metabolites were therefore evaluated for their genotoxicity potential prior to entering the large phase III program [as recommended in the FDA Guidance for Industry; Safety Testing of Drug Metabolites (2008)]. The presence of SB-823094 was demonstrated under the conditions of the darapladib Ames test, but SB-554008 was absent and required direct testing, which proved negative. Safety margins for general toxicity were also established for both metabolites prior to the start of phase III. Specific HPLC-MS/MS assays were developed, and the exposures of SB-554008 and SB-823094 were determined in humans post repeat dosing of the enteric clinical formulation, and in rats and dogs (at no adverse effect dose levels), with preclinical exposure margins for SB-823094 being established in both rats (~1.5-fold) and dogs (~14-fold). Given the chiral nature of SB-823094, the formation of each enantiomer was also confirmed, with no marked differences between rats, dogs, and humans. Safety margins for SB-554008 were attained in the dog only (~1.5-fold), whereas in the rat this metabolite was present at lower concentrations than in humans, which is consistent with the physiologic pH of the stomach in rats being higher than dogs in both fed and fasted states (McConnell et al., 2008; Sagawa et al., 2009). Interestingly, SB-554008 was not observed at all systemically after a single oral dose of the enteric coated tablet in humans (LLQ 0.1 ng/ml), whereas after a single oral solution dose of [^{14}C]darapladib, the mean individual pooled plasma concentration of SB-554008 was up to 4.5 nanogram equivalents/milliliter, clearly demonstrating that SB-554008 concentrations are substantially greater after oral dosing of solution than an enteric coated tablet, which protects darapladib from the low pH environment in the stomach. SB-554008 is detectable at low concentrations after dosing to steady-state, which is ascribed to the fact that, even at neutral pH, there is a very slow rate of hydrolysis of darapladib.

The pharmacological activity of SB-823094 was similar to that of darapladib and SB-553253, whereas that of SB-554008 was about 100-fold less. Since exposure to the metabolites in humans at steady state was much lower than darapladib (means of ≤5% of parent based on AUC), these metabolites are not expected to contribute significantly to the pharmacological activity. Based on the genotoxicity evaluation, general safety cover, and pharmacological activity, no further metabolite work was conducted.

Darapladib was eliminated both by metabolism and as unchanged drug, via the feces. The radiolabeled metabolite profiles in fecal extracts from all three dosing regimens were very similar, qualitatively and quantitatively, and were independent of the route and duration of administration. Darapladib was the primary component in feces, representing 43%–53% of the dose, whereas SB-823094 and SB-553253 accounted for 9%–19% of the dose. Several minor metabolites, each accounting for less than 4% of the dose, were also observed. Based on the structure of the metabolites, a simplified metabolic scheme is shown in Fig. 5.

Minimal absorption can be estimated in humans from urinary excretion post oral dosing or, where data exist, by comparing urinary excretion following i.v. and oral administrations of a radiolabeled drug (Gibaldi and Perrier, 1982). However, due to the negligible amounts of radioactive drug-related material in urine following [^{14}C]darapladib administration, neither approach was undertaken. Alternatively, absorption can be estimated from oral fecal metabolite profiles, assuming unchanged darapladib observed in these profiles (53% of the dose) is unabsorbed, and given the negligible degradation of darapladib by gastrointestinal microbiota. Possible acid degradation of darapladib to SB-554008 (up

Downloaded from dmd.aspetjournals.org at ASPET Journals on November 7, 2015

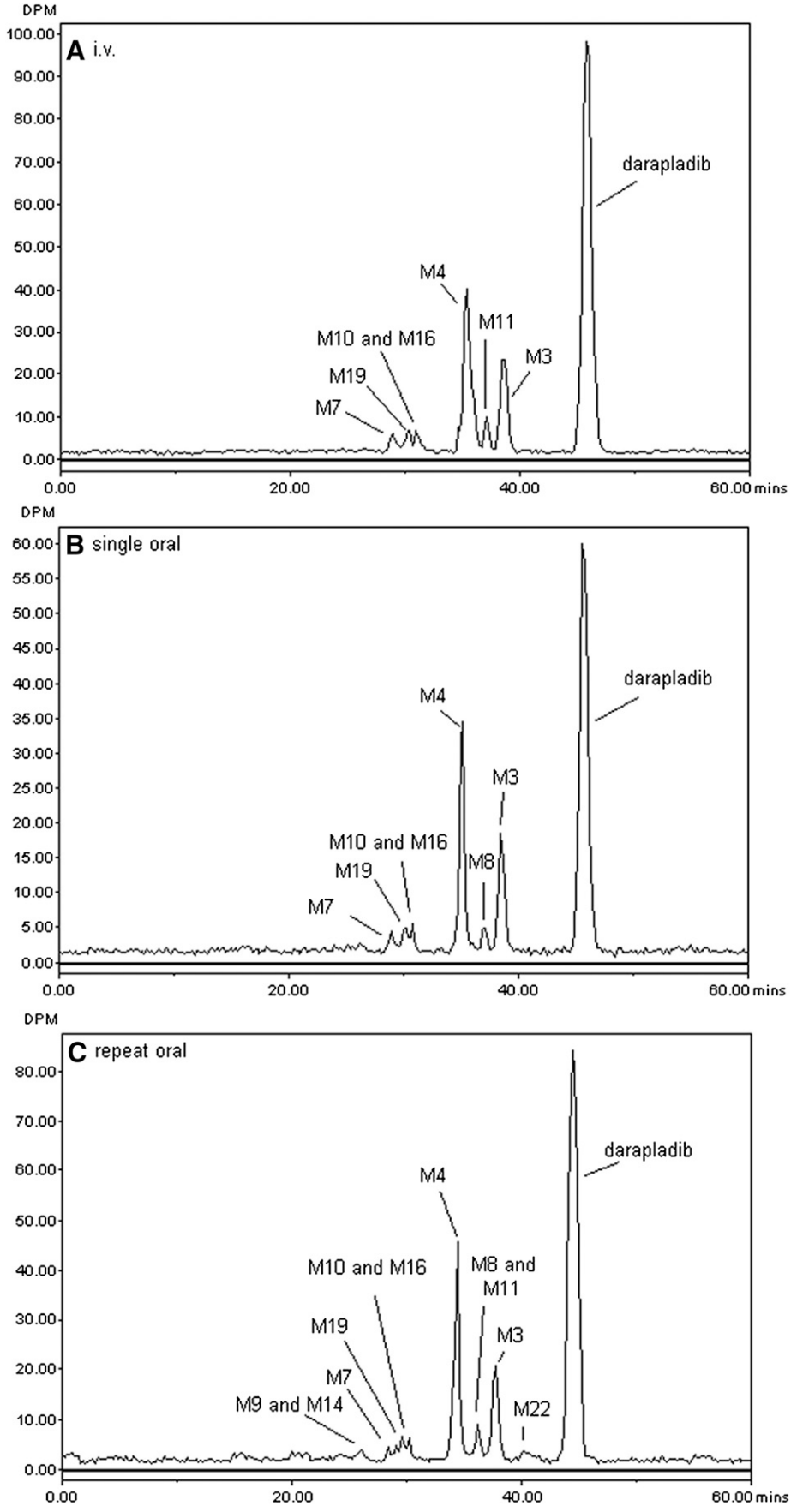

Fig. 4. Representative radiochromatograms of human fecal extracts following single i.v. (A), single oral (B), and repeat dose oral administration (C) of [^{14}C]darapladib to human volunteers.

Downloaded from dmd.aspetjournals.org at ASPET Journals on November 7, 2015

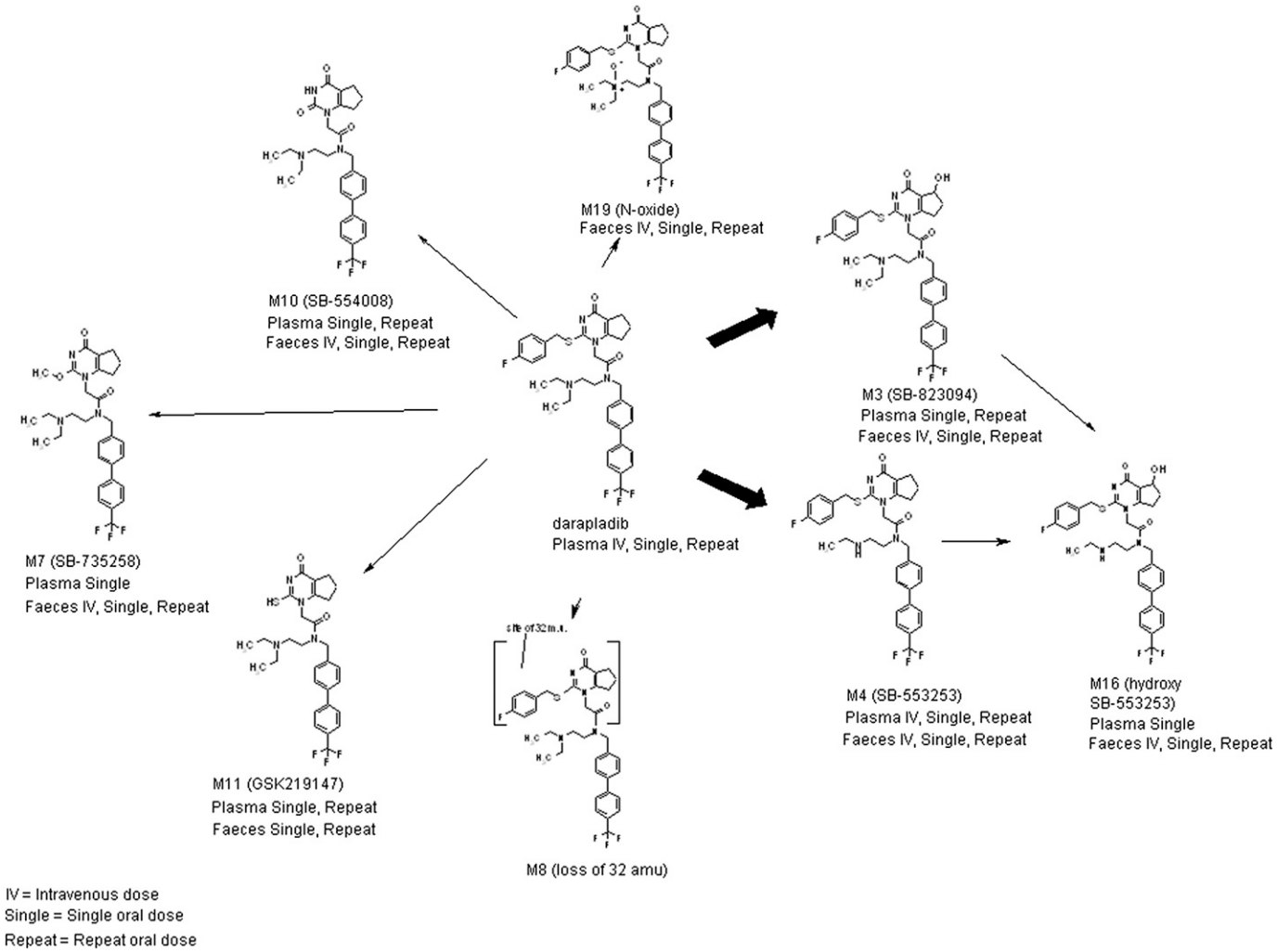

Fig. 5. Simplified metabolic scheme for darapladib in humans.

to 4% of the dose) was also considered, and together suggest absorption of darapladib is at least 43% of the dose. Moreover, i.v. fecal profiles showed a large proportion of the dose (43%) is secreted unchanged (via bile and/or direct gut) into feces, and therefore, oral absorption may well be substantially higher than the lower estimate of 43%. Absorption is defined as crossing the apical membrane of the enterocytes, and as darapladib is both a CYP3A and P-glycoprotein (PgP) substrate (as are metabolites SB-823094 and SB-553253), it is postulated that the oral fecal profiles observed in humans reflect metabolism and subsequent elimination at the level of the enterocyte (Hochman et al., 2000; Paine et al., 2006). Previous lower estimates of absorption from rats and dogs (based on urinary and biliary excretion of drug-related material) do not allow for this gut wall elimination, although a re-examination of oral fecal data in dogs suggested a higher absorption of at least 41%; however, this information is not available for rats. The similar levels of SB-823094 and SB-553253 in feces following oral and i.v. dosing are thought to reflect the varying contributions of hepatic and intestinal CYP3A to the overall metabolic clearance of darapladib, depending on the route of administration.

The systemic exposure to radioactivity following a single oral radioactive dose during steady-state dosing was about 30% lower than that following the first single oral radioactive dose. This observation is consistent with, and an independent confirmation of, the lower than expected accumulation of darapladib on repeat dosing. Given the CYP3A and Pgp substrate status of darapladib, the lower exposure to radioactivity may indicate lesser absorption of darapladib across the enterocyte after repeat oral dosing combined with greater extent of first-pass metabolism and/or efflux transport as a result of induction of enzyme and/or efflux transporter activity after repeat dosing. Due to the complexity of AMS analysis and the decision to only profile time-adjusted pooled plasma samples to 24 hours, it was not possible to confirm whether enzyme induction is the mechanism underlying the time-dependent pharmacokinetics. The question of CYP3A induction will be addressed in a planned drug-drug interaction study with midazolam.

In summary, this unusual study design utilizing different routes of administration, low-level AMS detection, and a repeat dose oral leg has allowed an enhanced understanding of the relative absorption, metabolism, and elimination of darapladib in humans, despite the absence of absolute metabolite quantification post repeat dose.

The increased availability and acceptance of AMS within the pharmaceutical industry (Smith 2011; Iyer et al., 2012; Lappin et al., 2012; Vuong et al., 2012; Bowers et al., 2013; Harrell et al., 2013) does facilitate replacing the traditional single-dose human radiolabeled study with a design using repeated therapeutic doses incorporating trace levels of radioactivity amenable to AMS detection, which in

Downloaded from dmd.aspetjournals.org at ASPET Journals on November 7, 2015

conjunction with MS and NMR techniques, would allow complete determination of metabolism and disposition under the more relevant steady-state conditions.

Acknowledgments

The authors thank Jackie Bloomer for her input into the study design; Will Ellis, Clive Felgate, and Steven Corless for providing technical assistance with AMS; Bianca Squillaci for technical assistance with metabolite identification; and Dave Lundberg, John Kratz, and Sherry Wang for bioanalysis of darapladib and SB-553253 (M4). The authors would also like to acknowledge Simon Harwood for the synthesis of [^{14}C]darapladib.

Authorship Contributions

Participated in research design: Young, Ellens, Magee, Boyle.

Conducted experiments: Dave, Nash, Young, Roberts, Taylor.

Performed data analysis: Dave, Nash, Young, Magee, Roberts, Taylor.

Wrote or contributed to the writing of the manuscript: Dave, Nash, Young, Ellens, Magee, Greenhill, Boyle.

References

Ames BN, Durston WE, Yamasaki E, and Lee FD (1973) Carcinogens are mutagens: a simple test system combining liver homogenates for activation and bacteria for detection. *Proc Natl Acad Sci USA* **70**:2281–2285.

Botta L, Gerber H-U, and Schmid K (1985) Measurement of radioactivity in biological experiments, in *Drug Fate and Metabolism, Methods and Techniques*, **Vol. 5** (Garrett ER and Hirtz JL eds) pp 99–134, Dekker, New York.

Bowers GD, Tenero D, Patel P, Huynh P, Sigafoos J, O'Mara K, Young GC, Dumont E, Cunningham E, and Kurtinecz M, et al. (2013) Disposition and metabolism of GSK2251052 in humans: a novel boron-containing antibiotic. *Drug Metab Dispos* **41**:1070–1081.

Bruin GJ, Waldmeier F, Boernsen KO, Pfaar U, Gross G, and Zollinger M (2006) A microplate solid scintillation counter as a radioactivity detector for high performance liquid chromatography in drug metabolism: validation and applications. *J Chromatogr A* **1133**:184–194.

Funk RS and Krise JP (2012) Cationic amphiphilic drugs cause a marked expansion of apparent lysosomal volume: implications for an intracellular distribution-based drug interaction. *Mol Pharm* **9**:1384–1395.

Gibaldi M and Perrier D (1982) *Pharmacokinetics*, 2nd ed, Dekker, New York.

Green MHL (1984) Mutagen testing using Trp+ reversion in *Escherichia coli*, in *Handbook of Mutagenicity Test Procedures*, Ed. 2nd, pp 161–187, Elsevier Science Publishing, New York.

Harrell AW, Siederer SK, Bal J, Patel NH, Young GC, Felgate CC, Pearce SJ, Roberts AD, Beaumont C, and Emmons AJ, et al. (2013) Metabolism and disposition of vilanterol, a long-acting β(2)-adrenoceptor agonist for inhalation use in humans. *Drug Metab Dispos* **41**:89–100.

Hochman JH, Chiba M, Nishime J, Yamazaki M, and Lin JH (2000) Influence of P-glycoprotein on the transport and metabolism of indinavir in Caco-2 cells expressing cytochrome P-450 3A4. *J Pharmacol Exp Ther* **292**:310–318.

Hop CECA, Wang Z, Chen Q, and Kwei G (1998) Plasma-pooling methods to increase throughput for in vivo pharmacokinetic screening. *J Pharm Sci* **87**:901–903.

Iyer GR, Patel Y, and Teuscher NS (2012) A novel study using accelerated mass spectrometry to evaluate the pharmacokinetics of total ^{14}C AL-8309 (tandospirone) following topical ocular administration in healthy male subjects. *Clinical Pharmacology in Drug Development* **1**:4–13.

Lappin G, Seymour M, Gross G, Jørgensen M, Kall M, and Kværnø L (2012) Meeting the MIST regulations: human metabolism in Phase I using AMS and a tiered bioanalytical approach. *Bioanalysis* **4**:407–416.

Maron DM and Ames BN (1983) Revised methods for the *Salmonella* mutagenicity test. *Mutat Res* **113**:173–215.

McConnell EL, Basit AW, and Murdan S (2008) Measurements of rat and mouse gastrointestinal pH, fluid and lymphoid tissue, and implications for in-vivo experiments. *J Pharm Pharmacol* **60**:63–70.

Mohler ER, 3rd, Ballantyne CM, Davidson MH, Hanefeld M, Ruilope LM, Johnson JL, and Zalewski A Darapladib Investigators (2008) The effect of darapladib on plasma lipoprotein-associated phospholipase A_2 activity and cardiovascular biomarkers in patients with stable coronary heart disease or coronary heart disease risk equivalent: the results of a multicenter, randomized, double-blind, placebo-controlled study. *J Am Coll Cardiol* **51**:1632–1641.

Oliveira EJ and Watson DG (2000) Liquid chromatography-mass spectrometry in the study of the metabolism of drugs and other xenobiotics. *Biomed Chromatogr* **14**:351–372.

Paine MF, Hart HL, Ludington SS, Haining RL, Rettie AE, and Zeldin DC (2006) The human intestinal cytochrome P450 "pie". *Drug Metab Dispos* **34**:880–886.

Reasor MJ and Kacew S (2001) Drug-induced phospholipidosis: are there functional consequences? *Exp Biol Med (Maywood)* **226**:825–830.

Roffey SJ, Obach RS, Gedge JI, and Smith DA (2007) What is the objective of the mass balance study? A retrospective analysis of data in animal and human excretion studies employing radiolabeled drugs. *Drug Metab Rev* **39**:17–43.

Sagawa K, Li F, Liese R, and Sutton SC (2009) Fed and fasted gastric pH and gastric residence time in conscious beagle dogs. *J Pharm Sci* **98**:2494–2500.

Serruys PW, García-García HM, Buszman P, Erne P, Verheye S, Aschermann M, Duckers H, Bleie O, Dudek D, and Bøtker HE, et al.; Integrated Biomarker and Imaging Study-2 Investigators (2008) Effects of the direct lipoprotein-associated phospholipase $A_{(2)}$ inhibitor darapladib on human coronary atherosclerotic plaque. *Circulation* **118**:1172–1182.

Smith DA (2011) The debate is over: accelerator MS provides the route to better drug-development paradigms/protocols. *Bioanalysis* **3**:391–392.

Thompson A, Gao P, Orfei L, Watson S, Di Angelantonio E, Kaptoge S, Ballantyne C, Cannon CP, Criqui M, and Cushman M, et al.; Lp-PLA(2) Studies Collaboration (2010) Lipoprotein-associated phospholipase $A_{(2)}$ and risk of coronary disease, stroke, and mortality: collaborative analysis of 32 prospective studies. *Lancet* **375**:1536–1544.

Vuong LT, Blood AB, Vogel JS, Anderson ME, and Goldstein B (2012) Applications of accelerator MS in pediatric drug evaluation. *Bioanalysis* **4**:1871–1882.

Young GC, Corless S, Felgate CC, and Colthup PV (2008) Comparison of a 250 kV single-stage accelerator mass spectrometer with a 5 MV tandem accelerator mass spectrometer—fitness for purpose in bioanalysis. *Rapid Commun Mass Spectrom* **22**:4035–4042.

Address correspondence to: Gary W. Boyle, DMPK, GlaxoSmithKline, Ware, UK. E-mail: Gary.W.Boyle@gsk.com

Downloaded from dmd.aspetjournals.org at ASPET Journals on November 7, 2015

The Journal of Clinical Pharmacology
53(9) 955–961
© 2013, The American College of Clinical Pharmacology
DOI: 10.1002/jcph.127

Concomitant Oral and Intravenous Pharmacokinetics of Dabrafenib, a BRAF Inhibitor, in Patients With BRAF V600 Mutation-Positive Solid Tumors

Cathrine L. Denton, PhD[1], Elisabeth Minthorn, BS[2], Stanley W. Carson, PharmD[1], Graeme C. Young, MSc[3], Lauren E. Richards-Peterson, PhD[4], Jeffrey Botbyl, MS[5], Chao Han, PhD[6], Royce A. Morrison, MD[7], Samuel C. Blackman, MD, PhD[8], and Daniele Ouellet, PhD[1]

Abstract

Dabrafenib is an orally bioavailable, potent, and selective inhibitor of human wild-type BRAF and CRAF kinases as well as mutant forms of BRAF kinase. The aim of this phase 1, single-center, open-label study in four patients with BRAF mutation-positive solid tumors was to determine the absolute bioavailability of a 150 mg oral dose of dabrafenib. A microtracer study approach, in which a 50 μg radiolabeled intravenous (IV) microdose of dabrafenib was given concomitantly with a 150 mg oral dose, was used to simultaneously recover IV and oral pharmacokinetic parameters. The least squares mean (90% CI) absolute bioavailability of dabrafenib (HPMC capsules) was 94.5% (81.3%, 109.7%). Median T_{max} after oral administration was 2.0 hours and the geometric mean terminal half-life was 4.8 hours. The geometric mean clearance and volume of distribution after IV administration were 12.0 L/h and 45.5 L, respectively. Human clearance and volume of distribution at steady state were in agreement with predictions made using allometric scaling of pharmacokinetic parameters from four preclinical species. In conclusion, dabrafenib absolute bioavailability was high, whereas first-pass metabolism was low. Furthermore, the microtracer approach provided an innovative and efficient method for assessing the absolute bioavailability of dabrafenib in patients with advanced cancer.

Keywords

bioavailability, dabrafenib, pharmacokinetic, intravenous, microtracer

Dabrafenib (GSK2118436) is an orally potent and selective small-molecule inhibitor of BRAF kinase activity that is currently being developed for the treatment of BRAF V600 mutation-positive malignant melanoma. Clinical activity was first observed in a phase 1 first-time-in-human (FTIH) study,[1] and efficacy of oral dabrafenib 150 mg twice daily was confirmed in a randomized phase 3 study[2] as well as a phase 2 study in patients with melanoma.[3]

The pharmacokinetics of dabrafenib after oral administration was characterized in the FTIH study.[1] Following a single oral dose of 150 mg dabrafenib, median T_{max} was recorded 2 hours after dosing and the mean terminal half-life ($t_{1/2}$) was 5.2 hours. Three major circulating metabolites were identified in the FTIH study and their pharmacokinetics characterized. Based on data from the mass balance study, the half-lives of hydroxy-, carboxy-, and desmethyl-dabrafenib were 5.7, 17.5, and 20.4 hours, respectively.[4]

Determination of absolute bioavailability improves our understanding and is required by several regulatory agencies, but such clinical studies have been fraught with the challenges and delays associated with preparing and administering a drug intravenously that has been developed for oral use. The use of intravenous (IV) radiolabeled microtracer studies offers an attractive alternative to conducting conventional crossover-design absolute bioavailability studies and provides

[1]GlaxoSmithKline, Research Triangle Park, NC, USA
[2]GlaxoSmithKline, Collegeville, PA, USA
[3]GlaxoSmithKline, Ware, UK
[4]GlaxoSmithKline, King of Prussia, PA, USA
[5]Provonix, Mullica Hill, NJ, USA
[6]Biologics Clinical Pharmacology, Janssen R&D, Spring House, PA, USA
[7]Comprehensive Clinical Development, Tacoma, WA, USA
[8]Translational Medicine, Seattle Genetics, Inc., Bothell, WA, USA

Submitted for publication 8 March 2013; accepted 4 June 2013.

Corresponding Author:
Cathrine L. Denton, PhD, GlaxoSmithKline, Clinical Pharmacology Modeling & Simulation, 5 Moore Drive, Research Triangle Park, NC 27709, USA
E-mail: cathrine.l.denton@gsk.com

characterization of the IV pharmacokinetics of a new compound. The microtracer approach involves administration of an unlabeled oral therapeutic dose with concomitant administration of a subtherapeutic radiolabeled IV microdose (pharmacologically inactive). A microdose is defined as less than 1/100th of the calculated clinical dose (based on animal data) needed to yield a pharmacologic effect, up to a maximum of 100 μg.[5,6] The radiolabeled microdose produces trivial exposure to ionizing radiation (<270 nCi), and does not require additional IV toxicity studies or extensive IV formulation development. The microtracer approach has the advantage of simultaneous recovery of IV and oral pharmacokinetic parameters to obtain within-subject, within-period comparison. As such, this approach reduces the variability of recovered pharmacokinetic parameters, reduces the number of subjects required, and provides a more precise estimate of absolute bioavailability than does the use of a traditional crossover design study. Microtracer studies have been used successfully to determine the absolute bioavailability of a number of compounds including fexofenadine, IDX899 and IDX989, SRT-2104 (GSK2245840), and saxagliptin.[7–11]

The purpose of this study was to characterize the oral and IV pharmacokinetics and determine the absolute oral bioavailability of dabrafenib using simultaneous administration of an unlabeled oral capsule dose (150 mg as two 75 mg capsules) and a radiolabeled IV microdose (50 μg) in patients with BRAF mutation-positive solid tumors. Clinical pharmacokinetic parameters were compared with preclinical pharmacokinetic parameters to better understand the predictability of the preclinical models.

Methods

Clinical Study Design

The study protocol (BRF113479; ClinicalTrials.gov identifier NCT01340833) and consent form were approved by a duly constituted institutional review board (Alpha Independent Review Board, San Clemente, CA), and the study was conducted in accordance with Good Clinical Practice and the guiding principles of the Declaration of Helsinki at Comprehensive Clinical Development NW, Inc. (Tacoma, WA). Signed and dated written informed consent was obtained from each patient before his or her participation in the study and before the performance of any procedures.

This was a phase 1, single-center, open-label study in patients with BRAF mutation-positive solid tumors. After obtaining informed consent, eligible participants were admitted to the clinical research unit on day −1. After an overnight fast, all participants received 150 mg of dabrafenib (as mesylate salt) as two 75 mg hydroxypropyl methylcellulose (HPMC) capsules and a single IV dose of 50 μg (7.4 kBq; 200 nCi) [^{14}C] dabrafenib, infused over 15 minutes, starting 1.75 hours after the oral dose (to coincide with oral T_{max}). The actual measured IV dose was determined by liquid scintillation counting of aliquots (300 μL) of the administered dabrafenib IV solution, and based on the predetermined specific activity of [^{14}C]-labeled dabrafenib. The participants continued fasting for 4 hours after the oral dose. Blood samples (two 6 mL samples at each time point) for analysis of dabrafenib, [^{14}C] dabrafenib, and total radioactivity were collected at several time points through 72 hours after the oral dose. The actual date and time of each blood sample collection were recorded. Plasma was separated from blood by centrifugation and stored frozen prior to analysis. After completion of the study, all participants entered an open-label rollover study of dabrafenib (no washout period or follow-up visit required) and continued receiving dabrafenib (BRF114144, ClinicalTrials.gov identifier NCT01231594).

Dose Selection

The recommended oral dose for phase 2 and phase 3 studies was 150 mg twice daily administered as two 75 mg HPMC capsules. An IV dose of 50 μg was selected, which is 3,000-fold lower than the oral dose, thus fitting the criteria of a microdose (i.e., <100th of the dose needed to yield a pharmacologic effect, up to a maximum of 100 μg). The exact IV dose administered was measured on site and used in absolute bioavailability calculations.

Study Participants

Men or women were eligible if they were ≥18 years of age with BRAF mutation-positive tumors, had an Eastern Cooperative Oncology Group (ECOG) performance status of 0 or 1, and had adequate organ function. A body weight of ≥45 kg and a body mass index of ≥19 kg/m^2 and ≤35 mg/m^2 were required. Participants were excluded if they had received cancer therapy, an investigational anticancer drug within 3 weeks, or any other investigational product within 30 days, five half-lives, or twice the duration of the biological effect of the investigational product. In addition, patients were excluded if they had participated in a ^{14}C human research study within 12 months preceding the administration of study medication. Consumption of food, herbal remedies, or medication known to interfere with cytochrome P (CYP) 3A, CYP2C8, or P-glycoprotein activity was prohibited. Disease-related exclusion criteria were the presence of invasive non-BRAF mutation-positive malignancy or presence of brain metastases that were symptomatic, treated but not clinically stable, or asymptomatic/untreated and >1 cm in the longest dimension. Patients with a corrected QT (QTc) interval ≥480 ms (note that QTc was assessed using Fridericia's correction) or with conditions affecting gastrointestinal absorption were excluded.

Dabrafenib UHPLC-MS/MS Analysis

Concentrations of dabrafenib in plasma samples at all time points were determined using a validated analytical ultrahigh performance liquid chromatography mass spectrometry/mass spectrometry (UHPLC-MS/MS) method, over the range of 1–1,000 ng/mL. Dabrafenib was extracted from 50 μL of human plasma by liquid–liquid extraction with ethyl acetate after the addition of isotopically labeled internal standards ([$^2H_9$]-dabrafenib). Extracts (4 μL) were injected onto a Waters Acquity BEH C_{18} column (50 mm × 2.1 mm; Waters Corporation, Milford, MA) maintained at 55°C. The mobile phase consisted of 0.1% formic acid in water (solvent A) and acetonitrile (solvent B). A flow rate of 0.8 mL/min was maintained for the entire run. The following 1.4-min linear gradient was used: start at 30% B, increase to 50% B over 0.5 minutes, maintain 50% B for 0.3 minutes, increase to 80% B over 0.2 minutes, and maintain at 80% B for 0.3 minutes. The column was reequilibrated after each injection. Detection was performed by positive-ion MS/MS using a TurboIon spray interface on an API 4000 mass spectrometer (Applied Biosystems/MDS Sciex, Concord, Ontario, Canada) with multiple reaction monitoring (*m/z* 520–*m/z* 277 for dabrafenib, *m/z* 529–*m/z* 280 for [$^2H_9$]-dabrafenib). Quantification was performed against dabrafenib-spiked recovery standards based on demonstrated linearity with $1/x^2$ weighted regression.

Each batch of experimental samples was run against freshly prepared calibration standards (n = 10). Replicate (n = 4) quality control (QC) samples at three concentrations were stored and also analyzed alongside study samples. For the analysis to be acceptable, no more than one-third of the total QC results and no more than one-half of the results from each concentration level could deviate from the nominal concentration by >15% (actual, <10.9%). In all cases, the coefficient of variation between the replicates could not deviate by >15% (actual, <5.6%). The applicable analytic runs met all predefined acceptance criteria. Twelve study samples (16.7% of the total study samples) were reanalyzed for incurred sample reproducibility (ISR), with all samples being within 20% of the mean of the original and ISR results.

[^{14}C] Dabrafenib and Total Radioactivity Analysis

Samples were analyzed for [^{14}C] dabrafenib and total plasma radioactivity using accelerator mass spectrometry (AMS) by Xceleron (Germantown, MD). Prior to analysis by AMS, the carbon within the samples was harvested and converted to graphite. This involved a two-stage process of sample combustion (oxidation) followed by graphitization (reduction), as previously published.[12] AMS provides an isotope ratio from which total radiocarbon per mg carbon is derived. The carbon content of plasma was taken into account to allow correction of the AMS data to determine the amount of radiocarbon in the samples. Carbon analysis was undertaken using a Costech Elemental Combustion System CHNS-O Analyzer (Costech Analytical Technologies, Inc., Valencia, CA) supplied by Pelican Scientific Ltd. (Cheshire, United Kingdom). The AMS was a 250 kV Single Stage Accelerator Mass Spectrometer (National Electrostatics Corp., Middleton, WI), operated via NEC proprietary "AccelNET" software on a Linux operating system. Post-acquisition data processing was performed using the NEC software "abc." Further details of the operating conditions have been previously published.[12] The lower limit of quantitation (LLQ) and higher limit of quantitation (HLQ) for total plasma radioactivity were 9.77 and 11,400 dabrafenib pg equiv/mL for a 60-μL aliquot of human plasma.

Plasma [^{14}C] dabrafenib concentrations at all time points were determined using a validated analytical LC + AMS method over the range of 1.86–456 pg/mL. Dabrafenib (including [^{14}C] dabrafenib as a tracer) was extracted from 400 μL (2 × 200-μL aliquots) of human plasma by protein precipitation using three volumes of acetonitrile containing nonlabeled dabrafenib at 10 μg/mL as an internal standard (IS). The protein precipitation plate was shaken for 5 minutes at medium setting on a plate shaker. Samples were drawn through the plate under vacuum and collected as two filtrates into polypropylene tubes. After drying one of the filtrates under nitrogen until ≈100 μL remained, the second filtrate was added and the combined filtrate was reduced to dryness under nitrogen at 20°C. The sample was reconstituted in 100 μL of 10-mM ammonium acetate (pH5) and 50 μL was injected onto the HPLC system. Isolation of dabrafenib was achieved using a Poroshell 120 EC-C18 column (2.7 μm packing, 3 × 50 mm; Agilent Technologies, Santa Clara, CA) maintained at 30°C. The mobile phase consisted of 10 mM ammonium acetate (pH 5; A) and acetonitrile (B). A flow rate of 1 mL/min was maintained for the entire run. The following 15-minutes gradient was used: start at 5% B, maintain at 5% B for 1 minutes, increase to 20% B over 1.4 minutes, increase to 35% B over 5.6 minutes, increase to 95% B over 4 minutes, and maintain at 95% B for 0.8 minutes, then decrease to 5% B over 0.1 minutes. The column was then reequilibrated at 5% B over 2.1 minutes. The area of the UV response of the IS was recorded, and the eluate corresponding to dabrafenib was collected as a discrete fraction into a quartz tube for further processing (to harvest graphite) and subsequent analysis by AMS. The assay had a linear dynamic range of 1.86–456 pg/mL, and quantification was performed against dabrafenib-spiked recovery standards based on demonstrated linearity with 1/x weighted regression.

During validation, QC samples (n = 3) at three concentrations were analyzed on two separate occasions. Eight of nine assay results on day 1 and 7 of 9 on day 2 were within 20% (25% at LLQ) of the actual value. Additionally, a set of spiked samples (n = 5) at five

concentrations ranging from 1.86–456 pg/mL was analyzed alongside the QC samples, giving a within-run precision of <13.6% and a 1/x-weighted R^2 value of 0.99.

Replicate (n = 3) QC samples at three concentrations were also analyzed alongside study samples. Only 2 of 36 samples failed to meet the established acceptance criteria (±20%) through four analytical runs. Ten study samples (≈16%) were reanalyzed for ISR, with all samples being within 20% of the mean of the original and ISR results.

Clinical Pharmacokinetics

Analysis of plasma concentration data via noncompartmental methods was conducted using WinNonlin Professional Edition version 5.2 (Pharsight Corporation, Mountain View, CA) noncompartmental Model 200 (for extravascular administration) for dabrafenib and noncompartmental Model 202 (for constant infusion) for [^{14}C] dabrafenib and total radioactivity by ICON Development Solutions (Marlow, United Kingdom). Standard noncompartmental pharmacokinetic parameters for dabrafenib, [^{14}C] dabrafenib, and total radioactivity were estimated based on actual sampling times. V_{ss} is described as the volume of distribution at steady state, and is based on mean residence time (MRT) and clearance (CL) where $V_{ss} = MRT_{(0-\infty)} \times CL$.

Preclinical Pharmacokinetics

Preclinical studies were conducted to characterize the IV and oral pharmacokinetic properties of dabrafenib in mice, rats, dogs, and monkeys. All animal studies were conducted in accordance with the GlaxoSmithKline (GSK) policy on the care, welfare, and treatment of laboratory animals, and were reviewed by the Institutional Animal Care and Use Committee at GSK (Collegeville, PA). The pharmacokinetics of dabrafenib was studied in male CD-1 mice, Sprague–Dawley rats, beagle dogs, and cynomolgus monkeys after a single IV bolus (mouse) or 1-hour infusion (rat, dog, and monkey) administration (n = 3/species). Doses were formulated in 1% DMSO and 10% Solutol in saline (pH 5.0–5.5) for injection (rodent) or 1% DMSO and 30% PEG400 in saline (pH 3.72 or 4.35) for injection (dog or monkey). Oral exposure was also determined after single oral gavage administration. Oral solution doses were formulated as the free base in 1% DMSO and 10% Solutol in ≈pH 5 water (rodent), 1% DMSO and 30% PEG400 in pH 4.07 water (dog), or in water (pH 4.92) alone (monkey). Serial blood samples were collected and assayed for dabrafenib by protein precipitation followed by LC/MS/MS analysis, and the resulting concentration–time data were analyzed by noncompartmental methods using WinNonlin Professional version 4.1. The linear relationship between log-transformed body weight and log-transformed CL or V_{ss} for all four preclinical species was used to estimate human CL and V_{ss}, prior to conducting the FTIH clinical study.

Statistical Analysis

Summary statistics were calculated for each pharmacokinetic parameter for data from each of the preclinical species and the human study. For calculation of absolute bioavailability, a mixed-effect model was fit to dose-normalized, $\log_e$-transformed area under the curve ($AUC_{[0-\infty]}$) with the subject as a random effect and treatment as a fixed effect (oral was the test, IV was the reference). Dose-normalized $AUC_{(0-\infty)}$ was obtained by dividing $AUC_{(0-\infty)}$ by the corresponding dose of the subject. The least squares mean difference and associated 90% CI in $AUC_{(0-\infty)}$ between the oral and IV doses were obtained from the model. This least squares mean difference was back-transformed to provide a point estimate and corresponding 90% CI for the absolute bioavailability (F). The oral dose and the actual measured IV dose were used in the calculation of absolute bioavailability.

Results

Participants

Four patients (two men, two women; all were white) were enrolled and underwent study procedures. Three patients had stage IV BRAF mutation-positive melanoma and one had stage IV BRAF mutation-positive small cell lung cancer. All patients had an ECOG performance status of 1 at screening. All received the oral and IV doses as planned. The measured IV dose of [^{14}C] dabrafenib received by each patient was between 53 and 59 μg, 106–118% of the target dose.

Clinical Pharmacokinetics

Mean concentration–time profiles following oral and IV microdose are illustrated in Figure 1. After IV administration, [^{14}C] dabrafenib, and total radioactivity were detectable in all four patients through 8 and 72 hours, respectively. Pharmacokinetic parameters for [^{14}C] dabrafenib and total radioactivity after IV administration and for dabrafenib after oral administration are summarized in Table 1.

For a targeted 3,000-fold difference between IV and oral dose, geometric mean C_{max} and $AUC_{(0-\infty)}$ were 766-fold and 2,560-fold lower, respectively, after IV microdose relative to the oral dose. The least squares mean (90% CI) absolute bioavailability of dabrafenib administered as HPMC capsules was 94.5% (81.3%, 109.7%), with individual values ranging from 79.3% to 105.9%.

Following IV administration, the geometric mean CL and V_{ss} of [^{14}C] dabrafenib were 12.0 L/h and 45.5 L, respectively. Geometric mean apparent CL after oral

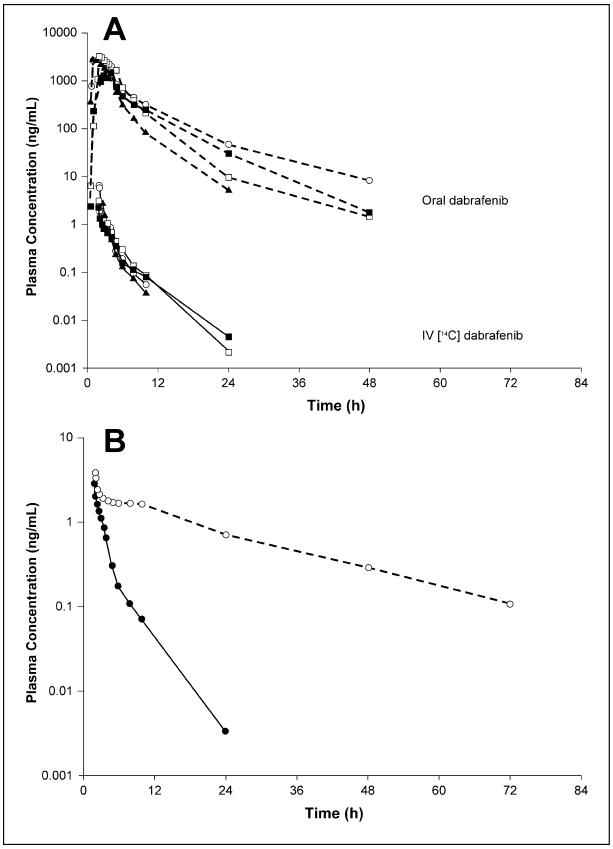

Figure 1. (A) Individual plasma dabrafenib and [^{14}C] dabrafenib concentration versus time profiles after oral (150 mg) and IV (50 μg) administration. The following symbols denote patient 1 (◯), patient 2 (■), patient 3 (□), and patient 4 (▲). The dashed lines represent oral dabrafenib, the solid lines represent IV [^{14}C] dabrafenib. (B) Mean plasma [^{14}C] dabrafenib (solid line, ng/mL) and total radioactivity (dashed line, ng equivalents of dabrafenib/mL) concentration versus time profile after intravenous (IV; 50 μg) administration (N = 4).

administration was 14.0 L/h. Plasma concentrations of [^{14}C] dabrafenib and dabrafenib declined in a biexponential fashion, and the geometric mean half-lives were 2.6 hours after IV [^{14}C] dabrafenib administration and 4.8 hours after oral dabrafenib administration. Median T_{max} after oral administration was 2.0 hours and coincided with the T_{max} observed at the end of the IV infusion (Table 1, Figure 1A and B).

C_{max} and $AUC_{(0-\infty)}$ of total radioactivity were 1.3-fold and 10.5-fold higher, respectively, than [^{14}C]-dabrafenib after IV dosing, consistent with the presence of circulating metabolites. The percentage of total radioactivity in the form of parent compound was ≈9.6% as assessed by the ratio of geometric mean plasma $AUC_{(0-\infty)}$ of [^{14}C] dabrafenib to total plasma radioactivity (Table 1). Terminal half-life was 18.3 hours for total radioactivity compared with 2.6 hours for [^{14}C] dabrafenib.

Adverse Events

All reported adverse events (AEs) were grade 1 or grade 2 and resolved within 6 days of onset. The most common AE was flushing (reported in two of four patients). All AEs except for upper respiratory tract infection were considered related to treatment with the study medication. There were no withdrawals due to AEs and no reports of AEs related to changes in clinical laboratory tests, echocardiograms, or vital signs. There were no reports of serious AEs.

Preclinical Pharmacokinetics and Allometry

Dabrafenib pharmacokinetic parameters after oral and IV dosing in preclinical species are summarized in Table 2. Following IV administration, dabrafenib CL was low and volume was small relative to body water in all preclinical species, resulting in half-lives ranging from 0.3 hours (mouse and monkey) to 2.8 hours (dogs). Oral bioavailability ranged from 46% to 82% across species and was lowest in monkeys.

Based on preclinical pharmacokinetic parameters, CL and volume in humans were originally predicted based on allometric scaling methods. Figure 2 shows the linear model used to describe the allometric relationship of log-

Table 1. Clinical Pharmacokinetics of Dabrafenib After Concomitant Oral and IV Administration (150 mg Dabrafenib Orally, 50 μg [^{14}C] Dabrafenib IV)

Parameter[a] (units)	Oral dabrafenib	IV [^{14}C] dabrafenib	IV Total radioactivity[b]
T_{max} (h)	2.0 (2.0, 4.0)	0.25 (0.22, 0.32)	0.29 (0.22, 0.33)
C_{max} (ng/mL)	2,527 (1,318, 4,845)	3.3 (1.6, 6.8)	4.2 (2.0, 8.6)
$AUC_{(0-t)}$ (ng × h/mL)	10,723 (6,989, 16,451)	4.1 (3.1, 5.3)	41.1 (21.4, 79.2)
$AUC_{(0-\infty)}$ (ng × h/mL)	10,751 (6,996, 16,523)	4.2 (3.2, 5.4)	43.9 (22.8, 84.5)
$t_{1/2}$ (h)	4.8 (3.0, 7.6)	2.6 (1.8, 3.7)	18.3 (14.7, 22.7)
CL or CL/F[c] (L/h)	14.0 (9.1, 21.4)	12.0 (9.2, 15.7)	NA
V_{ss} (L)	NA	45.5 (28.1, 73.7)	NA

Abbreviations: AUC, area under the curve; CL, clearance; F, absolute bioavailability; IV, intravenous; NA, not applicable; $t_{1/2}$, half-life; V_{ss}, volume of distribution at steady state.

[a]Results are presented as geometric mean (95% CI), except T_{max} as median (range), N = 4.

[b]Radioactivity concentrations are expressed as ng equivalents of dabrafenib/mL.

[c]CL for IV administration or CL/F for oral administration.

Table 2. Preclinical Pharmacokinetics After a Single IV or Oral Dose of Dabrafenib[a]

Specie	Dose (IV/oral) (mg/kg)	IV CL (mL/min/kg)	IV V_{ss} (L/kg)	IV $t_{1/2}$ (h)	F (%)
Mouse	2.5/10	43.5 (6.8)	1.0 (0.1)	0.3 (0.1)	70[b]
Rat	2.0/4.0	17.6 (4.3)	1.0 (0.1)	0.7 (0.1)	77 (21)
Monkey	0.5/1.0	22.5 (1.8)	0.5 (0.1)	0.3 (0.1)	46 (4)
Dog	0.6/0.7	3.6 (0.3)	0.4 (0.1)	2.8 (0.7)	82 (12)

Abbreviations: CL, clearance; F, absolute bioavailability; IV, intravenous; $t_{1/2}$, half-life; V_{ss}, volume of distribution at steady state.
[a]Pharmacokinetic parameters reported as mean (SD), N = 3.
[b]Noncrossover estimate of oral bioavailability from two separate studies.

transformed body weight and either CL or volume between species. Accordingly, human CL and volume were predicted to be 14.8 L/h (3.5 mL/min/kg) and 21.6 L (0.31 L/kg), respectively, resulting in a half-life of 61 min. Observed values for human CL and volume after IV dosing of [^{14}C] dabrafenib were 12.0 L/h and 45.5 L, respectively, and as such were consistent with values predicted from preclinical species.

Discussion

The primary objective of this study was to determine the absolute bioavailability of dabrafenib using concomitant administration of an unlabeled oral therapeutic dose (two 75 mg HPMC capsules) and a radiolabeled IV microtracer dose (50 μg). The absolute bioavailability of a 150 mg dose of dabrafenib was high (94.5%). Whereas the estimate given in the current publication uses the actual measured IV dose of [^{14}C] dabrafenib to estimate bioavailability, a preliminary estimate was published using prescribed dose 84.2% (72.3–98.1%).[13] Traditionally, absolute bioavailability has been determined via a randomized, 2-period crossover study design and typically requires ≈6–12 individuals. Although the sample size in this study was small (four patients), the reduced variability afforded by the microtracer approach, compared with the 2-period crossover design, allows for a robust estimate of absolute bioavailability.

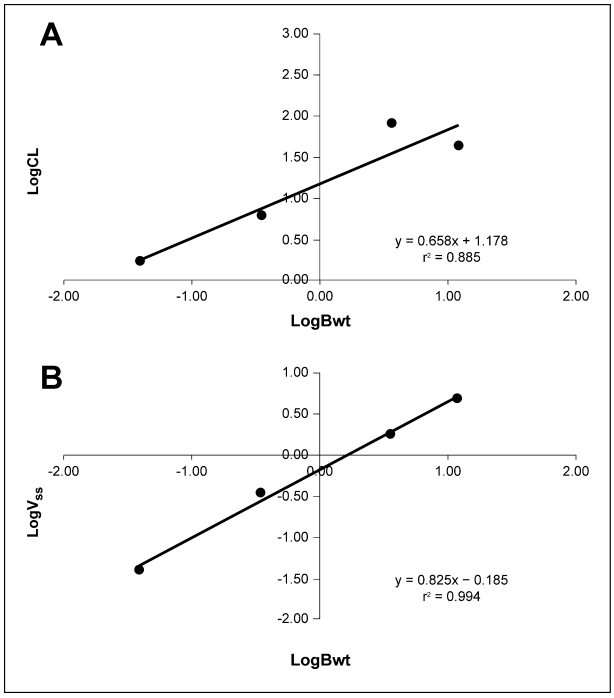

Figure 2. Allometric scaling of dabrafenib clearance and volume. Linear relationship between log-transformed body weight (LogBwt) and log-transformed (A) clearance (LogCL) or (B) volume of distribution at steady state ($LogV_{ss}$) in four preclinical species after intravenous administration of dabrafenib. Linear regression equation and r^2 (coefficient of determination) values are shown, inset.

The IV CL of dabrafenib was 12.0 L/h and, as such, was ≈30% of hepatic blood flow (where the hepatic blood flow is 81 L/h,[14] and the blood:plasma ratio is ≈0.5). The high absolute bioavailability and low CL suggested low hepatic extraction of dabrafenib in addition to low first-pass metabolism. Low first-pass metabolism likely contributed to low variability in exposure after oral dosing (28% between-subject variation). Despite low CL, dabrafenib $t_{1/2}$ was short, likely due to a small volume of distribution. Following oral administration, both the T_{max} and $t_{1/2}$ observed in this study were consistent with previous reports.[11] Dabrafenib $t_{1/2}$ was nearly twice as long after oral administration as that after IV administration, suggesting prolonged absorption, that is, flip–flop kinetics. Increased exposure to dabrafenib after oral administration is therefore dependent on the prolonged absorption phase, which contributes to a longer half-life and protracted decline in plasma concentrations than that after IV administration.

A longer $t_{1/2}$ was observed for total radioactivity than for [^{14}C] dabrafenib, likely due to the circulating dabrafenib metabolites carboxy-dabrafenib and desmethyl-dabrafenib, which have long $t_{1/2}$ (17.5 and 20.4 hours, respectively) and display elimination rate-limited pharmacokinetics. In contrast, the $t_{1/2}$ of hydroxy-dabrafenib after oral dosing was ≈5.7 hours, and the pharmacokinetic profile paralleled that of the parent. In terms of total plasma radioactivity $AUC_{(0-\infty)}$, the parent and the hydroxy-, carboxy-, and desmethyl-dabrafenib metabolites were found to account for 11%, 8%, 57%, and 3%, respectively, based on data from the mass balance study.[4] As observed in the present study, the fraction of

systemic parent $AUC_{(0-\infty)}$ compared with systemic total radioactivity $AUC_{(0-\infty)}$ after IV administration was 9.6%, generally consistent with both the value observed with oral dosing and the low first-pass metabolism.

The estimate of human CL from preclinical pharmacokinetic data was within 20% of the observed value in our study. For volume of distribution, the observed V_{ss} was about twofold higher than the predicted value. From a qualitative standpoint, however, scaling from preclinical data was consistent with the observed clinical data in that IV CL was low and volume was small relative to body water in preclinical species. Allometric scaling of dabrafenib $t_{1/2}$ in humans was estimated to be 61 minutes and, as such, was expected to pose a challenge to adequate dosing in the clinic. The uncertainty surrounding allometric predictions of human pharmacokinetics was addressed by including both single-dose and repeat-dose regimens in a flexible FTIH study during which the pharmacokinetics of dabrafenib was monitored.[1] Decisions about adequate dosing frequency could thus be made based on emerging pharmacokinetic data.

In conclusion, the IV microtracer study approach revealed the contribution of high oral bioavailability with low first-pass metabolism, a prolonged absorption phase, and the presence of long half-life metabolites to the pharmacokinetics of dabrafenib. Furthermore, this approach shortened the study time frame and allowed for simultaneous collection of IV and oral pharmacokinetic parameters, thus reducing variability. Particularly, where patients as clinical research participants are concerned, IV microtracer studies offer an innovative and efficient approach for assessing absolute bioavailability and may be applied across a range of therapeutic areas and compound classes.

Acknowledgments

Thanks to Catrin Dalton and Christopher Jefferds (ICON Clinical Research) who assisted with conduct of the trial, Jen Beyer (GlaxoSmithKline, data management), Ken Martin (Comprehensive Clinical Development), Marie Croft (Xceleron), and the patients who participated in this study. All listed authors meet the criteria for authorship set forth by the International Committee for Medical Journal Editors. Editorial support in the form of collating author comments, copyediting, referencing, and graphic services was provided by Clinical Thinking and was funded by GlaxoSmithKline.

Funding

Cathrine L. Denton, Elisabeth Minthorn, Stanley W. Carson, Graeme C. Young, Lauren E. Richards-Peterson, and Daniele Ouellet are full-time paid employees and stockholders of GlaxoSmithKline. As a statistical consultant, Jeffrey Botbyl's institution (Provonix) received consulting fees, fees for participation in review activities, and payment for writing and reviewing the manuscript from GlaxoSmithKline. Royce A. Morrison's institution received payment from GlaxoSmithKline to conduct the clinical research study. Chao Han and Samuel C. Blackman were former paid employees and stockholders of GlaxoSmithKline at the time of this study and analysis. Funding for this study (NCT01340833) was provided by GlaxoSmithKline.

References

1. Falchook GS, Long GV, Kurzrock R, et al. Dabrafenib in patients with melanoma, untreated brain metastases, and other solid tumours: a phase 1 dose-escalation trial. *Lancet.* 2012;379(9829):1893–1901.
2. Hauschild A, Grob JJ, Demidov LV, et al. Dabrafenib in BRAF-mutated metastatic melanoma: A multicentre, open-label, phase 3 randomised controlled trial. *Lancet.* 2012;380(9839):358–365.
3. Trefzer U, Minor D, Ribas A, et al. BREAK-2: a phase IIA trial of the selective BRAF kinase inhibitor GSK2118436 in patients with BRAF mutation-positive (V600E/K) metastatic melanoma. *Pigment Cell Melanoma Res.* 2011;24(5): Abstr LBA1-1.
4. Nebot N, Richards-Peterson LE, Bershas DA, et al. Characterization of the absorption, distribution, metabolism and elimination of a single oral ^{14}C labeled dose of dabrafenib in subjects with BRAF V600-mutation positive solid tumors. *Clin Pharmacol Ther.* 2013;93(S52–S86): PII-38.
5. Department of Health and Human Services, Center for Drug Evaluation and Research (CDER). FDA guidance for industry: bioavailability and bioequivalence studies for orally administered drug products - general considerations. http://www.fda.gov/downloads/Drugs/GuidanceComplianceRegulatoryInformation/Guidances/ucm070124.pdf. Updated 2003. Accessed February 26, 2013.
6. European Medicines Agency (EMEA). Committee for Medicinal Products for Human Use (CHMP). Position paper on non-clinical safety studies to support clinical trials with a single microdose. http://www.ema.europa.eu/ema/index.jsp?curl=pages/regulation/general/general_content_000400.jsp&mid=WC0b01ac0580029570. Updated 2004. Accessed February 26, 2013.
7. Boulton DW, Kasichayanula S, Keung CF, et al. Simultaneous oral therapeutic and intravenous (14) C-microdoses to determine the absolute oral bioavailability of saxagliptin and dapagliflozin. *Br J Clin Pharmacol.* 2013;75(3):763–768.
8. Hoffmann E, Wald J, Lavu S, et al. Pharmacokinetics and tolerability of SRT2104, a first-in-class small molecule activator of SIRT1, after single and repeated oral administration in man. *Br J Clin Pharmacol.* 2013;75(1):186–196.
9. Lappin G, Shishikura Y, Jochemsen R, et al. Pharmacokinetics of fexofenadine: evaluation of a microdose and assessment of absolute oral bioavailability. *Eur J Pharm Sci.* 2010;40(2):125–131.
10. Sarapa N, Hsyu PH, Lappin G, Garner RC. The application of accelerator mass spectrometry to absolute bioavailability studies in humans: simultaneous administration of an intravenous microdose of 14C-nelfinavir mesylate solution and oral nelfinavir to healthy volunteers. *J Clin Pharmacol.* 2005;45(10):1198–1205.
11. Zhou XJ, Garner RC, Nicholson S, Kissling CJ, Mayers D. Microdose pharmacokinetics of IDX899 and IDX989, candidate HIV-1 non-nucleoside reverse transcriptase inhibitors, following oral and intravenous administration in healthy male subjects. *J Clin Pharmacol.* 2009;49(12):1408–1416.
12. Young GC, Corless S, Felgate CC, Colthup PV. Comparison of a 250 kV single-stage accelerator mass spectrometer with a 5 MV tandem accelerator mass spectrometer–fitness for purpose in bioanalysis. *Rapid Commun Mass Spectrom.* 2008;22(24):4035–4042.
13. Denton CL, Carson SW, Young GC, et al. Absolute bioavailability of BRAF inhibitor GS K2118436: use of a microtracer study in patients with cancer. *Cancer Res.* 2012;72: Abstr 3773.
14. Rowland M, Tozer TN. *Clinical pharmacokinetics: concepts and applications*. 2nd ed. Philadelphia, PA: Lea & Febiger; 1989.

BJCP British Journal of Clinical Pharmacology

DOI:10.1111/bcp.12373

Concomitant oral and intravenous pharmacokinetics of trametinib, a MEK inhibitor, in subjects with solid tumours

Cathrine Leonowens,[1] Carolyn Pendry,[1] John Bauman,[1] Graeme C. Young,[2] May Ho,[3] Frank Henriquez,[4] Lei Fang,[1] Royce A. Morrison,[5] Keith Orford[4] & Daniele Ouellet[1]

[1]GlaxoSmithKline, Research Triangle Park, NC, USA, [2]GlaxoSmithKline, Ware, UK, [3]GlaxoSmithKline, King of Prussia, PA, [4]GlaxoSmithKline, Collegeville, PA and [5]Comprehensive Clinical Development, Tacoma, WA, USA

Correspondence
Cathrine Leonowens PhD, Clinical Pharmacology Modeling & Simulation, GlaxoSmithKline, 5 Moore Drive, Research Triangle Park, NC 27709, USA.
Tel.: +1 919 483 7588
Fax: +1 919 483 8948
E-mail: cathrine.x.leonowens@gsk.com

Keywords
bioavailability, intravenous, microtracer, pharmacokinetic, trametinib

Received
11 June 2013
Accepted
2 March 2014
Accepted Article Published Online
7 March 2014

WHAT IS ALREADY KNOWN ABOUT THIS SUBJECT

- Following oral dosing of 2 mg trametinib, median t_{max} was 1.5 h and the mean effective half-life ($t_{1/2}$) was approximately 4 days. Trametinib is greater than 95% protein bound. Trametinib accumulates about six-fold with repeat daily dosing, and the concentration–time profiles showed a flat profile at steady-state with a low peak : trough ratio.
- The absolute bioavailability of trametinib has not been previously reported.
- The microtracer approach has been used previously to recover i.v. and oral pharmacokinetic parameters, simultaneously, which are used to estimate absolute bioavailability.
- Determination of absolute bioavailability improves our understanding of the clinical pharmacology of a compound.

WHAT THIS STUDY ADDS

- Trametinib has moderate to high bioavailability (72.3%) following oral administration of a 2 mg tablet.
- The i.v. microtracer study approach revealed the contribution of high oral bioavailability with low first pass metabolism and a prolonged terminal elimination phase to the pharmacokinetics of trametinib.

AIMS

The aim of this phase 1, single centre, open label study in four patients with solid tumours was to determine the absolute bioavailability of a 2 mg oral dose of trametinib. Trametinib is an orally bioavailable, reversible and selective allosteric inhibitor of MEK1 and MEK2 activation and kinase activity.

METHODS

A microtracer study approach, in which a 5 μg radiolabelled i.v. microdose of trametinib was given concomitantly with an unlabelled 2 mg oral tablet formulation, was used to recover i.v. and oral pharmacokinetic parameters, simultaneously.

RESULTS

The least-squares mean (90% confidence interval) absolute bioavailability of trametinib (2 mg tablet) was 72.3% (50.0%, 104.6%). Median t_{max} after oral administration was 1.5 h and the geometric mean terminal half-life was 11 days. The geometric mean clearance and volume of distribution after i.v. administration were 3.21 l h^{-1} and 976 l, respectively, resulting in a terminal elimination half-life of 11 days.

CONCLUSIONS

Trametinib absolute bioavailability was moderate to high, whereas first pass metabolism was low.

© 2014 The British Pharmacological Society

Introduction

Trametinib is a reversible, highly selective allosteric inhibitor of MEK1/MEK2 activation and kinase activity [1, 2] which has been approved in the United States for the treatment of BRAF V600E or V600K mutation-positive melanoma. Clinical activity of trametinib in unresectable, BRAF V600 mutation-positive melanoma was observed in phase 1, 2 and 3 studies [3–5]. Significant improvement in overall survival and progression free survival over dacarbazine or paclitaxel was confirmed in the pivotal phase 3 study (METRIC) [5].

The pharmacokinetics (PK) of trametinib after oral administration were characterized in the first-time-in-human (FTIH) study [6]. Following oral dosing of 2 mg trametinib, median t_{max} was 1.5 h and the mean effective half-life ($t_{1/2}$) was approximately 4 days. Trametinib accumulates about six-fold with repeat daily dosing and the concentration–time profiles showed a flat profile at steady-state with a low peak : trough ratio.

Determination of absolute bioavailability improves our understanding of the clinical pharmacology of a compound (e.g. by characterizing the i.v. pharmacokinetics) and is required by several regulatory agencies [7]. Conventional crossover studies have been fraught with the challenges and delays associated with preparing and administering a drug intravenously that has been developed for oral use. The use of i.v. radiolabelled microtracer studies has become an attractive alternative to conducting conventional crossover design absolute bioavailability studies and provides characterization of the i.v. PK of a new compound. The microtracer approach involves administration of an unlabelled oral therapeutic dose with concomitant administration of a subtherapeutic radiolabelled i.v. microdose (pharmacologically inactive). A microdose is defined as less than 1/100th of the calculated clinical dose (based on animal data) needed to yield a pharmacologic effect, up to a maximum of 100 µg [8, 9]. The radiolabelled microdose (<270 nCi) produces trivial exposure to ionizing radiation and does not require additional i.v. toxicity studies or extensive i.v. formulation development. The microtracer approach has the advantage of simultaneous recovery of i.v. and oral pharmacokinetic parameters to obtain within-subject, within-period comparison. As such, this approach reduces the variability of recovered pharmacokinetic parameters, reduces the number of subjects required and provides a more precise estimate of absolute bioavailability than does the use of a traditional crossover design study. I.v. radiolabelled microtracer studies have been widely implemented at GlaxoSmithKline (GSK) within clinical pharmacology programmes and across diverse therapeutic areas. Microtracer studies have been used successfully to determine the absolute bioavailability of several compounds at GSK (dabrafenib [7], SRT-2104 (GSK2245840) [10], and GSK962040 [11]) and elsewhere (fexofenadine, IDX899, IDX989 and saxagliptin (dapagliflozin, SCH 900518) [12–17]) using either the marketed oral formulation or an oral microdose as the test treatment.

The purpose of this study was to characterize the oral and i.v. PK and to determine the absolute oral bioavailability of trametinib using simultaneous administration of an unlabelled oral dose (2 mg tablet) and a radiolabelled i.v. microdose (5 µg) in patients with solid tumours.

Methods

Clinical study design

The study protocol (MEK115064; ClinicalTrials.gov identifier NCT01416337) and consent form were approved by a duly constituted institutional review board (Alpha Independent Review Board, San Clemente, CA, USA), and the study was conducted in accordance with good clinical practice and the guiding principles of the Declaration of Helsinki at Comprehensive Clinical Development NW, Inc (Tacoma, WA, USA). Signed and dated written informed consent was obtained from each patient before his or her participation in the study and before any study-related procedures were performed.

This was a phase 1, single centre, open label study in patients with solid tumours. After obtaining informed consent, eligible participants were admitted to the clinical research unit on day −1. After fasting overnight for 8 h, all participants received trametinib as a single 2 mg tablet (with 240 ml water) and a single i.v. dose of 5 µg (7.4 kBq, 200 nCi) [^{14}C]-trametinib, administered 1.5 h after the oral dose (to coincide with oral t_{max}). The participants continued fasting for 4 h after the oral dose. The 5 µg (1 ml) i.v. microdose of [^{14}C]-trametinib (in 5% hydroxypropyl β-cyclodextrin [Cavitron] for injection) was injected as a slow i.v. push over 1 min into the infusion line through a 'Y' injection port co-administered with either a 50 ml solution of normal saline or 5% dextrose administered at a rate of 10 ml min^{-1}. All excipients used in the i.v. formulation had GRAS (generally regarded as safe) status. The i.v. infusion was given in the arm not being used for PK sampling.

Blood samples (two 6 ml samples at each time point) for analysis of trametinib, [^{14}C]-trametinib and total radioactivity were collected at several time points through 10 h on day 1 (pre-dose and 0.5, 1, 1.5, 1.75, 2, 2.5, 3, 4, 5, 6, 8, 10 h) and at single time points on days 2, 3, 4, 5, 8 and 11 after the oral dose. The actual date and time of each blood sample collection were recorded. Blood samples were stored on wet ice for a maximum of 1 h before plasma was separated from blood by centrifugation at 4°C and stored at −70°C prior to analysis. After completion of the study, all participants entered an open label rollover study of

trametinib (no washout period or follow-up visit required) and continued receiving trametinib (MEK114375, ClinicalTrials.gov identifier NCT01376310).

Dose selection

The recommended oral dose of trametinib is 2 mg once daily. The highest dosage strength (2 mg tablet) was used in this study. An i.v. dose of 5 µg was selected, which is 400-fold lower than the oral dose, thus fitting the criteria of a microdose (i.e. less than 100th of the dose needed to yield a pharmacologic effect, up to a maximum of 100 µg) [8, 9]. Due to the very low i.v. dose, a target detection limit of 2.5 pg ml^{-1} was considered acceptable to characterize the PK profile of trametinib. The lower limit achieved in developing the assay was 1.1 pg ml^{-1}.

Study participants

Men or women were eligible if they were ≥18 years of age with solid tumours, had an Eastern Cooperative Oncology Group (ECOG) performance status of 0 or 1, and had adequate organ function (total bilirubin ≤1.5 times ULN, ALT ≤2.5 times ULN, creatinine ≤1.5 times ULN, Cockroft–Gault creatinine clearance ≥50 ml min^{-1}, 24 h urine creatinine clearance ≥50 ml min^{-1}, LVEF ≥LLN by ECHO or MUGA). A body weight of ≥45 kg and a body mass index between 19 and 45 kg m^{-2} were required. Participants were excluded if they had received cancer therapy with delayed toxicity within 3 weeks, chemotherapy without delayed toxicity within 2 weeks, an investigational anticancer drug within 28 days, or any other investigational product within 30 days, five half-lives or twice the duration of the biological effect of the investigational product. In addition, patients were excluded if they had participated in a ^{14}C human research study within 12 months preceding administration of the study medication. Consumption of food, herbal remedies or medication known to interfere with cytochrome P450 (CYP) 3A activity was prohibited, although it was later confirmed that the major pathway of elimination of trametinib is not mediated by CYP3A4. Subjects with untreated leptomeningeal or brain metastases or spinal cord compression were excluded. Subjects with a Fridericia-corrected QT interval (QT_cF) or Bazett-corrected QT interval (QT_cB) ≥480 ms, with history or evidence of cardiovascular risk, with a history of interstitial lung disease or pneumonitis, with a history of retinal vein occlusion or central serous retinopathy or with conditions affecting gastrointestinal absorption were excluded.

Trametinib HPLC/MS/MS analysis

Trametinib was extracted from human plasma samples with an isotopically labelled standard ([$^{13}C_6$]-trametinib) by liquid-liquid extraction using ethyl acetate. Extracts were injected onto a BEH C18 column (50 × 2.1 mm, 1.7 µm; Waters Corporation, Milford, MA, USA), maintained at 65°C and eluted with a binary mobile phase gradient using 0.1% formic acid in water (A) and 0.1% formic acid in acetonitrile (B), with a constant flow rate of 0.7 ml min^{-1}. The initial mobile phase condition of 50 : 50 A : B was held until 0.8 min, when the composition changed to 35 : 65 A : B. From 0.81 to 1.0 min, the mobile phase held at 20:80 A:B and reverted back to the initial conditions (50 : 50 A : B) at 1.1 min. Detection was performed by positive ion MS/MS with multiple reaction monitoring (*m/z* 616 to *m/z* 491 for trametinib). The lower limit of quantification (LLQ) for trametinib was 0.25 ng ml^{-1} for a 50 µl aliquot of human plasma with a higher limit of quantification (HLQ) of 250 ng ml^{-1}. Quality control samples (QC), prepared at three different analyte concentrations (four replicates per concentration) and stored with the study samples, were analyzed with each batch of samples against separately prepared calibration standards. For the analysis to be acceptable, no more than one-third of the total QC results and no more than one-half of the results from each concentration level were to deviate from the nominal concentration by more than 15%. Data acquisition and quantitation were performed with Analyst version 1.4.2. The applicable analytical runs met all predefined run acceptance criteria.

[^{14}C]-trametinib and total radioactivity analysis

Samples were analyzed for [^{14}C]-trametinib and total plasma radioactivity using accelerator mass spectrometry (AMS). Prior to analysis by AMS, the carbon within the samples was harvested and converted to graphite. This involved a two stage process of sample combustion (oxidation) followed by graphitization (reduction), as previously published [18]. AMS provides an isotope ratio from which total radiocarbon per mg carbon is derived. The carbon content of plasma was taken into account to allow correction of the AMS data to determine the total amount of radiocarbon in the samples. Carbon analysis was undertaken using a Costech Elemental Combustion System CHNS-O Analyzer (Costech Analytical Technologies, Inc, Valencia, CA, USA) supplied by Pelican Scientific Ltd (Cheshire, UK). The AMS was a 250 kV Single Stage Accelerator Mass Spectrometer (National Electrostatics Corp., Middleton, WI, USA), operated via NEC proprietary 'AccelNET' software on a Linux operating system. Post-acquisition data processing was performed using the NEC software 'abc.' Further details of the operating conditions have been previously published [18]. The LLQ for total radioactivity was 0.95 pg equiv ml^{-1}.

Plasma [^{14}C]-trametinib concentrations at all time points were determined with a validated analytical LC + AMS method over the range of 1.1 to 101 pg ml^{-1}. Trametinib (including [^{14}C]-trametinib as a tracer) was extracted from 200 µl of human plasma by protein precipitation using three volumes of acetonitrile containing non-labelled trametinib at 2 µg ml^{-1} as an internal standard (IS). The samples were vortex-mixed and centrifuged at 3000 × *g*; the resultant supernatant was removed and dried using

a vacuum centrifuge. The sample was reconstituted in 250 µl of acetonitrile/water (50 : 50) and 50 µl was injected onto the HPLC system. Isolation of trametinib was achieved using a Phenomenex Synergi-Polar column (4 µm packing, 4.6 × 250 mm) maintained at 30°C. The mobile phase consisted of 10 mM ammonium acetate (pH 5) (A) and acetonitrile (B). A flow rate of 1 ml min^{-1} was maintained for the entire run. The following 70 min gradient was used: started at 5% B, increased to 20% B over 5 min, increased to 60% B over 40 min, increased to 95% B over 5 min and maintained at 95% B for 5 min, and decreased to 5% B over 5 min. The column was then re-equilibrated at 5% B over 5 min. The area of the u.v. response of the IS was recorded, and the eluate corresponding to trametinib was collected as a discrete fraction into a quartz tube for further processing to harvest graphite and subsequent analysis by AMS. The assay had a linear dynamic range of 1.1 to 101 pg ml^{-1} and quantification was performed against trametinib-spiked recovery standards based on demonstrated linearity with non-weighted linear regression.

During method validation, concentrations of [^{14}C]-trametinib in validation samples were determined on two occasions. Five of 33 validation samples failed to meet the acceptance criteria of being within 20% of the actual concentrations (25% at LLOQ). The bias was assessed to be <10% with a precision of <17.3%.

Study samples were analyzed as four separate batches with QC samples included in each batch. Individual QC results were deemed acceptable if the calculated concentration was within 20% of the actual concentration, and the analytical run was accepted if no more than one-third of the QCs exceeded the acceptable limit with at least one QC sample at each concentration within the acceptable limit. Only two of 36 samples failed to meet the established acceptance criteria (±20%) through four analytical runs.

Eight study samples (≈11%) were re-analyzed for incurred sample reproducibility (ISR) with all samples being within 20% of the mean of the original and ISR result.

Clinical pharmacokinetics

Analysis of plasma concentration data via non-compartmental methods was conducted using WinNonlin Professional Edition version 5.2 (Pharsight Corporation, Mountain View, CA, USA) non-compartmental Model 200 (for extravascular administration) for trametinib and non-compartmental Model 202 (for constant infusion) for [^{14}C]-trametinib and total radioactivity by ICON Development Solutions (Marlow, UK). Standard non-compartmental PK parameters, including maximum concentration (C_{max}), t_{max}, area under the concentration–time curve from time zero to 244 h or to infinity (AUC(0,t_{last}) and AUC(0,∞), respectively) and half-life ($t_{1/2}$) for trametinib, [^{14}C]-trametinib and total radioactivity, were estimated based on actual sampling times. Systemic clearance (CL) and apparent oral clearance (CL/*F*) were determined after i.v. and oral dosing, respectively. V_{ss} is described as the volume of distribution at steady-state following i.v. dosing and is based on mean residence time (MRT) and CL, where $V_{ss} = MRT(0,\infty) \times CL$. $V_{d,z}$ is described as the volume of distribution during the terminal phase and is calculated as $dose_{i.v.}/(\lambda_z \times AUC(0,\infty)_{i.v.})$, where λ_z is the terminal slope elimination rate constant and $AUC(0,\infty)_{i.v.}$ following i.v. administration of trametinib is defined above.

Statistical analysis

Summary statistics are reported for each PK parameter. For calculation of absolute bioavailability, a mixed-effect model (SAS, version 9.1.3, on the Windows SAS platform) was fitted to dose-normalized, log_e-transformed area under the curve (AUC(0,t_{last}) or AUC(0,∞)) with the subject as a random effect and treatment as a fixed effect (oral was the test, i.v. was the reference). Dose-normalized AUC(0,t_{last}) or AUC(0,∞) was obtained by dividing AUC(0,t_{last}) or AUC(0,∞) by dose for each subject. The least-squares mean difference and associated 90% confidence intervals (CIs) in AUC(0,t_{last}) or AUC(0,∞) between the oral and i.v. doses were obtained from the model. This least-squares mean difference was back-transformed to provide a point estimate and corresponding 90% CI for the absolute bioavailability (*F*). Due to the long elimination half-life and large extrapolation of area, the estimate of bioavailability is also reported based on AUC(0,t_{last}).

Results

Participants

Four patients (two White men and two White women;) were enrolled and underwent study procedures. All patients had metastatic (stage IV) cancer at screening, including oesophageal cancer, non-small cell lung cancer (NSCLC), ocular melanoma and bladder cancer. All patients had an ECOG performance status of 0 or 1 at screening. All received the oral and i.v. dose as planned.

Clinical pharmacokinetics

The geometric least squares mean (90% CI) absolute bioavailability (*F*) of the 2 mg trametinib tablet were 72.3% (50.0%, 104.6%) and 84.2% (66.1%, 107.2%) based on AUC(0,t_{last}) and AUC(0,∞), respectively. Individual values ranged from 45.7% to 92.8% and from 65.9% to 109% when *F* was determined using AUC(0,t_{last}) and AUC(0,∞), respectively.

Individual concentration–time profiles following oral dose and i.v. microdose are illustrated in Figure 1. Selected PK parameters for trametinib observed following oral administration and for [^{14}C]-trametinib and total radioactivity following i.v. administration are summarized in Table 1. For a 400-fold difference in dose, trametinib geometric mean C_{max} and AUC(0,t_{last}) were 76-fold and 289-fold

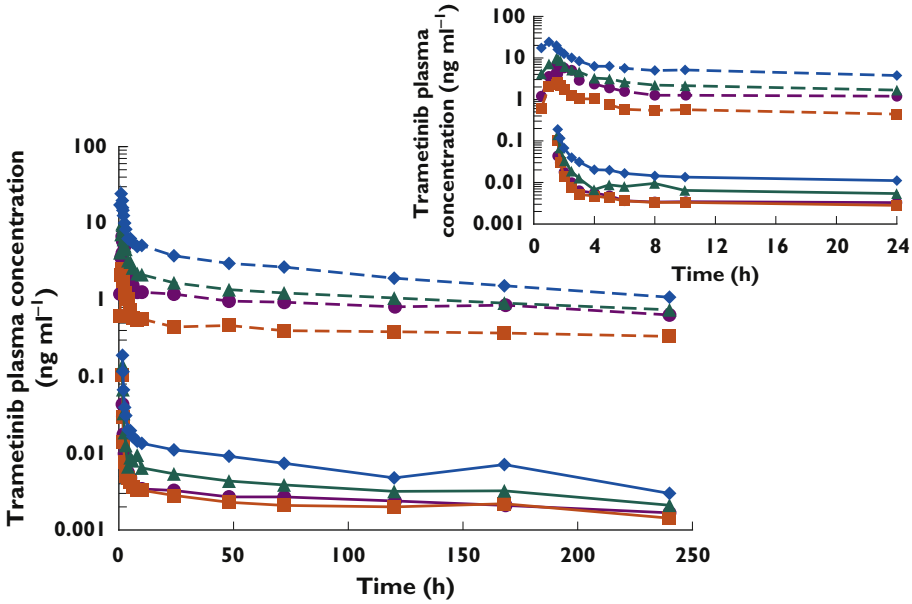

Figure 1

(A) Individual plasma trametinib and [^{14}C]-trametinib concentration *vs*. time profiles after oral (2 mg) and i.v. (5 μg) administration. Individual patients are denoted by symbols and colours. The dashed lines represent oral trametinib; the solid lines represent i.v. [^{14}C]-trametinib. Inset shows detail from 0 to 24 h post-dose

Table 1

Clinical pharmacokinetics of trametinib after concomitant oral and i.v. administration (2 mg trametinib orally, 5 μg [^{14}C]-trametinib i.v.)

Parameter (units)	Trametinib (oral)	[^{14}C]-trametinib (i.v.)	Total radioactivity* (i.v.)
t_{max}† (h)	1.50 (1.00, 1.58)	0.08 (0.08, 0.08)	0.08 (0.08,0.08)
C_{max}‡ (ng ml^{-1})	8.03 [118] (2.56, 24.31)	0.105 [71] (0.044, 0.190)	0.118 [54] (0.058, 0.177)
AUC(0,t)‡ (ng ml^{-1} h)	248 [83] (99.8, 580)	0.858 [57] (0.546, 1.76)	1.68 [56] (1.18, 3.60)
AUC(0,∞) (ng ml^{-1} h)	525 [36] (333, 783)‡	1.56 [31] (1.26, 2.39)‡	4.92§, 5.91§
$t_{1/2}$ (h)	264 [62] (130, 481)‡	229 [39] (144, 348)‡	643§, 176§
CL or CL/F‡ (l h^{-1})	3.81 [36] (2.56, 6.01)	3.21 [31] (2.09, 3.97)	ND
V_{ss}‡ (l)	ND	976 [79] (385, 1836)‡	ND
$V_{d,z}$‡ (l)	ND	1060 [75] (435, 1985)‡	ND

$t_{1/2}$, half-life; t_{max}, time to reach C_{max}; V_{ss}, volume of distribution at steady state; $V_{d,z}$, volume of distribution during the terminal phase. *Total radioactivity concentration units are ng equivalents trametinib ml^{-1}. †t_{max} results are presented as median (minimum, maximum). ‡Results are presented as geometric mean [%CV] (minimum, maximum) for n >2. §Elimination half-life and AUC(0,∞) for total radioactivity were estimated in only two of four subjects; individual subject values are listed. AUC(0,∞), area under the concentration–time curve from time zero to infinity; AUC(0,t), area under the concentration–time curve from time zero to time t; CL, systemic clearance; CL/F, apparent oral clearance; C_{max}, maximum concentration; ND, not determined.

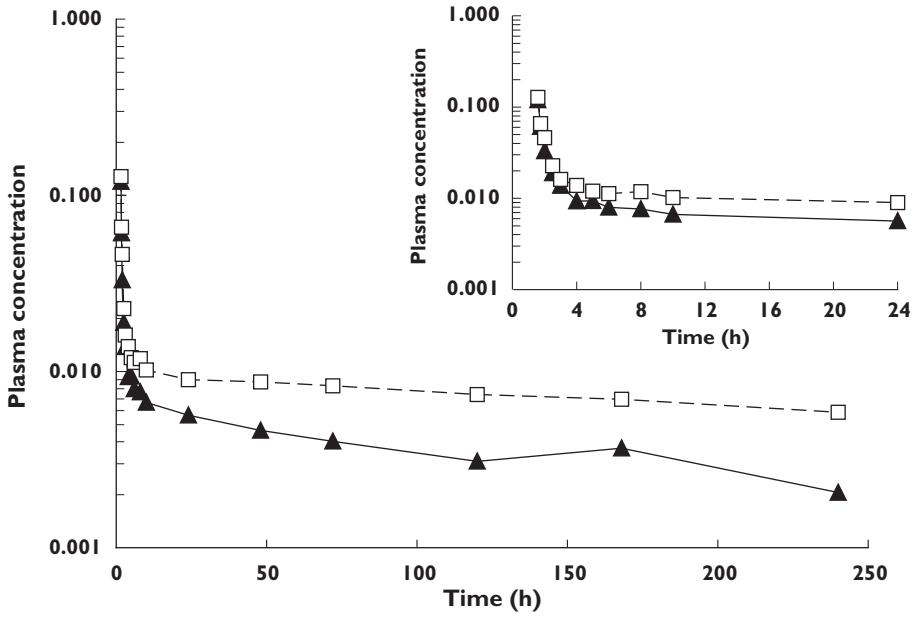

Figure 2

Mean plasma [^{14}C]-trametinib (solid line, ng ml^{-1}) and total radioactivity (dashed line, ng equivalents of trametinib ml^{-1}) concentration *vs*. time profile after i.v.; 5 μg administration (n = 4). Inset shows detail from 0 to 24 h post-dose. —▲—, [^{14}C]-trametinib; –□–, total radioactivity

lower, respectively, after i.v, microdose relative to the oral dose. Geometric mean i.v. trametinib plasma clearance, $V_{d,z}$, and V_{ss} were 3.21 l h^{-1}, 1060 l and 976 l, respectively, after administration of i.v. microdose. Apparent clearance following oral dose of trametinib was 3.81 l h^{-1}.

The median trametinib t_{max} after oral administration was 1.5 h and coincided with the t_{max} observed at the end of the i.v. infusion (0.08 h post-end of infusion). After t_{max}, a rapid distribution phase was observed as plasma concentrations decreased five-fold and 21-fold from t_{max} to 24 h post-oral and i.v. dose, respectively (Figure 1). The rapid distribution phase was followed by a prolonged terminal elimination phase after both oral and i.v. administration. The geometric mean terminal phase half-life for trametinib after oral dose and i.v. microdose administration was 264 h (≈11 days) and 229 h (≈10 days), respectively.

Mean profiles of [^{14}C]-trametinib and total radioactivity plasma concentration over time are shown in Figure 2. Trametinib as parent accounted for 52% (range: 43%–63%) of the total radioactivity observed after a single i.v. dose.

As shown in Figure 1, the rank order for each subject was consistent following oral and i.v. dosing, such that subjects with comparatively high exposure following oral administration also had high exposure after i.v. administration. This was further investigated by examining relationships between exposure and subject characteristics. Figure 3 shows trametinib and [^{14}C]-trametinib AUC(0,t_{last}) and C_{max} values by gender and by body weight. There was an apparent inverse relationship between body weight and trametinib exposure. Female subjects had higher exposure, consistent with their lower body weight.

Adverse events

All reported adverse events (AEs) were grade 1 and non-recurrent and most (except headache, ecchymosis and excoriation in one subject) resolved by the time subjects transitioned to the rollover study to continue receiving trametinib. None of the AEs was considered related to treatment with the study medication. There were no withdrawals due to AEs and no reports of AEs related to changes in clinical laboratory tests, echocardiograms or vital signs. There were no reports of serious AEs.

Discussion

The primary objective of this study was to determine the absolute bioavailability (F) of trametinib after concomitant administration of a radiolabelled i.v. microtracer dose (5 μg) and an unlabelled oral therapeutic dose (2 mg tablet formulation). To enable determination of concentrations following administration of the 5 μg i.v. microtracer dose, an AMS assay was validated with a lower limit of quantitation of 1.1 pg ml^{-1}. Based on AUC(0,t_{last}), the absolute bioavailability of trametinib was 72.3% (range, 45.7%–92.8% indicating moderate to high bioavailability of the 2 mg tablet following oral administration.

Trametinib had low i.v. plasma CL of 3.21 l h^{-1} (0.94 l h^{-1} blood clearance), which is approximately 1% of liver blood

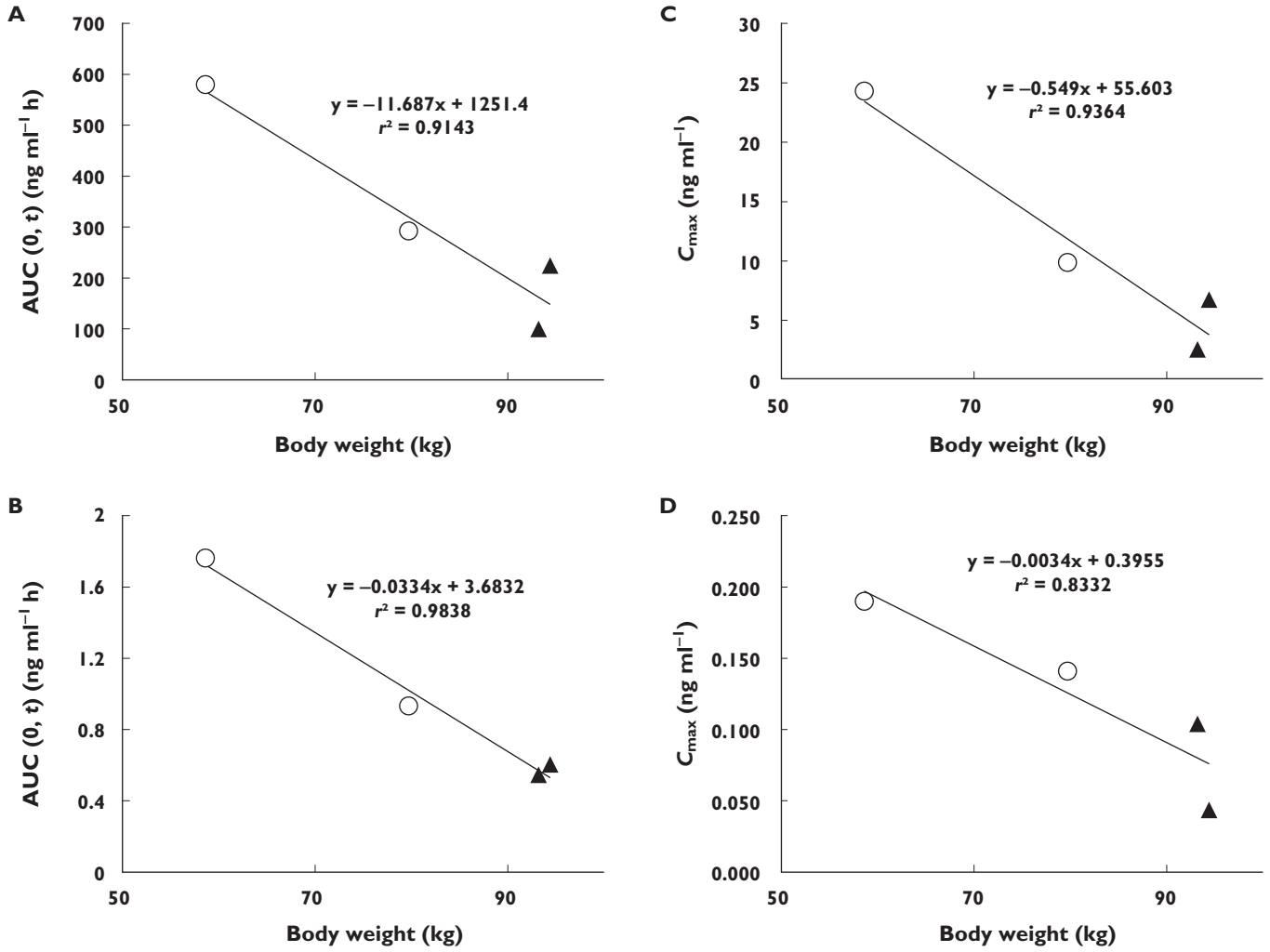

Figure 3

Individual AUC(0,t_{last}) and C_{max} values for a single 2 mg oral dose of trametinib (A,C) or a single 5 μg i.v. dose of [^{14}C]-trametinib (B,D). Symbols denote male (triangles) and female (circles) subjects

flow (where liver blood flow is 81 l h^{-1} [19] and a blood : plasma ratio of 3.4). High absolute bioavailability and low clearance suggest low hepatic extraction and limited first pass metabolism of trametinib. A large V_{ss} (976 l) suggests that trametinib distributes considerably to tissues. The distribution is rapid, as evidenced by the large initial decrease in concentrations after a single oral and i.v. dose (5- and 21-fold decrease within 24 h of t_{max}, respectively). Under steady-state conditions, a low peak : trough ratio of 1.8 was observed in subjects after once daily dosing of trametinib (2 mg) in the FTIH study. This may be attributable to the fact that the distribution processes are less pronounced with repeat dosing [6].

Subjects with comparatively high exposure following oral administration also had high exposure after i.v. administration. In addition, female subjects with lower body weight had higher exposure compared with male subjects with higher body weight, consistent with results from the population PK analysis where oral clearance (CL/*F*) was affected by both gender and weight, whereas the distributional clearance was affected by body weight [20].

The estimated half-lives after oral and i.v. administration were 11 and 10 days, respectively. The half-life determined in the food effect study (MEK113709 [21]) was approximately 5 days, likely due the shorter sampling period (up to 7 days) while the accumulation half-life was only 4 days. Using a population PK model, estimated terminal half-lives were 3.9 and 4.8 days for male and female subjects, respectively, and were consistent with the effective half-life [20]. Despite a lengthy elimination phase, it is expected that steady-state exposure following repeat daily dosing of 2 mg will be reached within 15 to 20 days. This is because the AUC attributed to the long elimination phase contributes little to total AUC.

Trametinib profiles following both oral and i.v. administration showed an initial rapid distribution phase

followed by a protracted elimination phase likely reflective of slow elimination from deep compartments. It has been shown that parent trametinib, but not metabolites, preferentially distributes to red blood cells and this accounts for the initial rapid distribution phase [22] and is supportive of the observation that following a single i.v. dose, parent trametinib accounts for 52% (range 43%–63%) of the total radioactivity in plasma. Following repeat dosing, as steady-state is reached, the fraction of parent trametinib in plasma accounts for >75%, while the two metabolites each accounted for approximately 10% of total radioactivity.

Given the long elimination half-life relative to the sample collection period and large extrapolation of AUC(0,∞), the primary estimate of *F* was based on AUC(0,t_{last}). In general, estimates of *F* using AUC(0,∞) agreed (within 17%) with estimates using AUC(0,t_{last}), except for one subject in whom the estimate of absolute bioavailability differed from that in the other three subjects by 44%. This subject had an elimination half-life for trametinib in plasma that was 1.5 times higher than the geometric mean half-life. For two subjects, accurate estimation of elimination half life (and AUC(0,∞)) was not possible due to a relatively flat elimination phase of the plasma concentration–time curve.

In conclusion, the i.v. microtracer study approach revealed the contribution of moderate/high oral bioavailability with low first pass metabolism and a prolonged terminal elimination phase to the PK of trametinib. Although this study had its limitations due to the study population, namely the small number of patients, the advantages of this approach was a shorter study time frame (compared with a traditional crossover design) and simultaneous collection of i.v. and oral pharmacokinetic parameters with reduced variability. In the case of trametinib, which has a long half-life, the i.v. microtracer approach is especially useful. This approach obviates the need for a lengthy washout period required in a conventional crossover study, and allows patients to receive treatment without delay by entering into the rollover study and also allows recruitment of a small number of patients while recovering the necessary PK parameters. As such, i.v. microtracer studies offer an innovative and efficient approach for assessing absolute bioavailability and may be applied across a range of therapeutic areas and compound classes.

Competing Interests Disclosure

All authors have completed the Unified Competing Interest form at http://www.icmje.org/coi_disclosure.pdf (available on request from the corresponding author) and declare CL, CP, JB, GCY, MH, FH, KO and DO are full-time paid employees and stockholders of GlaxoSmithKline. LF, an independent contractor, received payment from GlaxoSmithKline for statistical analysis related to this study and RAM's institution received payment from GlaxoSmithKline to conduct the clinical research study.

Thanks are due to Steven Corless and Mike Hobbs (DMPK, GlaxoSmithKline) for the analysis of samples by AMS and LC + AMS, Sherry Wang and Ciara Rodgers (DMPK, GlaxoSmithKline) for analysis by LC/MS/MS, Alexandra Piepszak (GlaxoSmithKline, data management), Veronique Fauvel and Christopher Jefferds (ICON Clinical Research) who assisted with the conduct of the trial, Ken Martin (Comprehensive Clinical Development) and the patients who participated in this study. Funding for this study was provided by GlaxoSmithKline (NCT01416337). All listed authors meet the criteria for authorship set forth by the International Committee for Medical Journal Editors. Editorial support in the form of collating author comments, copyediting, referencing, and graphic services was provided by Clinical Thinking and was funded by GlaxoSmithKline.

REFERENCES

1 Abe H, Kikuchi S, Hayakawa K, Iida T, Nagahashi N, Maeda K, Sakamoto J, Matsumoto N, Miura T, Matsumura K, Seki N, Inaba T, Kawasaki H, Yamaguchi T, Kakefuda R, Nanayama T, Kurachi H, Hori Y, Yoshida T, Kakegawa J, Watanabe Y, Gilmartin AG, Richter MC, Moss KG, Laquerre SG. Discovery of a highly potent and selective MEK inhibitor: GSK1120212 (JTP-74057 DMSO solvate). ACS Med Chem Lett 2011; 2: 320–4.

2 Gilmartin AG, Bleam MR, Groy A, Moss KG, Minthorn EA, Kulkarni SG, Rominger CM, Erskine S, Fisher KE, Yang J, Zappacosta F, Annan R, Sutton D, Laquerre SG. GSK1120212 (JTP-74057) is an inhibitor of MEK activity and activation with favorable pharmacokinetic properties for sustained *in vivo* pathway inhibition. Clin Cancer Res 2011; 17: 989–1000.

3 Falchook GS, Lewis KD, Infante JR, Gordon MS, Vogelzang NJ, DeMarini DJ, Sun P, Moy C, Szabo SA, Roadcap LT, Peddareddigari VG, Lebowitz PF, Le NT, Burris HAI, Messersmith WA, O'Dwyer PJ, Kim KB, Flaherty K, Bendell JC, Gonzalez R, Kurzrock R, Fecher LA. Activity of the oral MEK inhibitor trametinib in patients with advanced melanoma: a phase 1 dose-escalation trial. Lancet Oncol 2012; 13: 782–9.

4 Kim KB, Kefford R, Pavlick AC, Infante JR, Ribas A, Sosman JA, Fecher LA, Millward M, McArthur GA, Hwu P, Gonzalez R, Ott PA, Long GV, Gardner OS, Ouellet D, Xu Y, DeMarini DJ, Le NT, Patel K, Lewis KD. Phase II study of the MEK1/MEK2 inhibitor trametinib in patients with metastatic BRAF-mutant cutaneous melanoma previously treated with or without a BRAF inhibitor. J Clin Oncol 2013; 31: 482–9.

5 Flaherty KT, Robert C, Hersey P, Nathan P, Garbe C, Milhem M, Demidov LV, Hassel JC, Rutkowski P, Mohr P, Dummer R, Trefzer U, Larkin JM, Utikal J, Dreno B, Nyakas M, Middleton MR, Becker JC, Casey M, Sherman LJ, Wu FS, Ouellet D, Martin AM, Patel K, Schadendorf D. Improved survival with MEK inhibition in BRAF-mutated melanoma. N Engl J Med 2012; 367: 107–14.

6 Infante JR, Fecher LA, Falchook GS, Nallapareddy S, Gordon MS, Becerra C, DeMarini DJ, Cox DS, Xu Y, Morris SR,

Peddareddigari VG, Le NT, Hart L, Bendell JC, Eckhardt G, Kurzrock R, Flaherty K, Burris HAI, Messersmith WA. Safety, pharmacokinetic, pharmacodynamic, and efficacy data for the oral MEK inhibitor trametinib: a phase 1 dose-escalation trial. Lancet Oncol 2012; 13: 773–81.

7 Denton CL, Minthorn E, Carson SW, Young GC, Richards-Peterson LE, Botbyl J, Han C, Morrison RA, Blackman SC, Ouellet D. Concomitant oral and intravenous pharmacokinetics of dabrafenib, a BRAF inhibitor, in patients with BRAF V600 mutation-positive solid tumors. J Clin Pharmacol 2013; 53: 955–61.

8 Department of Health and Human Services, Center for Drug Evaluation and Research (CDER). FDA guidance for industry: bioavailability and bioequivalence studies for orally administered drug products – general considerations. 2003. Available at http://www.fda.gov/downloads/Drugs/GuidanceComplianceRegulatoryInformation/Guidances/ucm070124.pdf (last accessed 26 February 2013).

9 European Medicines Agency (EMEA), Committee for Medicinal Products for Human Use (CHMP). Position paper on non-clinical safety studies to support clinical trials with a single microdose, 2004. 2013. Available at http://www.ema.europa.eu/ema/index.jsp?curl=pages/regulation/general/general_content_000400.jsp&mid=WC0b01ac0580029570 (last accessed 26 February 2013).

10 Hoffmann E, Wald J, Lavu S, Roberts J, Beaumont C, Haddad J, Elliott P, Westphal C, Jacobson E. Pharmacokinetics and tolerability of SRT2104, a first-in-class small molecule activator of SIRT1, after single and repeated oral administration in man. Br J Clin Pharmacol 2013; 75: 186–96.

11 Vasist Johnson LS, Young MA, Stevens LA, Cozens SJ, Collier J, Robertson DC, Dukes GE. A microtracer study of GSK962040, a motilin receptor agonist, to support dosing regimens in the critical care setting. Clin Pharmacol Ther 2013; 93: S80.

12 Gao L, Li J, Kasserra C, Song Q, Arjomand A, Hesk D, Chowdhury SK. Precision and accuracy in the quantitative analysis of biological samples by accelerator mass spectrometry: application in microdose absolute bioavailability studies. Anal Chem 2011; 83: 5607–16.

13 Xu XS, Dueker SR, Christopher LJ, Lohstroh PN, Keung CF, Cao KK, Bonacorsi SJ, Cojocaru L, Shen JX, Humphreys WG, Stouffer B, Arnold ME. Overcoming bioanalytical challenges in an onglyza intravenous [(14)C]microdose absolute bioavailability study with accelerator MS. Bioanalysis 2012; 4: 1855–70.

14 Boulton DW, Kasichayanula S, Keung CF, Arnold ME, Christopher LJ, Xu XS, Lacreta F. Simultaneous oral therapeutic and intravenous ^{14}C-microdoses to determine the absolute oral bioavailability of saxagliptin and dapagliflozin. Br J Clin Pharmacol 2013; 75: 763–8.

15 Lappin G, Shishikura Y, Jochemsen R, Weaver RJ, Gesson C, Houston B, Oosterhuis B, Bjerrum OJ, Rowland M, Garner C. Pharmacokinetics of fexofenadine: evaluation of a microdose and assessment of absolute oral bioavailability. Eur J Pharm Sci 2010; 40: 125–31.

16 Sarapa N, Hsyu PH, Lappin G, Garner RC. The application of accelerator mass spectrometry to absolute bioavailability studies in humans: simultaneous administration of an intravenous microdose of 14C-nelfinavir mesylate solution and oral nelfinavir to healthy volunteers. J Clin Pharmacol 2005; 45: 1198–205.

17 Zhou XJ, Garner RC, Nicholson S, Kissling CJ, Mayers D. Microdose pharmacokinetics of IDX899 and IDX989, candidate HIV-1 non-nucleoside reverse transcriptase inhibitors, following oral and intravenous administration in healthy male subjects. J Clin Pharmacol 2009; 49: 1408–16.

18 Young GC, Corless S, Felgate CC, Colthup PV. Comparison of a 250 kV single-stage accelerator mass spectrometer with a 5 MV tandem accelerator mass spectrometer – fitness for purpose in bioanalysis. Rapid Commun Mass Spectrom 2008; 22: 4035–42.

19 Rowland M, Tozer TN. Clinical Pharmacokinetics: Concepts and Applications, 2nd ed edn. Philadelphia, PA: Lea & Febiger, 1989.

20 Kassir N, Mouksassi M, Cox DS, DeMarini DJ, Gardner OS, Sherman L, Crist WA, Ouellet D. Population pharmacokinetics (PK) of trametinib (GSK1120212), a MEK inhibitor, in subjects with cancer. Clin Pharmacol Ther 2013; 93: S69.

21 Cox DS, Papdopoulos KP, Fang L, Bauman J, LoRusso P, Tolcher AW, Patnaik A, Pendry C, Orford K, Ouellet D. Evaluation of the effects of food on the single-dose pharmacokinetics of trametinib, a first-in-class MEK inhibitor, in patients with cancer. J Clin Pharmacol 2013; 53: 946–54.

22 Ho MY, Morris MJ, Pirhalla JL, Bauman JW, Pendry CB, Orford KW, Morrison RA, Cox DS. Trametinib, a first-in-class oral MEK inhibitor mass balance study with limited enrollment of two male subjects with advanced cancers. Xenobiotica 2013; 44: 352–68.

GlaxoSmithKline Research
& Development Limited
Park Road
Ware
Hertfordshire
SG12 0DP

Tel. +44 (0)1920 469469
www.gsk.com

I confirm that Graeme C. Young contributed significantly to the clinical study design, support of the work performed and publication preparation as detailed in the paper –

Bowers, G. D., D. Tenero, P. Patel, P. Huynh, J. Sigafoos, K. O'Mara, **G. C.Young**, E. Dumont, E. Cunningham, M. Kurtinecz, P. Stump, J. J. Conde, J. P. Chism, M. J. Reese, Y. L. Yueh and J. F. Tomayko (2013). "Disposition and metabolism of GSK2251052 in humans: a novel boron-containing antibiotic." Drug Metab Dispos **41**(5): 1070-1081

1st December 2015

Dr. Gary Bowers, PhD.
(formerly of) GlaxoSmithKline Research and Development Ltd.
garybowers@me.com

Date

Registered in England & Wales
No. 835139

Registered office
980 Great West Road
Brentford, Middlesex. TW8 9GS

GlaxoSmithKline Research
& Development Limited
Park Road
Ware
Hertfordshire
SG12 0DP

Tel. +44 (0)1920 469469
www.gsk.com

I confirm that Graeme C. Young contributed significantly to the clinical study design, support of the work performed and publication preparation as detailed in the paper –

Harrell, A. W., S. K. Siederer, J. Bal, N. H. Patel, **G. C. Young**, C. C. Felgate, S. J. Pearce, A. D. Roberts, C. Beaumont, A. J. Emmons, A. I. Pereira and R. D. Kempsford (2013). "Metabolism and disposition of vilanterol, a long-acting beta(2)-adrenoceptor agonist for inhalation use in humans." Drug Metab Dispos **41**(1): 89-100.

A Harrell

1-Dec-2015

Andrew W. Harrell, BSc.
GlaxoSmithKline Research and Development Ltd.
Andrew.W.Harrell@gsk.com

Date

Registered in England & Wales
No. 835139

Registered office
980 Great West Road
Brentford, Middlesex. TW8 9GS

GlaxoSmithKline Research
& Development Limited
Park Road
Ware
Hertfordshire
SG12 0DP

Tel. +44 (0)1920 469469
www.gsk.com

I confirm that Graeme C. Young contributed significantly to the clinical study design, support of the work performed and publication preparation as detailed in the paper –

Dave, M., M. Nash, G. C. Young, H. Ellens, M. H. Magee, A. D. Roberts, M. A.Taylor, R. W. Greenhill and G. W. Boyle (2014). "Disposition and metabolism of darapladib, a lipoprotein-associated phospholipase A2 inhibitor, in humans." Drug Metab Dispos 42(3): 415-430

01-Dec-2015.

Mehul Dave, BSc. (Hons)
GlaxoSmithKline Research and Development Ltd.
Mehul.2.Dave@gsk.com

Date

Registered in England & Wales
No. 835139

Registered office
980 Great West Road
Brentford, Middlesex. TW8 9GS

GlaxoSmithKline

GlaxoSmithKline Research
& Development Limited
Park Road
Ware
Hertfordshire
SG12 0DP

Tel. +44 (0)1920 469469
www.gsk.com

I confirm that Graeme C. Young contributed significantly to the clinical study support work performed and publication preparation as detailed in the papers –

Denton, C. L., E. Minthorn, S. W. Carson, **G. C. Young**, L. E. Richards-Peterson, J. Botbyl, C. Han, R. A. Morrison, S. C. Blackman and D. Ouellet (2013)."Concomitant oral and intravenous pharmacokinetics of dabrafenib, a BRAF inhibitor, in patients with BRAF V600 mutation-positive solid tumors." J Clin Pharmacol **53**(9): 955-961

And -

Leonowens, C., C. Pendry, J. Bauman, **G. C. Young**, M. Ho, F. Henriquez, L.Fang, R. A. Morrison, K. Orford and D. Ouellet (2014). "Concomitant oral and intravenous pharmacokinetics of trametinib, a MEK inhibitor, in subjects with solid tumours." Br J Clin Pharmacol **78**(3): 524-532

Cleonowens

Dec. 2, 2015

Dr. Cathrine Leonowens (neé Denton), PhD.
(formerly of) GlaxoSmithKline Research and Development Ltd.
leonowens.c@gmail.com

Date

Registered in England & Wales
No. 835139

Registered office
980 Great West Road
Brentford, Middlesex. TW8 9GS

GlaxoSmithKline Research
& Development Limited
Park Road
Ware
Hertfordshire
SG12 0DP

Tel. +44 (0)1920 469469
www.gsk.com

To whom it may concern,

This statement is designed to explain the situation around authorship of publications from industry to assist The University of Lincoln and other interested parties in assessing the works included in the PhD Commentary by Graeme C. Young. All publications authored or co-authored by Graeme C. Young have been produced whilst he has been employed by GlaxoSmithKline Research and Development Ltd. (GSK), or a legacy company.

It is common practice in industry to have varied contributors for published papers as the work being published often arises through collaborations across multiple representative groups and drug development projects. The list of co-authors is then dictated by a number of influences and may not necessarily be all inclusive or indeed reflect, for example, the magnitude of the contribution. That said, there are strict guidelines concerning justification for inclusion of an individual as an author, which are adhered to *[GSK ensures that authorship selection is consistent with Good Publication Practice (GPP2) and the International Committee of Medical Journal Editors (ICMJE) guidelines (www.icmje.org)].*

In the case of clinical study data the lead author will usually come from the clinical arena eg. Clinical Pharmacology or Clinical Pharmacokinetics disciplines, and for Drug Metabolism based publications the lead author is often the individual who lead that overall effort for the development of the drug. It is often also the case that practical work carried out at a Contract Research Organisation may be published by GSK authors.

Additionally, sometimes the main architect for a study design may not be the lead author of the publication and may be listed as a co-author, or even just in the Acknowledgements, particularly where there is a restriction on the number of authors that can be included. This latter situation has also led to instances where other members of staff who have been involved in the works are given the opportunity to contribute by way of authorship of the publication, to the exclusion of another contributor *[in this case Graeme C. Young].*

The papers that Graeme C. Young is including in his PhD Commentary as examples of some of those that he has co-authored, reflect the common practices outlined above.

Yours faithfully,

Dr. Gordon Dear, PhD. [Industrial Supervisor for Graeme C. Young]

Director, GlaxoSmithKline Research and Development Ltd.

Registered in England & Wales
No. 835139

Registered office
980 Great West Road
Brentford, Middlesex. TW8 9GS